



The Global Center for Desiccant Technology

Mississippi State
UNIVERSITY

Mechanical Engineering

Advanced Desiccant Technology Research

For

Oak Ridge National Laboratory
And
Gas Technology Institute

October 2001

The Global Center for Desiccant Technology
Department of Mechanical Engineering
Mississippi State University
Mississippi State, MS 39762-5925
Phone: (662) 325-3260
Fax: (662) 325-7223

L. M. Chamra
B.K. Hodge
A. Jalalzadeh
C. A. James
W. G. Steele
J. W. Stevens



Mississippi State UNIVERSITY

Department of Mechanical Engineering
P. O. Box ME, 210 Carpenter Engineering
Mississippi State, MS 39762-5925
(662) 325-3260 Fax: (662) 325-7223

November 13, 2001

Dr. Jim Sand
Oak Ridge National Laboratory
1000 Bethel Valley Road
Bldg. 3147, MS 6070
Oak Ridge, TN 37831-6070

Re: Advanced Desiccant Technology Research Report

Dear Jim:

The Global Center for Desiccant Technology (GCDT) at Mississippi State University (MSU) is pleased to forward you a copy of the final report for the GCDT's Advanced Desiccant Technology Research project. This project, a 30-month research effort cofunded by Oak Ridge National Laboratory (ORNL), the Gas Research Institute (which became part of the Gas Technology Institute), and the Hearin Foundation, addressed three topics pertinent to enhancing the penetration of gas-fired desiccant systems in the HVAC sector. The first topic, presented as Chapter 2 in the report, examines the economics of desiccant-enhanced systems for eight building types in forty cities. The screening tool, DesiCalc, was used as were actual electrical and gas rate schedules from the forty cities. The second topic, contained in Chapter 3, presents a comprehensive study of the comfort literature relating to temperature and humidity. Additionally, results of an experimental human comfort study (utilizing the Environmental Laboratory at Kansas State University) that examined temperature/humidity conditions at the periphery of the ASHRAE comfort zone are presented and analyzed. The third topic, discussed in Chapter 4, uses field data and ORNL and MSU laboratory data to assess the validity of the DesiCalc screening tool.

The GCDT would appreciate receiving feedback and comments on the contents of the Advanced Desiccant Technology Research Report.

Sincerely,

B. K.

B. K. Hodge, PhD, PE
Professor and GCDT Director

CHAPTER 1

INTRODUCTION

1.1 BACKGROUND

Mississippi State University (MSU) houses the Global Center for Desiccant Technology (GCDT). In support of its mission to develop desiccant technologies, the GCDT engages in education, outreach, and research related to desiccant dehumidification devices. Additionally, the GCDT possesses a non-proprietary desiccant performance test loop. The research and enhancement activities of the GCDT supplement on-going efforts by the Department of Energy/Oak Ridge National Laboratory (DOE/ORNL) and the Gas Technology Institute (GTI) to develop this energy-efficient, comfort-oriented, and environmentally friendly technology.

Industry partnerships have been formed between conventional heating, ventilating, and air conditioning (HVAC) equipment companies, academe, manufacturers of desiccant air conditioning equipment, and the gas utilities. These collaborations serve to organize industrial, governmental, and academic support for desiccant technology, function as an advisory body on desiccant-related research, and perfect and expand the market acceptance of desiccant-based technologies in comfort air conditioning applications through workshops, professional symposia, and other methods of technical communication.

Some key research activities in promoting the acceptance of desiccant technologies in the established building air conditioning markets are

- Development of a clear analysis of the energy use and potential for energy savings associated with the use of desiccant systems as the latent load handling component in building ventilation and air conditioning systems,
- Verification and quantification of the effect of parameters such as temperature, humidity, and air velocity on the relative “comfort” felt by building occupants,
- Revision of the accepted “comfort zone” in the region of lower relative humidities and higher dry bulb temperatures that is indicative of desiccant-treated air, and
- Continued outreach and education efforts aimed at architects and building HVAC engineers highlighting the operation, main features, energy saving potential, enhanced comfort, and indoor air quality benefits of desiccant-treated air in commercial, governmental and municipal buildings.

Research tasks outlined in this document serve to address these key activities and to delineate the cost effectiveness, health and environmental aspects, comfort benefits, and needed educational outreach activities associated with expanded application and market growth of desiccant-based air conditioning equipment in the United States.

1.2 OBJECTIVES

The objectives of this research are to:

- 1) Prepare a nationwide analysis of energy savings associated with the use of desiccant systems in commercial buildings.
- 2) Review and verify the most important variables affecting human comfort levels within buildings and apply this knowledge to influence HVAC design and installation practices involving desiccant-based equipment.
- 3) Use field demonstration "case study" data coming out of the current DOE/ORNL and GTI desiccant equipment programs to validate the energy saving and comfort study predications developed in the first two activities.

Chapter 2, entitled "National Energy/Cost Savings," addresses the first objective. The second objective is addressed in Chapter 3, "Human Comfort Studies." The final objective is addressed in "Field Energy Savings Validation," Chapter 4.

CHAPTER 2

NATIONAL ENERGY/COST SAVINGS

2.1 INTRODUCTION

The objective of the National Energy/Cost Savings study is to provide a nationwide comparison of predicted operating costs between conventional HVAC systems and similar systems that include a gas-fired desiccant component. System operating costs and performance predictions were generated using the computer simulation program DesiCalc™, distributed by the Gas Technology Institute. The study included effects of geographic location (weather) and building type. Forty cities and eight building types for each city were selected for analysis. For each city, the local utility rate structures (natural gas and electricity) were obtained and used for the economic analysis. Weather information in the form of Typical Meteorological Year (TMY2) data was used for each city.

2.1.1 Literature Review

Desiccant systems have been widely studied for many years. Studies pertinent to this work examine the advantages of desiccant systems in controlling humidity and improving comfort.

Harriman et al. (1999) found an interesting pattern when comparing comfort differences to cost differences in movie theaters. The comfort differences are strongly influenced by climate, but in most cases the cost differences relate primarily to the cost of electrical power. Utility rates drive the operating cost advantages and limitations of each technology. Comfort has a value that varies according to its duration and the preferences of building owners. Clearly, it is useful to examine the local conditions of both climate and utility costs before making a generalization about the cost effectiveness of any given technology.

Busby (1996) discussed various aspects of humidity control in healthcare facilities using desiccant units. Humidity can be controlled separately with desiccant units that are simple to operate and maintain. Healthcare facilities are often ideal candidates for this strategy. He also affirmed that although desiccant-based dehumidifiers have been used in industrial applications for decades, recent advances in desiccant materials and system components have made modern packages more efficient and reliable for commercial buildings.

Downing (1996) discussed the development of a desiccant-based air conditioning system at the Georgia Institute of Technology. The desiccant-based system was installed in a dormitory to maintain acceptable indoor air quality with minimal energy consumption. For the dormitory design, outdoor ventilation air around the clock was considered necessary in order to alleviate indoor air quality concerns. Humidity loads were expected to fluctuate with occupancy levels and cooking and bathroom activities. The design solution uses an "outdoor air preconditioner" based on a desiccant system, which effectively decouples the outside ventilation load from the building's internal load. Heat recovery systems are used to recover energy from the exhaust air. Estimated first-cost savings resulted in immediate payback for the desiccant-based system.

Fischer (1999) performed a market analysis on the potential for active desiccant dehumidification systems in nursing homes, hospitals, research laboratories, retail stores, hotels, and school and university classrooms. He found that active desiccant systems could be competitive on the basis of cost and energy performance with conventional systems.

2.2 METHODOLOGY

This study includes the analysis of forty cities and eight building types. DesiCalc™ was used to generate the energy cost estimates and performance predictions. Required weather information for each city selected was obtained from Typical Meteorological Year (TMY2) data. Utility rate structures, including gas and electricity, were obtained from the utility companies serving the forty cities. For each building type, a building configuration was selected, as were equipment configurations for both conventional and desiccant-enhanced systems. Once the information was complete, DesiCalc™ was run to calculate the total annual energy usage and cost for each case.

2.2.1. Description of the DesiCalc™ Software.

DesiCalc™ is a desiccant screening software which provides analysis of the benefits of supplementing standard air-conditioning systems with desiccant based air-treatment equipment. DesiCalc™ employs DOE version 2.1E which runs in the background as the computational engine. The latest National Renewable Energy Laboratory (NREL) TMY2 meteorological weather database is used. DesiCalc™ provides templates for eleven building types and annual weather data sets for 236 U.S. locations. Eleven typical commercial buildings are included with the program: hospitals, small and large hotels, ice arenas, nursing homes, quick-service restaurants, retail stores, schools, supermarkets, movie theaters, and refrigerated warehouses.

The software includes weather data for 236 U.S. cities and representative utility rates (both gas and electric) for sixteen cities, including Atlanta, Baltimore, Charleston (SC), Chicago, Cleveland, Dallas, Houston, Jackson (MS), Miami, Minneapolis, Nashville, New Orleans, New York, Raleigh, St. Louis, and Tampa. The user can specify other utility rates by adapting rates from other cities or by adding new rate schedules. DesiCalc™ allows estimates of annual or monthly energy loads (using an hour-by-hour simulation) and energy costs for any of the eleven commercial buildings in any of the locations. The program uses electric equipment selected from a library of five typical systems. DesiCalc™ compares the performance of the selected system with that of the system supplemented with a desiccant dehumidifier.

Short (Figure 2.A.1 in Appendix 2.A) and detailed (Figure 2.A.2 in Appendix 2.A) summary reports can be generated. Short reports include the following information: job description, building, location and design weather data, equipment and energy descriptions (baseline equipment and desiccant-enhanced system alternatives). Short reports contain summaries of key calculated results including annual electric energy use (kWh), annual gas energy use (MBTU), annual electric energy cost, and annual occupied hours @ RH > 60%. Desiccant dehumidifier performance is also included.

A detailed report can also be produced. This report, entitled "Monthly Loads, Energy Consumption and Costs Report," includes the following information: job description, cooling and heating loads (baseline and alternative systems), electric energy consumption by equipment type, gas energy consumption by equipment type, total monthly electric consumption and electric energy cost, and total monthly gas consumption and gas energy cost.

In addition to the reports, the following charts can be generated (see Figure 2.A.3 of Appendix 2.A for an example): humidity control, electric energy use, electric demand, electric costs, gas energy use, gas costs, monthly energy costs, and annual energy costs.

2.2.2. Site Selection

Forty cities were selected so that regions where desiccant dehumidification was expected to be useful were covered. In addition, the cities chosen were representative of the population demographics in the United States. Table 2.1 lists all the cities included in the study.

Table 2.1 Cities Included in the Study

1	Albany, NY	15	Houston, TX	29	Omaha, NE
2	Asheville, NC	16	Huntington, WV	30	Pittsburgh, PA
3	Atlanta, GA	17	Indianapolis, IN	31	Portland, ME
4	Baltimore, MD	18	Jackson, MS	32	Portland, OR
5	Boston, MA	19	Little Rock, AR	33	Raleigh, NC
6	Burlington, VT	20	Los Angeles, CA	34	Rochester, NY
7	Charleston, SC	21	Louisville, KY	35	San Francisco, CA
8	Chicago, IL	22	Miami, FL	36	Seattle, WA
9	Cleveland, OH	23	Milwaukee, WI	37	St. Louis, MO
10	Corpus Christi, TX	24	Minneapolis, MN	38	Tallahassee, FL
11	Detroit, MI	25	Nashville, TN	39	Tampa, FL
12	Fargo, ND	26	New Orleans, LA	40	Wichita, KS
13	Fort Worth, TX	27	New York, NY		
14	Honolulu, HI	28	Norfolk, VA		

Figure 2.1 shows the distribution of the geographic locations of the selected cities, with the exception of Honolulu, HI. Following the divisions to be used by the 2000 U.S. census, the forty cities considered were divided in four geographic regions: northeast, midwest, south, and west. Table 2.2 shows the cities included in each region.



Figure 2.1 Locations of Cities used in the Study

Table 2.2 Census Regions

Region 1: Northeast	Region 2: Midwest	Region 3: South	Region 4: West
Portland, ME	Cleveland, OH	Baltimore, MD	Seattle, WA
Burlington, VT	Indianapolis, IN	Norfolk, VA	Portland, OR
Boston, MA	Chicago, IL	Huntington, WV	San Francisco, CA
New York, NY	Detroit, MI	Asheville, NC	Los Angeles, CA
Albany, NY	Milwaukee, WI	Raleigh, NC	Honolulu, HI
Rochester, NY	Minneapolis, MN	Charleston, SC	
Pittsburgh, PA	St. Louis, MO	Atlanta, GA	
	Fargo, ND	Miami, FL	
	Omaha, NE	Tampa, FL	
	Wichita, KS	Tallahassee, FL	
		Louisville, KY	
		Nashville, TN	
		Jackson, MS	
		Little Rock, AR	
		New Orleans, LA	
		Fort Worth, TX	
		Houston, TX	
		Corpus Christi, TX	

2.2.3. Utility Rate Schedules

Full utility rate data were required for a total of 80 cases (gas and electricity rates for each city). With help from the Technical Marketing Group at Mississippi Valley Gas Company, the 80 rate schedules were collected and tabulated. The help from Mississippi Valley Gas was invaluable in completing this portion of the study.

The electric rate schedule type can be defined as either a stepped or a time-of-use rate structure. Electric rate season information can be introduced by identifying the months of the year for which summer or winter rates are applicable. In stepped-rate schedules, the unit price of energy varies based on the rate of consumption. A utility may offer inverted-rate blocks (where the rate increases as consumption decreases), declining-rate blocks (where the rate decreases as consumption increases), or flat-rate blocks. In time-of-use rate schedules, the unit price of energy varies depending on the time of day. For this study, stepped rate schedules were used for all cases.

The gas rate structure uses stepped energy rates. The unit-price cost for all gas consumption is defined within a step or block. Rates are entered for both summer and winter, and the gas rate season information is introduced by defining which months of the year pertain to the summer and winter rates, respectively.

2.2.4. Building Selection and Configuration

DesiCalc™ has the capacity to analyze eleven different building types. These eleven types are: hospital, large hotel, small hotel, ice arena, nursing home, quick-service restaurant, retail store, school, supermarket, theater, and refrigerated warehouse. The eight building types used in this study are large hotel, retail store, school, hospital, nursing home, refrigerated warehouse, quick-serve restaurant, and supermarket. These choices were made on the basis of greatest current market potential for desiccants. Ice arenas and theaters, although ideal candidates for desiccant equipment, were not included because they represent only a small portion of the potential market. The following descriptions of the eight building types considered in this study are taken from the *DesiCalc™ 1.1 User's Manual* (GRI, 1998):

- Large Hotel - Six-story building with lobby and meeting rooms on first floor, guestrooms on upper floors. Desiccant system serves only ventilation air for the guestrooms (70% of total floor area). Maximum allowable glazing percentage is 80%.
- Retail Store - Single-story slab on grade construction, typical of a national-chain discount department store. Maximum allowable glazing percentage is 28%.
- School - Single-story slab on grade construction, typical of a suburban secondary school. Desiccant system serves classrooms and library only (73% of total floor area). Assumed to operate on summer schedule during Jun-Aug, 8 am-12 noon, M-F, kitchen closed. Because of the allocation of glazing to classrooms and the remaining portions of the school, the maximum fraction of glazing varies with the overall size of the school.

- Supermarket - Single-story slab on grade construction, typical of a large 24-hr supermarket. Maximum allowable glazing percentage is 4%. Desiccant system serves only the core sales and checkout area (67% of total floor area, everything except the bakery, office, stock room and equipment room).
- Hospital - 6-story hospital. Desiccant system serves only the surgical suites (4.4% of total floor area). Maximum allowable glazing percentage is 80%.
- Nursing home - Single-story slab on grade construction with attic. Desiccant system serves only ventilation air for the patient wings (56% of total floor area). Maximum allowable glazing percentage is 43%.
- Refrigerated Warehouse - Single-story slab on grade construction, with refrigerated storage for meats, deli, produce, and freezer, loading dock and small office. Glazing is not user controllable (fixed amount of glazing is modeled for office only). Desiccant system serves only the loading dock (8% of total floor area).
- Quick-Serve Restaurant – Single-story slab on grade construction, typical of a national-chain hamburger restaurant. Maximum allowable glazing percentage is 65%.

The building configuration, loads, and comfort control setpoints for each of the eight building types are shown in Table 2.3. This information includes total floor area, glazing area, and room configurations and was taken directly from the DesiCalc™ manual. User configurable information includes total floor area, glazing fraction, internal loads, ventilation and infiltration, and comfort control setpoints.

Table 2.3 Building Configuration and Load Specification

Building	Configuration	Load
Retail Store	Retail Store; single-story slab on grade construction typical of a larger department store with 10 % wall glazing. Humidity control air treatment applies to 60000 sf floor area. Internal loads and ventilation values apply to humidity controlled areas. Building total floor area is 60000 sf. Comfort control settings: Cooling temp/setback = 75/80 F, Heating temp/setback = 72/60 F, 60% RH	Occupancy: 100 sf/person Lighting: 2.3 Watt/sf Other Electric: 0.25 Watt/sf Infiltration: 0.3 air exch./hr. Ventilation: 0.3 cfm/sf
Large Hotel	Large Hotel; 6-story building with 40 % wall glazing. Lobby and meeting rooms on first floor. Guest rooms on upper floors. Humidity control air treatment applies to 210000 sf of guest rooms. Internal loads and ventilation values apply to humidity controlled areas. Building total floor area is 300000 sf. Comfort control settings: Cooling temp/setback = 75/80 F, Heating temp/setback = 72/65 F, 60% RH	Occupancy: 100 sf/person Lighting: 2.3 Watt/sf Other Electric: 0.25 Watt/sf Infiltration: 0.3 air exch./hr. Ventilation: 65 cfm/room
School	School; single-story slab on grade construction typical of suburban secondary school with 20 % wall glazing. Humidity control air treatment applies to 120450 sf of classrooms and library. Internal loads and ventilation values apply to humidity controlled areas. Building total floor area is 165000 sf. Comfort control settings: Cooling temp setback = 75/85 F, Heating temp/setback = 72/65 F, 60% RH	Occupancy: 25 sf/person Lighting: 2.2 Watt/sf Other Electric: 0.5 Watt/sf Infiltration: 0.5 air exch./hr. Ventilation: 15 cfm/pers.

Hospital	Hospital; 6-story building with 15 % wall glazing. Humidity control air treatment applies to 22000 sf of surgical suites. Internal loads and ventilation values apply to humidity controlled areas. Building total floor area is 500000 sf. Comfort control settings: Cooling temp/setback = 65/75 F, Heating temp/setback = 65/65 F, 50% RH	Occupancy: 275.0 sf/person Lighting: 4.00 Watt/sf Other Electric: 3.00Watt/sf Infiltration: 0.00 air exch./hr Ventilation: 100%
Nursing Home	Nursing Home; 1-story slab on grade construction with attic and 25 % wall glazing. Humidity control air treatment applies to 25200 sf of patient rooms wings. Internal loads and ventilation values apply to humidity controlled areas. Building total floor area is 45000 sf. Comfort control settings: Cooling temp/setback = 75/75 F, Heating temp/setback = 74/74 F, 60% RH	Occupancy: 175.0 sf/person Lighting: 2.00 Watt/sf Other Electric: 0.20 Watt/sf Infiltration: 0.75 air exch./hr Ventilation: 25.00 cfm/pers
Refrigerated Warehouse	Refrigerated Warehouse; Single-story slab on grade construction, with refrigerated storage for meats, deli, produce, and freezer, loading dock and small office. Glazing is not user controllable (fixed amount of glazing is modeled for office only). Humidity control air treatment applies to 4000 sf floor area of loading dock. Internal loads and ventilation values apply to humidity controlled areas. Building total floor area is 50000 sf. Comfort control settings: Cooling temp/setback = 35/35 F, Heating temp/setback = 33/33 F, 80% RH	Occupancy: 1,000 sf/person Lighting: 1.50 Watt/sf Other Electric: 0.00 Watt/sf Infiltration: 2.00 air exch./hr Ventilation: 0.12 cfm/pers
Supermarket	Supermarket; single-story slab on grade construction typical of 24-hr supermarket with 3 % wall glazing. Humidity control air treatment applies to 21440 sf of core sales and checkout area. Internal loads and ventilation values apply to humidity controlled areas. Building total floor area is 32000 sf. Comfort control settings: Cooling temp/setback = 72/72 F, Heating temp/setback = 70/70 F, 55% RH	Occupancy: 125 sf/person Lighting: 1.75 Watt/sf Other Electric: 0.15 Watt/sf Infiltration: 0.75 air exch./hr. Ventilation: 15 cfm/pers.
Quick-serve Restaurant	Quick-serve restaurant; 1-story slab on grade construction based on standard design of a national chain with 30 % wall glazing. Humidity control air treatment applies to 2000 sf floor area. Internal loads and ventilation values apply to humidity controlled areas. Building total floor area is 2000 sf. Comfort control settings: Cooling temp/setback = 75/99 F, Heating temp/setback = 70/65 F, 60% RH	Occupancy: 35.0 sf/person Lighting: 4.00 Watt/sf Other Electric: 8.00 Watt/sf Infiltration: 2.00 air exch./hr. Ventilation: 1.60 cfm/sf.

DesiCalc™ allows comfort control settings for the baseline system and the desiccant enhanced system to be defined independently. Although most baseline systems installed today do not incorporate a humidistat, operating cost comparisons are meaningful only if the comfort control settings for the baseline system and the desiccant-enhanced system are identical. Therefore, in this study, comfort control setpoints (cooling temperature, heating temperature, and relative humidity) for the baseline and desiccant-enhanced equipment are defined identically. Specifying a relative humidity setpoint for the baseline equipment implicitly defines reheat as the humidity control mechanism for the baseline system. Other humidity control options for the baseline system can be explicitly defined using equipment selection options as discussed in the next section.

2.2.5. Equipment Selection

DesiCalc™ can model three air conditioning equipment options. The following is a summary of the description of these options taken from the DesiCalc™ User's Manual (1998):

1. An air conditioning system with a rooftop unit with direct expansion (DX) cooling coil, air-cooled condenser, and electric or gas heating coil can be selected. Temperature (dry-bulb) or enthalpy (wet-bulb) economizer, and any one of the following: sensible or enthalpy heat recovery, dedicated outside air DX unit (100% outside air), dual path, and wrap-around heat pipe are available options of the system.
2. An air conditioning system consisting of a packaged terminal unit, an exhaust air unit, and a make-up air unit with direct expansion (DX) cooling coil, air-cooled condenser, and electric or gas heating coil can be selected for the large hotel, small hotel/motel, nursing home, and school applications. A separate make-up air unit supplies make-up for air exhausted from the space either directly to the conditioned space or indirectly from an adjacent corridor. Temperature (dry-bulb) or enthalpy (wet-bulb) economizer is an available option. Additional options for the make-up air unit include: sensible or enthalpy heat recovery, dedicated outside air DX unit (100% outside air), dual path, and wrap-around heat pipe.
3. An air conditioning system with a central chiller plant, rooftop unit with chilled water cooling coil, air or water cooled condenser, and electric or gas heating coil. Available system options are temperature (dry-bulb) or enthalpy (wet-bulb) economizer, and any one of the following: sensible or enthalpy heat recovery, dedicated outside air DX unit (100% outside air), dual path, and wrap-around heat pipe.

Table 2.4 gives details of the HVAC equipment configurations selected for the eight building types. The description of the equipment was taken directly from the DesiCalc™ user input screen. Rooftop units were selected for three of the eight building types. For the other cases, rooftop units were not an option and central plant chilled water systems were selected. Gas heating was specified for both the conventional and desiccant-enhanced systems. The reheat energy source for the conventional system is set by the program to be the same as the heating energy source. Neither evaporative coolers nor humidifiers were used in either the conventional or the desiccant-enhanced systems. The desiccant-enhanced systems included heat recovery wheels with 70% effectiveness. Heat recovery wheels are generally standard, integral components of commercially available gas-fired rotary desiccant dehumidifiers because they perform a function which is natural and beneficial to the desiccant dehumidification process. The sensible recovery wheel exchanges heat between two adjacent, counterflow airstreams which are already flowing through the dehumidifier unit: the incoming regeneration air stream (which must be heated anyway) and the exiting process air stream (which must be cooled anyway). The result is lower post-cooling requirements of the dehumidified process air stream and lower heat input required to regenerate the desiccant material. Conversely, heat recovery components are generally not integral components of conventional air conditioning equipment. Such components are usually separate pieces of equipment known as heat recovery ventilators (HRV's for sensible recovery) or energy recovery ventilators (ERV's for sensible and latent recovery), and oftentimes additional fans and considerable ductwork are required to obtain a balanced flow of exhaust air and makeup air to the recovery unit. Since such components are, with few exceptions, aftermarket add-ons rather than integral components of conventional air-conditioning equipment, heat recovery components were not specified for the conventional baseline equipment. Similarly, the wrap-around heat pipe option was not considered in this

study because it also is an add-on component rather than a standard option in most conventional equipment configurations.

Table 2.4 Equipment Selection

Building	Baseline	Desiccant
Retail Store	Constant volume 8.9 EER packaged DX rooftop unit with temperature economizer. System does not use heat recovery. System equipped with gas source heating. Humidifier not used.	Constant volume 8.9 EER packaged DX rooftop unit with temperature economizer. System equipped with gas source heating. Outside air treated by a gas-fired desiccant dehumidifier with 70 % eff. heat exch. (downstream sensible exchange with relief air heat recovery). Dehumidifier configured without evap. cooler option. Humidifier not used.
Large Hotel	Const. vol. chilled water system with 0.68 kW/ton electric chiller (water cooled) without economizer. System does not use heat recovery. System equipped with gas source heating. Humidifier not used.	Constant volume chilled water system with 0.68 kW/ton electric chiller (water cooled) without economizer. System equipped with gas source heating. Outside air treated by gas-fired desiccant dehumidifier with 70 % eff. heat exch. (downstream sensible exchange with relief air heat recovery). Dehumidifier configured without evap. cooler option. Humidifier not used.
School	Constant volume 8.9 EER packaged DX rooftop unit with temperature economizer. System does not use heat recovery. System equipped with gas source heating. Humidifier not used.	Constant volume 8.9 EER packaged DX rooftop unit with temperature economizer. System equipped with gas source heating. Outside air treated by a gas-fired desiccant dehumidifier with 70 % eff. heat exch. (downstream sensible exchange with relief air heat recovery). Dehumidifier configured without evap. cooler option. Humidifier not used.
Super-market	Constant volume 8.9 EER packaged DX rooftop unit with temperature economizer. System does not use heat recovery. Condenser heat utilized for heating/reheating. System equipped with gas source heating. Humidifier not used.	Constant volume 8.9 EER packaged DX rooftop unit with temperature economizer. Condenser heat utilized for heating/reheating. System equipped with gas source heating. Outside air treated by a gas-fired desiccant dehumidifier with 70 % eff. heat exch. (downstream sensible exchange with outside air heat recovery). Dehumidifier configured without evap. cooler option. Humidifier not used.
Hospital	Const. vol. chilled water system with 0.68 kW/ton electric chiller (water cooled) without economizer. System does not use heat recovery. System equipped with gas source heating. Humidifier not used.	Constant volume chilled water system with 0.68 kW/ton electric chiller (water cooled) without economizer. System equipped with gas source heating. Outside air treated by gas-fired desiccant dehumidifier with 70 % eff. heat exch. (downstream sensible exchange with relief air heat recovery). Dehumidifier configured without evap. cooler option. Humidifier not used.
Nursing Home	Const. vol. chilled water system with 0.68 kW/ton electric chiller (water cooled) without economizer. System does not use heat recovery. System equipped with gas source heating. Humidifier not used.	Constant volume chilled water system with 0.68 kW/ton electric chiller (water cooled) without economizer. System equipped with gas source heating. Outside air treated by gas-fired desiccant dehumidifier with 70 % eff. heat exch. (downstream sensible exchange with relief air heat recovery). Dehumidifier configured without evap. cooler option. Humidifier not used.

Refrigerated Warehouse	Const. vol. chilled water system with 0.93 kW/ton electric chiller (water cooled) without economizer. System does not use heat recovery. System equipped with gas source heating. Humidifier not used.	Constant volume chilled water system with 0.93 kW/ton electric chiller (water cooled) without economizer. System equipped with gas source heating. Outside air treated by gas-fired desiccant dehumidifier with 70 % eff. heat exch. (downstream sensible exchange with outside air heat recovery). Dehumidifier configured without evap. cooler option. Humidifier not used.
Quick-serve Restaurant	Constant volume 8.9 EER packaged DX rooftop unit with temperature economizer. System does not use heat recovery. System equipped with gas source heating. Humidifier not used.	Constant volume 8.9 EER packaged DX rooftop unit with temperature economizer. System equipped with gas source heating. Outside air treated by a gas-fired desiccant dehumidifier with 70 % eff. heat exch. (downstream sensible exchange with outside air heat recovery). Dehumidifier configured without evap. cooler option. Humidifier not used.

2.2.6. Simulation Runs

Simulations were run for the forty cities and eight building types described earlier in this section. Once the DesiCalc™ runs were completed for the 320 cases (40 cities x 8 building types), the results were compiled and analyzed. Details of the analysis and conclusions are explored in the following section.

2.3 TOTAL ANNUAL ENERGY COST RATIO

The main parameter used in this study is the total annual energy cost ratio, defined as the ratio of the total annual energy cost of the conventional system to the total annual energy cost of the desiccant-enhanced system. Defined in this manner, ratios greater than unity indicate that the use of desiccant-enhanced systems result in energy cost savings. Conversely, ratios less than unity indicate that desiccant-enhanced systems result in an energy cost increase.

Figures 2.B.1 to 2.B.8 in Appendix 2.B present results of the simulation runs in a graphical form for the forty cities. Each figure represents a different building type. The total (gas and electricity) annual energy cost ratio between the conventional system and the desiccant system for each of the 320 cases is plotted. The locations have been sorted in order of increasing cost ratio. Most of the ratios are larger than unity for the eight building types, indicating that the desiccant-enhanced system is favored for nearly all the cities included in this study.

Table 2.B.1 in Appendix 2.B shows the results (total annual energy cost ratios) of the simulation runs for the forty cities and eight building types. For brevity in comparisons, the ratios of Table 2.B.1 can be described with percentages relative to unity. For example, if the ratio is larger than unity, as in the case of a hospital in Albany, NY (1.030), the percentage above 100% (3.0%, in this case) indicates that the desiccant-enhanced systems would be slightly favored in this application. If the ratio is lower than unity, as in the case of supermarket in Cleveland, OH (0.994), the percentage (-0.6%) is slightly in favor of conventional systems. Negative numbers indicate that the percentage is in favor of conventional systems. Table 2.5 shows the four highest and the four lowest values of these percentages for each building type and the corresponding city. The highest values are found in the cases of retail stores for the cities of Pittsburgh, PA (66.2%), Huntington, WV (59.7%), and Cleveland, OH (55.7%), and schools for

the cities of Miami, FL (46.1%) and Tampa, FL (45.2%). Those are the cases where desiccant-enhanced systems show the greatest relative advantage in energy cost savings. On the other hand, the lowest ratios are found for Fort Worth, TX (-40.7%), Huntington, WV (-34.1%), and Pittsburgh, PA (-25%) in the case of refrigerated warehouses. All these cases favor conventional systems. Fort Worth, TX was not expected to be included in the group of cities with the lowest ratios, but the high cost of the gas in this city affected the results.

The cities that show a persistent high percentage in favor of desiccant-enhanced systems are Miami, FL, which appears in six building types, Tampa, FL, which is included in five building types, and New Orleans, LA, which appears in four building types. All these cities have humid and hot weather, which should favor the use of desiccant systems. However, some cities with hot and humid weather such as Tallahassee, FL, Fort Worth, TX, and Houston, TX appear in the group of cities with lower ratios. The cities that appear more frequently with the lowest ratios are San Francisco, CA, Fort Worth, TX, Seattle, WA, and Portland, OR. Some cities such as Pittsburgh, PA, Huntington, WV, Fargo, ND, and Houston, TX are found in both the highest and the lowest ratios for different building types. These inconsistencies in trends regarding geographic location (weather) indicate that local variations in utility rates can have a greater effect than climate on the economic favorability of gas-fired desiccant systems.

Table 2.5 Highest and Lowest Percentages for Total Annual Energy Cost

Building	Higher Ratios		Lower Ratios	
	City	%	City	%
Hospital	Miami, FL	14.5	Huntington, WV	2.4
	Tampa, FL	12.8	Chicago, IL	2.2
	Little Rock, AR	11.5	Seattle, WA	1.9
	New Orleans, LA	10.8	Fort Worth, TX	-0.3
Large Hotel	Cleveland, OH	27.7	Tallahassee, FL	5.5
	Pittsburgh, PA	25.8	Albany, NY	4.8
	Fargo, ND	22.5	San Francisco, CA	4.1
	Huntington, WV	19.5	Houston, TX	1.9
Nursing Home	Pittsburgh, PA	16.8	Burlington, VT	3.5
	Fargo, ND	15.5	Tallahassee, FL	3.2
	Cleveland, OH	14.9	Fort Worth, TX	1.6
	Miami, FL	13.7	Houston, TX	0.0
Quick-serve restaurant	Miami, FL	19.2	Fargo, ND	0.8
	Tampa, FL	18.5	Portland, OR	0.6
	Charleston, SC	16.2	Seattle, WA	-0.6
	New Orleans, LA	14.4	San Francisco, CA	-0.8
Retail Store	Pittsburgh, PA	66.2	Seattle, WA	13.8
	Huntington, WV	59.7	Portland, OR	7.7
	Cleveland, OH	55.7	Los Angeles, CA	5.0
	Fargo, ND	45.3	San Francisco, CA	-0.4

School	Miami, FL	46.1	Albany, NY	12.2
	Tampa, FL	45.2	Los Angeles, CA	8.8
	Charleston, SC	44.1	Portland, OR	5.9
	Houston, TX	40.9	San Francisco, CA	4.4
Supermarket	Miami, FL	11.4	Omaha, NE	-5.8
	Tampa, FL	10.8	Fort Worth, TX	-12.5
	Little Rock, AR	8.8	Fargo, ND	-14.4
	New Orleans, LA	8.8	Jackson, MS	-20.1
Refrigerated Warehouse	Miami, FL	14.7	Norfolk, VA	-13.6
	Tampa, FL	12.9	Pittsburgh, PA	-25.1
	Little Rock, AR	10.2	Huntington, WV	-34.1
	New Orleans, LA	10.1	Fort Worth, TX	-40.7

Figure 2.2 shows the averages of the total annual cost ratio of all forty cities for each building. This parameter helps to focus on the effect of building type on energy cost while ignoring the effect of climate.

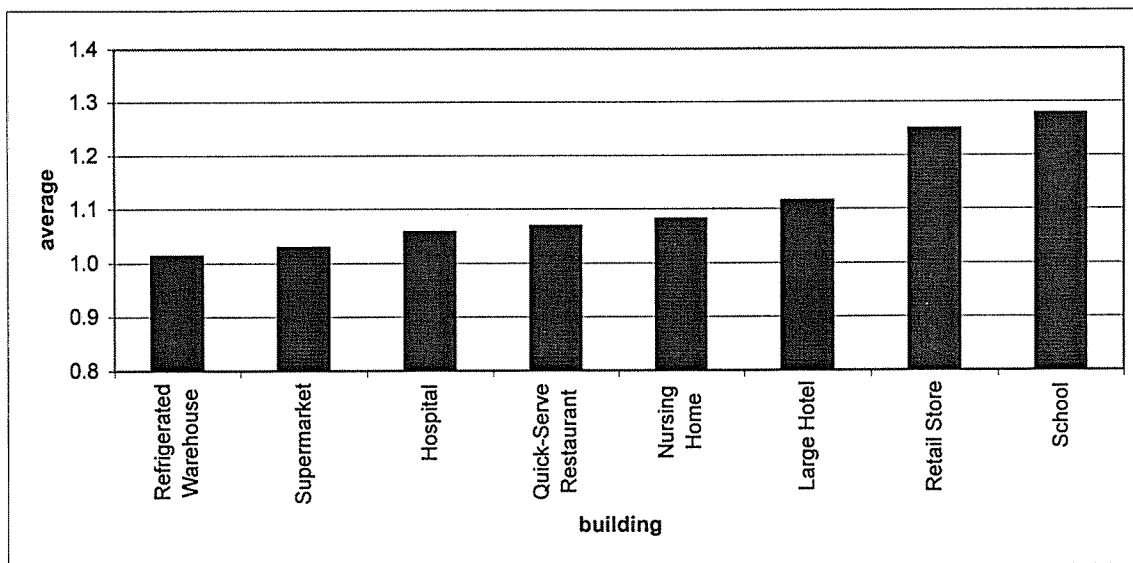


Figure 2.2 Averages of the Total Annual Cost Ratio

All the values are greater than unity, but in the cases of refrigerated warehouse and supermarket, the cost savings due to the use of desiccant system are very low compared with the 28% and 25% savings in the cases of school and retail store, respectively.

The performance of the buildings with the lower ratios can be attributed to limitations imposed by DesiCalc™ on the particular building type. In the case of the refrigerated warehouse, for example, the desiccant system serves only the loading dock (representing only 8% of the total floor area), and the heat recovery option is limited to outside air heat recovery rather than relief air heat recovery. Similarly, heat recovery options for the supermarket are limited to outside air

heat recovery only, and the desiccant system is limited to serving only 67% of the total floor area. The hospital desiccant system serves only the surgical suites (4.4% of the total floor area) and is not used to advantage in other areas of high latent loads. Heat recovery options for the quick-serve restaurant are limited to outside air heat recovery only. In the nursing home, the desiccant system serves only ventilation air for patient wings (56% of the floor area), neglecting other areas of high latent loads. In the large hotel, the desiccant system serves only ventilation air for the guest rooms (70% of total floor area) and does not take advantage of other high latent load areas such as lobbies, conference rooms, and restaurants. For the retail store, the building type with the second highest ratio, the desiccant system serves the entire area and is allowed to take advantage of relief air heat recovery. For the school, which has the highest ratio, although the desiccant system serves only 73% of the floor area (classrooms and library), these areas, compared to the remaining 27% of floor area, have a very high occupant density with correspondingly high ventilation loads for which the desiccant system is used advantageously. The school desiccant system also benefits from using relief air heat recovery.

The above limitations imposed by the DesiCalc™ program are not arbitrarily imposed by DesiCalc™, but rather, are practical limitations imposed by the building itself. For example, the DesiCalc™ Manual points out in its description of the outside air heat recovery option,

This type of system is used in applications where significant amounts of exhaust air cause the relief air volume to be insufficient. For example, this type of system might be applied in a quick-service restaurant, because the outdoor air volumes are based on balancing the kitchen exhaust air volumes, and due to grease contamination, the exhaust air cannot be used for heat exchange.

Pointing out these limitations, however, helps alert the designer of potential desiccant-enhanced air-conditioning systems to conditions within certain building types which limit the effectiveness of desiccant systems. Knowing these limitations, in certain situations, allows the designer to eliminate or overcome these situations. Consider for example, the quick-service restaurant example cited above. By using a short-circuit type kitchen exhaust hood (one in which roughly 80% of the required makeup air is supplied directly into the hood) and/or by carefully introducing the hood makeup air in such a manner that it is quickly captured by the hood, there is no need to condition the hood makeup air. Since the hood exhaust is balanced by other means, the desiccant unit can utilize the relief air heat recovery configuration to treat only the occupant ventilation air.

2.4 ASHRAE DESIGN TEMPERATURES AND LATITUDE

This section examines the effect of ASHRAE extreme design temperature and latitude. The ASHRAE *Handbook of Fundamentals* (1997) lists extreme conditions of dry bulb temperature, wet bulb temperature, and dew point. It also tabulates an extreme (cold) dry bulb temperature for purposes of heating. These temperatures are listed by annual hourly frequency of occurrence. For instance, a 1% dry bulb specification of 90°F means that in that particular location, the temperature typically will exceed 90°F for 1% of the hours (approximately 88 in a year). This specification is useful for sizing cooling systems. A similar specification is useful for sizing heating systems. This specification is called "heating temperature" and the local temperature is typically lower than the specified temperature for only about 88 hours in a year. The two dry bulb temperatures reflect extremes in the hottest and the coldest sensible

temperatures. The *Handbook* describes extremes in wet bulb temperatures as representative of extremes of "total sensible plus latent heat of outdoor air." The extremes in dew point temperature are representative of peaks in the humidity.

The extreme design temperature specifications represent only the extreme conditions and do not represent the weather at a particular location. But these specifications can be an indicator of the local climate and might be used as one preliminary guide for the potential of desiccant-enhanced systems for a particular location. This section explores that possibility.

The eight figures in Appendix 2.C present the total cost ratio as a function of the 1% dry bulb temperature for the forty cities. Each figure represents one building type. Even though the data are dispersed, the best fit line through the data tends to average out the effects of local utility rates and give some indication of the effect of dry bulb temperature. For the cases of retail store, quick-serve restaurant, school, and hospital there is an increase in cost ratio with increasing 1% dry bulb temperature. For the remaining four, however, there is a decrease in cost ratio with increasing 1% dry bulb temperature.

Appendix 2.D shows similar information to Appendix 2.C, but instead of 1% dry bulb temperature, 1% wet bulb temperature is plotted. In this case, as in the one before, there is an increase in cost ratio with increasing 1% wet bulb temperature for retail store, quick-serve restaurant, hospital, and school. The rest of the building types show no significant correlation with 1% wet bulb temperature.

Appendix 2.E is analogous to Appendices 2.C and 2.D, but the 1% dew point temperatures are shown. Again, the cases of retail store, quick-serve restaurant, hospital, and school show an increase in the cost ratio when the dew point temperature is increased. The remainder show no significant correlation.

Appendix 2.F represents the effect of latitude on the annual cost ratio. For the hospital, quick-serve restaurant, school, and supermarket, the cost ratio decreases with increasing latitude. For the large hotel, nursing home, and retail store, the cost ratio increases with increasing latitude. The refrigerated warehouse shows no significant trend.

Appendix 2.G shows the annual cost ratio as a function of the heating temperature. Cost ratios for the hospital, quick-serve restaurant, school, and supermarket increase with increasing heating temperature, while for the large hotel, nursing home, and retail store, cost ratios decrease. Again, the refrigerated warehouse shows no significant trend.

The intention of this analysis was to identify parameters that may serve as indicators or predictors for conditions that are favorable for desiccant-enhanced systems. Dry bulb, wet bulb, and dew point extreme design temperatures appear to function as indicators for retail stores, schools, quick-serve restaurants and hospitals, but there is no obvious common factor among these four building types to justify the apparent correlation. No significant trends could be identified for the four other building types or for other parameters. According to these results, general rules for indicators cannot be established using these parameters.

2.5 PHOENIX, AZ AND SALT LAKE CITY, UT

Gas-fired desiccant equipment is typically integrated into a commercial air conditioning system to increase the latent capacity (lower the sensible heat ratio) of the system. Thus, intuition would expect desiccant-enhanced systems to be favored only in humid climates (either hot and humid or cool and humid). However, the previous two sections indicate that building type and local variations in utility rates have a greater effect than climate on the economic favorability of gas-fired desiccant systems. No significant trends relating climate indicators to the economic favorability of gas-fired desiccant systems were evident. Moreover, desiccant-enhanced systems were favored in nearly all cities included in this study. The arid southwest and mountain west states were deliberately omitted from these forty cities (Table 2.1 and Figure 2.1) since humidity control is of much less interest in those areas. In view of the results of the previous two sections, two additional cities (from the southwest and mountain west regions of the United States) were selected for analysis.

Salt Lake City, UT is located at a latitude similar to Philadelphia, PA, but at an elevation of around 5000 feet above sea level. Phoenix, AZ is close to Atlanta, GA in latitude and is close to sea level in elevation. Both cities are characterized by relatively arid climates.

Table 2.6 summarizes the results for Phoenix, AZ and Salt Lake City, UT in terms of the total annual energy cost ratio. This is the same parameter presented in Table 2.B.1 for the main data set. Comparison with Table 2.B.1 and Table 2.5 reveals that the cost ratios for these two cities tend to fall toward the low end of the spectrum of 42 cities, but are not necessarily the lowest. In fact, only the retail stores and schools for Phoenix and the quick-serve restaurants for Salt Lake City would have been among the four lowest cost ratios as presented in Table 2.5. In nearly all cases, the cost ratio remains greater than unity, indicating that the desiccant-enhanced system would provide lower operational costs.

Table 2.6 Total Annual Energy Cost Ratio for Phoenix, AZ and Salt Lake City, UT

Building	Phoenix, AZ	Salt Lake City, UT
Hospital	1.0664	1.0556
Large Hotel	1.0784	1.1551
Nursing Home	1.0403	1.1182
Quick-Serve Restaurant	1.0133	1.0007
Retail Store	1.1121	1.2922
School	1.1055	1.2024
Supermarket	1.0282	1.0307
Refrigerated Warehouse	0.9926	1.0273

These results reaffirm the conclusion from Sections 2.3 and 2.4 that climate is not the main factor in determining the economic favorability of desiccant-enhanced systems. Yet it is certainly counter-intuitive that desiccant-enhanced systems are favored even in the very arid climates of the western United States. There are two possible reasons:

1. Internal latent loads are relatively constant year round. While the desiccant dehumidifier is in operation, the sensible load dumped into the space (which is inherent in the desiccant dehumidification process) serves as “free heat” during the heating season.
2. The dehumidifier’s sensible heat recovery wheel, which normally functions to simultaneously preheat the regeneration air and post cool the dehumidified process air, can also function as a heat recovery ventilator (HRV) when configured to use relief air heat recovery. Similarly, the desiccant wheel can function as an energy recovery ventilator (ERV) or enthalpy wheel if configured to use relief air for the regeneration airstream.

The fact that the first reason is valid is evident upon examination of the “Gas Energy Consumption by End Use” page of a typical detailed DesiCalc™ report (Figure 2.A.2). Space heating requirements are significantly lower for the alternative (desiccant-enhanced) system than for the baseline system.

The second reason is valid only if the dehumidifier’s control system allows the sensible heat recovery wheel to operate as a heat recovery ventilator or allows the desiccant wheel to operate as an energy recovery ventilator when dehumidification is not called for by the humidistat. Conversations with Mike Witte, technical support for DesiCalc™ (877-DESICALC), confirm that DesiCalc™ allows the sensible heat recovery wheel to function as a heat recovery ventilator whenever the desiccant unit is not actively dehumidifying. This function alone could result in significant energy savings compared with the conventional system without heat recovery and could be the reason that desiccant-enhanced systems were overwhelmingly favored in nearly all cities included in this study. If such were the case, the obvious question would be, “Why not use an HRV or ERV rather than a gas-fired desiccant dehumidifier?” To answer this question, the next section explores the effects of including a heat recovery option in the conventional system.

2.6 ALTERNATIVE CONFIGURATION

To explore the effects of including a heat recovery option in the conventional system, an alternative configuration analysis was made using the large hotel as the building type (representative of the average annual cost ratio for all building types, Figure 2.2) and the nineteen cities listed in Table 2.7.

Table 2.7 Cities for the Alternative Configuration

1	Atlanta, GA	11	Nashville, TN
2	Baltimore, MD	12	New Orleans, LA
3	Charleston, SC	13	New York, NY
4	Detroit, MI	14	Raleigh, NC
5	Fort Worth, TX	15	Rochester, NY
6	Honolulu, HI	16	San Francisco, CA
7	Huntington, WV	17	Seattle, WA
8	Jackson, MS	18	St. Louis, MO
9	Miami, FL	19	Tallahassee, FL
10	Minneapolis, MN		

Table 2.8 presents descriptions of the equipment for the alternative configurations. These descriptions were taken directly from the DesiCalc™ manual. The two additional configurations examined were a conventional system with heat recovery and a desiccant-enhanced system without heat recovery.

Table 2.8 Equipment Selection for Alternative Configuration

Building	Baseline	desiccant
Large Hotel	Const. vol. chilled water system with 0.68 kW/ton electric chiller (water cooled) without economizer. System equipped with 70 % effective sensible heat heat recovery. System equipped with gas source heating. Humidifier not used. Default Config.	Constant volume chilled water system with 0.68 kW/ton electric chiller (water cooled) without economizer. System equipped with gas source heating. Outside air treated by gas-fired desiccant dehumidifier with 0 % eff. heat exch. (without heat recovery). Dehumidifier configured without evap. cooler option. Humidifier not used. Default Config.

Table 2.9 summarizes the results of the total annual energy cost for the four cases: (1) conventional system with heat recovery, (2) desiccant system with heat recovery, (3) conventional system without heat recovery, and (4) desiccant systems without heat recovery.

Table 2.9 Total Annual Energy Cost (10³\$) Large Hotel

City	w/ heat recovery		w/o heat recovery	
	conventional	desiccant	conventional	desiccant
Atlanta, GA	469	439	486	469
Baltimore, MD	348	333	362	339
Charleston, SC	502	473	523	519
Detroit, MI	553	531	584	579
Fort Worth, TX	892	967	1024	1192
Honolulu, HI	576	543	579	577
Huntington, WV	1140	1174	1403	1500
Jackson, MS	354	338	369	371
Miami, FL	12719	10960	12858	11697
Minneapolis, MN	342	331	379	373
Nashville, TN	374	363	395	402
New Orleans, LA	258	236	262	252
New York, NY	440	420	466	455
Raleigh, NC	375	352	390	385
Rochester, NY	531	513	563	550
San Francisco, CA	611	602	626	616
Seattle, WA	189	187	206	204
St. Louis, MO	365	342	393	382
Tallahassee, FL	381	379	400	425

In general, the most expensive operating-cost configuration would be, in descending order: (1) a conventional system without heat recovery, (2) a desiccant system without heat

recovery, (3) a conventional system with heat recovery, and (4) a desiccant system with heat recovery.

For ease of comparison, the data of Table 2.9 are presented in Figure 2.3 in terms of the familiar total annual cost ratio used in Section 2.3. The denominator in each case is the total annual operating cost of the desiccant system with heat recovery, and the ratio is calculated for each of the other three configurations. The black solid bar represents the same numbers shown in Figure 2.B.2; i.e., the ratio of the conventional system without heat recovery to the desiccant system with heat recovery. Nearly all ratios in Figure 2.3 are greater than unity, indicating that the desiccant system with heat recovery is generally the least expensive option in terms of operating costs. The only two cities where the conventional system with heat recovery is less expensive than the desiccant system with heat recovery are Fort Worth, TX and Huntington, WV. The conventional system without heat recovery is usually the most expensive configuration. However, in a few cities (Tallahassee, Fort Worth, Nashville, Jackson, and Huntington) the desiccant system without heat recovery is the most expensive.

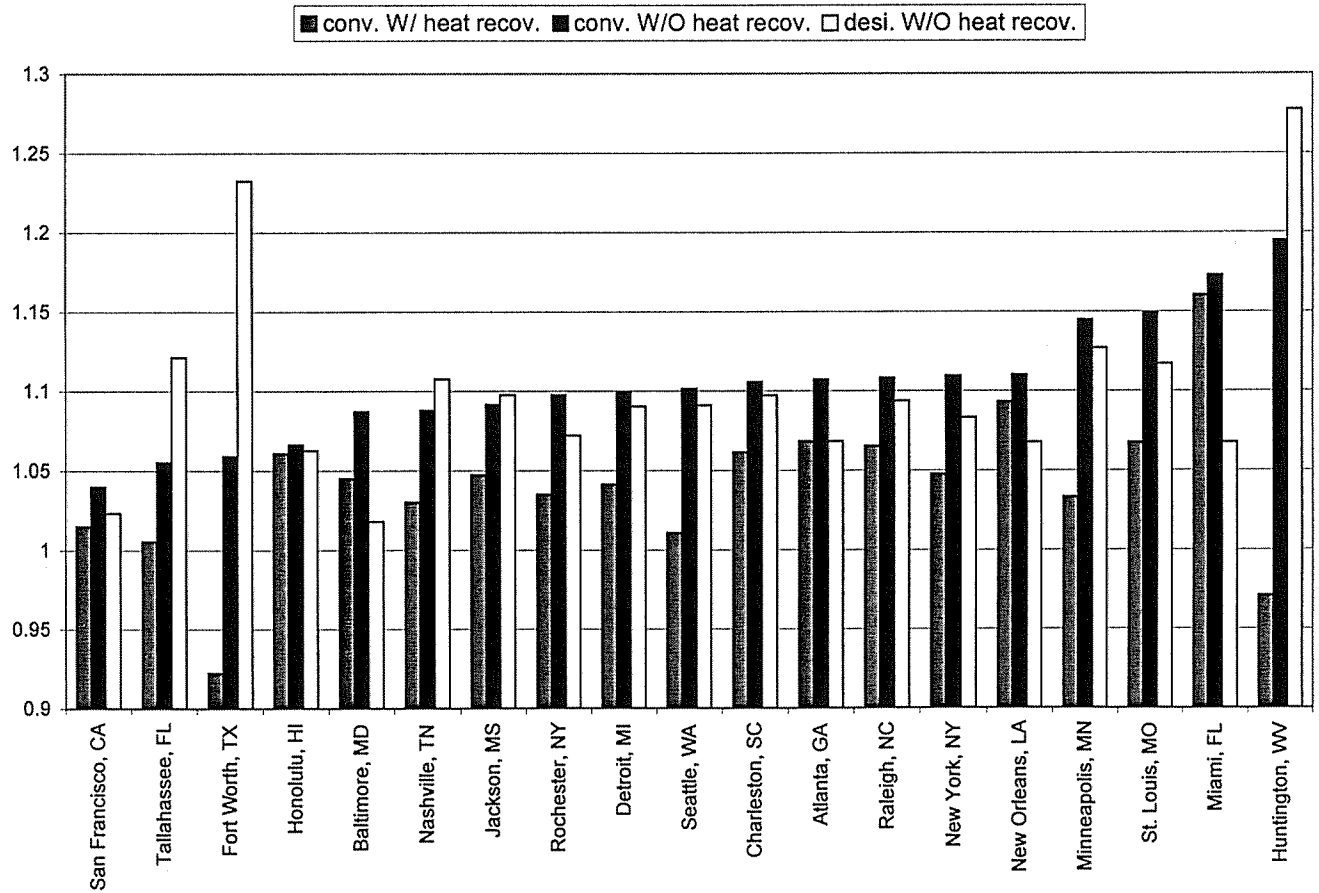


Figure 2.3 Cost Ratio Comparisons

These results confirm that the economic favorability of desiccant-enhanced systems was not the result of an unfair comparison between the desiccant-enhanced system with heat recovery and the baseline system without heat recovery. The desiccant-enhanced system with heat recovery generally results in savings over the conventional system even when the conventional system utilizes heat recovery. Additionally, the results confirm the earlier statement that sensible heat recovery should be considered an integral component of gas-fired desiccant dehumidifiers used in air-conditioning applications. The desiccant system without heat recovery is always more expensive to operate than the desiccant system with heat recovery and sometimes more expensive than the conventional system without heat recovery. When energy savings are a concern, a desiccant system without sensible heat recovery should not be considered an option.

2.7 SUMMARY AND CONCLUSIONS

In this study, energy costs for conventional HVAC systems and desiccant-enhanced systems were compared as a function of location, building type, and energy rates. The total annual energy cost ratio was the parameter used to make this comparison and was defined as the ratio of the total annual energy cost of the conventional system to the total annual energy cost of the desiccant-enhanced system. Simulation runs were completed for forty cities and eight building types. The desiccant screening tool DesiCalc™ was used to generate all annual cost information for the comparisons.

The overwhelming majority of the cost ratios for the 320 cases initially considered (40 cities x 8 building types) were greater than unity, which indicates that desiccant-enhanced systems have a clear advantage over conventional systems, regardless of geographic location. Inconsistencies in trends regarding geographic location (weather) indicate that local variations in utility rates have a greater effect than climate. Effects of weather and geographic location were further examined by considering correlations between the total annual energy cost ratio and climate related parameters, such as the ASHRAE 1% design values for dry bulb, wet bulb, and dew point temperatures, and latitude. This analysis confirmed that no significant trends relating total annual energy cost ratio to climate could be identified. These results prompted the addition of two cities from the arid southwest and mountain west states, which were initially omitted from the study on the basis that humidity control is of much less interest in these areas. For the two cities included in the arid climate comparison, Salt Lake City, UT, and Phoenix, AZ, the total annual energy cost ratios were toward the low end of the spectrum of 42 cities, but were not necessarily the lowest. Even in the arid climates, the cost ratio for nearly every case examined was greater than unity, indicating that the desiccant-enhanced system would provide lower operating costs. Two possible reasons for these counter-intuitive results were examined, and verified. During the heating season, a desiccant dehumidifier can function as a free heater. Moreover, under certain conditions, the sensible heat recovery wheel within a desiccant dehumidifier can function as a heat recovery ventilator (HRV). DesiCalc™ models both of these effects.

To determine whether the economic favorability of the desiccant-enhanced system was the result of the active dehumidification or was simply the result of the dehumidifier functioning as a heat or energy recovery device when not actively dehumidifying, an additional analysis was made to explore the effects of including a heat recovery option in the conventional system. The

alternative configuration analysis was made using the large hotel as the building type, representative of the average annual cost ratio for all building types, and nineteen cities geographically representative of the forty original cities. The results of this analysis confirm that the desiccant-enhanced system with heat recovery generally results in savings over the conventional system even when the conventional system utilizes heat recovery. Conversely, the desiccant-enhanced system without heat recovery can result in more expensive operating costs than the conventional system without heat recovery and should generally not be considered if energy savings are important.

Although most conventional air-conditioning systems installed today do not incorporate a humidistat (i.e., do not "control" humidity levels), all conventional systems in this study were defined with comfort control settings identical to the desiccant-enhanced system—including humidity setpoints. Had the conventional baseline systems been defined without humidity control, the results would not have been overwhelmingly in favor of desiccant-enhanced systems. However, an operating-cost-savings comparison between a system which maintains humidity control and a system which does not is meaningless unless reasonably accurate cost estimates associated with not maintaining humidity control are included in the comparison. Such a task is beyond the scope of this study.

In comparing the energy costs for conventional systems and desiccant enhanced systems as a function of the building type, the best applications for desiccant-enhanced systems (in terms of operating costs) are schools, which show an average of 28% advantage over conventional systems, followed by retail stores, with 25%, and large hotels, with 12%. The least favorable applications were refrigerated warehouses, with 1%, and supermarkets, with 3%. The dependence of building type on the favorability of desiccant systems is a result of limitations imposed by DesiCalc™ for each particular building type. These limitations, however, are not a fault of DesiCalc™, but rather are an attempt to model practical limitations often imposed by the buildings themselves. Nevertheless, these limitations are identified so that designers of potential desiccant systems may identify and possibly overcome these practical limitations in the design process.

2.8 REFERENCES

ASHRAE, 1997, *ASHRAE Handbook--Fundamentals*, American Society of Heating, Refrigerating and Air-Conditioning Engineers, Inc., Atlanta, GA.

Busby, R.L., 1996, "Relieving the Headache of Humidity Control," *Engineered Systems*, Vol. 13, No. 9, p 45-49.

GRI, 1998, *DesiCalc™ User's Manual, Version 1.1*, Chicago, IL.

Downing, C., 1996, "No Place Like Home," *Engineered Systems*, Vol. 13, No. 1, p 61-66.

Fischer, J., 1999, "Active Desiccant-Based Preconditioning Market Analysis and Product Development," ORNL Sub/94-SV044/1, Oak Ridge National Laboratory, Oak Ridge, TN.

Harriman, L.G., Witte, M.J., Czachorski, M., and Kosar, D.R., 1999, "Evaluating Active Desiccant Systems for Ventilating Commercial Buildings," *ASHRAE Journal*, Vol. 41, No.10, p 28-37.

Stevens, J.W., Jalalzadeh, A., and Hodge, B.K., 1996, *Desiccant Dehumidification Curriculum Module for Engineering/Technology HVAC Courses*, Mississippi State University, Mississippi State, MS.

APPENDIX 2.A
DESICALC EXAMPLES

JOB DESCRIPTION

Project: Unnamed Project Location: Atlanta, GA Program User: Isabel Gandica Comments: Retail Store.
--

BUILDING

Retail Store; single-story slab on grade construction typical of a larger department store with 10 % wall glazing. Humidity control air treatment applies to 60000 sf floor area. Internal loads and ventilation values apply to humidity controlled areas. Building total floor area is 60000 sf. Application Comfort Controls - Default Controls

Internal Loads and Ventilation

Occupancy:	100.0 sf/person
Lighting:	2.30 Watt/sf
Other Electric:	0.25 Watt/sf
Infiltration:	0.30 air exchanges/hour
Ventilation:	0.30 cfm/sf

LOCATION & DESIGN WEATHER

Atlanta GA - Lat./Long. 34N/84W Summer 1% Design Dry Bulb/Mean-Coincident Wet Bulb: 91/74°F (Humidity Ratio 104 gr/lb) Summer 1% Design Dew-Point/Mean-Coincident Dry Bulb: 73/81°F (Humidity Ratio 128 gr/lb). Energy Rates - GA: GA Pwr PLM-2/Atl Gas Lt G-11&GAC

Equipment Sizing Design Point: 1% DB & 1% DP
Equipment Oversize: 20 %

<u>Comfort Controls</u>	<u>Baseline</u>	<u>Des. Enhanced</u>
Cooling Temp./Setback	75 / 80 F	75 / 80 F
Heating Temp./Setback	72 / 60 F	72 / 60 F
Maximum Humidity	60 %	60 %
Minimum Humidity	0 %	0 %

EQUIPMENT & ENERGY

<u>Baseline Equipment Alternative</u>	<u>Desiccant Enhanced System Alternative</u>																
Constant volume 8.9 EER packaged DX rooftop unit with temperature economizer. System does not use heat recovery. System equipped with gas source heating. Humidifier not used. Default Config.	Constant volume 8.9 EER packaged DX rooftop unit with temperature economizer. System equipped with gas source heating. Outside air treated by a gas-fired desiccant dehumidifier with 70 % eff. heat exch. (downstream sensible exchange with relief air heat recovery). Dehumidifier configured without evap. cooler option. Humidifier not used. Default Config.																
<table style="width: 100%; border-collapse: collapse;"> <tr> <td style="padding: 2px;">Design Cooling Capacity:</td> <td style="padding: 2px;">216.37 RT</td> </tr> <tr> <td style="padding: 2px;">Design Heating Capacity:</td> <td style="padding: 2px;">2,050,861 Btu/hr</td> </tr> <tr> <td style="padding: 2px;">Supply Fans Capacity:</td> <td style="padding: 2px;">72,264 CFM</td> </tr> <tr> <td style="padding: 2px;">Outside Air:</td> <td style="padding: 2px;">18,716 CFM</td> </tr> </table>	Design Cooling Capacity:	216.37 RT	Design Heating Capacity:	2,050,861 Btu/hr	Supply Fans Capacity:	72,264 CFM	Outside Air:	18,716 CFM	<table style="width: 100%; border-collapse: collapse;"> <tr> <td style="padding: 2px;">Design Cooling Capacity:</td> <td style="padding: 2px;">133.60 RT</td> </tr> <tr> <td style="padding: 2px;">Design Heating Capacity:</td> <td style="padding: 2px;">1,350,826 Btu/hr</td> </tr> <tr> <td style="padding: 2px;">Supply Fans Capacity:</td> <td style="padding: 2px;">55,463 CFM</td> </tr> <tr> <td style="padding: 2px;">Outside Air :</td> <td style="padding: 2px;">18,746 CFM</td> </tr> </table>	Design Cooling Capacity:	133.60 RT	Design Heating Capacity:	1,350,826 Btu/hr	Supply Fans Capacity:	55,463 CFM	Outside Air :	18,746 CFM
Design Cooling Capacity:	216.37 RT																
Design Heating Capacity:	2,050,861 Btu/hr																
Supply Fans Capacity:	72,264 CFM																
Outside Air:	18,716 CFM																
Design Cooling Capacity:	133.60 RT																
Design Heating Capacity:	1,350,826 Btu/hr																
Supply Fans Capacity:	55,463 CFM																
Outside Air :	18,746 CFM																
<table style="width: 100%; border-collapse: collapse;"> <tr> <td style="padding: 2px;">Annual Electric Energy Use:</td> <td style="padding: 2px;">1,438,230 kWh</td> </tr> <tr> <td style="padding: 2px;">Annual Gas Energy Use:</td> <td style="padding: 2px;">3,534 MMBtu</td> </tr> </table>	Annual Electric Energy Use:	1,438,230 kWh	Annual Gas Energy Use:	3,534 MMBtu	<table style="width: 100%; border-collapse: collapse;"> <tr> <td style="padding: 2px;">Annual Electric Energy Use:</td> <td style="padding: 2px;">1,238,824 kWh</td> </tr> <tr> <td style="padding: 2px;">Annual Gas Energy Use:</td> <td style="padding: 2px;">2,279 MMBtu</td> </tr> </table>	Annual Electric Energy Use:	1,238,824 kWh	Annual Gas Energy Use:	2,279 MMBtu								
Annual Electric Energy Use:	1,438,230 kWh																
Annual Gas Energy Use:	3,534 MMBtu																
Annual Electric Energy Use:	1,238,824 kWh																
Annual Gas Energy Use:	2,279 MMBtu																
<table style="width: 100%; border-collapse: collapse;"> <tr> <td style="padding: 2px;">Annual Electric Energy Cost:</td> <td style="padding: 2px;">126,383 \$</td> </tr> <tr> <td style="padding: 2px;">Annual Gas Energy Cost:</td> <td style="padding: 2px;">17,486 \$</td> </tr> <tr> <td style="padding: 2px;">Total Annual Energy Cost</td> <td style="padding: 2px;">143,869 \$</td> </tr> </table>	Annual Electric Energy Cost:	126,383 \$	Annual Gas Energy Cost:	17,486 \$	Total Annual Energy Cost	143,869 \$	<table style="width: 100%; border-collapse: collapse;"> <tr> <td style="padding: 2px;">Annual Electric Energy Cost:</td> <td style="padding: 2px;">109,234 \$</td> </tr> <tr> <td style="padding: 2px;">Annual Gas Energy Cost:</td> <td style="padding: 2px;">7,777 \$</td> </tr> <tr> <td style="padding: 2px;">Total Annual Energy Cost</td> <td style="padding: 2px;">117,011 \$</td> </tr> </table>	Annual Electric Energy Cost:	109,234 \$	Annual Gas Energy Cost:	7,777 \$	Total Annual Energy Cost	117,011 \$				
Annual Electric Energy Cost:	126,383 \$																
Annual Gas Energy Cost:	17,486 \$																
Total Annual Energy Cost	143,869 \$																
Annual Electric Energy Cost:	109,234 \$																
Annual Gas Energy Cost:	7,777 \$																
Total Annual Energy Cost	117,011 \$																
<table style="width: 100%; border-collapse: collapse;"> <tr> <td style="padding: 2px;">Annual Occupied Hours @ RH>60%</td> <td style="padding: 2px;">92</td> </tr> </table>	Annual Occupied Hours @ RH>60%	92	<table style="width: 100%; border-collapse: collapse;"> <tr> <td style="padding: 2px;">Annual Occupied Hours @ RH>60%</td> <td style="padding: 2px;">0</td> </tr> </table>	Annual Occupied Hours @ RH>60%	0												
Annual Occupied Hours @ RH>60%	92																
Annual Occupied Hours @ RH>60%	0																

Figure 2.A.1 Short Report

DESICCANT DEHUMIDIFIER UNIT PERFORMANCE SPECIFICATION
(ARI Standard 940P Rating Conditions)

		Process Air Flow Face Velocity: 400		fpm
		Dehumidifier Capacity: 18,746		CFM
DB	WB	Humidity	Water Removed	Specific Energy Input
(F)	(F)	(gr/lb)	(lb/hr)	(Btu/lb_removed water)
95	75	100.0	479	1,713
80	75	124.5	798	1,548

Regeneration air source is relief air preheated by post-cool sensible HX.

DESICCANT WHEEL MATRIX PERFORMANCE SPECIFICATION
(ARI Standard 940P Rating Conditions)

		Process Air Flow Face Velocity: 400		fpm
DB	WB	Humidity	Water Removed	Specific Energy Input
(F)	(F)	(gr/lb)	(lb/hr)	(Btu/lb_removed water)
95	75	100.0	479	1,772
80	75	124.5	798	1,776

Note. The annual energy consumption and costs given in this report reflect facility total energy use including lights, equipment, and HVAC equipment. Details of monthly energy consumption by end use are given in Detailed Report.

Units Used

RT = 12,000 Btu/hr

MMBtu = 1,000,000 Btu

Figure 2.A.1 (continued)

Cooling and Heating Coil Loads

Unnamed Project
 Atlanta, GA
 Isabel Gandica
 Retail Store.

Baseline System

Month	Cooling Sensible MMBtu	Cooling Latent MMBtu	Cooling Total MMBtu	Heating/Reheatin Total MMBtu
JAN	16	4	20	323
FEB	35	6	41	266
MAR	85	17	102	175
APR	232	60	292	143
MAY	424	132	556	142
JUN	587	220	807	175
JUL	703	354	1,057	212
AUG	710	349	1,059	230
SEP	648	308	956	254
OCT	301	98	399	143
NOV	87	22	109	160
DEC	50	17	67	320
Total	3,877	1,587	5,464	2,543

Alternative System

Month	Cooling Sensible MMBtu	Cooling Latent MMBtu	Cooling Total MMBtu	Heating Total MMBtu
JAN	30	5	35	97
FEB	31	4	35	87
MAR	64	10	73	42
APR	140	26	166	13
MAY	267	56	323	0
JUN	382	80	462	0
JUL	486	98	584	0
AUG	482	102	584	0
SEP	404	98	502	0
OCT	187	41	228	2
NOV	58	11	69	27
DEC	27	4	31	97
Total	2,557	536	3,093	366

Figure 2.A.2 Detailed Report

Electric Energy Consumption by End Use

Baseline System										
Month	Lights kWh	Misc. Equip. kWh	Space Cooling kWh	Pumps & Misc. kWh	Fans Vent. kWh	Space Heating kWh	Heat Reject. kWh	Refrig. kWh	Dom.Hot Water kWh	Total kWh
JAN	61,879	6,726	1,562	307	10,804	0	0	0	0	81,278
FEB	55,710	6,056	3,141	706	9,732	0	0	0	0	75,345
MAR	62,252	6,767	8,005	1,624	10,857	0	0	0	0	89,505
APR	59,823	6,503	23,682	3,744	10,447	0	0	0	0	104,199
MAY	61,879	6,726	46,152	6,085	10,804	0	0	0	0	131,646
JUN	60,195	6,543	68,128	7,171	10,500	0	0	0	0	152,537
JUL	61,506	6,686	89,911	7,787	10,750	0	0	0	0	176,640
AUG	62,252	6,767	89,093	7,926	10,857	0	0	0	0	176,895
SEP	59,450	6,462	78,605	7,539	10,393	0	0	0	0	162,449
OCT	61,879	6,726	32,122	4,657	10,804	0	0	0	0	116,188
NOV	59,450	6,462	8,516	1,674	10,393	0	0	0	0	86,495
DEC	61,506	6,686	5,308	801	10,750	0	0	0	0	85,051
Total	727,781	79,110	454,225	50,021	127,091	0	0	0	0	1,438,228

Alternative System										
Month	Lights kWh	Misc. Equip. kWh	Space Cooling kWh	Pumps & Misc. kWh	Fans Vent. kWh	Space Heating kWh	Heat Reject. kWh	Refrig. kWh	Dom.Hot Water kWh	Total kWh
JAN	61,879	6,726	5,337	904	8,292	0	0	0	0	83,138
FEB	55,710	6,056	4,940	897	7,470	0	0	0	0	75,073
MAR	62,252	6,767	8,264	1,708	8,333	0	0	0	0	87,324
APR	59,823	6,503	16,004	3,052	8,018	0	0	0	0	93,400
MAY	61,879	6,726	29,637	4,823	8,292	0	0	0	0	111,357
JUN	60,195	6,543	42,507	5,631	8,059	0	0	0	0	122,935
JUL	61,506	6,686	54,380	5,998	8,251	0	0	0	0	136,821
AUG	62,252	6,767	53,550	6,076	8,333	0	0	0	0	136,978
SEP	59,450	6,462	45,104	5,729	7,977	0	0	0	0	124,722
OCT	61,879	6,726	20,977	3,796	8,292	0	0	0	0	101,670
NOV	59,450	6,462	7,689	1,652	7,977	0	0	0	0	83,230
DEC	61,506	6,686	4,925	813	8,251	0	0	0	0	82,181
Total	727,781	79,110	293,314	41,079	97,545	0	0	0	0	1,238,829

Figure 2.A.2 (continued)

Gas Energy Consumption by End Use
--

Baseline System							Total
Month	Space Heating MMBtu	Space Cooling MMBtu	Dom. Water MMBtu	Hot Misc. Domest. MMBtu	Supl. Heating MMBtu	Ext. Misc. MMBtu	MMBtu
JAN	431	0	13	0	0	0	444
FEB	355	0	12	0	0	0	366
MAR	234	0	13	0	0	0	247
APR	191	0	12	0	0	0	203
MAY	190	0	12	0	0	0	202
JUN	234	0	11	0	0	0	246
JUL	284	0	11	0	0	0	295
AUG	308	0	11	0	0	0	318
SEP	339	0	10	0	0	0	349
OCT	191	0	11	0	0	0	202
NOV	213	0	11	0	0	0	224
DEC	427	0	12	0	0	0	439
Total	3,397	0	138	0	0	0	3,535

Alternative System							Total
Month	Space Heating MMBtu	Space Cooling MMBtu	Dom. Water MMBtu	Hot Misc. Domest. MMBtu	Supl. Heating MMBtu	Ext. Misc. MMBtu	MMBtu
JAN	129	4	13	0	0	0	146
FEB	117	2	12	0	0	0	130
MAR	57	11	13	0	0	0	80
APR	18	35	12	0	0	0	65
MAY	1	103	12	0	0	0	116
JUN	0	215	11	0	0	0	226
JUL	0	431	11	0	0	0	441
AUG	0	412	11	0	0	0	422
SEP	0	343	10	0	0	0	353
OCT	3	75	11	0	0	0	89
NOV	36	13	11	0	0	0	60
DEC	129	11	12	0	0	0	153
Total	489	1,653	138	0	0	0	2,280

Figure 2.A.2 (continued)

DesiCalc

Monthly Loads, Energy Consumption and Costs Report

7/14/99 1:48:13PM

Version 1.1

Page 4 of 5

Total Monthly Electric Consumption and Electric Energy Cost

Baseline System

Month	Metered Energy kWh	Metered Demand kW	Energy Charge (\$)	Demand Charge (\$)	Energy Cost Adj (\$)	Taxes (\$)	Surch. (\$)	Fixed Charge (\$)	Min. Charge (\$)	Total Charge (\$)
JAN	81,279	278	7,198	0	0	0	0	17	0	7,215
FEB	75,346	272	6,688	0	0	0	0	17	0	6,704
MAR	89,505	290	7,905	0	0	0	0	17	0	7,922
APR	104,198	320	9,169	0	0	0	0	17	0	9,186
MAY	131,646	347	11,529	0	0	0	0	17	0	11,546
JUN	152,538	358	13,326	0	0	0	0	17	0	13,343
JUL	176,641	370	15,399	0	0	0	0	17	0	15,416
AUG	176,895	361	15,421	0	0	0	0	17	0	15,438
SEP	162,449	354	14,178	0	0	0	0	17	0	14,195
OCT	116,189	322	10,200	0	0	0	0	17	0	10,217
NOV	86,495	288	7,646	0	0	0	0	17	0	7,663
DEC	85,052	295	7,522	0	0	0	0	17	0	7,539
Total	1,438,233	3,855	126,181	0	0	0	0	204	0	126,384

Alternative System

Month	Metered Energy kWh	Metered Demand kW	Energy Charge (\$)	Demand Charge (\$)	Energy Cost Adj (\$)	Taxes (\$)	Surch. (\$)	Fixed Charge (\$)	Min. Charge (\$)	Total Charge (\$)
JAN	83,137	204	7,358	0	0	0	0	17	0	7,374
FEB	75,073	208	6,664	0	0	0	0	17	0	6,681
MAR	87,323	222	7,718	0	0	0	0	17	0	7,734
APR	93,399	248	8,240	0	0	0	0	17	0	8,257
MAY	111,358	275	9,785	0	0	0	0	17	0	9,801
JUN	122,935	284	10,780	0	0	0	0	17	0	10,797
JUL	136,821	311	11,974	0	0	0	0	17	0	11,991
AUG	136,977	301	11,988	0	0	0	0	17	0	12,005
SEP	124,722	285	10,934	0	0	0	0	17	0	10,951
OCT	101,670	264	8,951	0	0	0	0	17	0	8,968
NOV	83,231	224	7,366	0	0	0	0	17	0	7,382
DEC	82,182	206	7,275	0	0	0	0	17	0	7,292
Total	1,238,828	3,030	109,033	0	0	0	0	204	0	109,233

Figure 2.A.2 (continued)

DesiCalc

Monthly Loads, Energy Consumption and Costs Report

7/14/99

1:48:13PM

Version 1.1

Page 5 of 5

Total Monthly Gas Consumption and Gas Energy Cost

Baseline System

Month	Metered Energy Therms	Metered Demand Therms/Day	Energy Charge (\$)	Demand Charge (\$)	Energy Cost Adj (\$)	Taxes (\$)	Surch. (\$)	Fixed Charge (\$)	Min. Charge (\$)	Total Charge (\$)
JAN	4,435	381	2,056	0	0	151	0	13	0	2,220
FEB	3,664	343	1,701	0	0	125	0	13	0	1,839
MAR	2,473	239	1,153	0	0	85	0	13	0	1,251
APR	2,030	164	949	0	0	70	0	13	0	1,032
MAY	2,020	187	901	0	0	67	0	13	0	981
JUN	2,455	148	1,092	0	0	80	0	13	0	1,186
JUL	2,947	142	1,308	0	0	96	0	13	0	1,417
AUG	3,181	130	1,411	0	0	104	0	13	0	1,527
SEP	3,492	172	1,547	0	0	114	0	13	0	1,674
OCT	2,018	203	943	0	0	70	0	13	0	1,026
NOV	2,243	207	1,047	0	0	77	0	13	0	1,137
DEC	4,387	332	2,034	0	0	149	0	13	0	2,196
Total	35,345	2,649	16,142	0	0	1,188	0	156	0	17,486

Alternative System

Month	Metered Energy Therms	Metered Demand Therms/Day	Energy Charge (\$)	Demand Charge (\$)	Energy Cost Adj (\$)	Taxes (\$)	Surch. (\$)	Fixed Charge (\$)	Min. Charge (\$)	Total Charge (\$)
JAN	1,461	234	678	0	0	51	0	13	0	742
FEB	1,304	181	610	0	0	45	0	13	0	668
MAR	801	143	358	0	0	27	0	13	0	398
APR	648	103	232	0	0	17	0	13	0	262
MAY	1,156	136	317	0	0	24	0	13	0	355
JUN	2,257	199	588	0	0	44	0	13	0	645
JUL	4,413	214	1,124	0	0	83	0	13	0	1,220
AUG	4,222	193	1,076	0	0	80	0	13	0	1,169
SEP	3,525	203	902	0	0	66	0	13	0	981
OCT	892	134	257	0	0	20	0	13	0	289
NOV	596	117	256	0	0	19	0	13	0	290
DEC	1,527	211	693	0	0	51	0	13	0	758
Total	22,802	2,068	7,091	0	0	527	0	156	0	7,777

Figure 2.A.2 (continued)

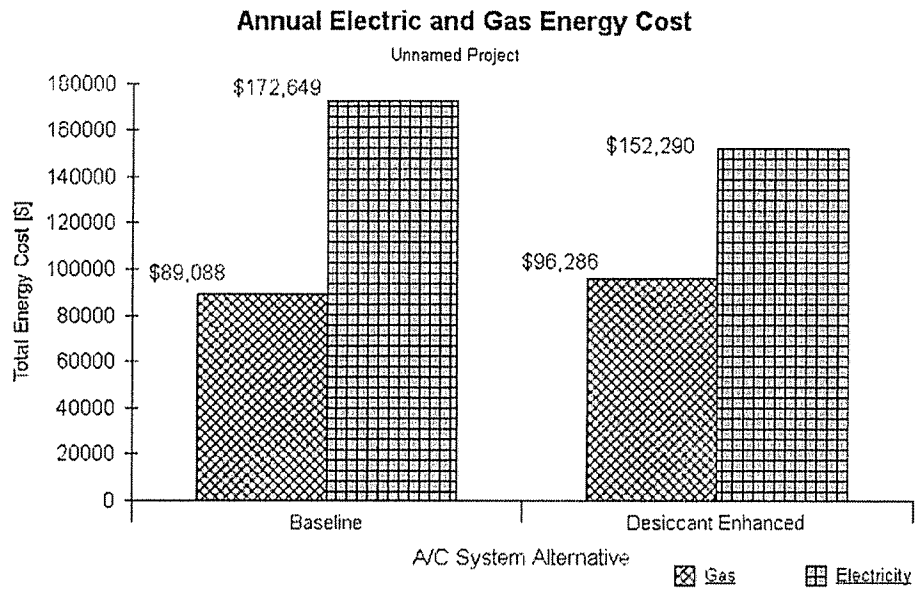


Figure 2.A.3 Annual Electric and Gas Energy Cost Chart

APPENDIX 2.B
TOTAL ANNUAL ENERGY COST RATIO

Table 2.B.1 Total Annual Energy Cost Ratios

City \ Building	Hospital	Large Hotel	Nursing Home	Quick-Serve Restaurant	Retail Store	School	Super market	Refrigerated Warehouse
Albany, NY	1.030	1.048	1.063	1.038	1.171	1.122	1.054	1.047
Asheville, NC	1.058	1.109	1.082	1.062	1.211	1.228	1.064	1.063
Atlanta, GA	1.061	1.107	1.080	1.106	1.230	1.267	1.069	1.090
Baltimore, MD	1.062	1.090	1.068	1.089	1.184	1.213	1.066	1.055
Boston, MA	1.041	1.155	1.100	1.035	1.296	1.273	1.034	1.024
Burlington, VT	1.042	1.100	1.035	1.027	1.160	1.191	1.053	1.076
Charleston, SC	1.069	1.107	1.072	1.162	1.336	1.441	1.074	1.058
Chicago, IL	1.022	1.111	1.131	1.057	1.230	1.256	1.058	1.100
Cleveland, OH	1.045	1.277	1.149	1.024	1.557	1.356	0.994	0.871
Corpus Christi, TX	1.089	1.076	1.048	1.136	1.230	1.369	1.059	1.064
Detroit, MI	1.035	1.100	1.071	1.035	1.164	1.182	1.047	1.051
Fargo, ND	1.077	1.225	1.155	1.008	1.453	1.301	0.856	1.010
Fort Worth, TX	0.997	1.059	1.016	1.060	1.316	1.343	0.875	0.593
Honolulu, HI	1.086	1.066	1.042	1.098	1.142	1.311	1.044	0.965
Houston, TX	1.053	1.019	1.000	1.092	1.156	1.409	0.994	0.944
Huntington, WV	1.024	1.195	1.122	1.039	1.597	1.394	0.954	0.659
Indianapolis, IN	1.046	1.104	1.069	1.059	1.192	1.223	1.050	1.060
Jackson, MS	1.064	1.091	1.059	1.065	1.220	1.405	0.799	1.045
Little Rock, AR	1.115	1.114	1.082	1.134	1.266	1.390	1.088	1.102
Los Angeles, CA	1.068	1.065	1.050	1.062	1.050	1.088	1.048	1.082
Louisville, KY	1.058	1.111	1.079	1.082	1.200	1.252	1.061	1.055
Miami, FL	1.145	1.173	1.137	1.192	1.279	1.461	1.114	1.147
Milwaukee, WI	1.036	1.105	1.073	1.041	1.193	1.191	1.044	1.062
Minneapolis, MN	1.060	1.147	1.107	1.026	1.265	1.234	1.046	1.043
Nashville, TN	1.038	1.090	1.081	1.079	1.259	1.179	1.058	1.035
New Orleans, LA	1.108	1.112	1.076	1.144	1.208	1.369	1.088	1.101
New York, NY	1.046	1.109	1.073	1.047	1.188	1.219	1.044	1.039
Norfolk, VA	1.053	1.128	1.082	1.067	1.358	1.401	0.979	0.864
Omaha, NE	1.064	1.150	1.104	1.053	1.335	1.292	0.942	1.026
Pittsburgh, PA	1.053	1.258	1.168	1.021	1.662	1.404	0.984	0.749
Portland, ME	1.050	1.123	1.093	1.035	1.217	1.236	1.053	1.057
Portland, OR	1.038	1.150	1.096	1.006	1.077	1.059	1.037	1.001
Raleigh, NC	1.069	1.106	1.086	1.102	1.248	1.321	1.061	1.073
Rochester, NY	1.037	1.098	1.066	1.035	1.158	1.174	1.047	1.046
San Francisco, CA	1.025	1.041	1.037	0.992	0.996	1.044	1.037	1.033
Seattle, WA	1.019	1.099	1.070	0.994	1.138	1.165	1.035	1.052
St. Louis, MO	1.079	1.147	1.103	1.089	1.295	1.298	1.062	1.051
Tallahassee, FL	1.060	1.055	1.032	1.101	1.170	1.366	1.039	0.977
Tampa, FL	1.128	1.152	1.115	1.185	1.274	1.452	1.108	1.129
Wichita, KS	1.057	1.131	1.090	1.053	1.309	1.230	1.029	1.012

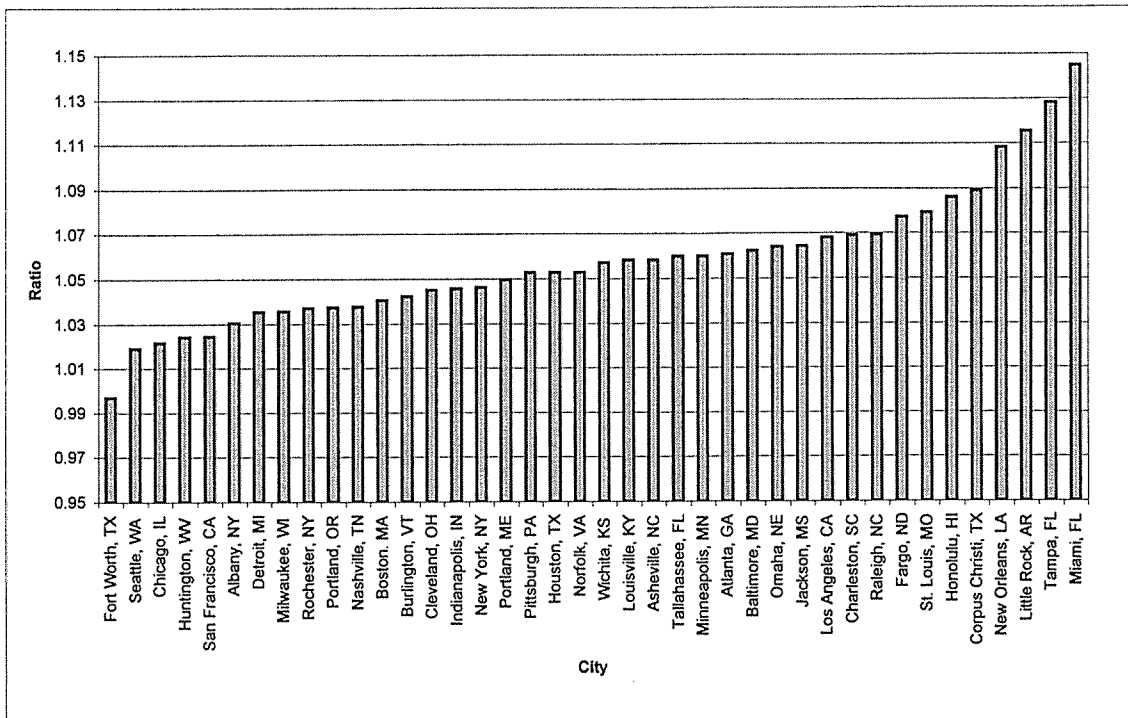


Figure 2.B.1 Total Annual Energy Cost Ratio. Building type: Hospital

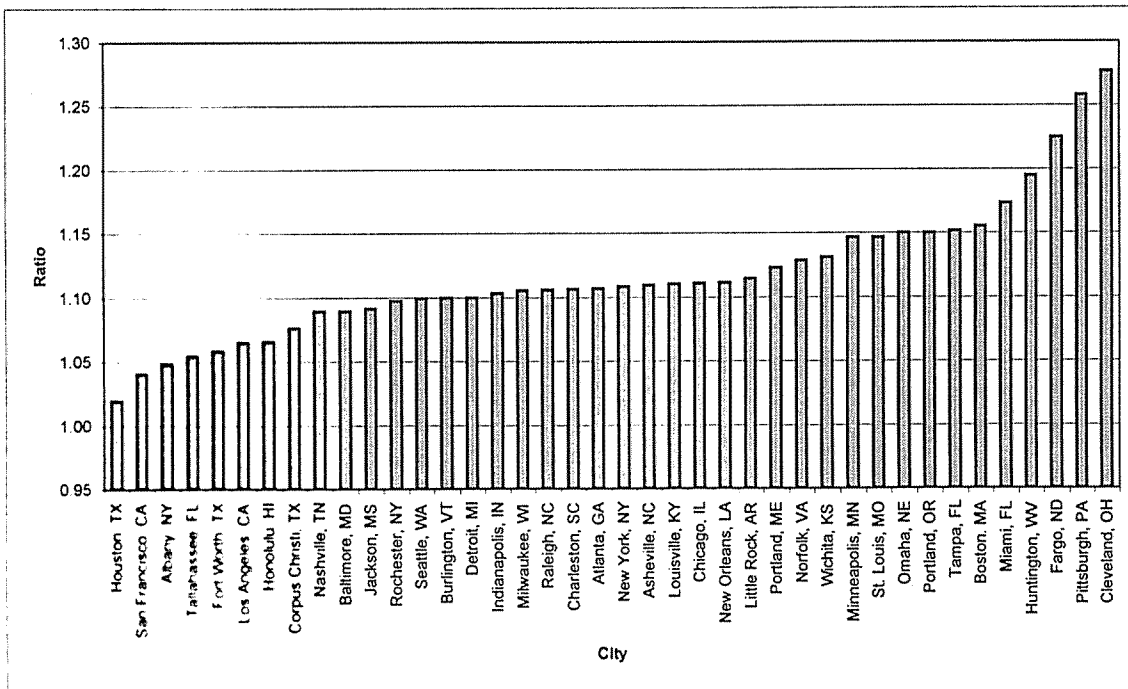


Figure 2.B.2 Total Annual Energy Cost Ratio. Building type: Large Hotel

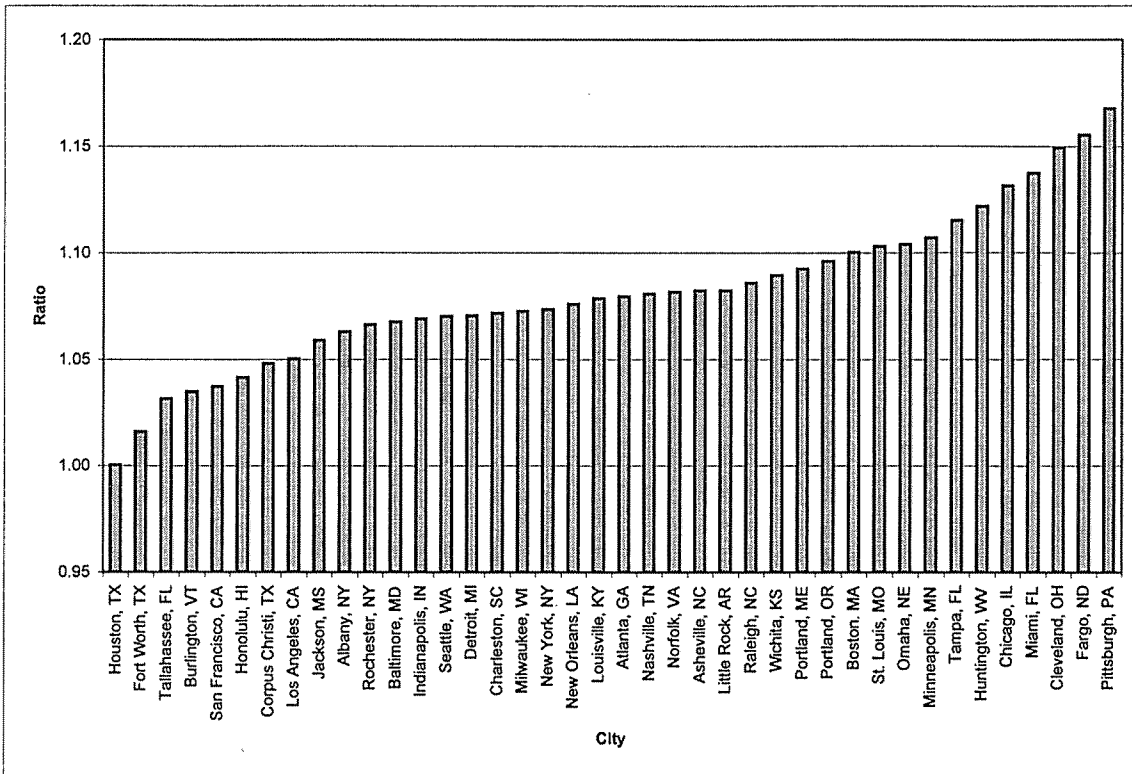


Figure 2.B.3 Total Annual Energy Cost Ratio. Building type: Nursing Home

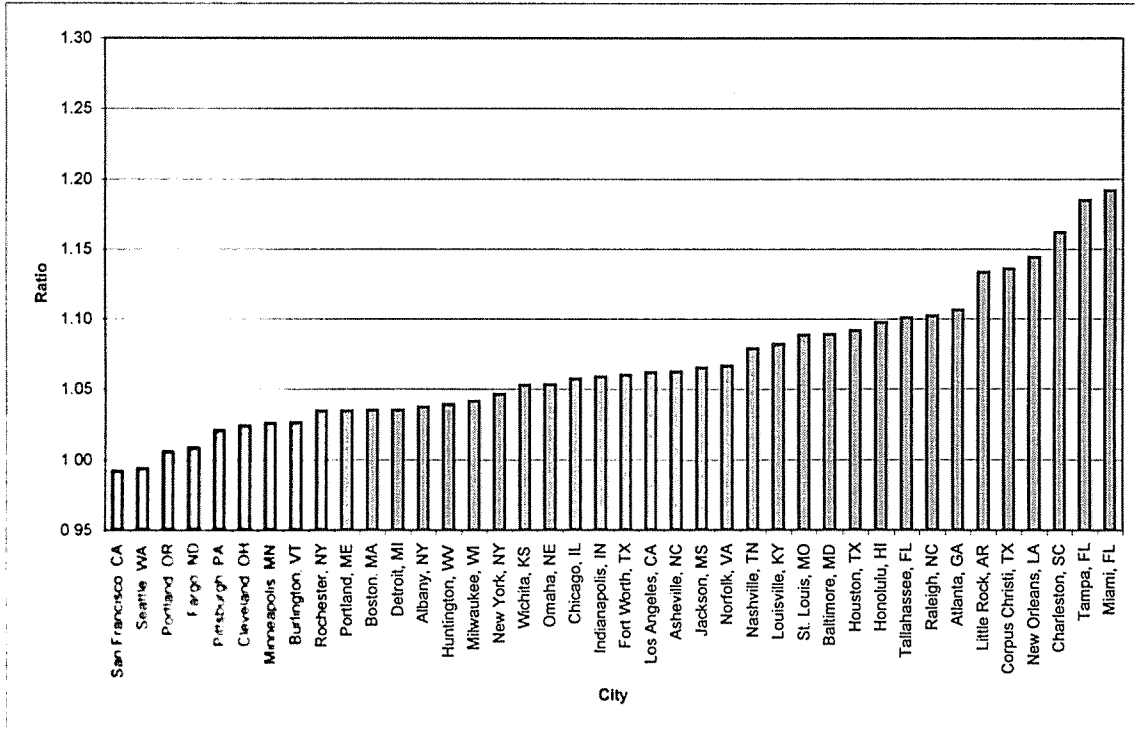


Figure 2.B.4 Total Annual Energy Cost Ratio. Building type: Quick-Serve Restaurant

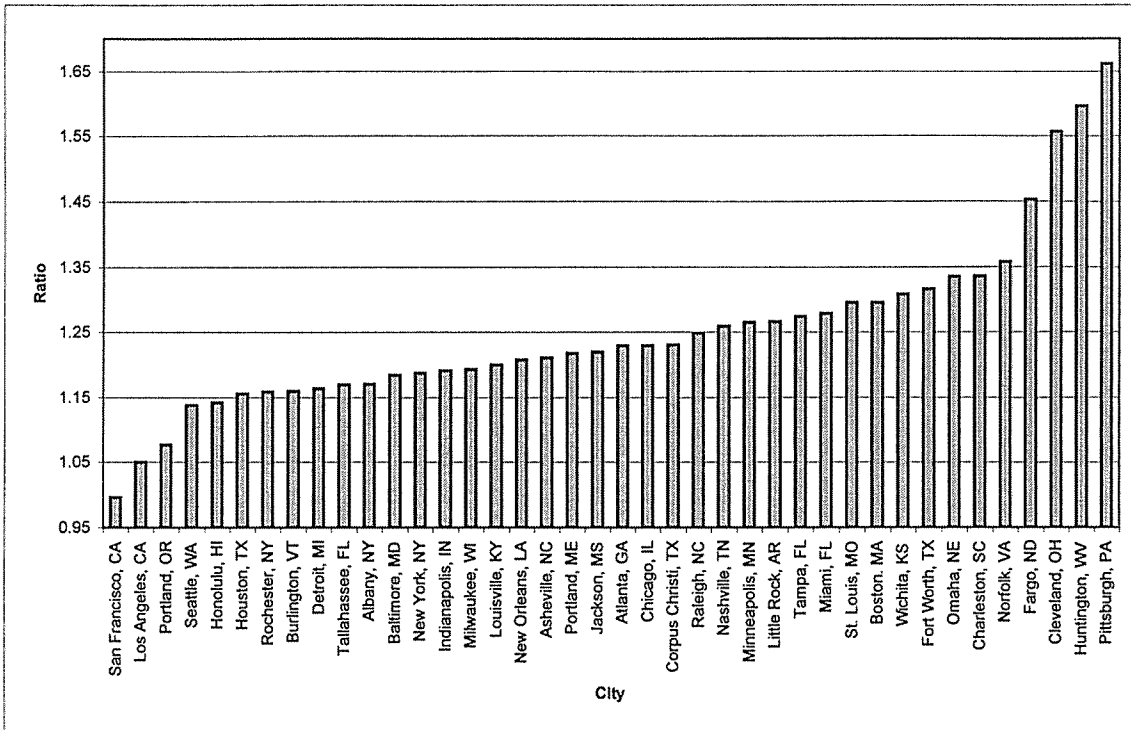


Figure 2.B.5 Total Annual Energy Cost Ratio. Building type: Retail Store

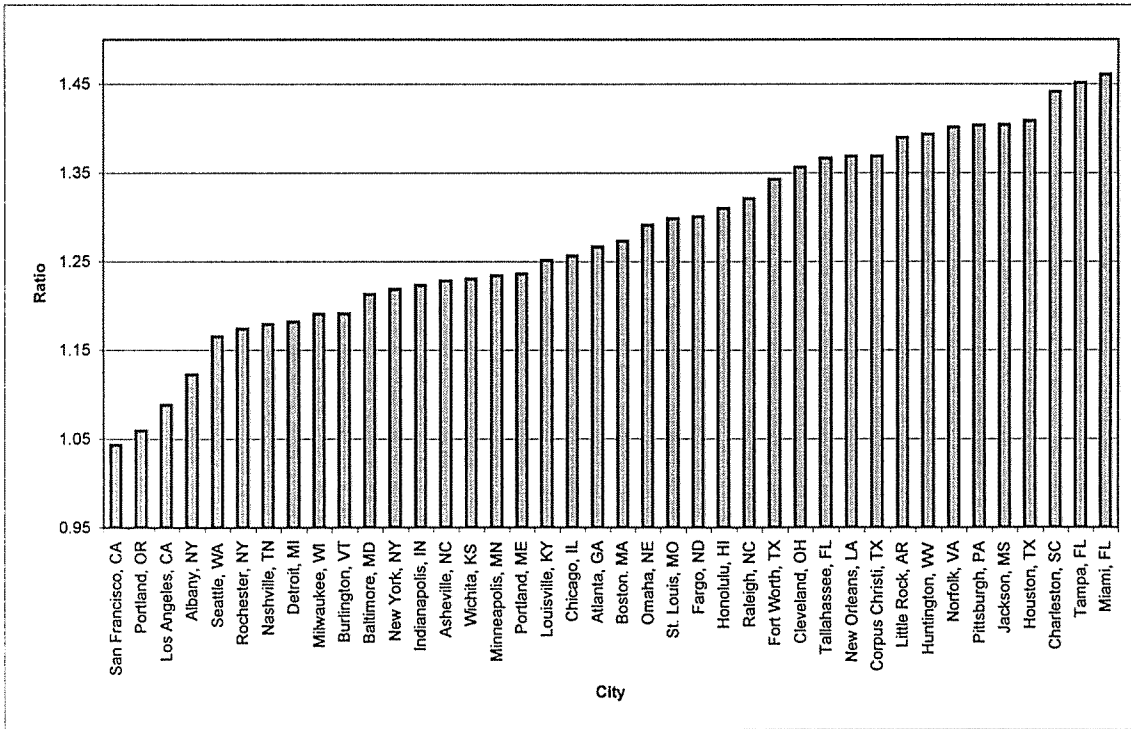


Figure 2.B.6 Total Annual Energy Cost Ratio. Building type: School

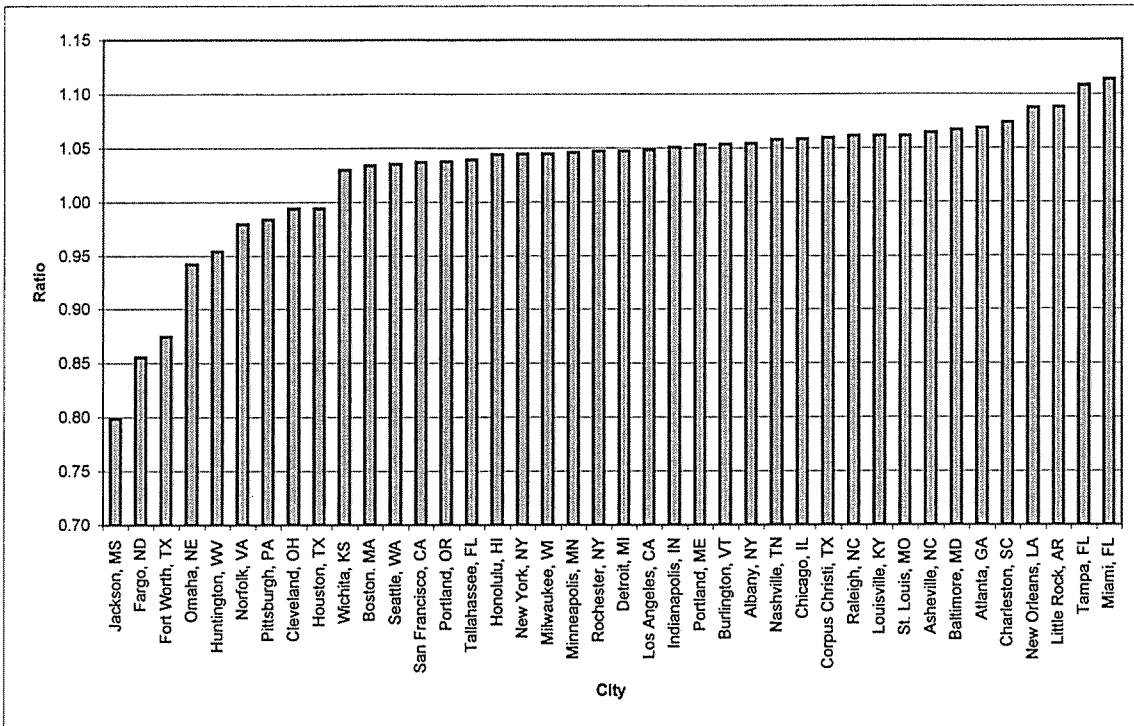


Figure 2.B.7 Total Annual Energy Cost Ratio. Building type: Supermarket

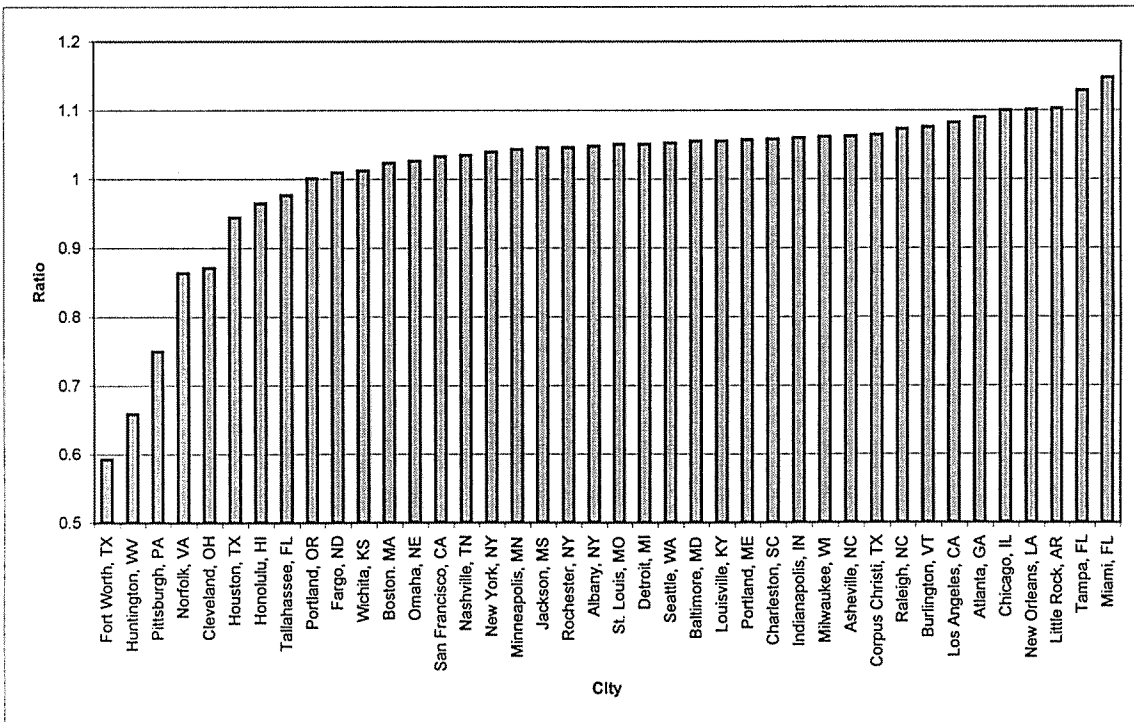


Figure 2.B.8 Total Annual Energy Cost Ratio. Building type: Refrigerated Warehouse

APPENDIX 2.C

EFFECT OF EXTREME DESIGN DRY-BULB TEMPERATURE

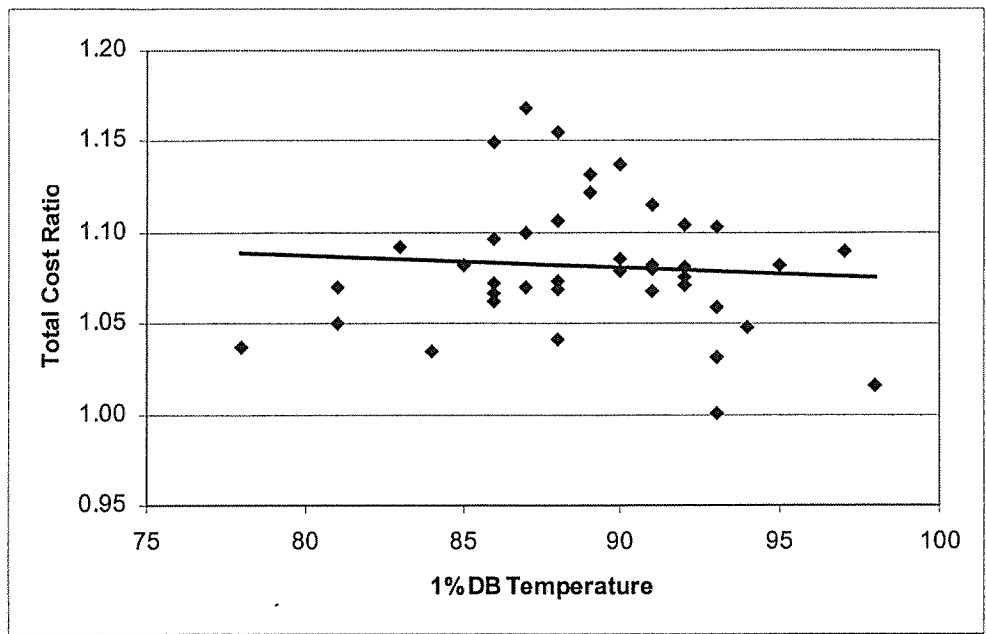


Figure 2.C.3 Effect of Extreme Design Dry-Bulb Temperature. Building: Nursing Home

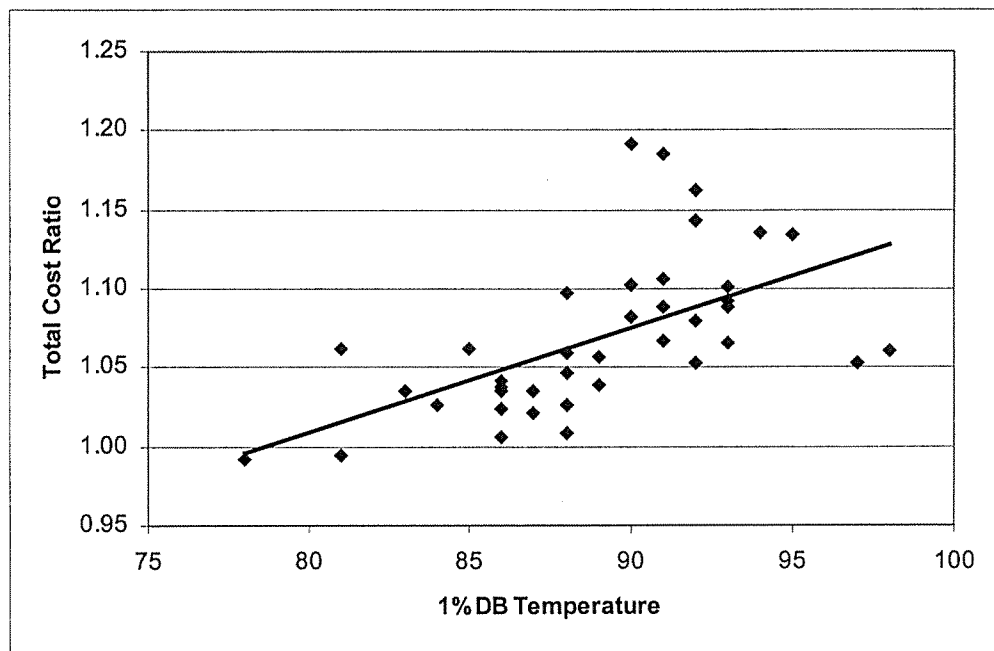


Figure 2.C.4 Effect of Extreme Design Dry-Bulb Temperature. Building: Quick-Serve Restaurant

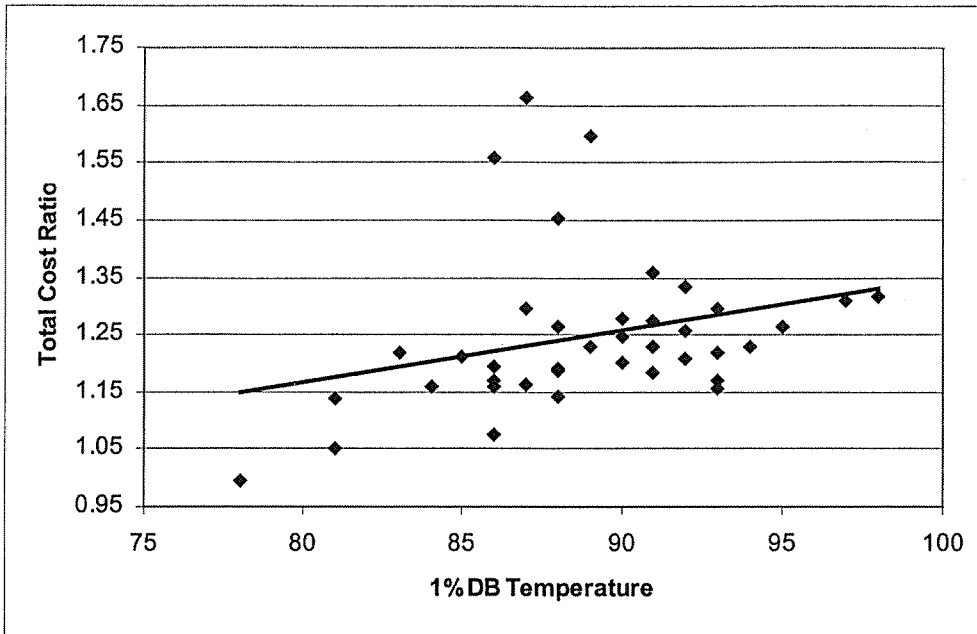


Figure 2.C.5 Effect of Extreme Design Dry-Bulb Temperature. Building: Retail Store

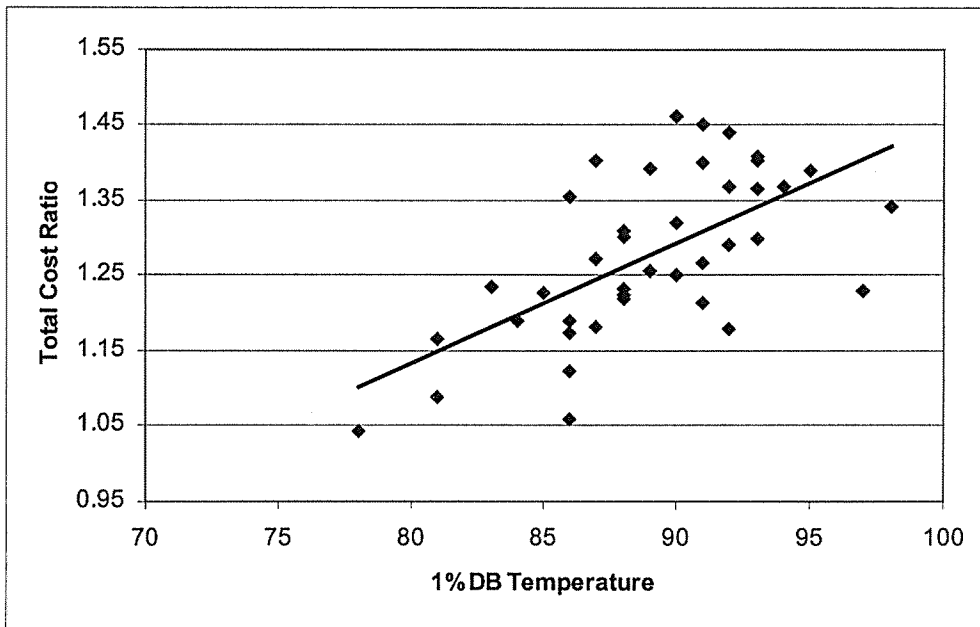


Figure 2.C.6 Effect of Extreme Design Dry-Bulb Temperature. Building: School

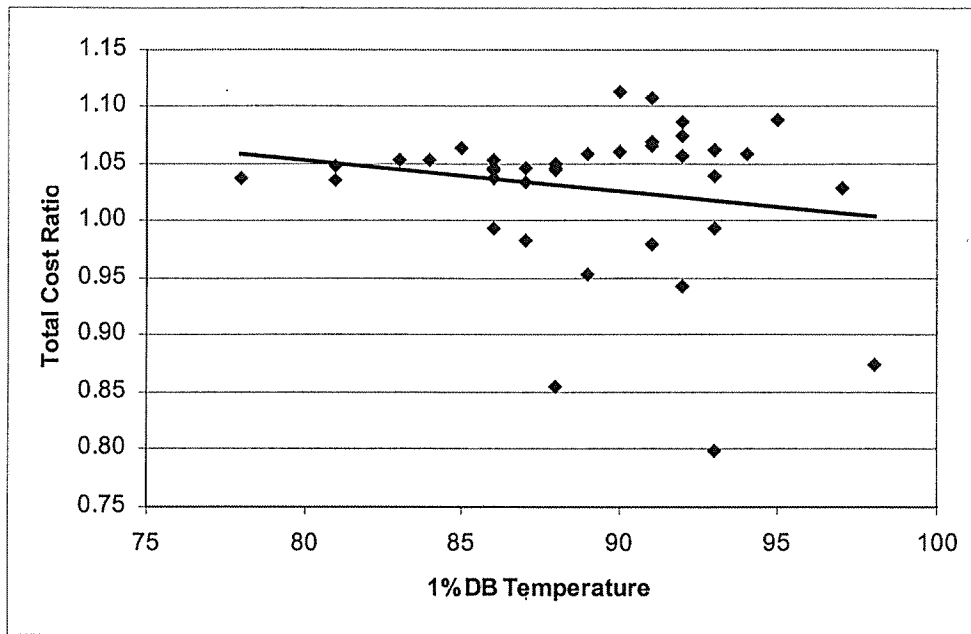


Figure 2.C.7 Effect of Extreme Design Dry-Bulb Temperature. Building: Supermarket

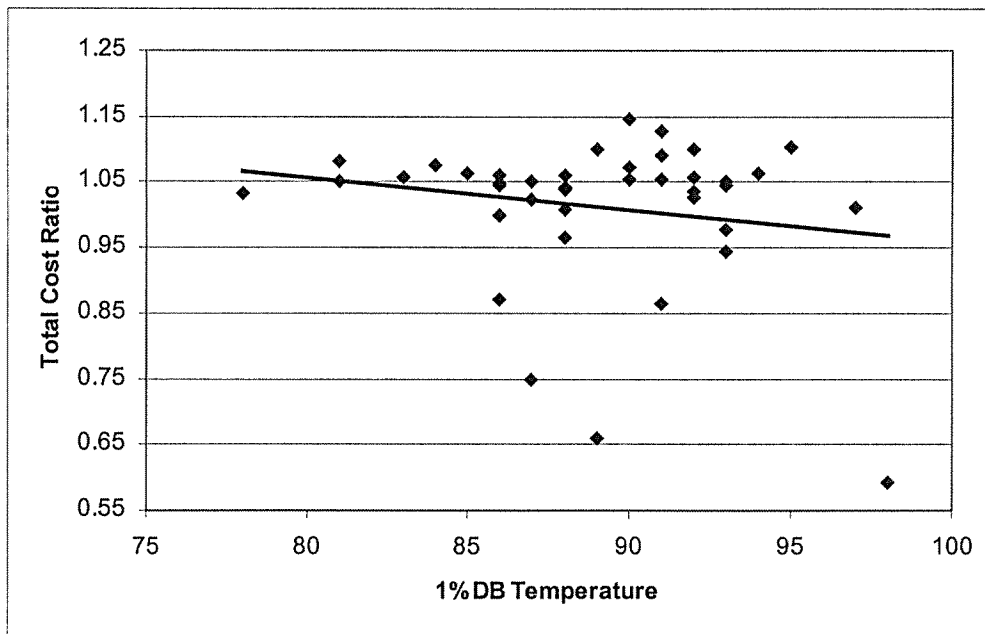


Figure 2.C.8 Effect of Extreme Design Dry-Bulb Temperature. Building: Refrigerated Warehouse

APPENDIX 2.D
EFFECT OF EXTREME DESIGN WET-BULB TEMPERATURE

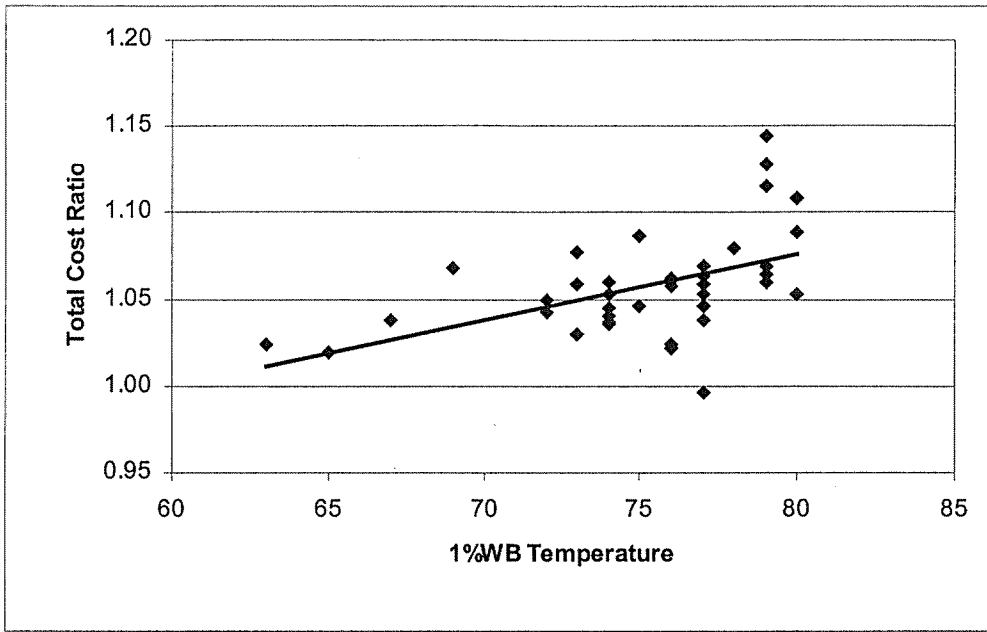


Figure 2.D.1 Effect of Extreme Design Wet-Bulb Temperature. Building: Hospital

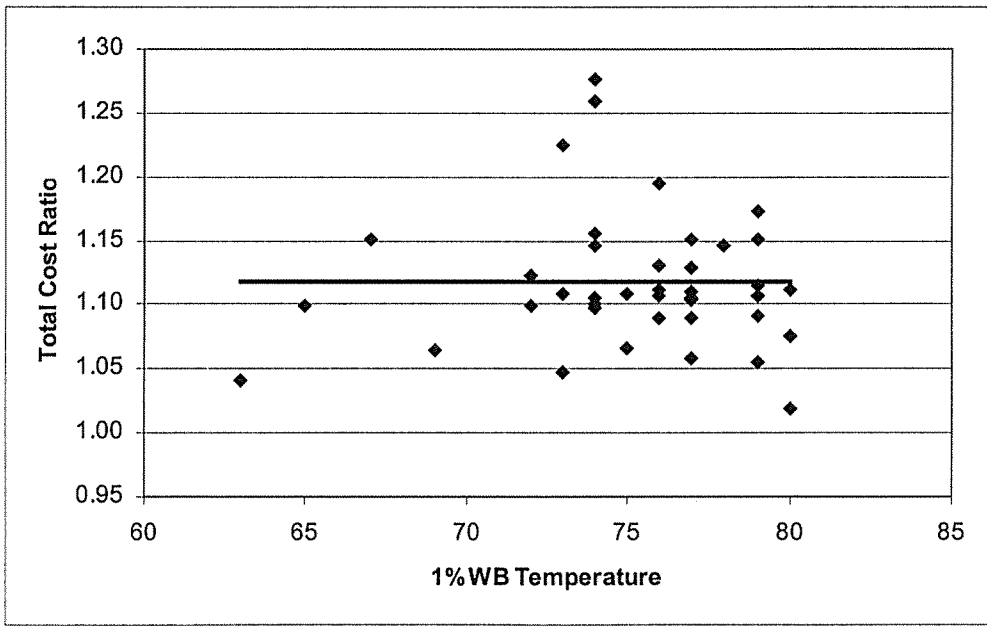


Figure 2.D.2 Effect of Extreme Design Wet-Bulb Temperature. Building: Large Hotel

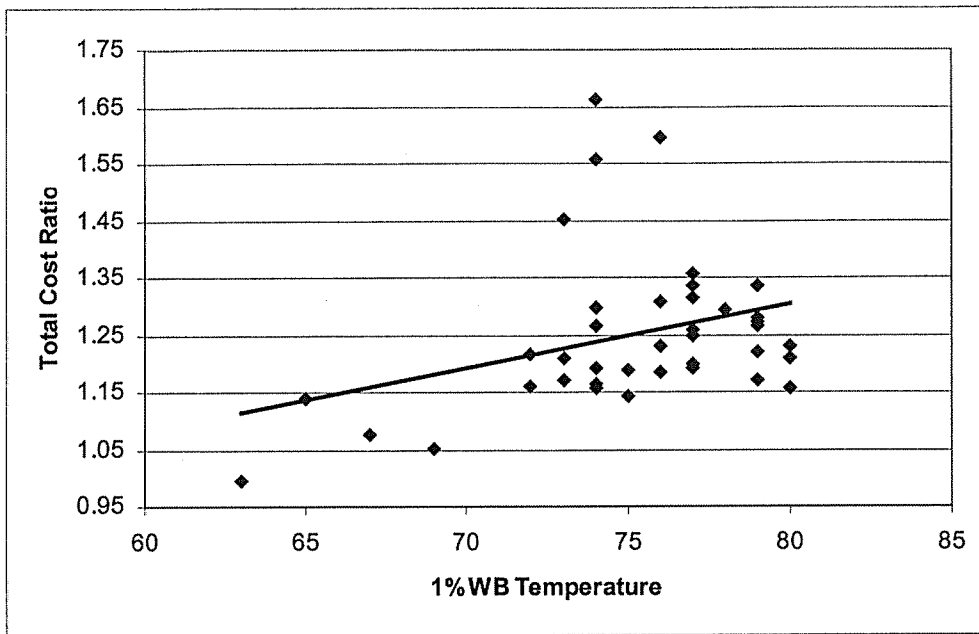


Figure 2.D.5 Effect of Extreme Design Wet-Bulb Temperature. Building: Retail Store

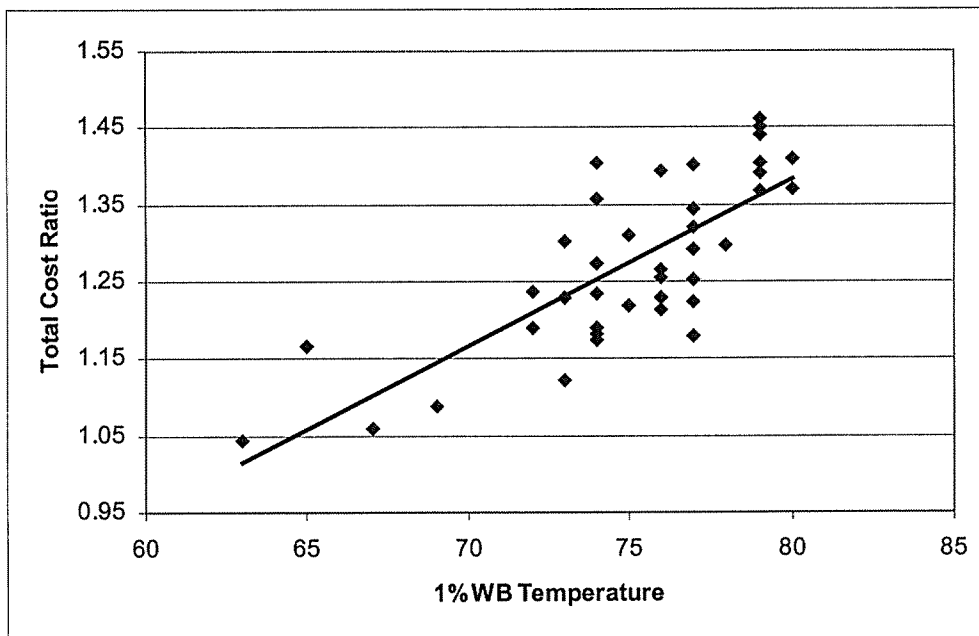


Figure 2.D.6 Effect of Extreme Design Wet-Bulb Temperature. Building: School

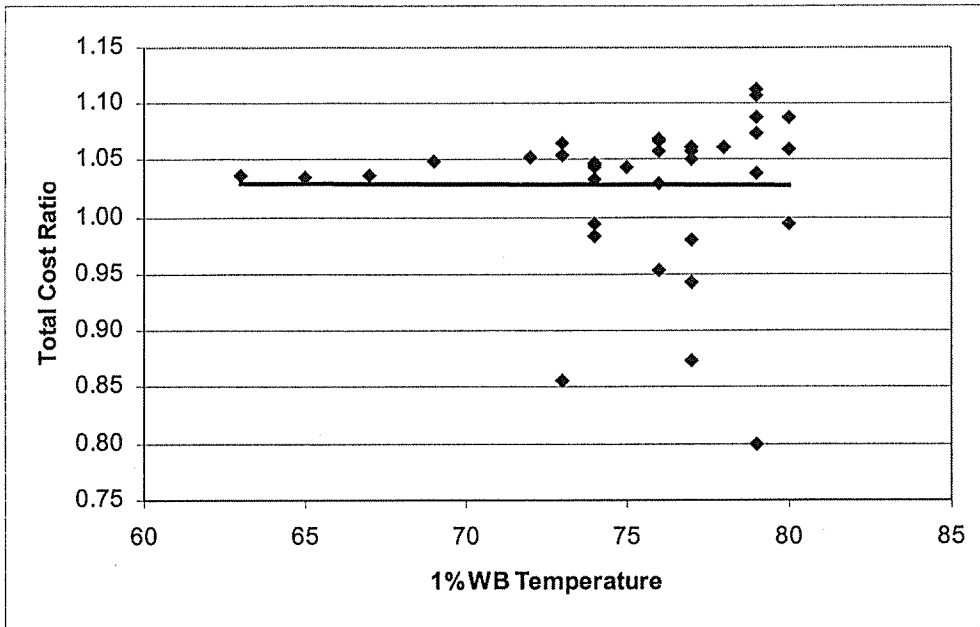


Figure 2.D.7 Effect of Extreme Design Wet-Bulb Temperature. Building: Supermarket

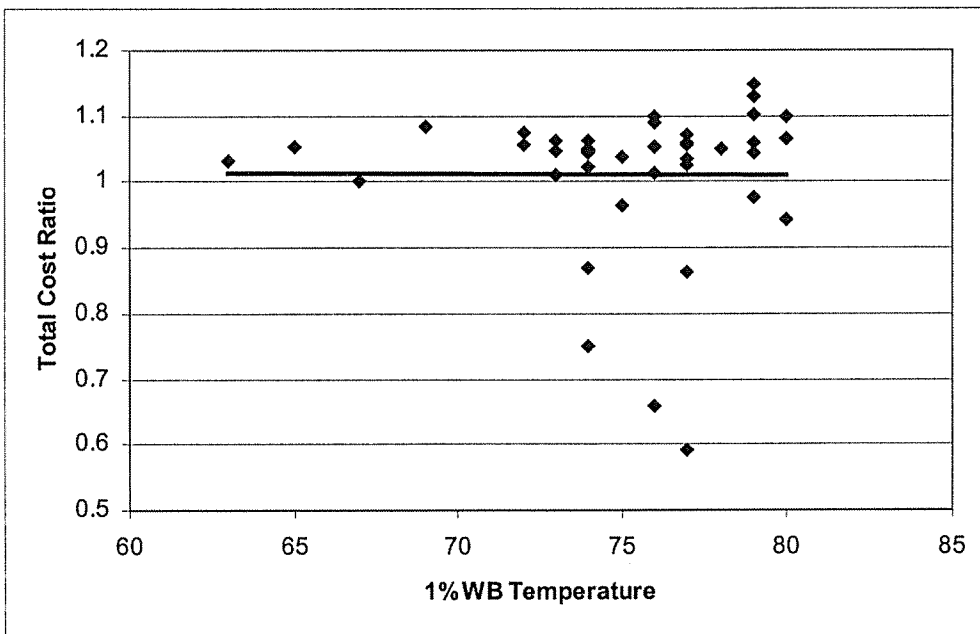


Figure 2.D.8 Effect of Extreme Design Wet-Bulb Temperature. Building: Refrigerated Warehouse

APPENDIX 2.E

EFFECT OF EXTREME DESIGN DEW-POINT TEMPERATURE

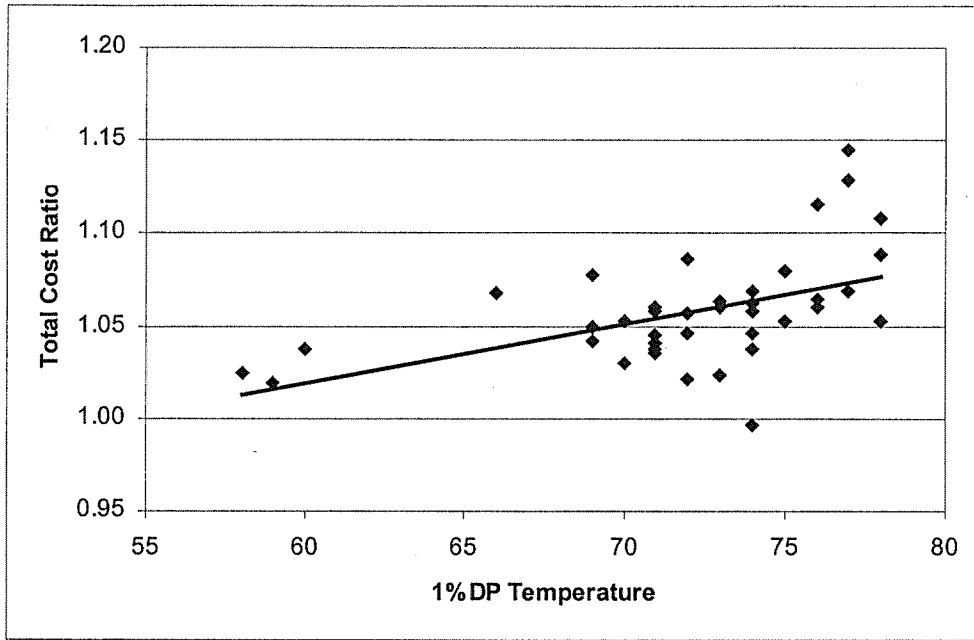


Figure 2.E.1 Effect of Extreme Design Dew-Point Temperature. Building: Hospital

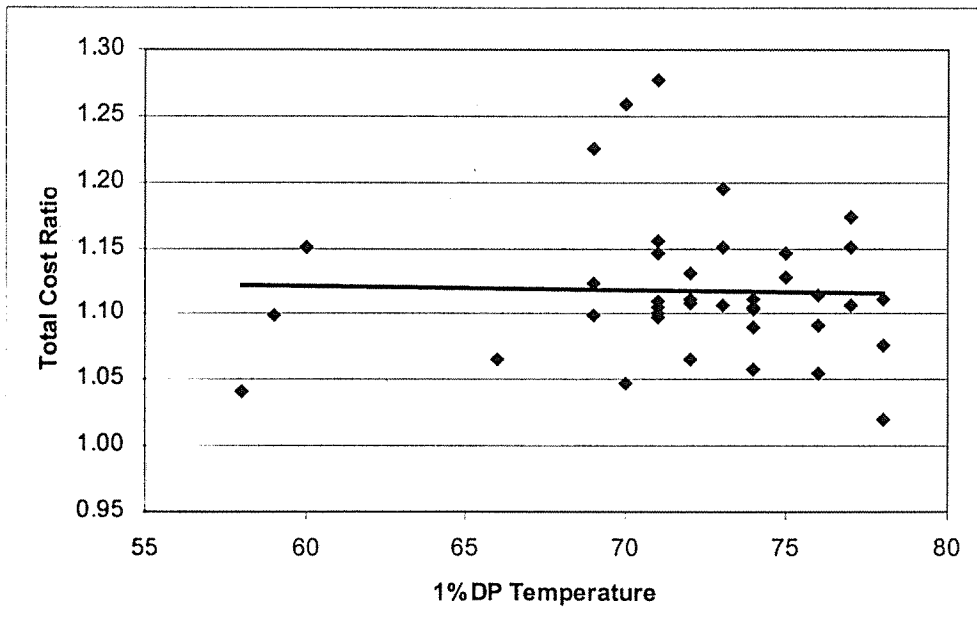


Figure 2.E.2 Effect of Extreme Design Dew-Point Temperature. Building: Large Hotel

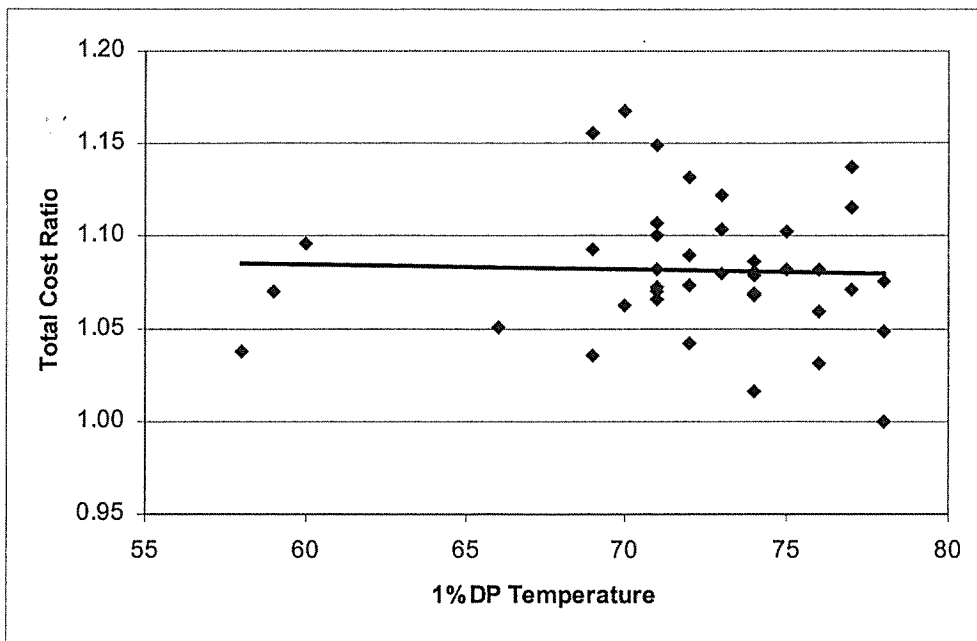


Figure 2.E.3 Effect of Extreme Design Dew-Point Temperature. Building: Nursing Home

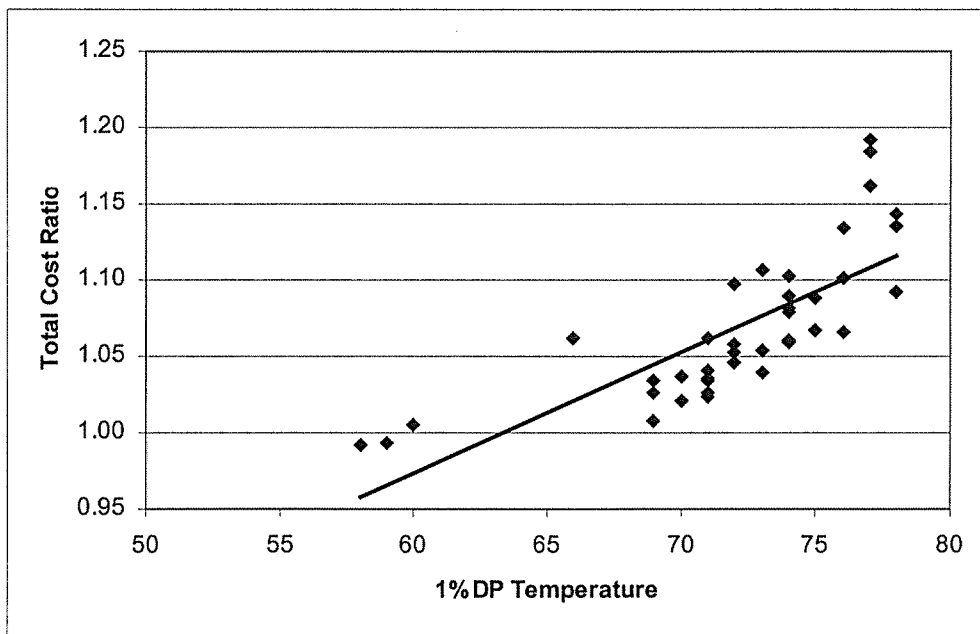


Figure 2.E.4 Effect of Extreme Design Dew-Point Temperature. Building: Quick-Serve Restaurant

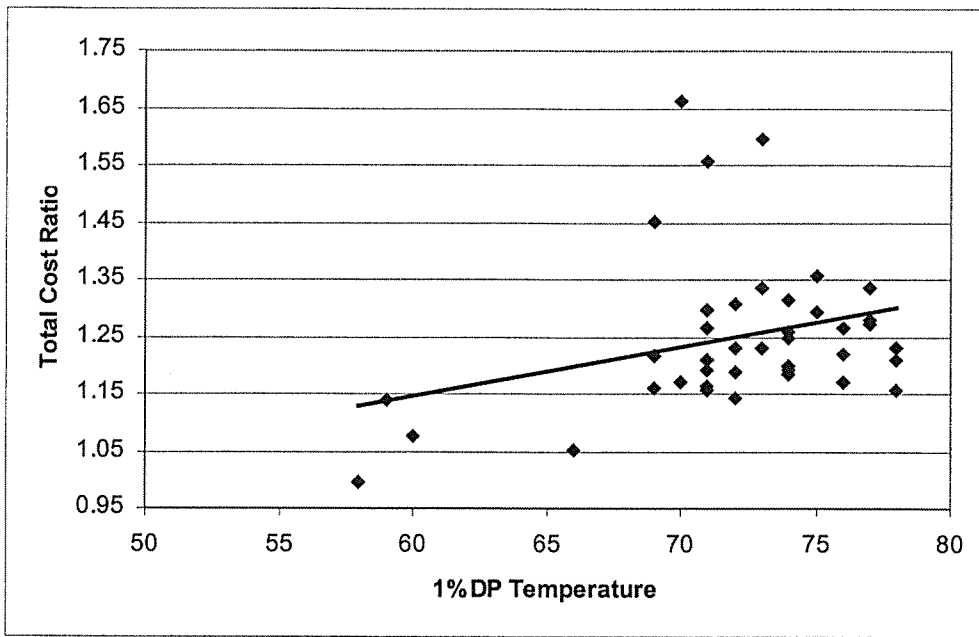


Figure 2.E.5 Effect of Extreme Design Dew-Point Temperature. Building: Retail Store

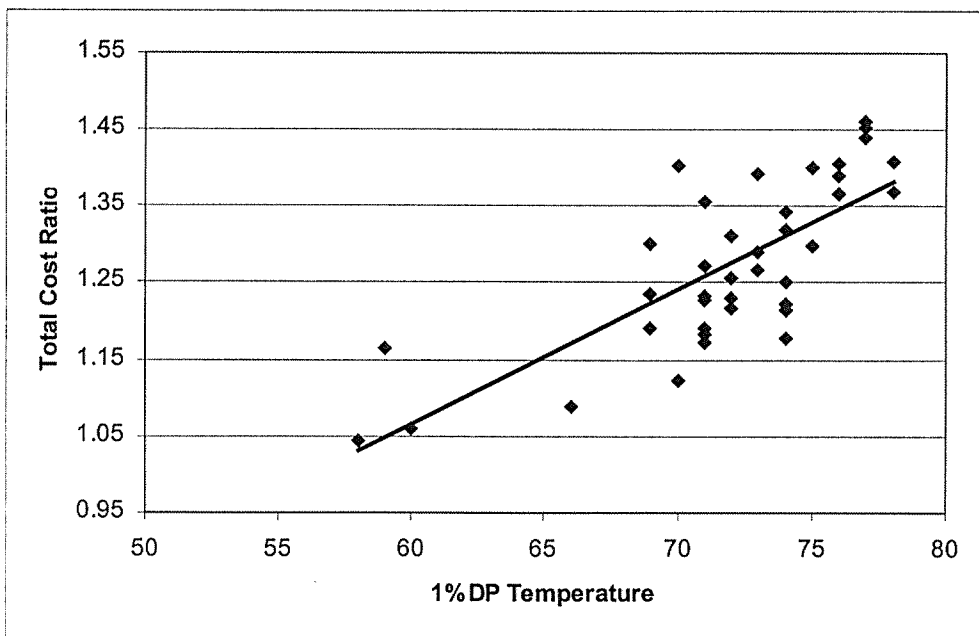


Figure 2.E.6 Effect of Extreme Design Dew-Point Temperature. Building: School

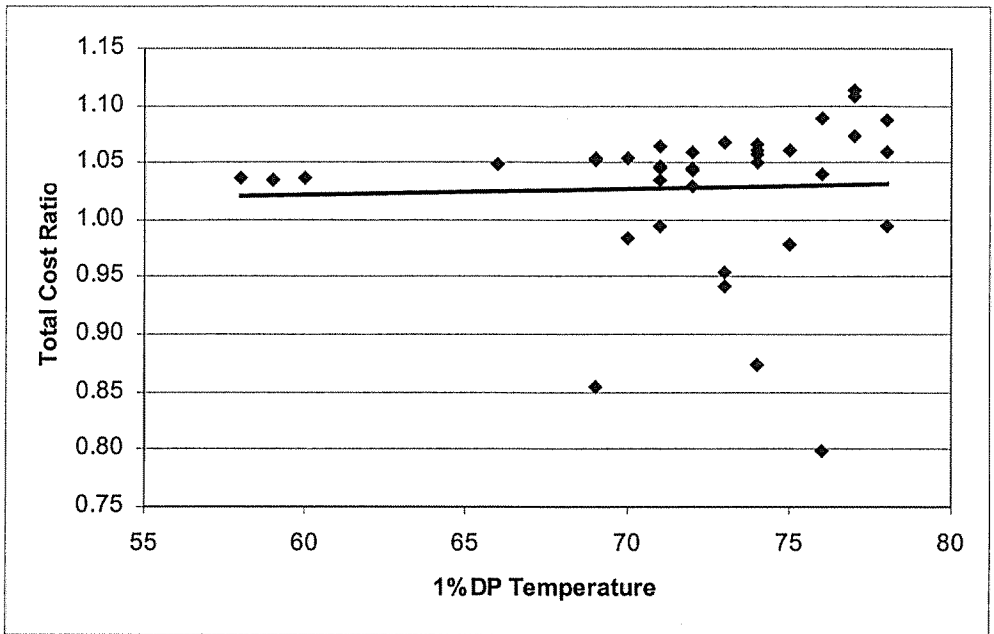


Figure 2.E.7 Effect of Extreme Design Wet-Bulb Temperature. Building: Supermarket

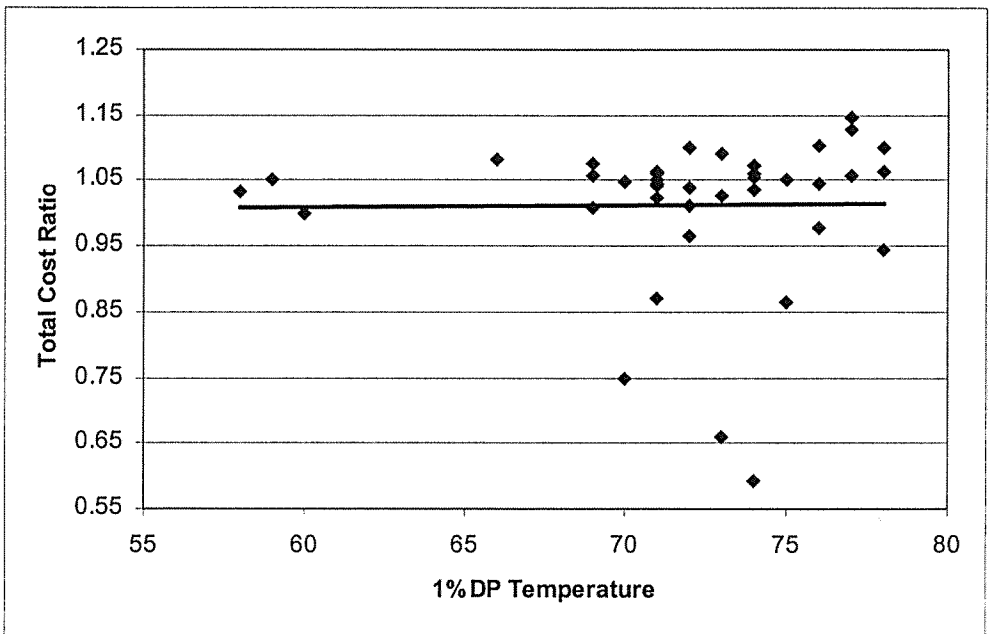


Figure 2.E.8 Effect of Extreme Design Dew-Point Temperature. Building: Refrigerated

APPENDIX 2.F
EFFECT OF LATITUDE

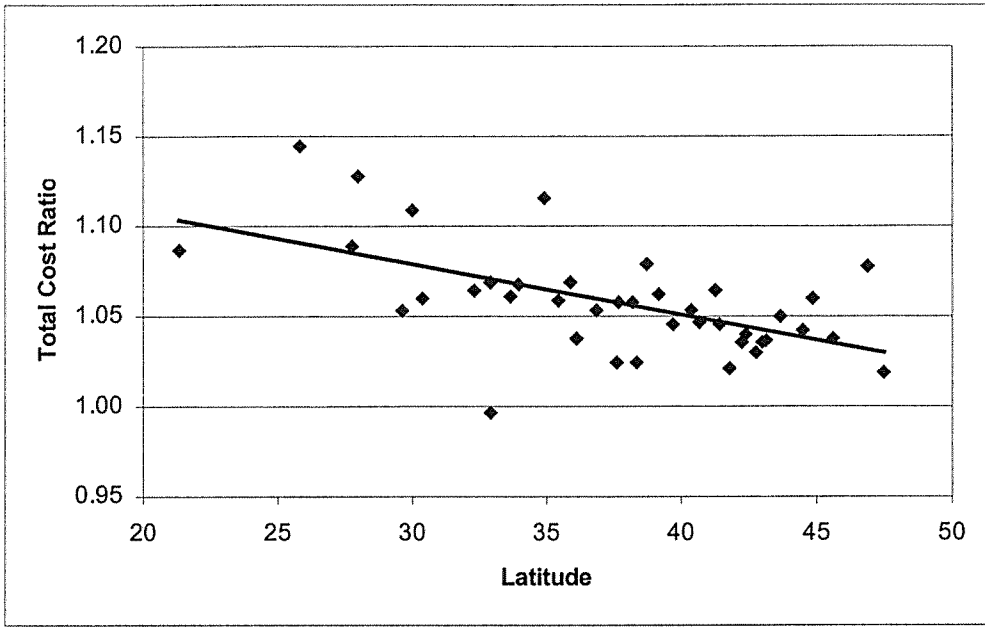


Figure 2.F.1 Effect of Latitude. Building: Hospital

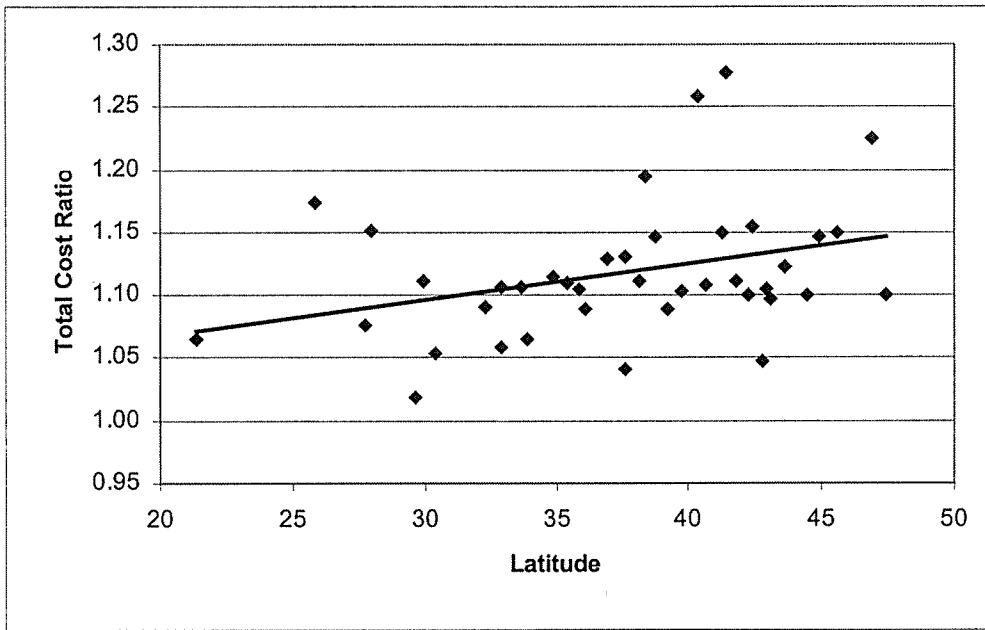


Figure 2.F.2 Effect of Latitude. Building: Large Hotel

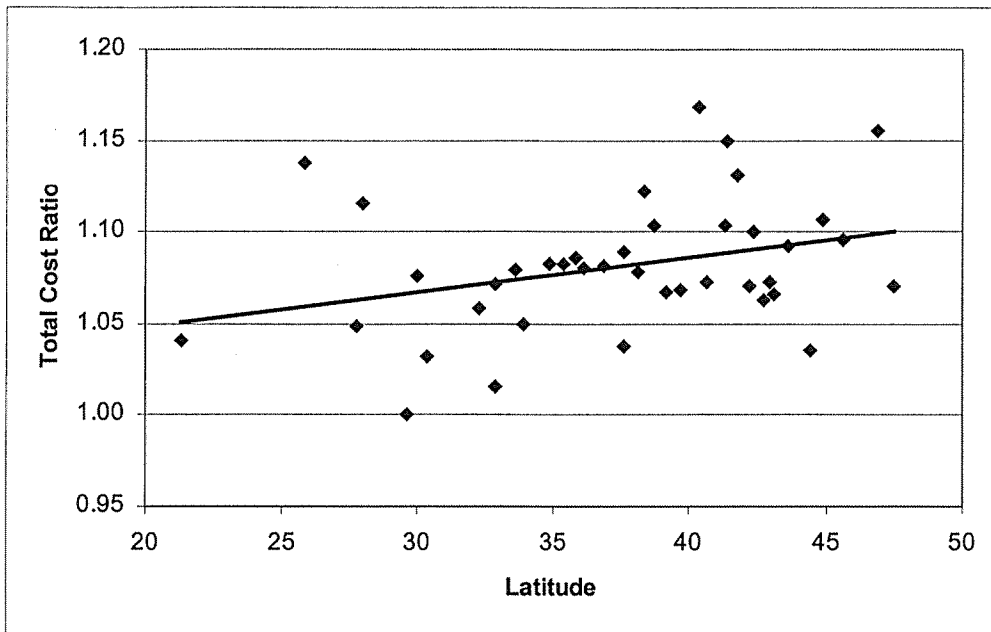


Figure 2.F.3 Effect of Latitude. Building: Nursing Home

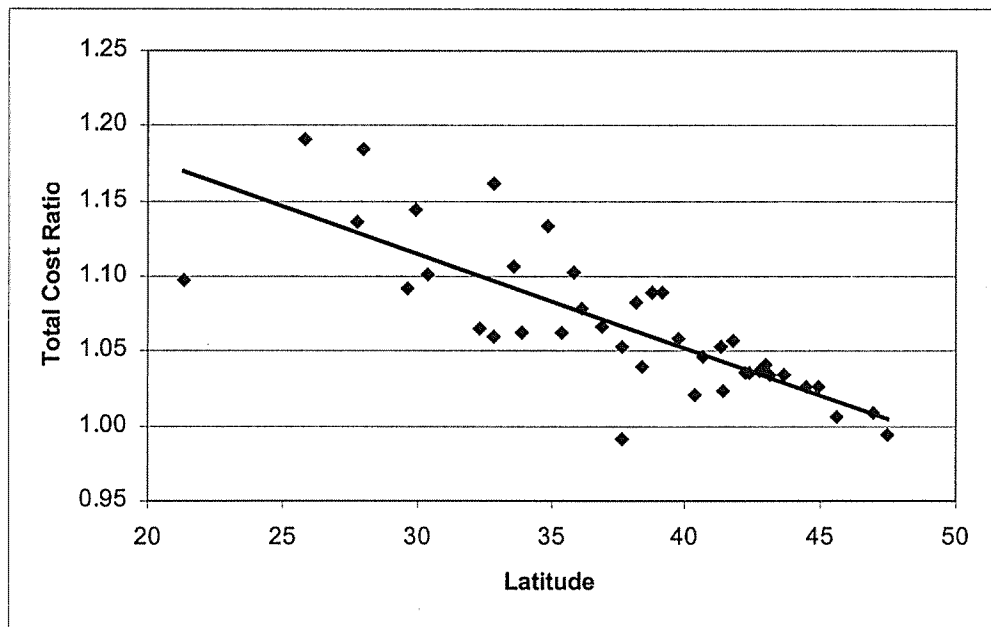


Figure 2.F.4 Effect of Latitude. Building: Quick-Serve Restaurant

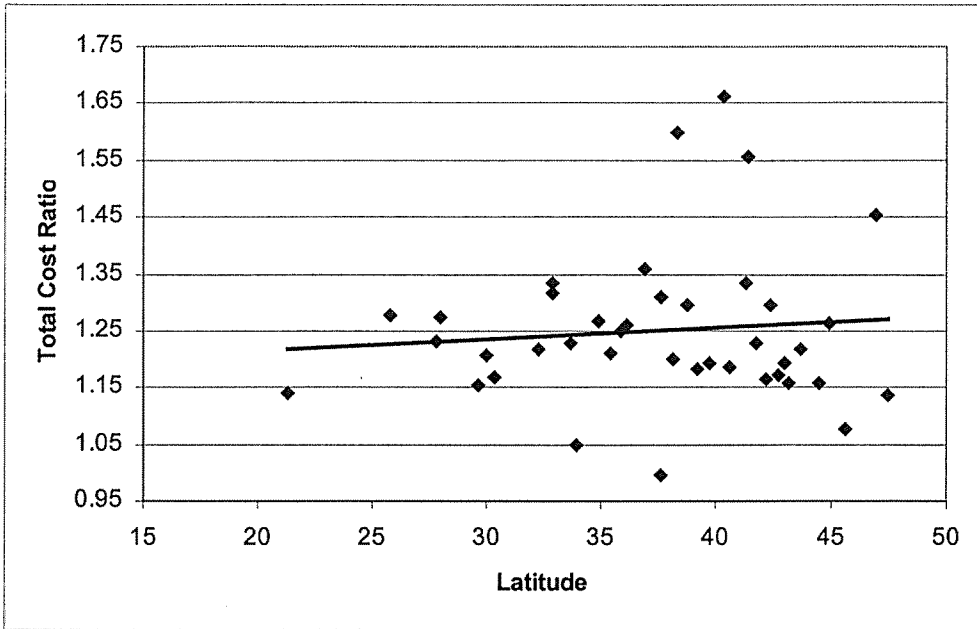


Figure 2.F.5 Effect of Latitude. Building: Retail Store

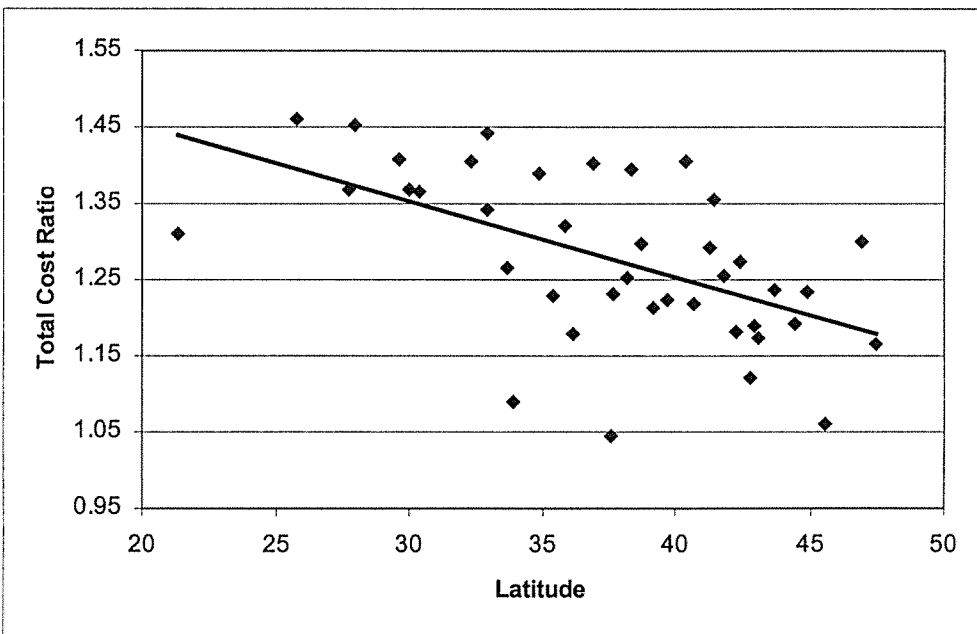


Figure 2.F.6 Effect of Latitude. Building: School

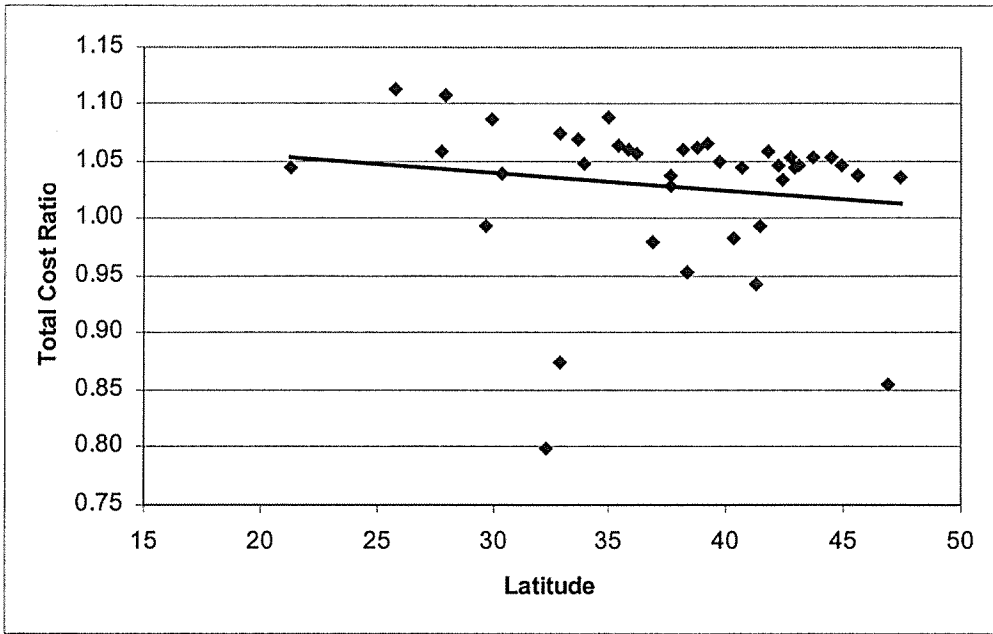


Figure 2.F.7 Effect of Latitude. Building: Supermarket

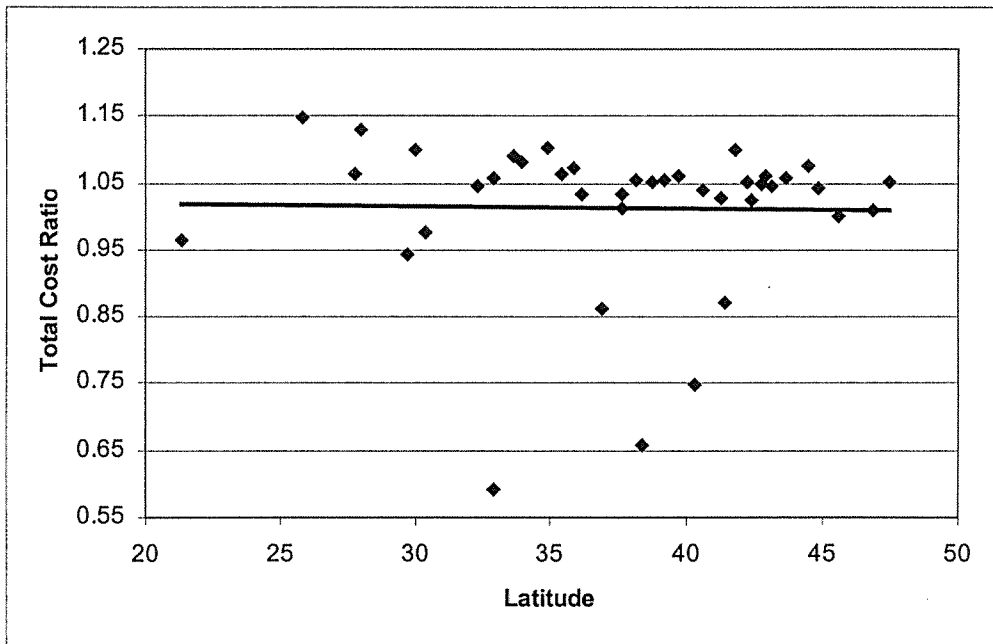


Figure 2.F.8 Effect of Latitude. Building: Refrigerated Warehouse

APPENDIX 2.G
EFFECT OF HEATING TEMPERATURE

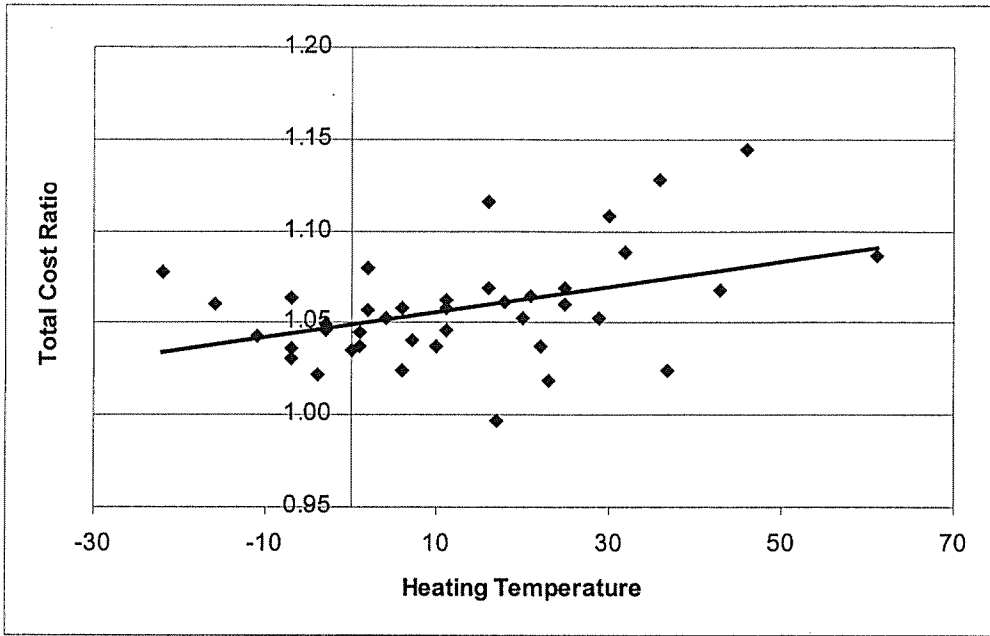


Figure 2.G.1 Effect of Heating Temperature. Building: Hospital

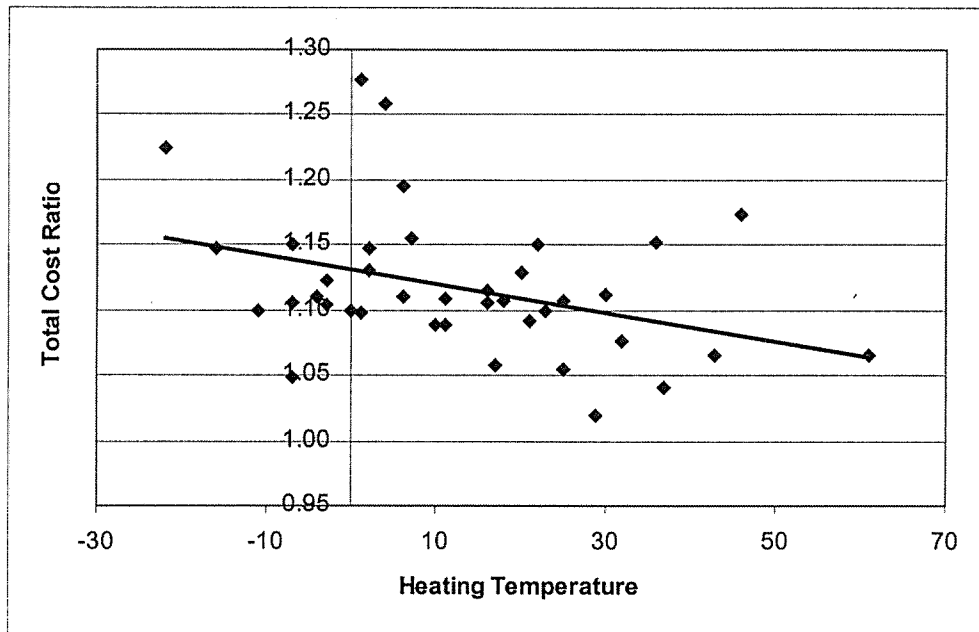


Figure 2.G.2 Effect of Heating Temperature. Building: Large Hotel

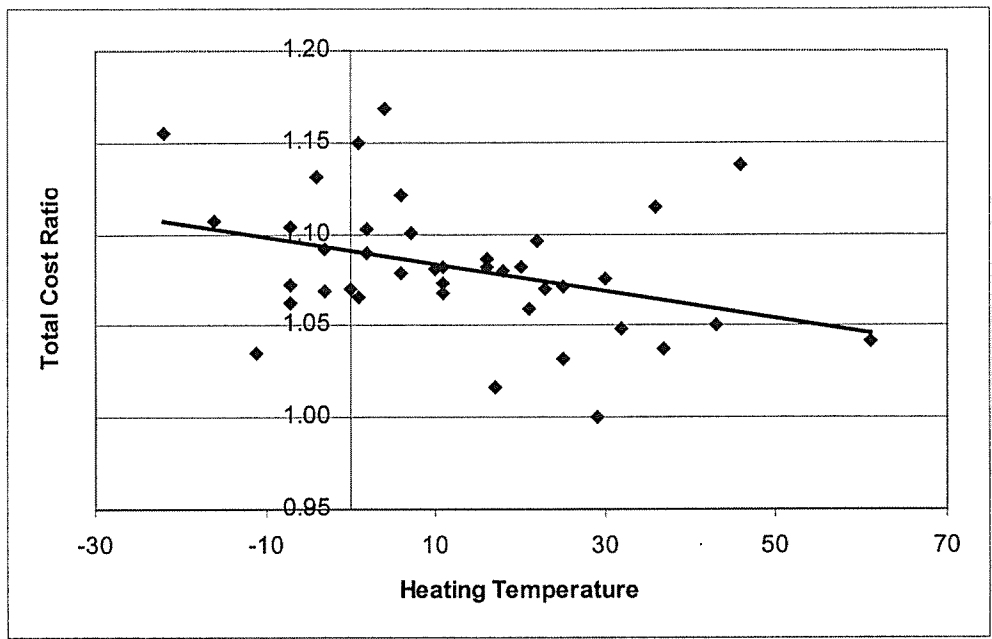


Figure 2.G.3 Effect of Heating Temperature. Building: Nursing Home

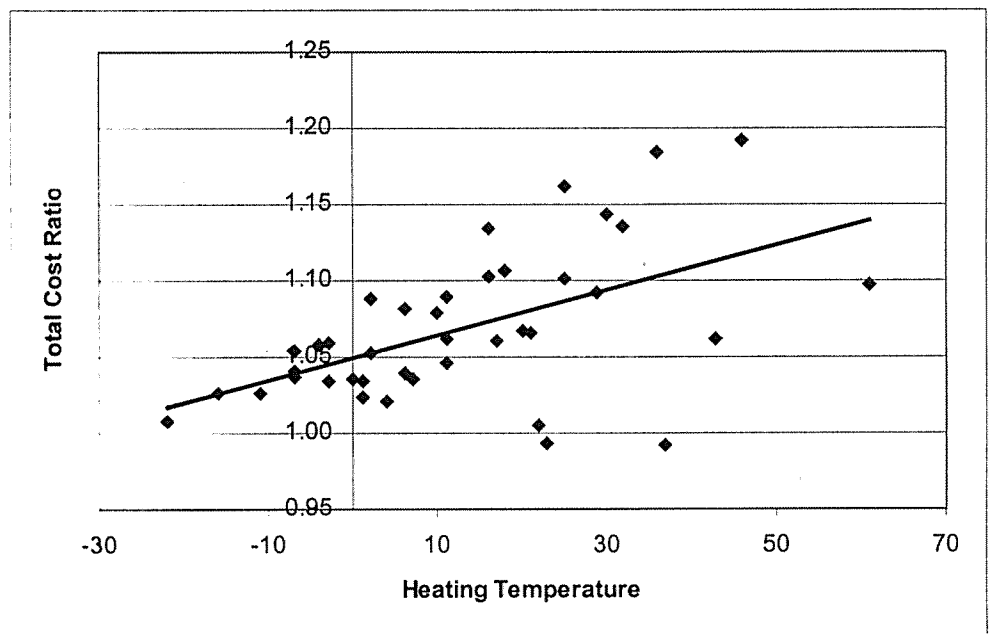


Figure 2.G.4 Effect of Heating Temperature. Building: Quick-Serve Restaurant

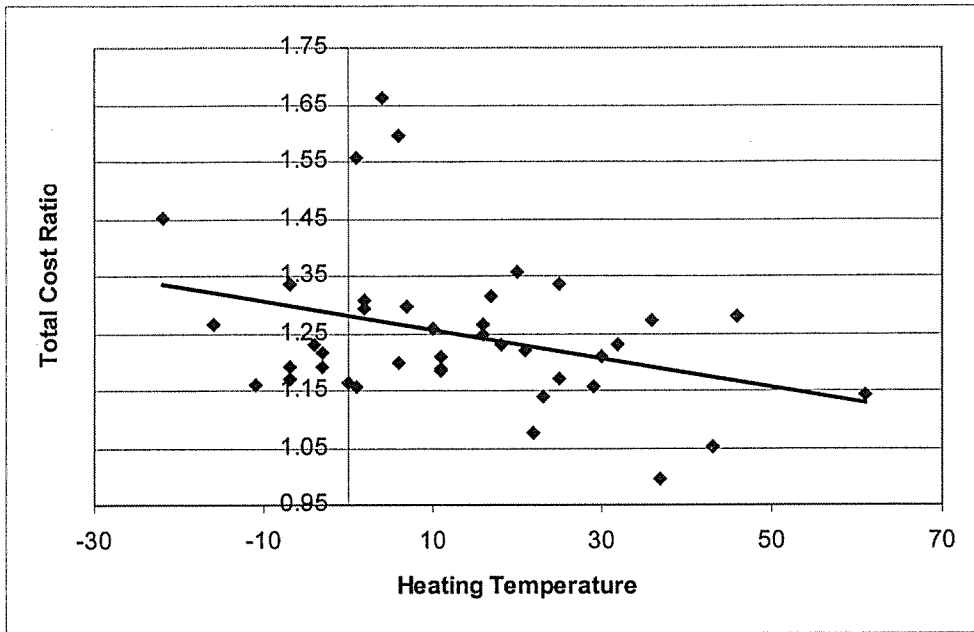


Figure 2.G.5 Effect of Heating Temperature. Building: Retail Store

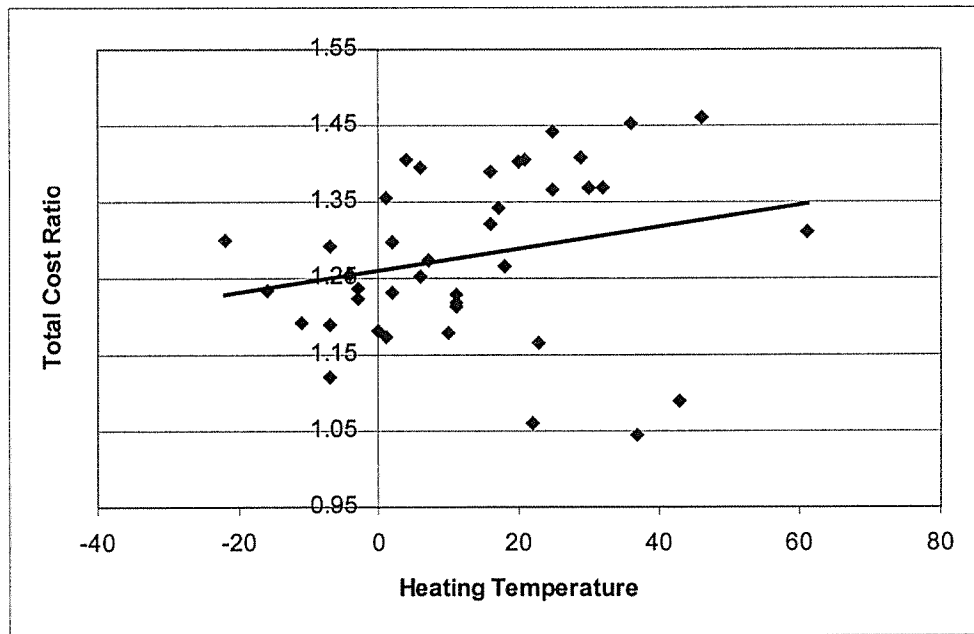


Figure 2.G.6 Effect of Heating Temperature. Building: School

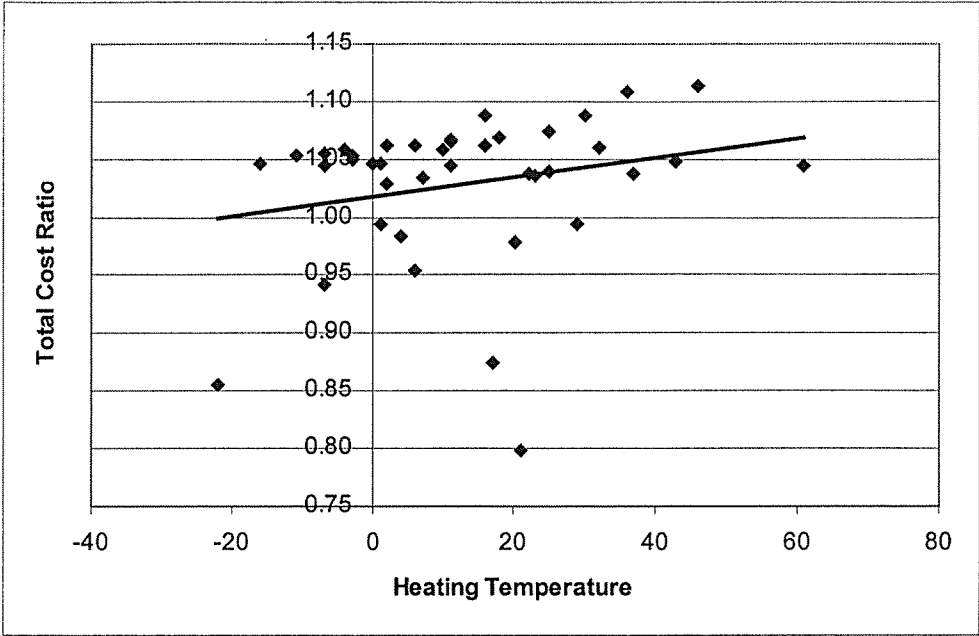


Figure 2.G.7 Effect of Heating Temperature. Building: Supermarket

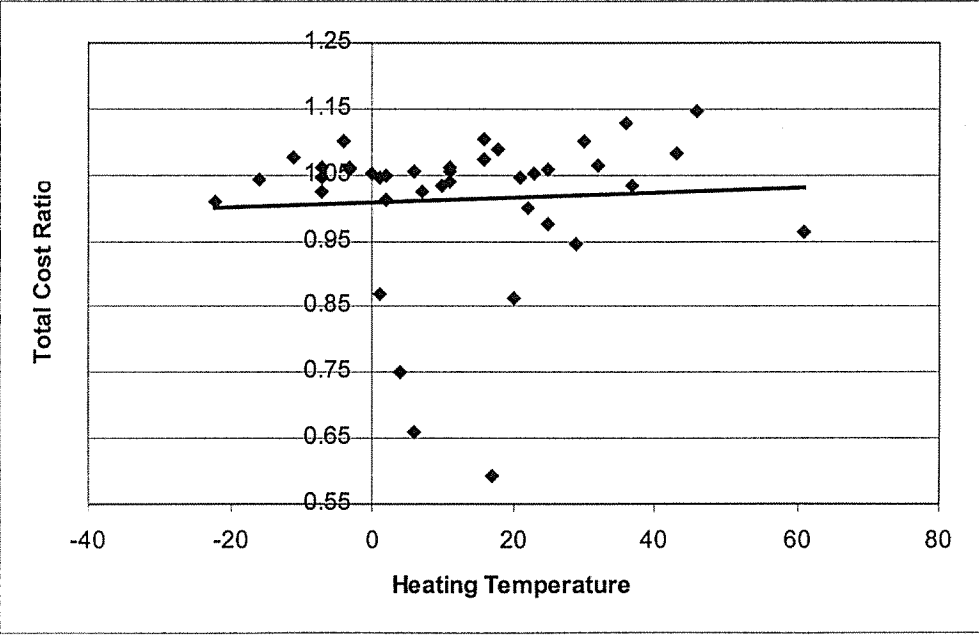
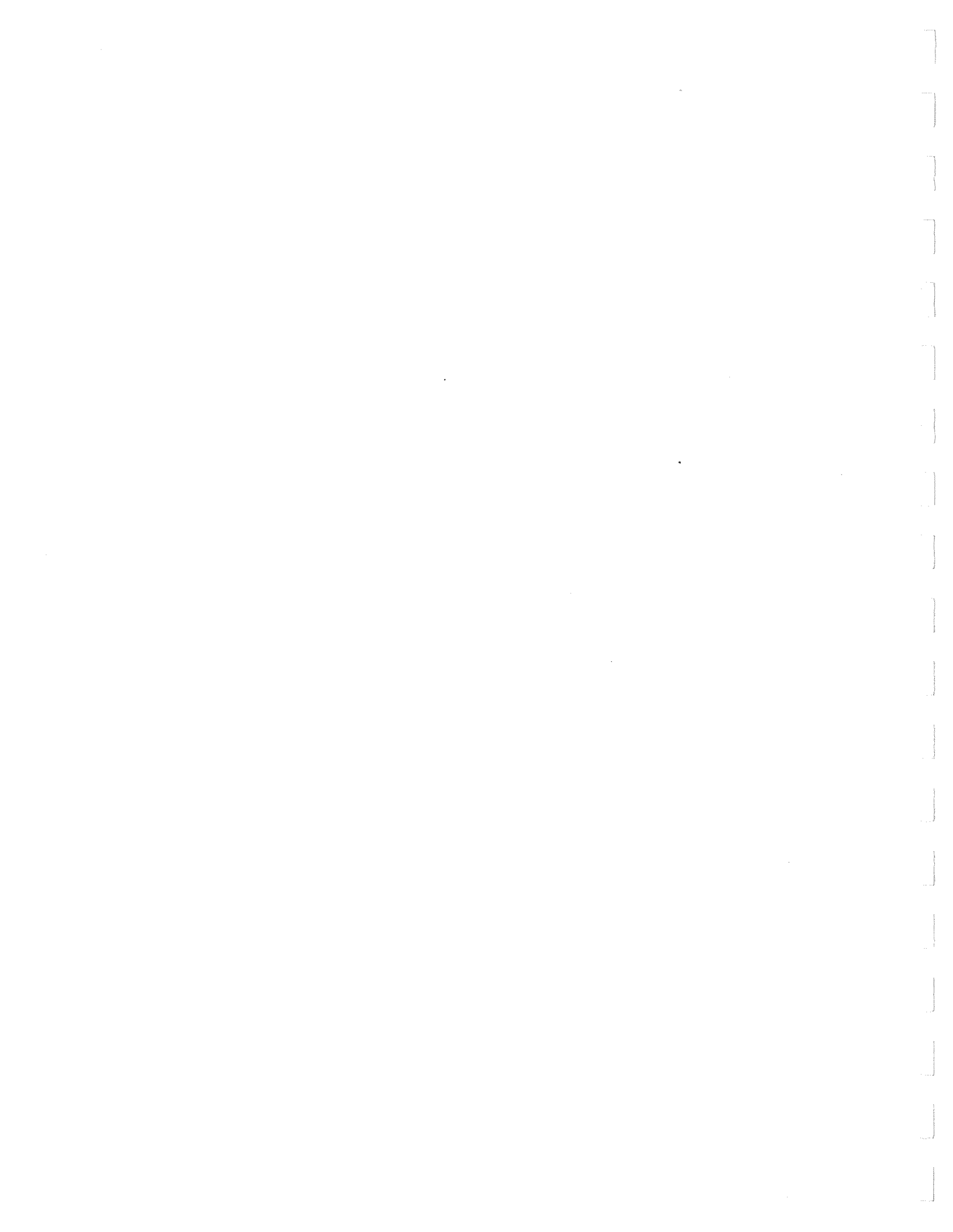


Figure 2.G.8 Effect of Heating Temperature. Building: Refrigerated Warehouse



CHAPTER 3

HUMAN COMFORT STUDIES

3.1 INTRODUCTION

3.1.1 Background

The American Society of Heating, Refrigerating and Air-Conditioning Engineers (ASHRAE) defines thermal comfort as “that condition of mind in which satisfaction is expressed with the thermal environment.” Basically, thermal comfort is influenced by four environmental parameters and two personal parameters. The environmental parameters are dry bulb temperature, mean radiant temperature, relative humidity and air velocity. The personal parameters that can significantly affect the perception of thermal comfort are clothing insulation and level of activity.

Professor John Sheppard first introduced the term “comfort zone” during the period 1913 to 1923 (Houghten and Yaglou, 1923). Houghten and Yaglou (1923) introduced the term effective temperature (ET) by combining the dry bulb temperature and the relative humidity into a single index. The first comfort chart was published in 1924 in the *American Society of Heating and Ventilating Engineers (ASHVE) Transactions*. Yaglou and Drinker (1929) modified the 1924 ASHVE comfort chart. The first minimum code for air conditioning comfort was published in the *ASHVE Transactions* in 1938. Because additional knowledge on the subject was crucial and long-term programs were anticipated, the first ASHRAE Research Laboratory was formed by Koch, Jennings, and Humphreys in Cleveland in 1956 (Koch et al. 1960). In 1958, the first data on human comfort were produced, and the data were presented the following year. An ASHRAE standard on thermal environment conditions for human occupancy was first introduced in 1966. In 1974, 1981, 1992, and 1995 the standard was revised and reissued.

ANSI/ASHRAE Standard 55 is the standard for “Thermal Environmental Conditions for Human Occupancy.” This standard specifies conditions for which 80 percent of sedentary (or slightly active) persons find the environment thermally acceptable. Figure 3.1 shows the acceptable regions of temperature and humidity for people in typical summer or winter clothing during light and sedentary activity. The Comfort Zone is based on a 20 percent dissatisfaction criterion, which means 20 percent of the test subjects will feel discomfort.

The 1981 ASHRAE Comfort Zone permitted relative humidities above 70 %, which lead to mildew and fungi growth. In 1992 the Comfort Zone was modified to limit relative humidity to 60%. The latest revision (the 1995 Comfort Zone) is shown in Figure 3.1. In this figure, the *operative temperature* is the uniform temperature of an imaginary black enclosure in which an occupant would exchange the same heat by radiation and convection as in the actual environment and is numerically the average of the ambient air temperature and mean radiant temperature, weighted by their respective heat transfer coefficients. For the 1995 ASHRAE Comfort Zone, the comfort regions in summer and winter are delineated as follows:

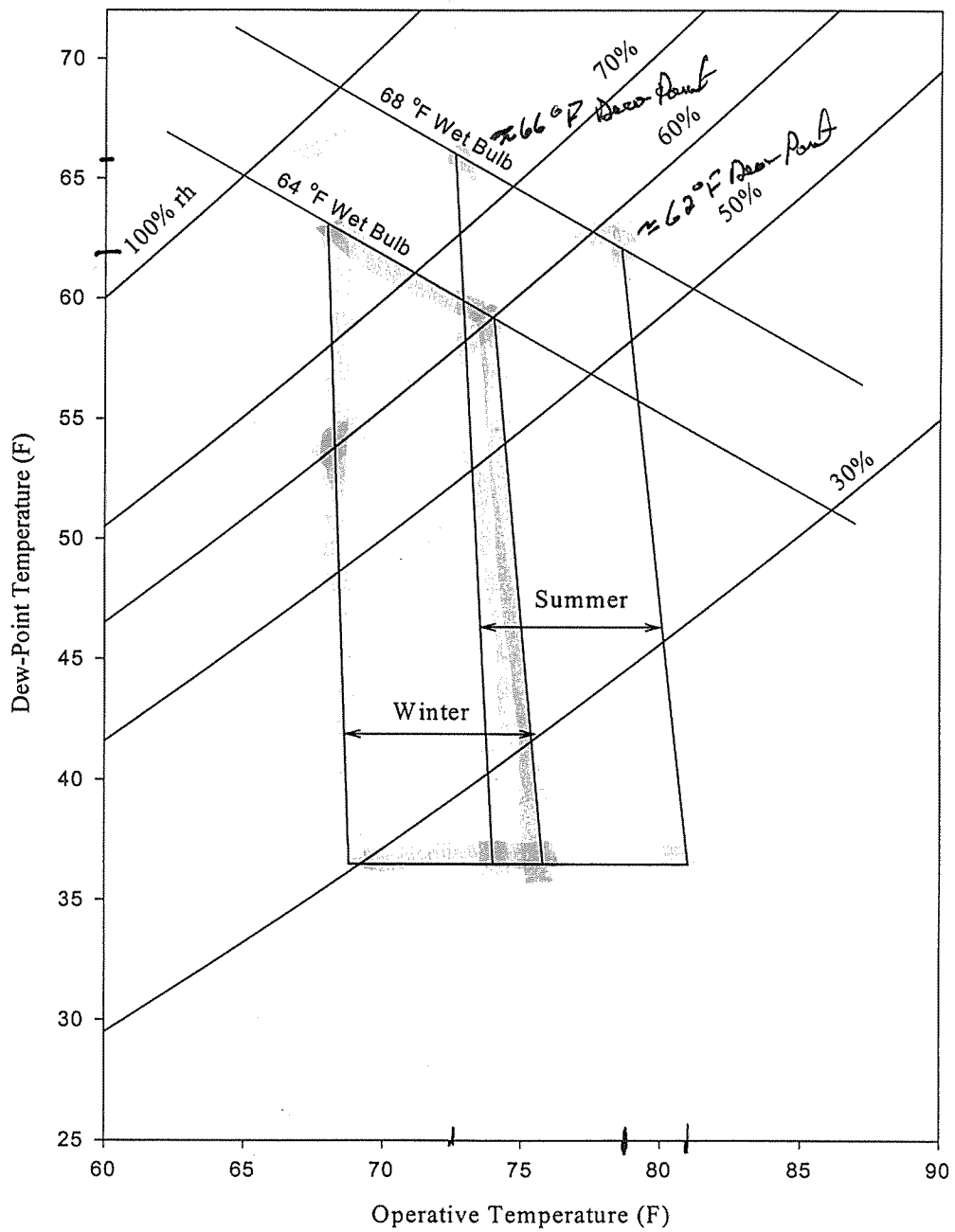


Figure 3.1 1995 ASHRAE Comfort Zone

Summer The left and right boundaries correspond to effective temperature lines of 73°F and 79°F, respectively. The lower boundary corresponds to 36°F dewpoint, and the upper boundary corresponds to 68°F wet bulb.

Winter The left and right boundaries correspond to effective temperature lines of 68°F and 74°F, respectively. The lower boundary corresponds to 36°F dewpoint, and the upper boundary corresponds to 64°F wet bulb.

The *effective temperature* is the operative temperature of an enclosure at 50% relative humidity in which an occupant would exchange the same total heat (sensible plus latent) as in the actual environment. Although ASHRAE Standard 55-1995 allows relative humidity to exceed 60% based on consideration of thermal comfort only, other standards governing indoor air quality such as ASHRAE Standard 62 impose limits on relative humidity (30% to 60%) to prevent the growth of mildew and fungi.

ASHRAE Standard 55 as well as the chapter on “Thermal Comfort” in the ASHRAE *Fundamentals Handbook* is based on limited experimental data from studies of human thermal comfort and, to a larger extent, predictions using analytical or empirical models of human responses to the thermal environment. A method widely used in both experimental and analytical comfort studies is known as the Standard Thermal Sensation Scale. In this scale, a subject’s conscious feeling is graded into the categories shown in Table 3.1.

Table 3.1 Standard Thermal Sensation Scale (ASHRAE)

<u>Thermal Sensation</u>	<u>Numerical Code</u>	<u>Vote Number</u>
Hot	+ 3	1
Warm	+ 2	2
Slightly Warm	+ 1	3
Neutral	0	4
Slightly Cool	- 1	5
Cool	- 2	6
Cold	- 3	7

The thermal sensation is represented with a vote from 1 to 7 and with a numerical value from + 3 to – 3. A numerical value of + 3 is the same as a vote 1 which corresponds to a “hot” thermal sensation. The vote of numerical code “0” was changed from “comfortable” to “neutral” since a person would prefer neither a warmer nor a cooler environment when the body is thermally neutral. Even though a person may feel “slightly warm” (vote number 3) or “slightly cool” (vote number 5), with a vote of 3 to 5, most occupants would feel comfortable with the thermal environment of the occupied space.

The Standard Thermal Sensation Scale originated from Fanger’s (1967) Predicted Mean Vote (PMV) which he related to a Predicted Percentage Dissatisfied (PPD), a method used to predict acceptable and unacceptable comfort conditions for occupants. According to Fanger,

occupants will begin to feel discomfort at numerical values beyond ± 1 from the neutral thermal sensation. Figure 3.2 shows a plot of the PPD as a function of the PMV. From this figure, when the mean vote (PMV) is ± 1 , 28 % of the occupants are dissatisfied. As the mean vote deviates from zero, the value of the PPD increases. A derivative of this method has been incorporated into the ASHRAE Thermal Comfort Program (WinComf) (www.dnai.com/~fountain/) developed by Fountain and Huizenga (1995).

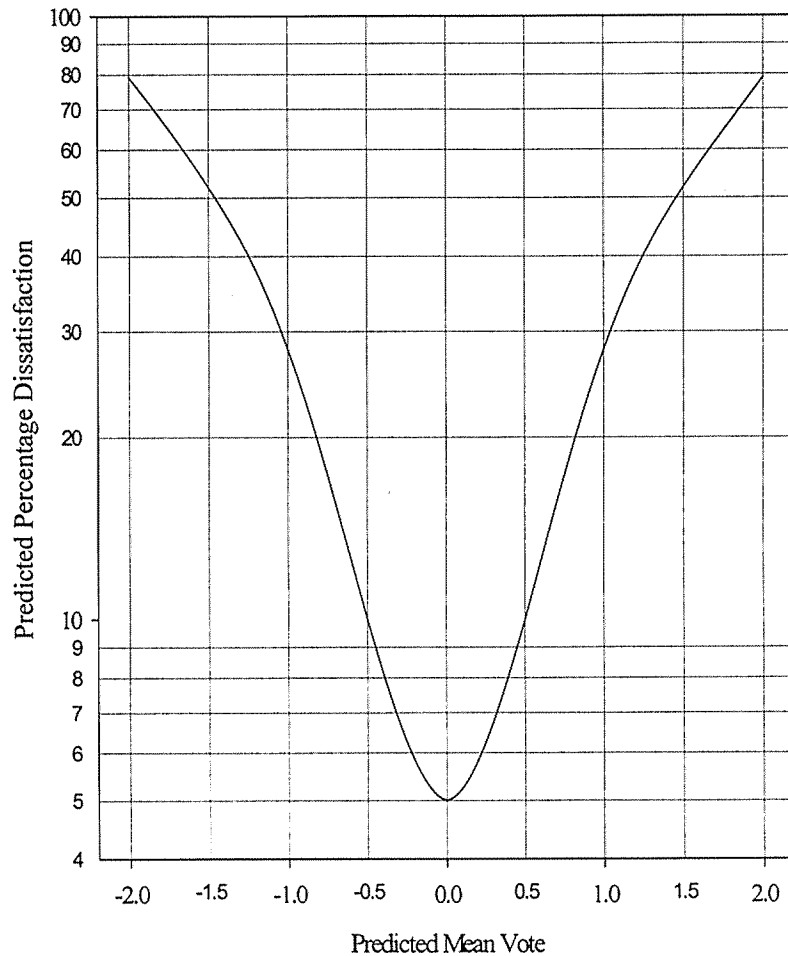


Figure 3.2 Predicted Percentage Dissatisfaction (PPD) as Function of Predicted Mean Vote (PMV) [ASHRAE (2001)]

3.1.2 Purpose of This Research

Within the overall objective of promoting the use of desiccant-based equipment within the mainstream building air conditioning market, the purpose of this particular research task is as follows: Review existing literature on air-conditioning-related human comfort studies and experiments. Based on findings of the literature survey, develop a test plan and implement a test using human subjects to gather and evaluate additional data on the effects of the thermal environment on human comfort. Finally, compare the results to the ASHRAE Comfort Zone.

The contents of this chapter are arranged according to the order of tasks in the above-stated purpose. The literature survey is contained in Section 3.2. Section 3.3 describes the experimental study conducted on the basis of the literature review. In Section 3.4, the data obtained from these tests are compared to the ASHRAE Standard 55-1995 Comfort Zone and the Fanger (1982) steady-state-energy-balance thermal comfort model on which much of the ASHRAE Standard 55 is based. Section 3.5 examines the experimental data in accordance with one of the newer approaches for evaluation of thermal comfort (Laviana and Rohles, 1987). Finally, conclusions are drawn in Section 3.6.

3.2 LITERATURE SURVEY

As mentioned in the Introduction, human thermal comfort is dependent on four environmental parameters (dry bulb temperature, mean radiant temperature, relative humidity, and air velocity) and two personal parameters (activity level and clothing insulation). These parameters have been the subject of considerable research, as evident from the following review of the literature. Before proceeding with the literature survey, a brief introduction of each of the environmental and personal parameters is in order.

The dry bulb temperature is basically the ambient air temperature. By definition, the radiant temperature is the temperature of an exposed surface in the environment. The temperatures of individual surfaces are usually combined into a mean radiant temperature. The mean radiant temperature can be further explained as the uniform surface temperature of an imaginary black enclosure in which an occupant would exchange the same amount of radiant heat as in the actual nonuniform-surface-temperature space. The effects of mean radiant temperature are generally more applicable to heating than to air conditioning (cooling); therefore, such studies are not included in this survey.

The relative humidity of moist air is by definition the ratio of the partial pressure of water vapor to the saturation pressure of water corresponding to the dry bulb temperature, expressed as a percentage. It can be interpreted as the actual moisture content (humidity) of the air relative to the air's maximum possible moisture content corresponding to the dry bulb temperature. Equally valid measures of humidity are dewpoint temperature, wet-bulb temperature, humidity ratio, degree of saturation, and vapor pressure. These variables, combined with dry bulb temperature, all are measure of humidity and are often referred to as psychrometric variables. Vapor pressure is the form used in the Fanger (1982) model because vapor pressure is most directly related to the physics and physiology of evaporative heat loss. Although most human comfort studies related to humidity are expressed in terms of relative humidity or dewpoint, given any two

psychrometric variables, the corresponding vapor pressure, or any other psychrometric variable, can be determined from psychrometric relations or charts such as those published in the ASHRAE *Fundamentals Handbook* (2001).

The importance of air velocity in human comfort is evident in the recommended selection procedures published in catalogs of major air distribution component manufacturers. Grilles and diffusers are selected based on capacity (cfm) corresponding to a particular noise level and throw (ft), which is the distance from the diffuser for which the jet issuing from the diffuser reaches terminal velocity (i.e., 50 fpm, which is the maximum recommended velocity for sedentary occupants in summer clothing according to ASHRAE Standard 55).

Activity level (resting, walking, etc.) is expressed in terms of measurable physical units as the metabolic rate. By ASHRAE definition, the metabolic rate is the rate of energy production of the body and is expressed in met units. One met is defined as $18.4 \text{ Btu/hr}\cdot\text{ft}^2$, which is the energy produced per unit surface area of a seated person. The ASHRAE Comfort Zone is valid for metabolic rates no greater than 1.2 met. Estimated met levels for other levels of activity are found in the ASHRAE *Fundamentals Handbook* (2001).

Clothing insulation is measured in terms of the unit clo, defined as the resistance to sensible heat transfer provided by a clothing ensemble (more than one garment). One clo is equivalent to $0.880 \text{ }^\circ\text{F}\cdot\text{ft}^2\cdot\text{h/Btu}$ and is described as the intrinsic insulation from the skin to the clothing surface, not including the resistance provided by the air layer around the clothed body. The ASHRAE *Fundamentals Handbook* (2001) lists estimates of clothing insulation values for various clothing ensembles.

Organization of the literature review into the effects of each of the above parameters on thermal comfort is difficult because the interrelations among the parameters affecting thermal comfort are complex. A small number of the studies varied a single parameter while holding other parameters constant. The majority, however, varied two or more parameters. The order of discussion, therefore, is based on the logic of the following paragraph.

First examined are those studies which considered the effects of only a single parameter. These are, in order, dry bulb temperature only and relative humidity only. Next are the studies which examined the coupled effects of two or more parameters on thermal comfort. These are the coupled effects of dry bulb temperature, humidity, and activity level followed by the coupled effects of velocity, dry bulb temperature, and humidity. At this point, the discussion will link the previously discussed studies of human perception of thermal comfort (psychological responses) to studies of human physiological responses to the parameters which affect thermal comfort. The final studies examined are those which use models of human physiological responses to predict human psychological responses (i.e., the perception of thermal comfort) to the thermal environment. The findings of the literature survey are used to form the basis for the experimental study of Section 3.3

3.2.1 The Effects of Dry Bulb Temperature on Thermal Comfort

Sprague and McNall (1970) conducted a two-part study on the effects of fluctuating temperature and relative humidity on the thermal sensation (thermal comfort) of sedentary subjects. A total of 156 subjects (78 male and 78 female) participated in the test for fluctuating temperature. The experiment was conducted at the KSU-ASHRAE Environmental Test Chamber. The subjects wore KSU Standard Clothing (cotton twill shirt, trousers, and sweat socks) of about 0.6 clo. The test conditions for the temperature fluctuations ranged from a peak-to-peak amplitude of 5 °F with a period of a half-hour to a peak-to-peak amplitude of 6 °F with a period of one hour. The air velocity was held constant at either 25 or 30 ft/min. The mean radiant temperature remained constant at 78 °F, and the mean dry bulb temperature for the tests was 79 °F. Sprague and McNall concluded that for conditioned spaces where dry bulb air temperatures fluctuate periodically, no serious occupancy complaints would occur due to temperature fluctuations if $[\Delta T^2 \times (\text{CPH})] < 15$, where ΔT (°F) is the peak-to-peak amplitude of the temperature fluctuation and CPH (cycles/hr) is the cycling frequency.

Fanger (1972) reported the preferred ambient temperature for various subjects according to age, geographic nationality, and gender. The results are tabulated in Tables 3.2, 3.3, and 3.4. In these studies, the clothing insulation, relative velocity, and relative humidity were held constant at 0.6 clo, 0.1 m/s, and 50%, respectively. In all cases, the mean radiant temperature was equal to the ambient air temperature.

Table 3.2 Comfort Conditions for Different Age Groups (Fanger, 1972)

Sedentary Activity, Clothing: 0.6 clo, Rel. Velocity < 0.1 m/s (19.7 ft/min), Relative Humidity: 50%, Mean Radiant Temperature = Air temperature

Study	Mean Age Years	Preferred Ambient Temp. (°C)	Mean Skin Temp. at Comfort (°C)	Evaporative Weight Loss During Comfort (g/m ² -h)	Number of Subjects
Nevins et al 1966	21	25.6 (78.1 °F)			720
Fanger 1970	23	25.7 (78.3 °F)		19.2* (3.93 x 10 ⁻³ lb/ft ² -h)	128
Fanger 1970	68	25.7 (78.3 °F)		15.3* (3.13 x 10 ⁻³ lb/ft ² -h)	128
Rohles et al 1972	74	24.5 (76.1 °F)			228
Tech. Univ. of Denmark 1972	24	25.4 (77.7 °F)	33.5 (92.3 °F)	19.2 (3.93 x 10 ⁻³ lb/ft ² -h)	32
Tech. Univ. of Denmark 1972	84	25.4 (77.7 °F)	33.2 (91.8 °F)	12.4 (2.54 x 10 ⁻³ lb/ft ² -h)	16
Comfort Equation Fanger 1967		25.6 (78.1 °F)			

* The originally published data for weight loss were slightly higher, since the weight loss due to the dry gas exchange was included (expired CO₂ weighs more than inspired O₂: 2.4 g/m²-h (4.92 x 10⁻⁴ lb/ft²-h) for young, 2.1 g/m²-h (4.3 x 10⁻⁴ lb/ft²-h) for elderly).

Table 3.3 Comfort Conditions for Different National-Geographic Groups of People Regularly Exposed to Extreme Cold or Heat (Fanger, 1972)

Sedentary Activity, Clothing: 0.6 clo, Rel. Velocity < 0.1 m/s, Relative Humidity: 50%, Mean Radiant Temperature = Air temperature

Group	Study	Preferred Ambient Temp. (°C)	Mean Skin Temp. at Comfort (°C)	Evaporative Weight Loss During Comfort (g/m ² -h)	Number of Subjects
Americans	Nevins et al 1966	25.6 (78.1 °F)			720
Danes	Fanger 1970	25.7 (78.1 °F)			256
Danes	Tech. Univ. of Denmark 1972	25.4 (77.7 °F)	33.5 (92.3 °F)	19.2* (3.93 x 10 ⁻³ lb/ft ² -h)	32
People from the Tropics	Tech. Univ. of Denmark 1972	26.2 (79.2 °F)	33.5 (92.3 °F)	17.1 (3.5 x 10 ⁻³ lb/ft ² -h)	16
Danes working in the Cold Meat-packing Industry	Olesen et al 1971	24.7 (76.5 °F)	33.6 (92.5 °F)	17.1* (3.5 x 10 ⁻³ lb/ft ² -h)	16
Danish winter swimmers	Tech. Univ. of Denmark 1972	25 (77 °F)	33.3 (91.9 °F)	16.6 (3.4 x 10 ⁻³ lb/ft ² -h)	16
Comfort Equation	Fanger 1967	25.6 (78.1 °F)			

* The originally published data for weight loss were slightly higher, since the weight loss due to the dry gas exchange was included (expired CO₂ weighs 2.4 g/m²-h (4.92 x 10⁻⁴ lb/ft²-h) more than inspired O₂).

Table 3.4 Comfort Conditions for Males and Females (Fanger, 1972)

Sedentary Activity, Clothing: 0.6 clo, Rel. Velocity < 0.1 m/s, Relative Humidity: 50%, Mean Radiant Temperature = Air temperature

Study	Sex	Preferred Ambient Temp. (°C)	Mean Skin Temp. at Comfort (°C)	Evaporative Weight Loss During Comfort (g/m ² -h)	Number of Subjects
Nevins et al 1966	Males	25.4 (77.7 °F)			488
Fanger 1970 (both studies combined)	Females	25.8 (78.4 °F)			488
Tech. Univ. of Denmark 1972	Males	25.5 (77.9 °F)	33.5 (92.3 °F)	21.3 (4.36 x 10 ⁻³ lb/ft ² -h)	16
	Females	25.3 (77.5 °F)	33.4 (92.1 °F)	17.1 (3.5 x 10 ⁻³ lb/ft ² -h)	16
Comfort Equation		25.6 (78.1 °F)			
Fanger 1967					

McIntyre (1975) conducted an experiment at the Electricity Council Research Centre (E.C.R.C.) to determine individual preferred temperatures. Fifteen male employees from E.C.R.C. participated as subjects. The subjects were given remote controls and allowed to select their own preferred temperature. Two starting temperatures were used [26°C (78.8°F) and 19°C (66.2°F)] and were maintained for the first one-half hour of a 2-hour session. Air velocity was less than 0.1 m/s (19.7 ft/min). McIntyre found that a subject's preferred temperature was not affected by the initial temperature in the chamber. A subject's preferred temperature was determined by allowing the subject direct control and by evaluation of the Bedford warmth scale (which is similar to the Standard Thermal Sensation Scale). Two separate tests using the same subjects resulted in a difference in preferred temperature of 1.5°C (2.7°F).

3.2.2 The Effects of Relative Humidity on Thermal Comfort and Health

In the Sprague and McNall (1970) study mentioned in the previous section, 96 subjects (48 male and 48 female) were involved in the test for fluctuating relative humidity. During this test, all other parameters were held constant. The exposure time was 3 hours for all tests. The ranges for the relative humidity fluctuation were a 3 % peak-to-peak fluctuation amplitude with a half-hour fluctuation period and a 14 % peak-to-peak fluctuation amplitude with a fluctuation period of one hour. From the study, the investigators found that there were no serious occupancy complaints from fluctuations of relative humidity.

The relative humidity range is important not only for comfort, but also for health issues. According to Sterling et al. (1985), an increase in relative humidity encourages mildew growth, but low relative humidity can result in respiratory problems due to dryness. They reported that bacterial populations typically increase below 30 % and above 60 % relative humidity. Relative humidity below 40 % may cause respiratory infections. Chemical interaction will take place in high relative humidity environments with the majority of problems occurring for a relative humidity above 50 %. Conversely, ozone production that generates irritants to the mucous and eyes will occur in low relative humidity.

Generally, bacteria and viruses have better chances to survive in high relative humidity. However, Wright et al. (1968) revealed that bacteria such as *mycoplasma laidlawii* prefer relative humidity either above 75 % or below 25 % (Sterling et al., 1985). From the health literature of relevant biological and chemical interactions, Sterling et al. identified an optimal range of humidity where overall health risks would be minimized. Figure 3.3 shows the optimum relative humidity ranges for health, and the bar widths represent the effects of biological contaminants, pathogens causing respiratory problems, and chemical interactions including ozone production with respect to relative humidity. Sterling et al. concluded that the relative humidity range should be between 40 % to 60 %. This range of relative humidity is included in the recommendation for ASHRAE Standard 55 and is illustrated in Figure 3.4.

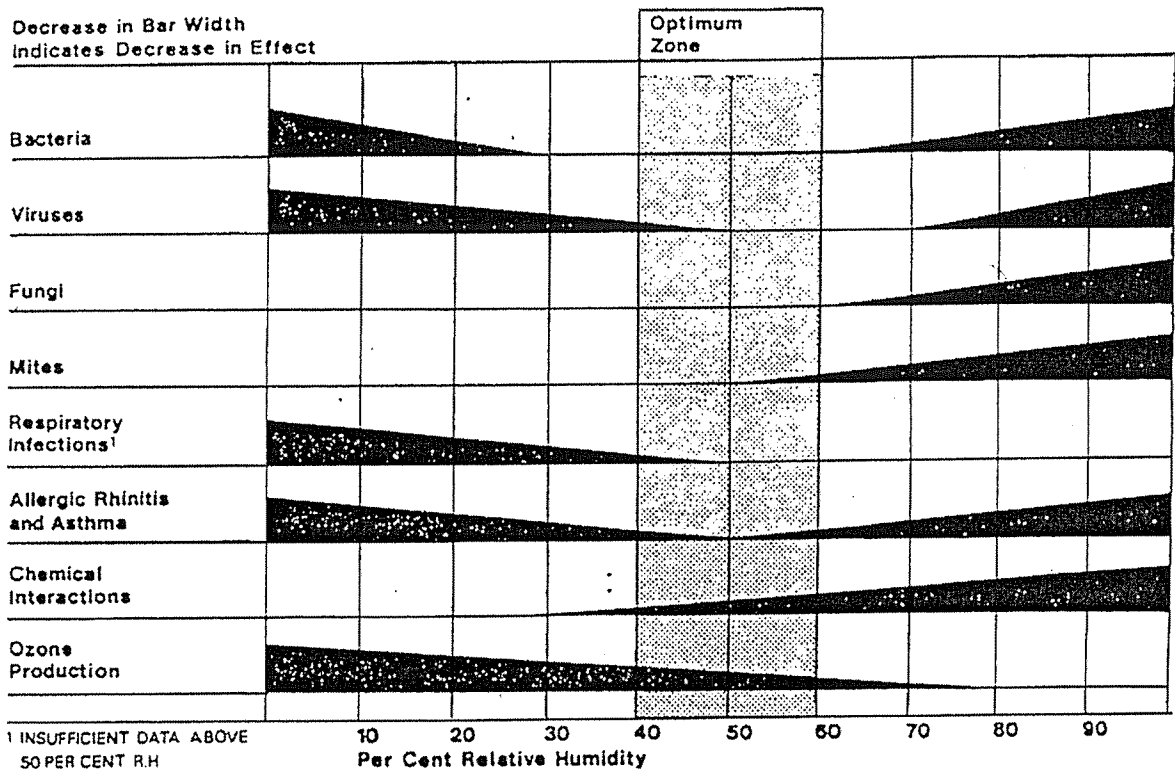


Figure 3.3 Optimum Relative Humidity Ranges for Health (Sterling et al., 1985)

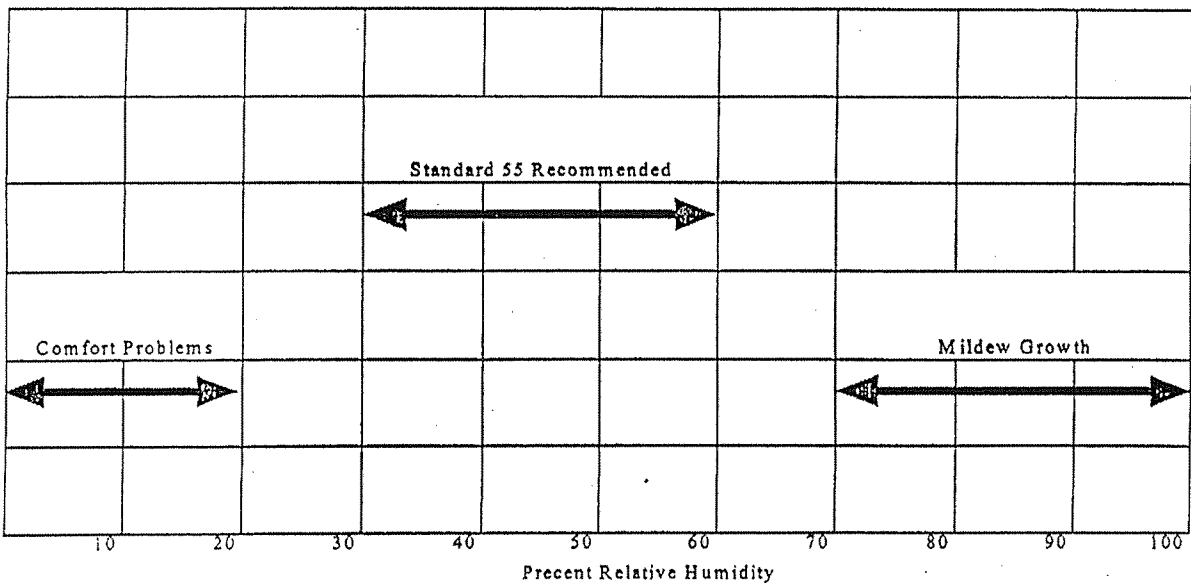


Figure 3.4 ASHRAE Standard 55 Recommended Relative Humidity (ASHRAE)

3.2.3 The Effects of Dry Bulb Temperature, Humidity, and Activity on Thermal Comfort

Koch et al. (1960) presented their results on the sensation responses to temperature and humidity under still air conditions in the comfort range. The study was carried out in the ASHRAE Environment Laboratory located at Cleveland. There were a total of three groups (each group has 6, 8, and 8 subjects, respectively) in the experiment for three different sequences. The clothing insulation of each subject was 0.5 clo, and the sedentary-activity subjects were exposed to uniform air flows of less than 20 ft/min. The investigators found that for a neutral thermal sensation, an increase in relative humidity from 20 % to 80 % could be compensated for by a 1.5 °F reduction in dry bulb temperature. They concluded that the optimum comfort conditions for both winter and summer ranged from 77.6 °F at 30 % relative humidity to 76.5 °F at 85 % relative humidity. In 1963, the ASHRAE Environmental Test Chamber was moved from Cleveland and placed in operation at Kansas State University. The floor plan of the KSU-ASHRAE environmental facilities is shown in Figure 3.5.

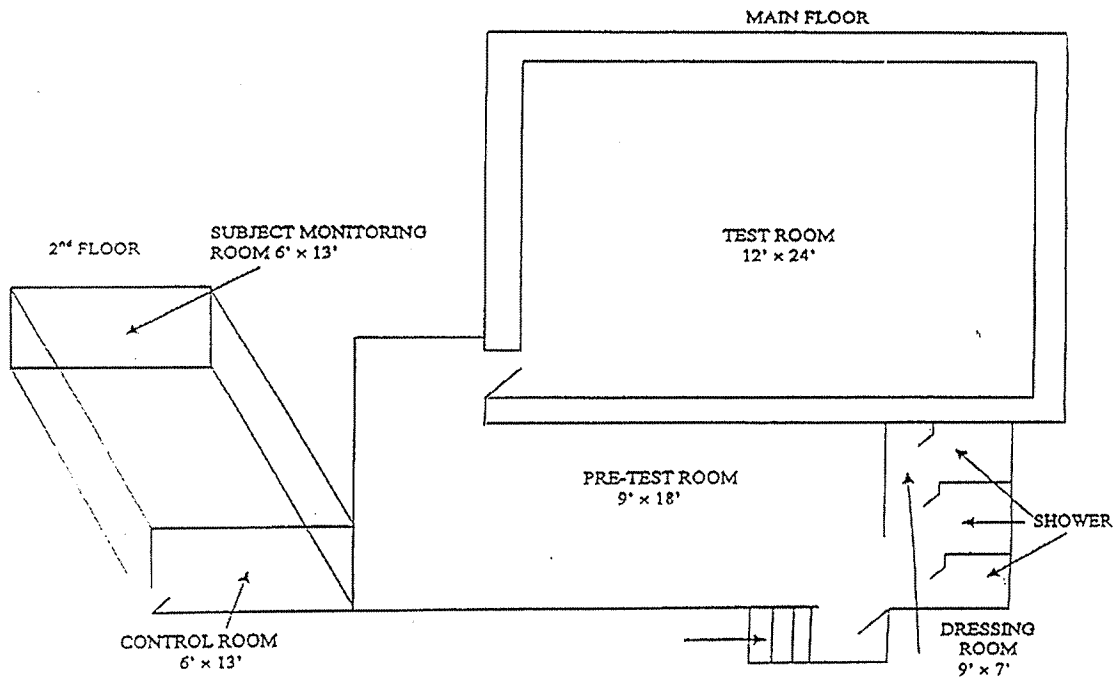


Figure 3.5 Floor Plan of KSU-ASHRAE Environmental Facilities (Nevins et al., 1966)

From 1963 to 1965, Nevins, Rohles, Springer, and Feyerherm (1966), using the KSU-ASHRAE Environmental Test Chamber, conducted a series of experiments on 720 subjects (360 male and 360 female college-age students). These subjects were exposed for periods of 3 hours to dry bulb temperatures of 66 to 80 °F (in 2 °F increments) and to relative humidities from 15 to 85 % (in 10 % increments), constituting 72 experimental conditions. In the occupied zone (area where test subjects were present), the air velocity was less than 45 ft/min, and the room surface

temperatures were held at the same level as the room air temperature. The sedentary-activity subjects' clothing insulation was 0.52 clo. In Figure 3.6, the experimental data are compared to that of Koch et al. (1960). The agreement at the higher relative humidity range is good; however, there is a difference of approximately 2 °F in the dry bulb temperature for the same wet bulb temperature at the lower end. Figure 3.7 presents the comfort lines for a thermal sensation vote of number 4 for males and females and for the two combined.

Rohles and Nevins (1971) studied the nature of thermal comfort for sedentary men and women. The tests were conducted at the KSU-ASHRAE Environmental Test Chamber. A total of 1600 (800 male and 800 female) college students participated in the experiment. This study involved 160 test conditions that included 20 dry bulb temperatures ranging from 60 °F to 98 °F (in 2 °F increments) at each of 8 relative humidity levels (15, 25, 35, 45, 55, 65, 75 and 85 %). The subjects wore KSU Standard Clothing of 0.6 clo. From these 160 tests, the researchers found that some subjects voted "comfortable" for temperatures between 72 °F to 81 °F and relative humidities between 15 % to 85 % for an exposure of 3 hours. Approximately 1.5 hours were needed for men to adapt to their thermal environments. Furthermore, the results showed that men felt warmer than women during the first hour at a given thermal condition. The results of these studies are depicted in Figures 3.8, and 3.9. The comfort lines for one, two, or three hours of exposure in Figures 3.8 and 3.9 represent the cases where the subjects considered the conditions "slightly cool," "comfortable," and "slightly warm." From a regression analysis, Rohles and Nevins concluded that there was a high positive linear relationship between the temperature and the relative humidity and thermal sensation. According to them, when the variations in temperature and humidity were equal (i.e., 1 °F change in temperature and 1 % change in relative humidity), temperature is seven times more important than relative humidity in influencing how men felt. Furthermore, for women, temperature is nine times more important than relative humidity. Figures 3.8 and 3.9 show that gender differences have significant effects on the perceived thermal sensation during the first hour. For one-hour exposure, men feel comfortable at 78 °F ambient air temperature and 15 % relative humidity whereas women feel comfortable at 81 °F ambient air temperature and 15 % relative humidity. The investigators found that the male subjects adapted to their thermal environments faster than the female subjects.

Berglund and Cain (1989) conducted a test to determine the perceived air quality and thermal comfort in an occupied space. Twenty subjects (10 male and 10 female) were involved in this study, and three activities were performed. The activities were sedentary (1 met), 5-minutes walking and 5-minutes standing (2 met), and continuous walking (3 met). The temperatures were 70 °F, 75 °F and 81 °F with dew point temperatures of 36 °F, 52 °F, and 68 °F and an air velocity of 10 ft/min. Figures 3.10, 3.11, and 3.12 represent the perceived humidity levels of the ambient environment at activity levels of 1, 2 and 3 met. The results show that for high relative humidity (68 °F dew point temperature with a relative humidity range from 65 % to 90 %) and an activity level of 3 met, the environment is somewhat humid for a range of temperature from 70 °F to 81 °F whereas for low relative humidity (36 °F dew point temperature with a relative humidity range from 20 % to 30 %) and an activity level of 3 met, the environment is considered neutral.

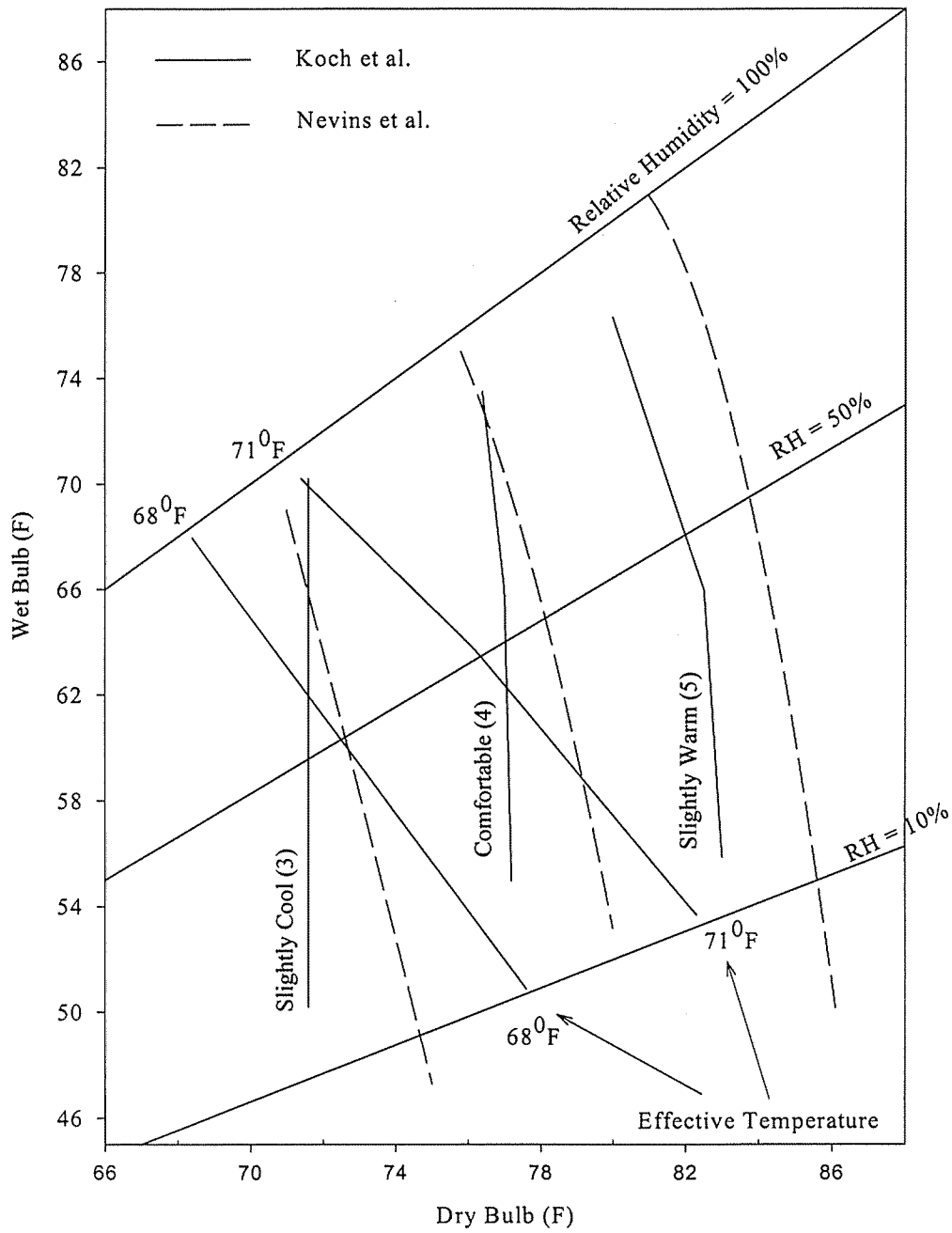


Figure 3.6 Results from Nevins et al. (1966) Compared With Those of Koch et al. (1960) (Nevins et al., 1966)

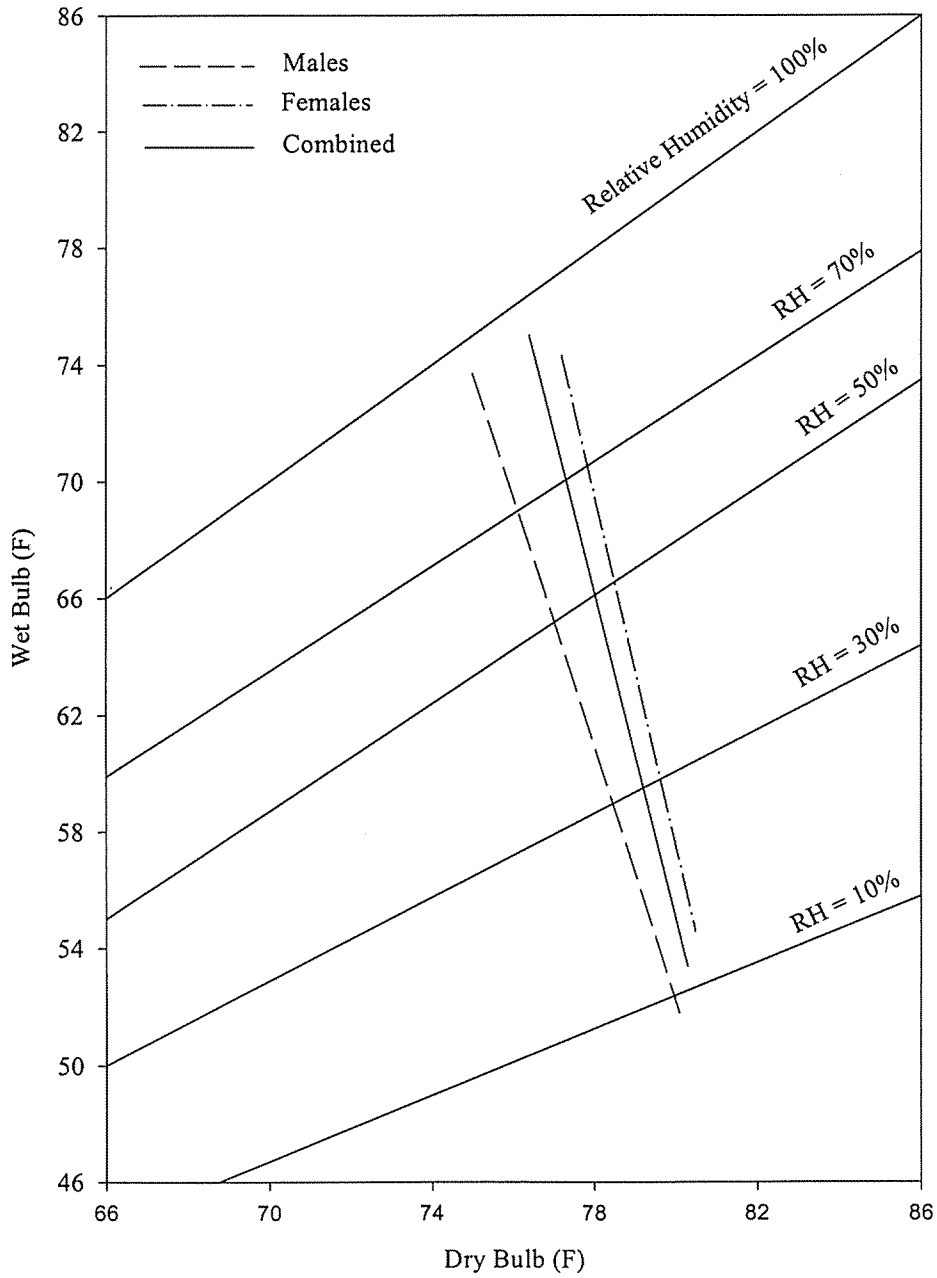


Figure 3.7 A Comfort Vote of No. 4 (Comfortable) For Males, Females, and the Two Combined (Nevins et al., 1966)

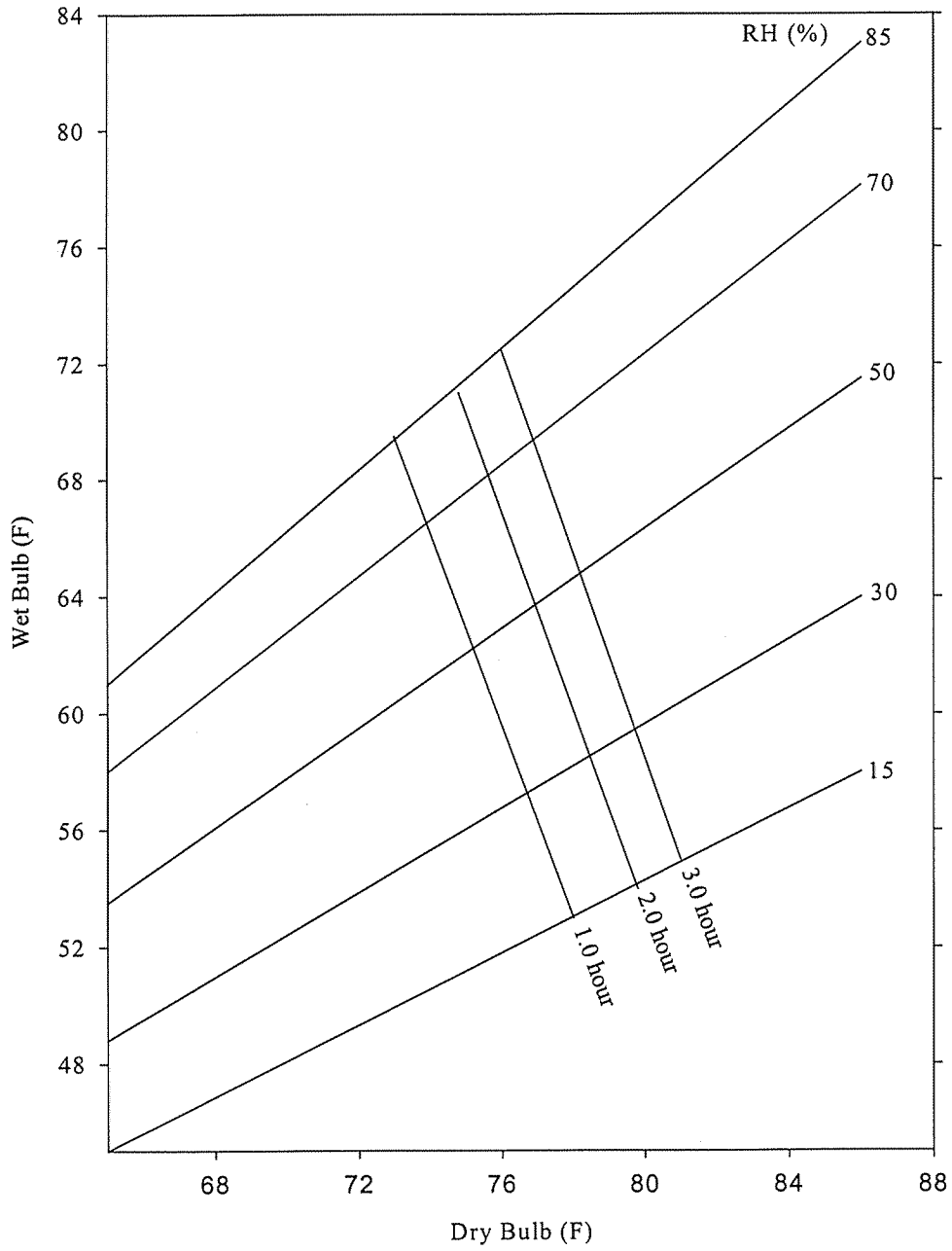


Figure 3.8 Comfortable Lines for Men for Exposure Periods of 1.0, 2.0, and 3.0 Hours (Rohles and Nevins, 1971)

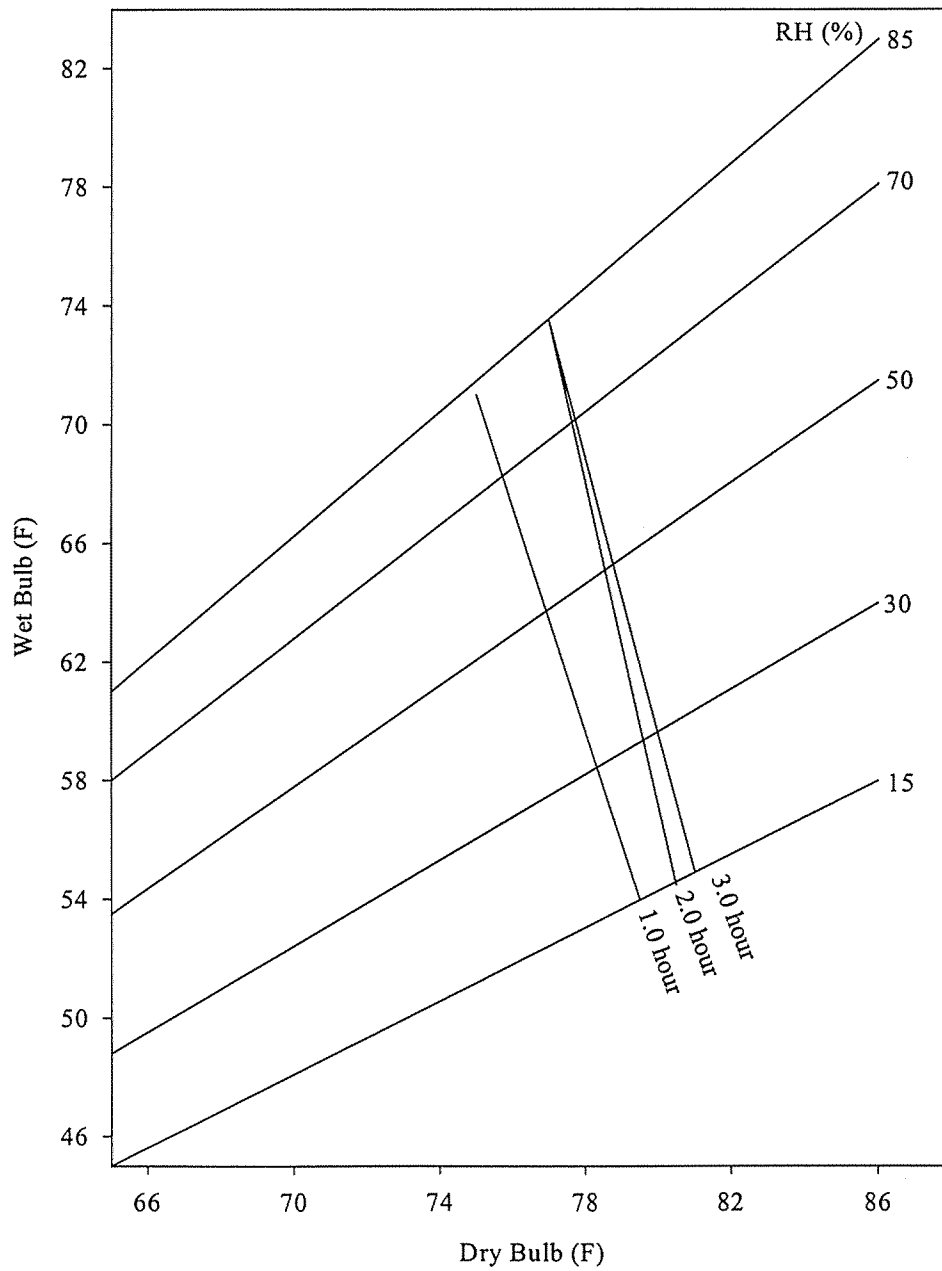


Figure 3.9 Comfortable Lines for Women for Exposure Periods of 1.0, 2.0, 3.0 hours (Rohles and Nevins, 1971)

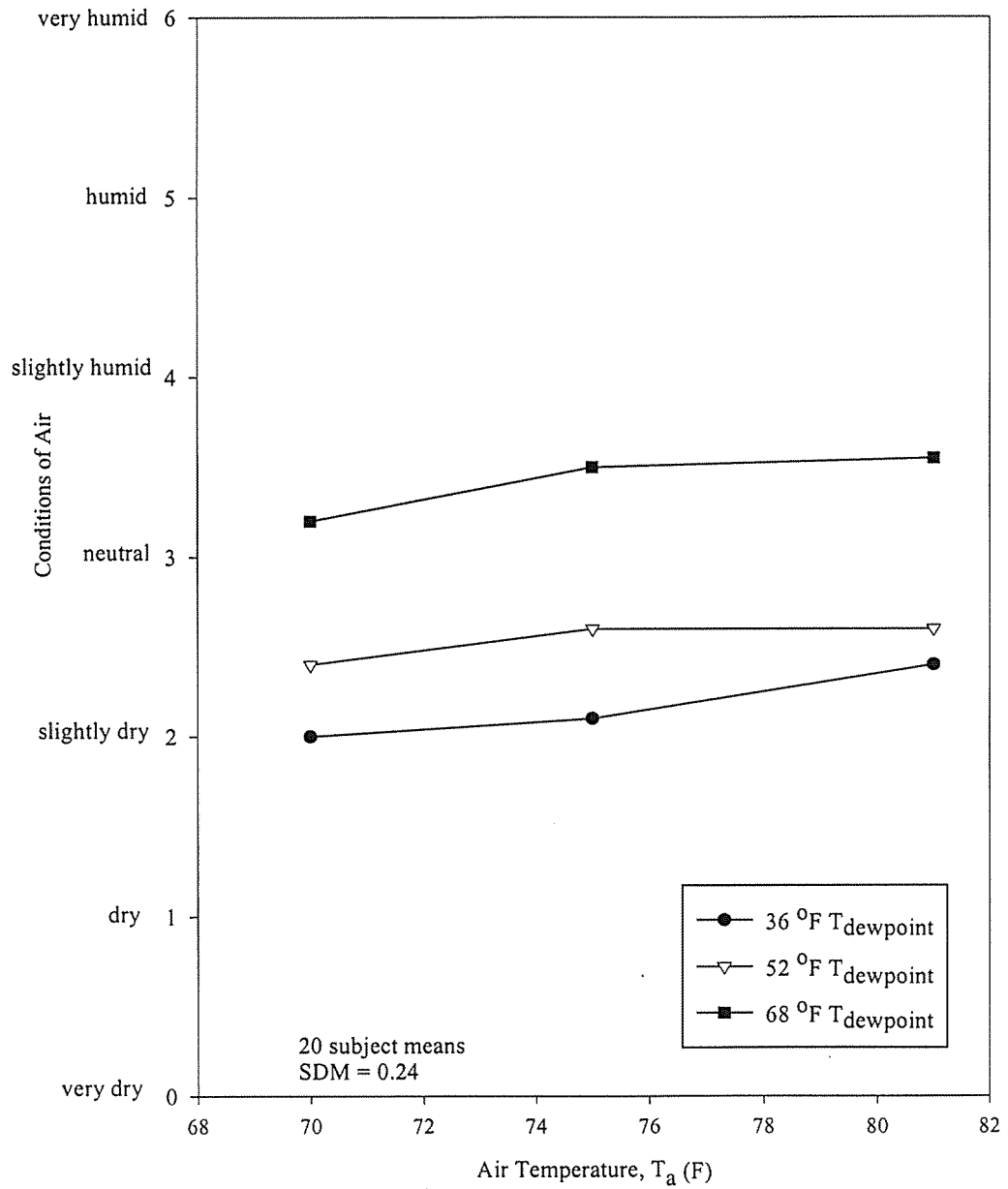


Figure 3.10 Plot of Conditions of Air to Ambient Temperature for 1-Met Activity (Berglund and Cain, 1989)

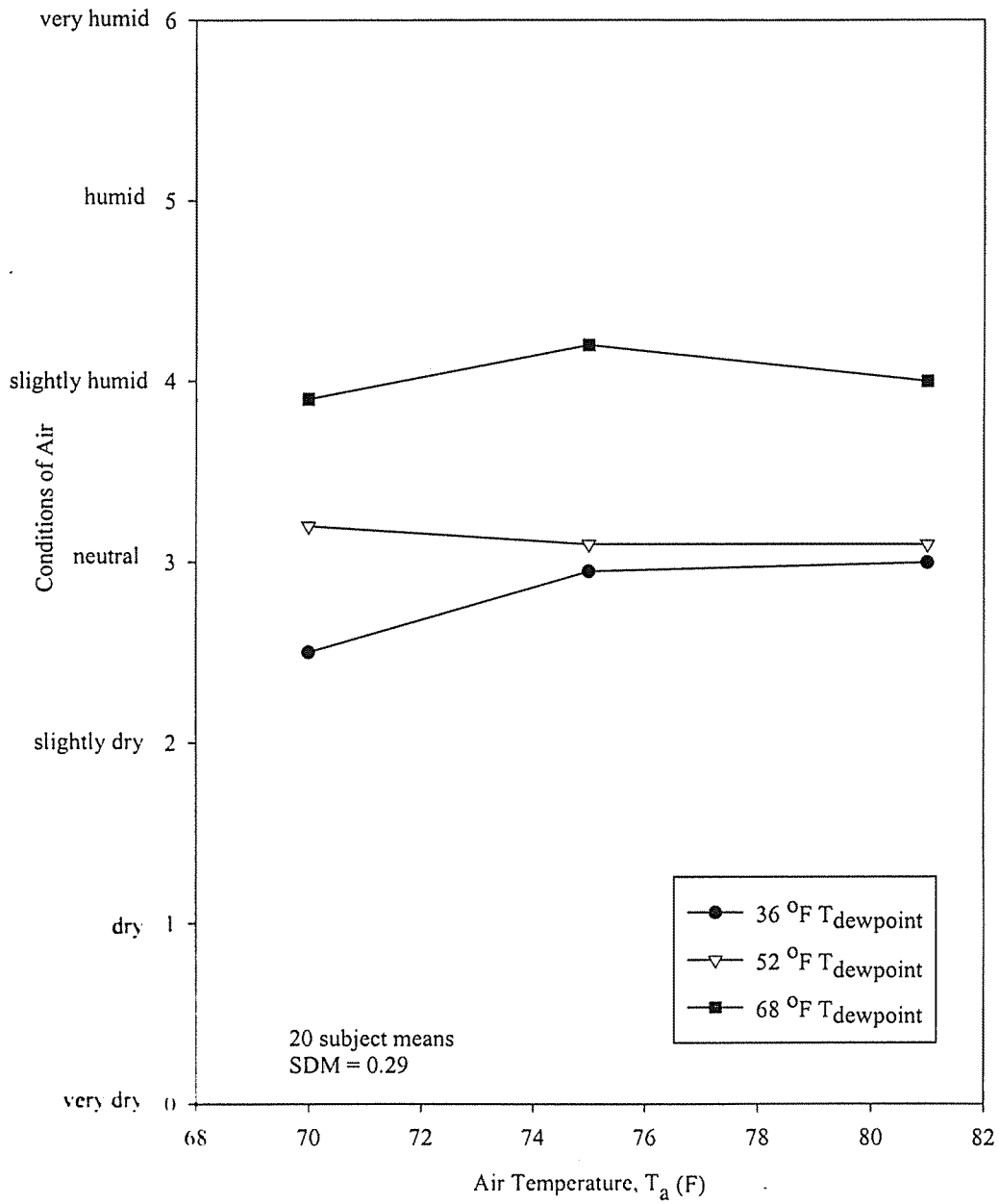


Figure 3.11 Plot of Conditions of Air to Ambient Temperature for 2-Met Activity (Berglund and Cain, 1989)

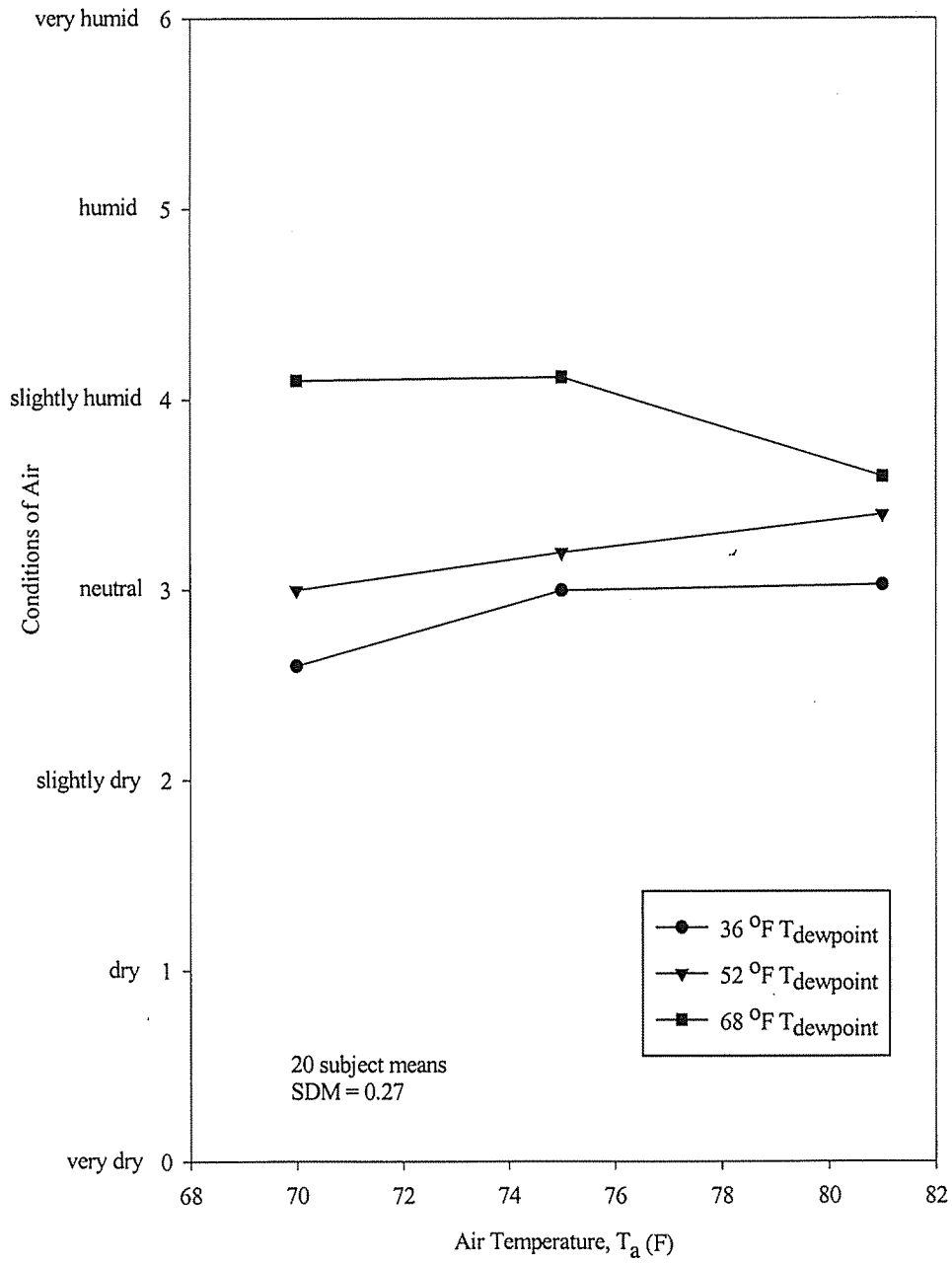


Figure 3.12 Plot of Conditions of Air to Ambient Temperature for 3-Met Activity (Berglund and Cain, 1989)

The perceived quality of air in an occupied space is also an essential consideration. The definition of "acceptability" of air quality by Berglund and Cain (1989) is that the subjects judged whether or not the air quality was acceptable, under instructions that an unacceptable condition would evoke a behavioral action to improve the climate and/or reduce discomfort, e.g., open a window, turn on a fan, change the thermostat setting, complain, or leave. In this context, the term "air quality" is concerned only with the quality of comfort and does not consider factors usually associated with the term "indoor air quality" or IAQ, particularly those of airborne contaminant levels and health issues. Figures 3.13, 3.14, and 3.15 show perceived air quality assessments as a function of temperature, dewpoint, and met levels. From the tests, Berglund and Cain concluded that air was perceived to be fresher and less stuffy with both decreasing temperature (i.e., the air temperature was decreased to about 70 °F) and humidity (i.e., the relative humidity of air was about 20 %). The effect of temperature in influencing perceived air quality was stronger than the effect of humidity.

3.2.4 The Effects of Velocity, Dry Bulb Temperature, and Humidity on Thermal Comfort

Air velocity has profound effects on thermal comfort. An increase in the temperature in an enclosed space can be offset by increasing the air velocity. The study conducted by McIntyre (1978) showed that the subjects chose air velocities that increased with air temperature to a maximum of about 2 m/s (394 ft/min) at 30 °C (86 °F). Eleven subjects participated in the test. In this study, the temperature ranged from 22 °C (71.6 °F) to 30 °C (86 °F) and the relative humidity was held constant at 50 %. The clothing insulations of male and female subjects were 0.48 clo and 0.38 clo, respectively. According to McIntyre, the perception of the strength of an air flow increases as the square of the air velocity while the cooling effect increases as the square root of the velocity. For warmer ambient temperatures, regulating the fan speed (increasing air velocity) can reduce discomfort. However, the upper limit for comfort was 28 °C (82.4 °F). For a temperature above 28 °C (82.4 °F), the increased air movement required to maintain comfort causes too many disturbances (i.e., noise and papers blown about). McIntyre further concluded that an occupant should have the capability to control the local air velocity.

In Figure 3.16, the starting point of the curves at 0.2 m/s (40 ft/min) corresponds to the recommended air velocity limit for the summer comfort zone at 26 °C (78.8 °F). ASHRAE Standard 55 recommends a maximum mean velocity of 30 ft/min for winter and 50 ft/min for summer. The figure shows that increases in the ambient temperature can be compensated with increases in the air velocity. Nevertheless, ASHRAE Standard 55 specifies that acceptance of the increased air speed depends on the occupant's ability to control the local air speed.

Tanabe and Kimura (1989) studied the importance of air movement for thermal comfort under hot and humid conditions. Their study can be divided into two parts. The first part deals with the effects of air movement on thermal comfort in a naturally-ventilated space and was based on their own previously obtained experimental data. For the second part of the study, Tanabe and Kimura investigated the effects of fluctuating air movement on thermal comfort in forced ventilated spaces. Sixty four subjects (32 male and 32 female) participated in both parts, and the duration for each test was 3 hours. The clothing insulation was estimated to be 0.5 clo, and both parts were for sedentary activity (1 met).

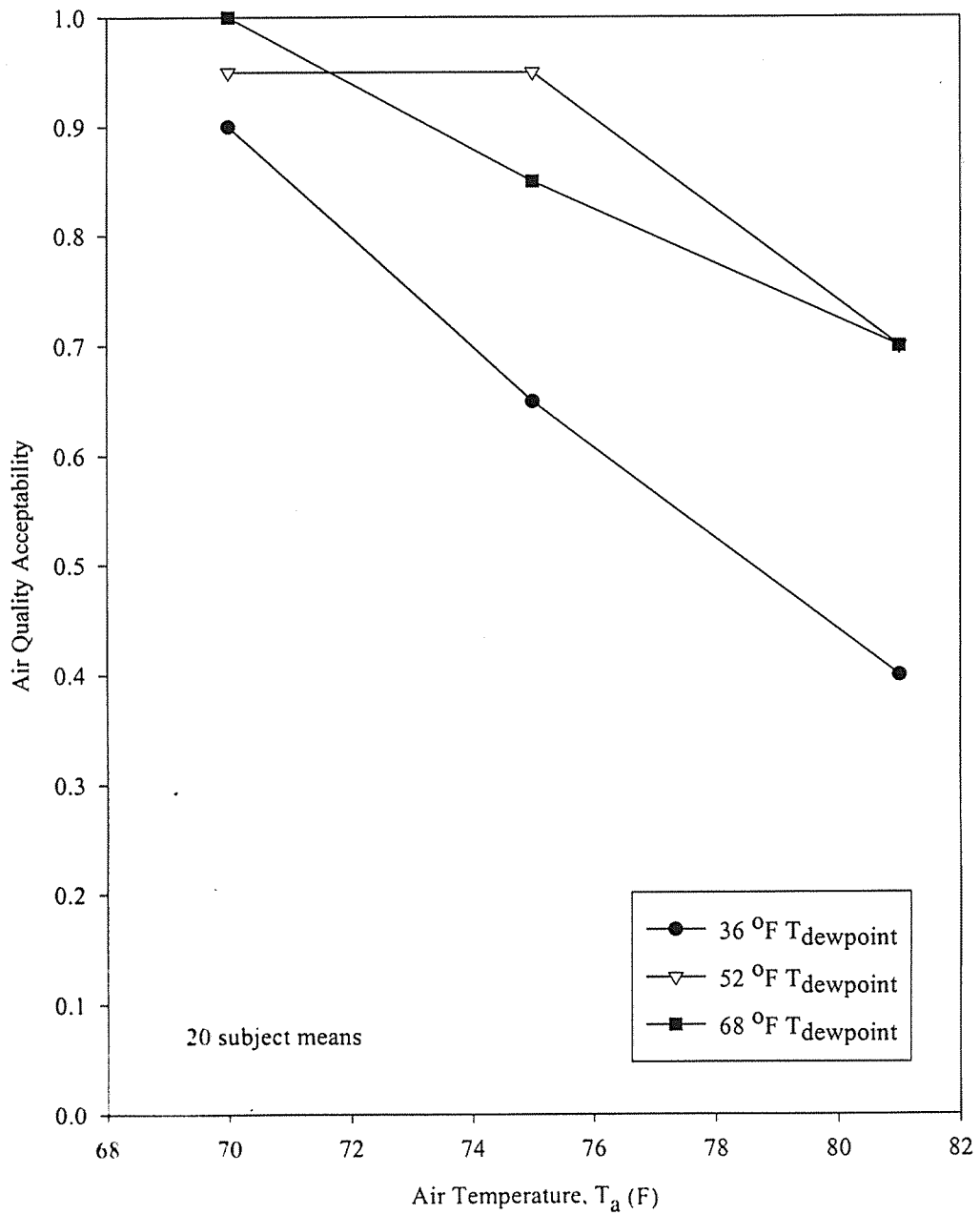


Figure 3.13 Plot of Air Quality Acceptability to Ambient Temperature for 1-Met Activity (Berglund and Cain, 1989)

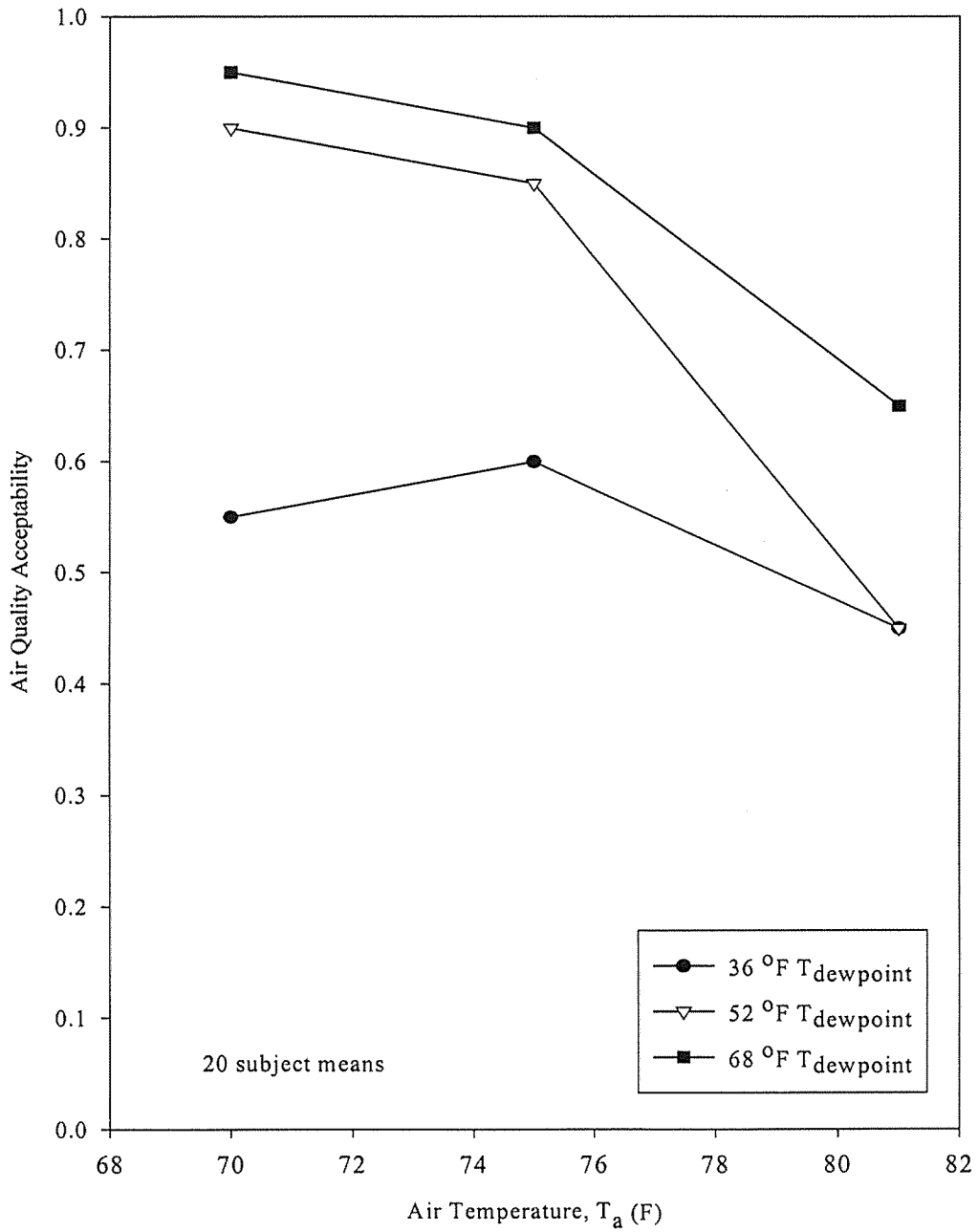


Figure 3.14 Plot of Air Quality Acceptability to Ambient Temperature for 2-Met Activity (Bergland and Cain, 1989)

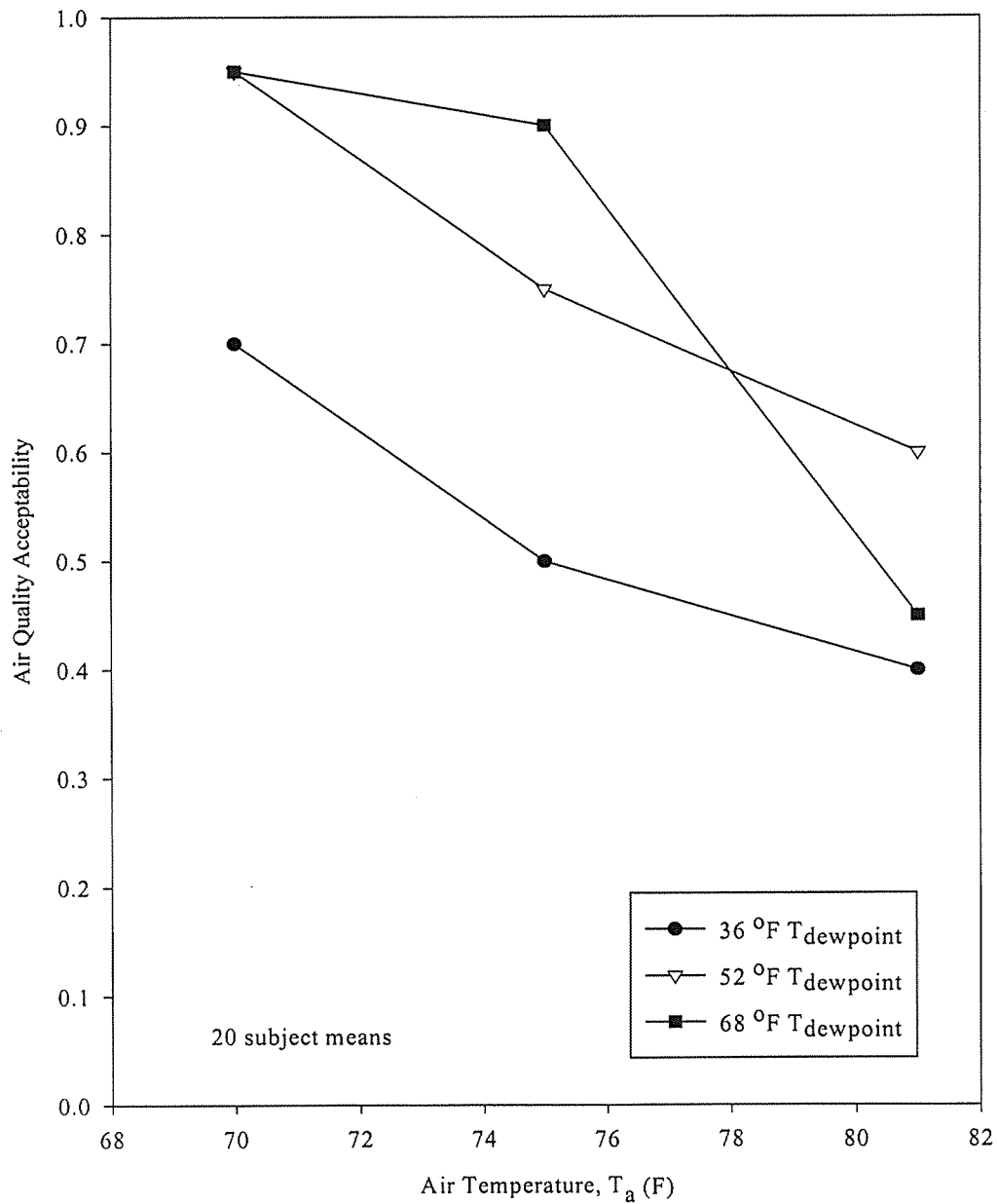


Figure 3.15 Plot of Air Quality Acceptability to Ambient Temperature for 3-Met Activity (Berglund and Cain, 1989)

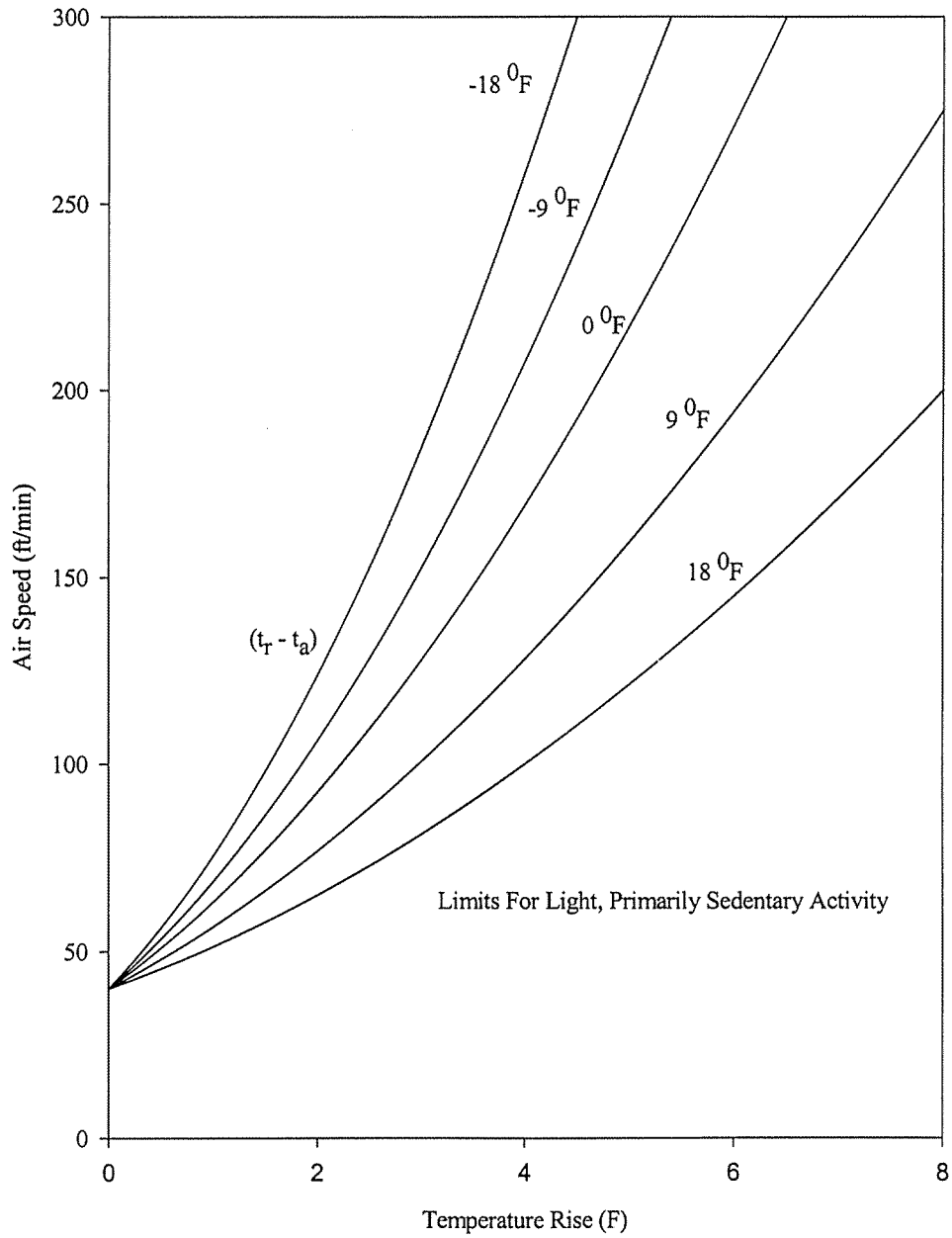


Figure 3.16 ASHRAE Standard 55-1995 Recommended Air Speed

For the first part of the study, six air velocities ranging from 0.13 m/s (25.6 ft/min) to 1.63 m/s (320.9 ft/min) were used. The air temperature ranged from 27.9 °C (82.2 °F) to 31.5 °C (88.7 °F), and the relative humidity was either 50 % or 80 %. For this part, Tanabe and Kimura concluded that the reduction of thermal insulation of clothing and skin diffusion (temperature gain or loss through skin) should be considered when the effects of air movement are evaluated in a space ventilated with outside air. Furthermore, the air velocity preferred by the subjects at 27 °C (80.6 °F)/50 % RH was 1.0 m/s (196 ft/min), at 29 °C (84.2 °F)/50 % RH was 1.2 m/s (236 ft/min), at 29 °C (84.2 °F)/80 % RH was 1.4 m/s (276 ft/min), and at 31 °C (87.8 °F)/50 % RH was 1.6 m/s (315 ft/min). From this study, the air velocity must be increased from 1.0 m/s (196 ft/min) to 1.6 m/s (315 ft/min) to maintain occupant comfort if the relative humidity remained constant at 50 % and the temperature increased from 27 °C (80.6 °F) to 31 °C (87.8 °F). By increasing the air velocity from 1.2 m/s (236 ft/min) to 1.4 m/s (276 ft/min) at an ambient air temperature of 29 °C (84.2 °F), the relative humidity can be increased from 50 % to 80 % with occupant comfort maintained.

In the second part, Tanabe and Kimura (1989) tested seven different air velocities by using a wind box to induce air fluctuations in the chamber. A schematic diagram of the wind box is shown in Figure 3.17. Figure 3.18 illustrates the air movements measured under seven different fluctuating patterns. For the first 40 minutes, the air velocity in the chamber was maintained at 0.13 m/s (26 ft/min). During the following seven 20-minute periods, the subjects were exposed to seven different air movements. "Sin(10)," "sin(30)," and "sin(60)" were with sine-wave fluctuations with periods of 10 s, 30 s, and 60 s, respectively. "Sinmax" was a sine wave with a period of 30 s with its maximum air velocity equal to the air velocity preferred by the subjects. "Const." was a constant velocity, and "Random" was a random wave. "Pulse" was a pulse wave [air velocity increased from 0.5 m/s (98.4 ft/min) to 2 m/s (394 ft/min)] with a period of 30 s. Tanabe and Kimura found that air movements that varied in a sine-wave pattern had more cooling effect on subjective thermal sensation than those of constant, pulse, and random patterns. Furthermore, air movements of sine-wave patterns of sin(10), sin(30), and sin(60) had more cooling effect on the mean skin temperatures than those of sinmax, constant, pulse, and random patterns.

Rohles, Woods, and Nevins (1974) investigated the effects of air movement and temperature on the thermal sensations of sedentary subjects. Ninety subjects (45 male and 45 female) participated in the 3-hour experiment. The air velocities selected for the study were 40, 80, and 160 ft/min, and the temperatures were 72 °F, 78.6 °F, and 85.2 °F. The study was conducted in the KSU-ASHRAE Environmental Test Chamber, and all the participants wore KSU Standard Clothing of 0.6 clo insulation. The relative humidity was 50 % throughout the study. The investigators found that the mean skin temperatures were significantly influenced by air temperatures and velocities. Furthermore, the skin temperature exhibited significant interactions with air movement, temperature, and the exposure period. Because of secondary interactions, thermal sensation and air motion can affect skin temperature significantly. No important gender differences existed in the thermal sensations at the higher velocities in the 3-hour test. Although this study reported on the thermal environment's effects on skin temperature (a physiological response) rather than thermal comfort (a psychological response), human perception of thermal comfort is linked to certain physiological responses, as discussed in the following section.

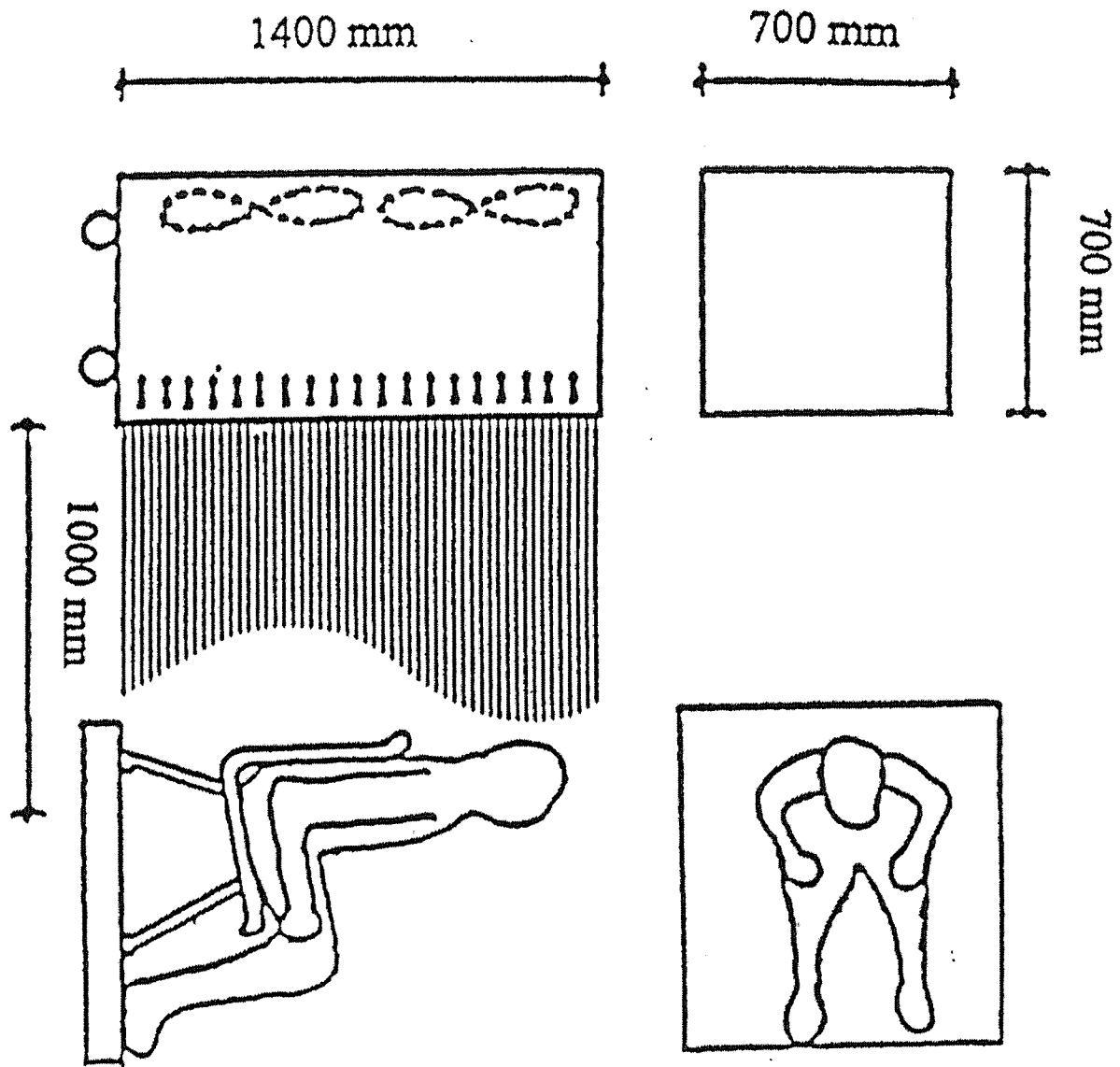


Figure 3.17 Experimental Setup with Subject Exposed to Air Movement from the Back (Tanabe and Kimura, 1989)

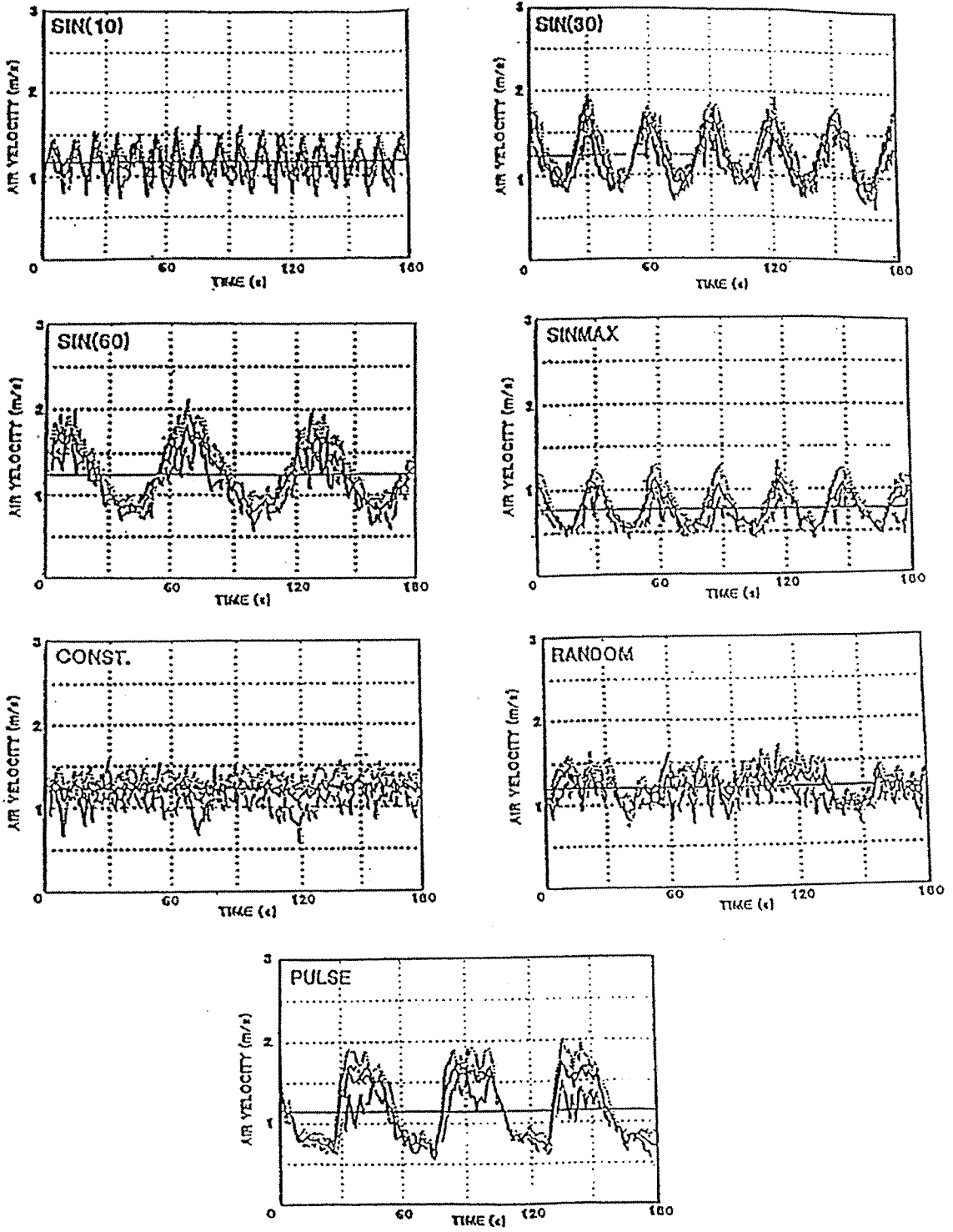


Figure 3.18 Pattern of Air Movement for Experiments (Tanabe and Kimura, 1989)

3.2.5 Human Physiological Responses to the Thermal Environment

Since Fanger's (1967) introduction of relating thermal comfort to empirically-based physiological variables (to be discussed in greater detail in Section 3.2.6), several studies using physical models to simulate human physiological responses to the thermal environment have been reported. Physiological responses to the thermal environment are manifested as changes in skin temperature, body core temperature, rectal temperature, sweat secretion rate, and metabolic rate. A number of computer-based models have been used to simulate human physiological responses to both steady and unsteady thermal conditions, and these models have been compared extensively to experimental data sets.

Takemori, Nakajima, and Shoji (1995) developed a model of the human thermal system for the prediction of thermal comfort. This model is known as the AVA Model and is able to predict heat transfer by blood flow considerations. Basically, the model is composed of two parts, an arteriovenous anastomoses model (AVA) of the extremities and a dual vascular network (macro and microcirculation). An experimental study on eight college-age male subjects in sedentary activity was conducted using the following thermal conditions: steady thermal conditions at 22 °C (71.6 °F), 28 °C (82.4 °F), and 34 °C (93.2 °F) and unsteady thermal conditions where the temperature was modulated stepwise from 28.1 °C (82.6 °F) (1-hour duration) to 47.1 °C (116.8 °F) (2-hour duration) and finally to 28.3 °C (82.9 °F) (1-hour duration). The relative humidity for steady and unsteady thermal conditions was maintained at 45 %. The model results were compared with the experimental data and with the Smith (1991) model (a conventional human thermal systems model).

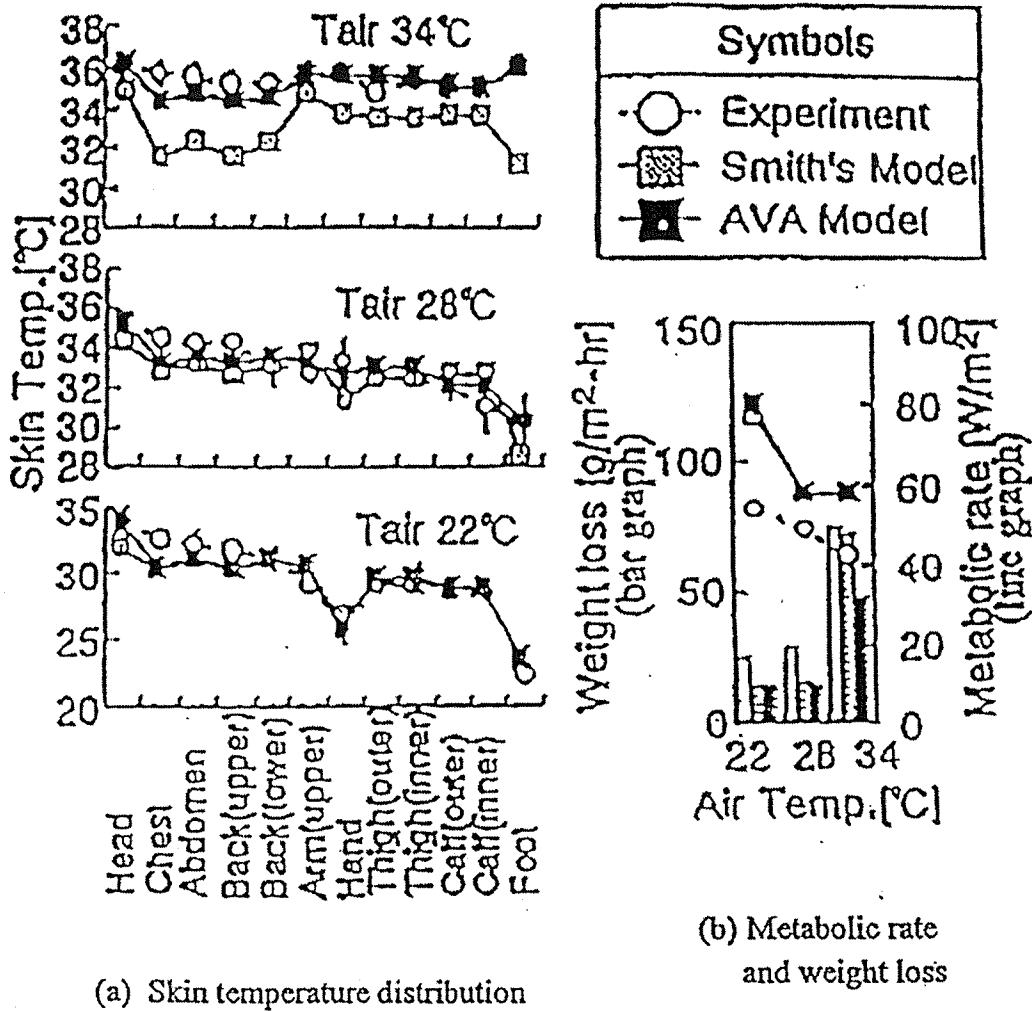
Under both steady and unsteady thermal conditions, the skin temperatures and the core (internal organs) temperatures predicted by the AVA model agreed with the experimental data whereas Smith's model agreed only with the experimental data at 22 °C (71.6 °F) for the steady thermal condition. The results are illustrated in Figures 3.19 and 3.20. The predicted skin and body temperature distributions agreed qualitatively in physiological terms.

Haslam and Parsons (1988) evaluated computer-based models that predict human responses to the thermal environment. Four models were compared. These models were Stolwijk and Hardy's (1977) 25-node model of human thermoregulation (lut 25), the Pierce 2-node model (Nishi and Gagge, 1977) of human thermoregulation (lut 2), Givoni and Goldman's (1972) model of rectal temperature response (luttre), and the ISO/DIS 7933 (1987) model (lutiso). The predictions of the four models were compared with the data of Chappuis et al. (1976), Kobayashi et al. (1980), Young et al. (1986), and Henane et al. (1979). These data sets are discussed in the following paragraphs.

For the study conducted by Chappuis et al. (1976), eleven subjects with clothing insulation of 0.1 clo were exposed to three sets of thermal conditions with temperatures of 20 °C (68 °F), 25 °C (77 °F), and 30 °C (86 °F) and metabolic rates of 57 W/m² (about 1 met, 18.43 Btu/h·ft²), 150 W/m² (about 2.5 met, 46.08 Btu/h·ft²), and 257 W/m² (about 4.5 met, 82.94 Btu/h·ft²). The relative humidity was 30 %, and room air velocity was 0.2 m/s (39.4 ft/min).

For the study of Kobayashi et al. (1980), five subjects were exposed to a temperature of 49.5 °C (121.1 °F), an air velocity of 0.1 m/s (19.7 ft/min), and a relative humidity of 32 % with

clothing insulation of 0.1 clo and moderate work activity of 204 W/m^2 (3.5 met, $64.51 \text{ Btu/h}\cdot\text{ft}^2$) or heavy work activity of 306 W/m^2 (about 5 met, $92.15 \text{ Btu/h}\cdot\text{ft}^2$).



Air Temperature	22°C		28°C		34°C	
	T_{core}	T_{skin}	T_{core}	T_{skin}	T_{core}	T_{skin}
Experiment	-	-	36.90	33.84	37.10	35.21
Smith's Model	36.69	30.00	36.91	32.72	37.06	32.75
AVA Model	36.64	30.35	36.74	33.45	36.96	34.97

(c) Core temperature and mean skin temperature

Figure 3.19 Comparison Between Experimental Data and Predictions (Takemori et al., 1995)

	1st hr	2nd hr	3rd hr	4th hr
Ambient Temperature ($^{\circ}\text{C}$)	28.1	47.8	47.8	28.3
Relative Humidity (%)	43	27	27	44

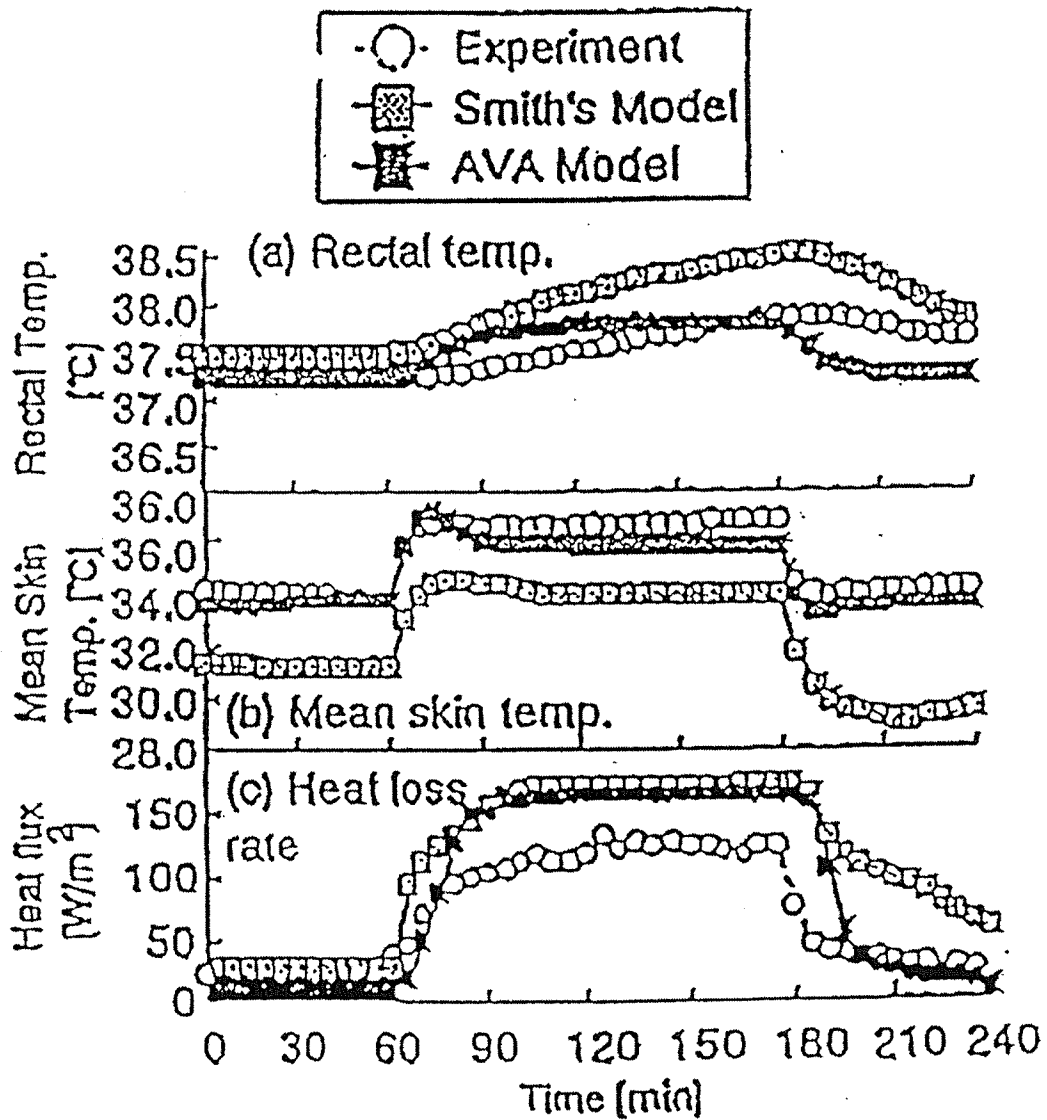


Figure 3.20 Comparisons Between Experimental Data and Predictions in an Unsteady Thermal Environment (Takemori et al., 1995)

The data from Young et al. (1986) were for seven subjects, resting males with metabolic rates of 60 W/m^2 (about 1 met, $18.43 \text{ Btu/h}\cdot\text{ft}^2$) and clothing insulation of 0.1 clo exposed for 90 minutes to an environment where the temperature was $5 \text{ }^\circ\text{C}$ ($41 \text{ }^\circ\text{F}$), the air velocity was 0.1 m/s (19.7 ft/min), and relative humidity was 30 %.

Henane et al. (1979) conducted a study where eleven subjects were exposed to the following environment conditions: a temperature of $35 \text{ }^\circ\text{C}$ ($95 \text{ }^\circ\text{F}$), an air velocity of 1 m/s (196.9 ft/min), a relative humidity of 54 %, and clothing insulations of 0.1 clo, 1 clo, and 2.6 clo. The metabolic rates were 165 W/m^2 (about 2.8 met, $51.6 \text{ Btu/h}\cdot\text{ft}^2$), 191 W/m^2 (3.2 met, $59 \text{ Btu/h}\cdot\text{ft}^2$), and 209 W/m^2 (about 3.6 met, $66.35 \text{ Btu/h}\cdot\text{ft}^2$).

Using the data from the above-mentioned tests, Haslam and Parsons (1988) found that few of the models' predictions were wildly inaccurate and that often the models were capable of providing sufficient accuracy to be of practical use. Predictions by the lut 2 and the lut 25 models on tympanic temperature, auditory canal temperature, and esophageal temperature were more accurate than predictions on rectal temperature. Predictions by the lut 2 model were similar to those of the lut 25 model, except for cold conditions or when the subjects were exercising. In general, the luttre model predicted the rectal temperature more accurately than core temperatures (deep body temperature). However, under certain circumstances, the lut 2 and the lut 25 models provided better predictions of rectal temperature than the luttre model.

3.2.6 Human Thermal Comfort Models

Thermal energy exchanges between a body and the environment are frequently modeled by using classical heat transfer theory as a rational starting basis and introducing empirical equations describing the effects of physiological regulatory controls (sweating or shivering). Two models are commonly used to predict human thermal comfort. These models are the steady-state energy balance model developed by Fanger (1967) and the two-node transient energy balance model developed by Gagge et al. (1971a).

3.2.6.1 Two-Node Transient Energy Balance Model

The two-node model developed by Gagge et al. (1971a) divides the human body into two parts. The first part is a passive system representing the skin layer where the body exchanges heat through direct contact with the environment and through the thermoregulatory-controlled peripheral blood flow. The other part is an inner cylinder, which models the body core (skeleton, muscle, and internal organs). The losses in the body core are associated with metabolic heat production, external work, and respiration. Figure 3.21 shows a schematic of the two-node model. The skin temperature and the body core temperature are used to regulate the body temperature.

For the Gagge et al. model, the three major parameters that influence comfort and thermal sensation are the skin and core temperatures and the skin wettedness. This model takes into account the effects of vasoconstriction (associated with the sense of cold), vasodilation (occurs during sweating and increases the sense of warmth), and sweat secretion. Vasoconstriction is

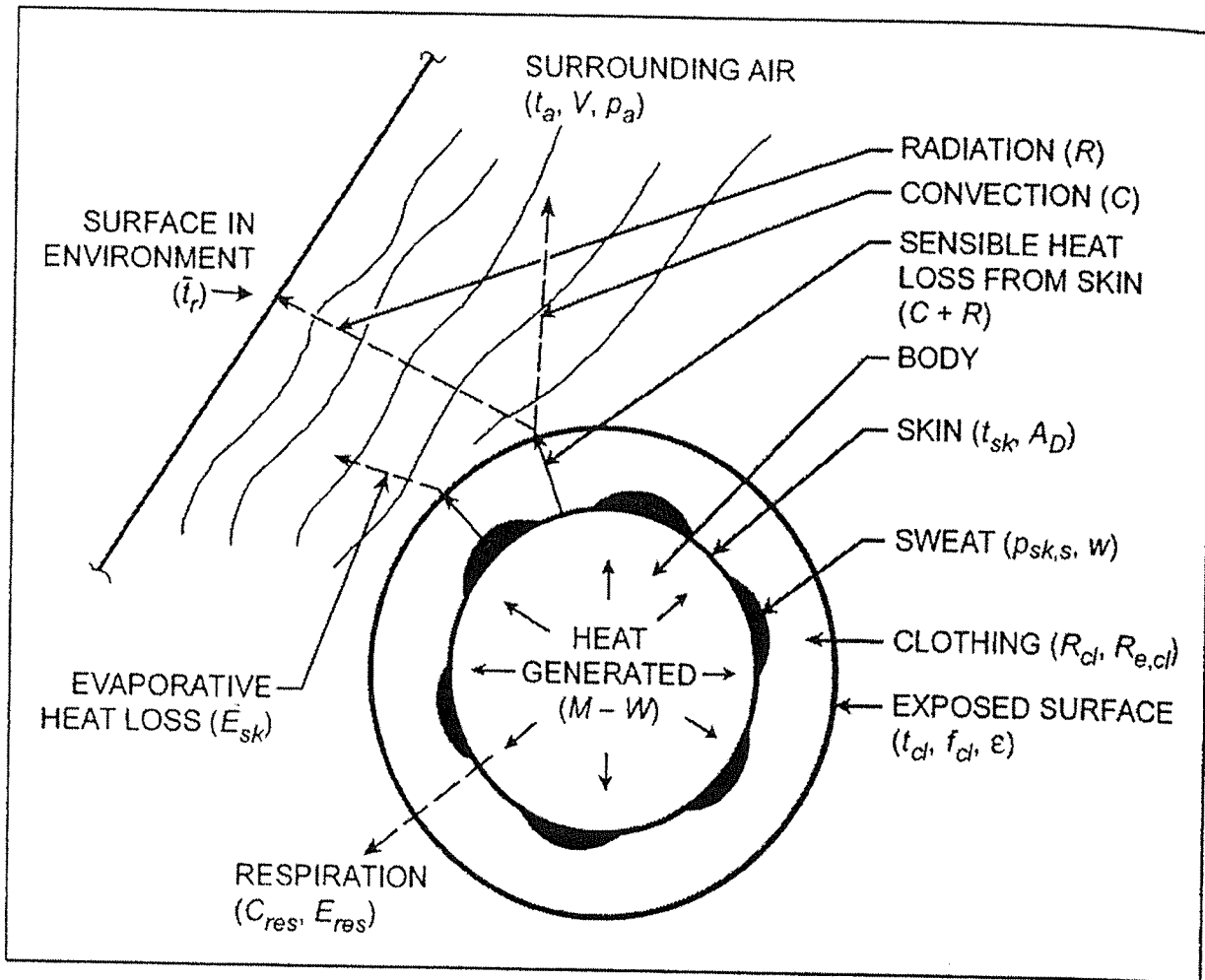


Figure 3.21 Schematic of Two-node Transient Energy Balance Model (Gagge et al., 1971a)

governed by cold signals from the skin, and vasodilation is governed by the warm signals from the core. According to Gagge et al., a warm signal from the skin plays a more important role in body temperature regulation by governing sweating than does vasodilation.

Even though this model contains many physiologically dependent as well as physiologically independent variables to predict comfort and thermal sensation, the model is limited to exposure times of one hour or less. Because of this limitation, the two-node model will not be considered further in this study.

3.2.6.2 Steady-State Energy Balance Model

In 1967, Fanger determined that for steady-state conditions, the mean skin temperature, t_{sk} , and the sweat secretion rate, E_{TSW} , required for thermal comfort could be predicted by the following equations:

$$t_{sk} = 96.3 - 0.156 \times (M - W) \quad (^\circ\text{F}) \quad (3.1)$$

$$E_{rsw} = 0.42 \times (M - W - 18.43) \quad (\text{Btu/h-ft}^2) \quad (3.2)$$

where

t_s	= mean skin temperature ($^{\circ}\text{F}$)
E_{rsw}	= sweat secretion rate (Btu/h-ft^2)
M	= metabolic rate per unit body surface area (Btu/h-ft^2)
W	= external work done by muscles (Btu/h-ft^2)

From Equation (3-1), the skin temperature required for comfort for sedentary activity ($M - W = 18.43 \text{ Btu/h-ft}^2$) is approximately 93.4°F . From Equation (3-2) for sedentary activity, the sweat secretion rate for comfort is zero.

For Fanger's model, the body is in a state of thermal equilibrium with negligible heat storage. Furthermore, Fanger assumes that when the body is near thermal neutrality there will be no shivering, and vasoregulation is not considered because the core and skin are modeled as a single entity. The general equation for neutrality (steady-state) when the rate of heat generation equals the rate of heat loss is

$$\begin{aligned} M - W &= Q_{sk} + Q_{res} \\ &= (C + R + E_{sk}) + (C_{res} + E_{res}) \end{aligned} \quad (3.3)$$

where

M	= rate of metabolic heat production
W	= rate of mechanical work accomplished
Q_{res}	= total rate of heat loss through respiration
Q_{sk}	= total rate of heat loss from skin
$C + R$	= sensible heat loss from skin (convection plus radiation)
E_{sk}	= rate of total evaporative heat loss from skin
C_{res}	= rate of convective heat loss due to respiration
E_{res}	= rate of evaporative heat loss due to respiration

Fanger assumes that all sweat generated is evaporated, thus eliminating clothing moisture permeability concerns. Fanger explains that the assumption is valid for normal indoor clothing worn in typical indoor environments with low or moderate activity levels. Fanger used fundamental principles (i.e., the Stefan-Boltzmann law for radiative heat transfer from the skin) for the terms in Equation (3.3) (C , R , E_{sk} , C_{res} , and E_{res}). By using these fundamental principles and Equations (3.1) and (3.2), the thermal neutrality of an occupant can be expressed as

$$\begin{aligned} M - W &= 1.196 \times 10^{-9} f_c \left[(t_{cl} + 460)^4 - (t_r + 460)^4 \right] + f_{cl} h_c (t_{cl} - t_a) \\ &+ 0.97 [5.73 - 0.022(M - W) - 6.9p_a] + 0.42 [(M - W) - 18.43] \\ &+ 0.0173M(5.87 - 6.9p_a) + 0.0007M(93.2 - t_a) \end{aligned} \quad (3.4)$$

where

- f_{cl} = clothing area factor
- t_{cl} = clothing surface temperature
- t_r = mean radiant temperature
- t_a = ambient air temperature
- p_a = ambient air water vapor pressure
- h_c = convection at surface

The meaning of each term in Equation (3.4) is explained in Table 3.5. Equation (3.4) is valid only for Inch-Pounds units.

Table 3.5 Meaning of Terms in Equation (3-4)

Term	Meaning
$M - W$	Internal heat production
$1.196 \times 10^{-9} f_c [(t_{cl} + 460)^4 - (t_r - 460)^4]$	Heat loss by radiation from skin
$f_{cl} h_c (t_{cl} - t_a)$	Heat loss by convection from skin
$0.97 [5.73 - 0.022 (M - W) - 6.9 p_a]$	Evaporative heat loss from skin
$0.42 [(M - W) - 18.43]$	Sweat secretion rate
$0.0173 M (5.87 - 6.9 p_a)$	Evaporative heat loss due to respiration
$0.0007 M (93.2 - t_a)$	Sensible heat loss due to respiration

Fanger (1970) related the Predicted Mean Vote (PMV) to the imbalance between the actual heat flow from the body in a given environment and the heat flow required for optimum comfort at a specific activity level. Furthermore, he expressed the PPD as a function of the PMV as follows:

$$PMV = [0.303 \exp (- 0.036 M) + 0.028] L \quad (3.5)$$

$$PPD = 100 - 95 \exp [- (0.03353 PMV^4 + 0.2179 PMV^2)] \quad (3.6)$$

where L is the thermal load on the body which is defined as the difference between the internal heat production and the heat loss to the environment for a human hypothetically kept at the comfort values of the mean skin temperature and the sweat secretion rate for the actual activity level. In other words, L is the difference between the left and right sides of Equation (3.4). When L is zero, the PMV is zero and the mean vote for the test is 'neutral.' From the Predicted

Percentage of Dissatisfied (PPD) for a PMV of zero, 5% of the occupants are dissatisfied with the neutral thermal environment because of individual variations.

Fanger compared the steady-state energy balance model with the results by Rohles and Nevins (1971) (who conducted the study at Kansas State University), and the model results agreed very well with the data. The Rohles and Nevins data included dry bulb temperatures ranging from 60°F to 98°F and relative humidities ranging from 15% to 18%. Subjects were sedentary (~ 1 met) and wore standard clothing (0.6 clo).

3.2.7 Basis for Experimental Study

According to the findings of this literature survey, the Fanger model has been validated over a wide range of relative humidities and dry bulb temperatures for sedentary subjects in standard clothing, but has not been substantially validated for higher met levels, varying air velocity, and heavier clothing insulation. Although a number of studies in this survey reported the effects of higher met levels, higher clothing insulation, and increased air velocities, none were presented in the form of PMV or the ASHRAE Standard Thermal Sensation Scale and, thus, are not suitable for comparison with the Fanger model or the ASHRAE 55 Comfort Zone. Therefore, a test plan was developed to obtain data suitable for further validation of the Fanger model, the ASHRAE 55 Comfort Zone, and the ASHRAE Thermal Comfort Program. The scope, procedure, and results of the experimental study are discussed in detail in the following Section.

3.3 EXPERIMENTAL STUDY

3.3.1 Introduction

The purpose of the experimental study was to obtain data suitable for further validation of the ASHRAE 55-1995 Comfort Zone, the ASHRAE Thermal Comfort Program, and the Fanger model upon which much of the Comfort Zone and Thermal Comfort Program are based. As stated in Section 3.2.7, the data needed for further validation are for higher met levels, varying air velocity, and heavier clothing insulation. In keeping with the overall objective of promoting widespread use of desiccant-based air conditioning equipment, the scope of this experimental study was limited to higher met levels and varying air velocity. Heavier clothing insulations are generally not of interest for summer air conditioning applications.

3.3.2 Test Conditions

Eight thermal conditions were selected for the study. These conditions are listed in Table 3.6. Figure 3.22 shows part of a psychrometric chart with both summer and winter comfort regions identified and with the eight test conditions for the study shown. With the exception of the 82/20 condition, all conditions are within the summer comfort zone, corresponding to a summer clothing insulation level of 0.5 clo. The 82/20 condition was included to determine if the comfort zone could be stretched to include higher dry bulb temperatures at the very low relative humidities attainable with desiccant-based air conditioning equipment.

Table 3.6 Eight Thermal Conditions Used in This Study

Condition	Temperature (°F, °C)/Relative Humidity (%)
1	79, (26.1)/20
2	82, (27.8)/20
3	77, (25)/35
4	80, (26.7)/35
5	75, (23.9)/50
6	78, (25.6)/50
7	73, (22.8)/65
8	76, (24.4)/65

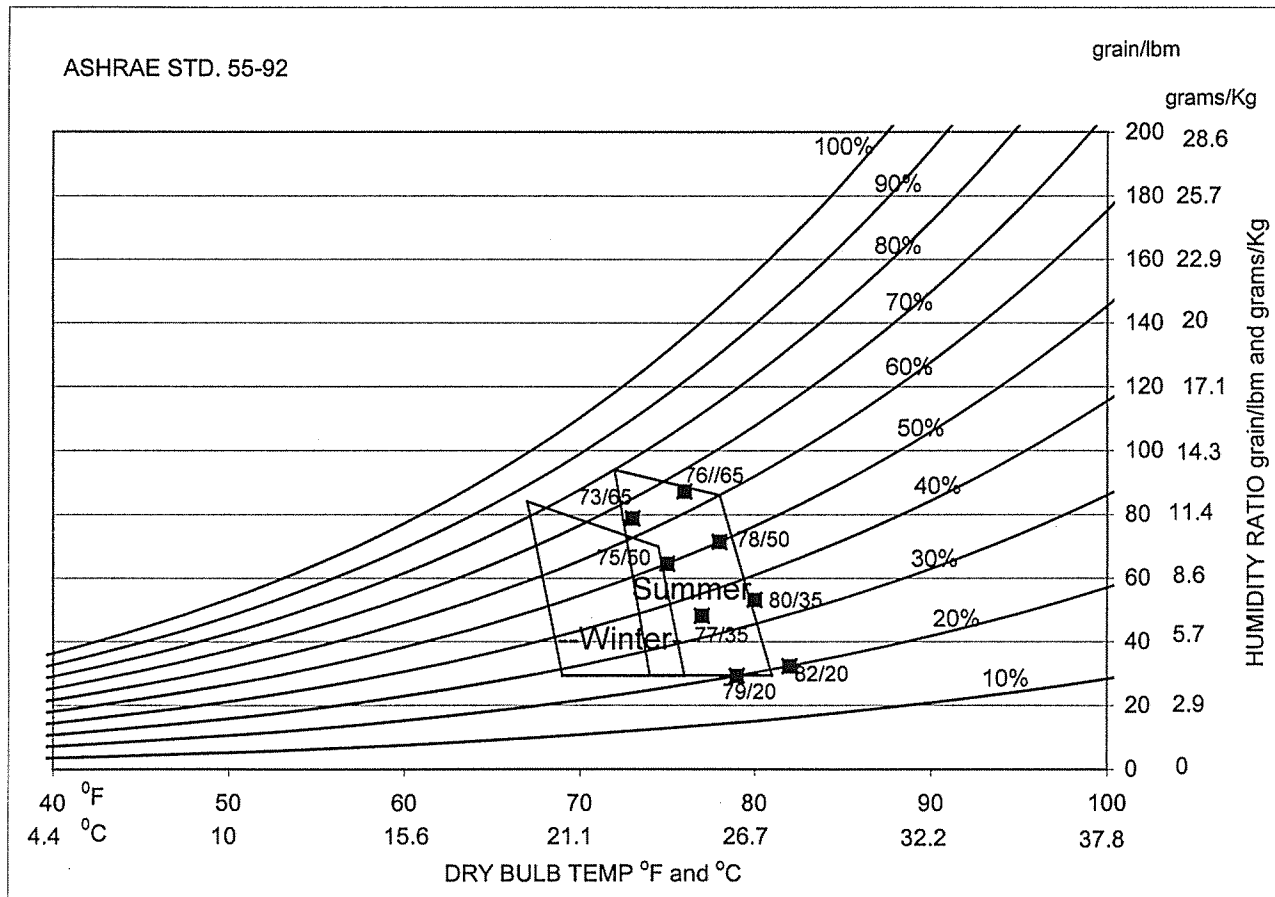


Figure 3.22 Psychrometric Chart of Both Summer and Winter Comfort Zones

At each of the eight temperature-humidity conditions, two activity levels, 1.0 met and 2.3 met, were examined. The purpose of the 1.0 met activity level was to establish the validity of the

experimental procedure by comparing results with similar studies of sedentary activity levels and the ASHRAE Comfort Zone, which is based on sedentary activity. The 2.3 met level is characteristic of moderate activities such as walking and light standing work.

Two air velocities, 30 fpm and 50 fpm, were employed at each of the sixteen temperature-humidity-activity combinations. These are the maximum air velocities recommended by ASHRAE 55 for winter and summer, respectively. Much higher velocities may be tolerated (even preferred) by occupants with higher activity levels. However, since activity levels exceeding 1.2 met occur only sporadically in typical air-conditioned buildings, room air distribution systems are normally designed for sedentary occupancy (≤ 50 fpm terminal velocity in the occupied zone). Maintaining reasonable comfort levels for sustained moderate to high activity levels can be accomplished by either (1) lowering the temperature setpoint (or humidity setpoint if humidity control is available) or (2) increasing air velocity with ceiling/portable fans. Air velocities greater than 50 fpm (corresponding to option 2) are tangent to the overall objective of this work (promoting the use of desiccant based air conditioning equipment) and, therefore, were not examined in this study.

The combination of eight thermal conditions, two activity levels, and two air velocities resulted in a total of 32 test conditions (8 temperature/humidity x 2 activity levels x 2 velocities). For each of these conditions, the clothing insulation was 0.6 clo, and the mean radiant temperature was maintained equal to the air temperature.

3.3.3 Facilities and Test Procedures

All tests took place in two adjacent environmental chambers at the ASHRAE Environmental Test Chamber of the Institute for Environmental Research at Kansas State University (KSU). Each chamber measured 11ft x 11ft with a ceiling height of 9 feet. Four computer stations were set up in one chamber for the lower activity level (1 met). The second chamber was used for the 2.3 met activity level with four Master Step Tests.

For the 1-met condition, the subjects were seated at computers and typed from selected material, solved simple arithmetic problems, solved anagrams, or worked seek-and-find word games. These activities were chosen to represent activities of a typical office worker. The typing activity was conducted in the first and third half-hour of the two-hour work session. The reading/writing activity was done in the second and fourth half-hour of the session. For the 2.3 met conditions, the subjects walked half-way across an 11-foot long environmental chamber, stepped up and down two 9-inch steps, (Master Step Test), and continued to the other side of the room and turned around. They rested there for 8 seconds and then repeated the walking and stepping. The total time for walk, step, and rest was 15 seconds. This activity as well as the lower activity level (1 met) lasted for a total of two hours. After each 30-minute activity, the subjects were given a 3-minute break to fill out ballots and drink water, if needed. Table 3.7 shows the subjective rating used in the thermal comfort test. In addition to subjectively rating thermal comfort according to Table 3.7, subjects were asked to rate the perceived quality of the conditioned environment according to the subjective air quality scale developed by Laviana and Rholes (1987). The perceived air quality portion of this study is discussed in Section 3.5.

Table 3.7 Subjective Thermal Environment Ratings Ballot

Rating	Subjective Rating
9	Hot
8	Hot/Warm
7	Warm
6	Warm/Comfort
5	Comfort
4	Comfort/Cool
3	Cool
2	Cold/Cool
1	Cold

The 32 conditions were assigned to the chambers in a completely random fashion with two replicates of each condition. For each replicate, two men and two women were tested in each chamber. Thus, four (4) men and four (4) women were tested under each of the 32 conditions, resulting in a total of 256 subjects (128 men and 128 women).

3.3.4 Subjects

Subjects were recruited from advertisements in the college and local newspapers. After reading all the procedures and requirements for the tests (Subject Orientation And Informed Consent Statement), the 256 subjects (128 men and 128 women) signed up for the test and were scheduled. On the day of the test, the subjects reported to the Institute for Environmental Research where a nurse ascertained that their oral temperatures were normal. They then donned the clothing ensemble and were read an orientation statement which explained the subjective ballots and voting procedures. Two men and two women were randomly assigned to each chamber, they entered the chambers, and the tests began. Votes were taken at half-hour intervals: 0.5, 1.0, 1.5, and 2.0 hours. After two hours, the subjects changed back into their own clothes, were paid \$25, and were dismissed.

3.3.5 Results

Thermal comfort votes were subjected to a factor analysis with the main sources of variance being temperature/relative humidity, velocity, activity level, and gender. Figure 3.23 presents the mean vote results for 1 met and 2.3 met with a standard clothing insulation of 0.6 clo and an air velocity of 30 fpm for the eight given conditions. The reported thermal vote is the average vote of all four ballots taken at 0.5, 1.0, 1.5, and 2.0 hours.

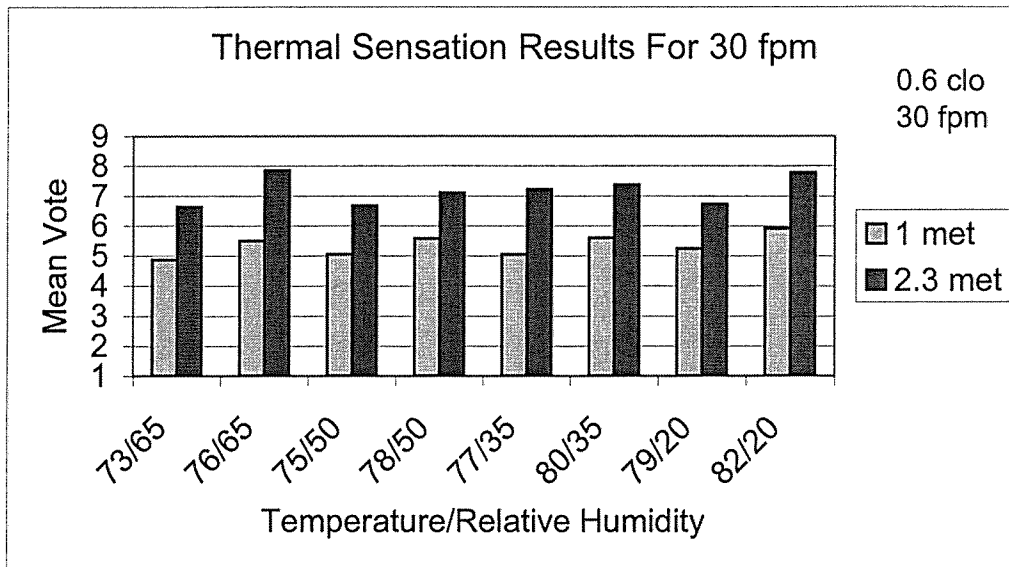


Figure 3.23 Thermal Sensation Results for 30 fpm (1 met and 2.3 met).

Figure 3.23 clearly shows that all conditions ranged from comfort (vote of 5) to warm/comfort (vote between 5 and 6) for the 1-met level. However, the thermal sensation votes become uncomfortably warm and hot/warm when the activity level increases to 2.3 met. The four combinations (temperature/relative humidity) of 73/65, 75/50, 77/35, and 79/20 resulted in identical thermal mean vote for 1 met. Examining these points on the Psychrometric chart of Figure 3.22 reveals that these points correspond to a straight line with slope corresponding roughly to the effective temperature (ET) lines which form the leftmost and rightmost boundaries of the comfort zone. The effective temperature is defined as the temperature of an environment at 50% relative humidity that results in the same total heat loss from the skin as would the actual environment, and the slope of the ET line is dependent upon several factors including activity level, skin wettedness, clothing insulation, clothing moisture permeability, and air velocity (ASHRAE *Fundamentals Handbook*, 2001). The fact that these four different temperature conditions received the same thermal sensation vote and lie on a straight line with slope corresponding roughly to the ET lines reaffirms the link between human physiological responses (heat loss from the skin, the basis for ET) and human psychological responses (perception of thermal comfort determined experimentally). Likewise, it reaffirms the notion implied by the definition of effective temperature that an increase in temperature from an original condition perceived as “comfortable” can be offset by a corresponding decrease in relative humidity to achieve the same thermal sensation of comfort. The slope of the experimental data line shows a greater sensitivity to humidity (i.e., it is more horizontal) than the ET lines. This could be a result of slight differences between the experimental factors which affect the ET and the factors assumed in computing the ET, or it could mean that the correspondence between the physiological and psychological responses to the thermal environment is not exactly one-to-one. The combinations of 76/65, 78/50, 80/35, and 82/20 for 1 met also resulted in nearly identical thermal votes, although the 82/20 condition was perceived as slightly warmer, yet not uncomfortable. The same trend occurs in the 2.3 met level, even though most subjects felt uncomfortable at the higher activity level.

Figure 3.24 shows the thermal sensation for 1-met and 2.3-met activity levels when the air velocity is increased to 50 fpm. At a velocity of 50 fpm, the subjects reported thermal

sensations ranging from comfort/cool to comfort for 1-met activity level. As the activity level increased to 2.3 met, the thermal sensations increased to between warm and hot/warm.

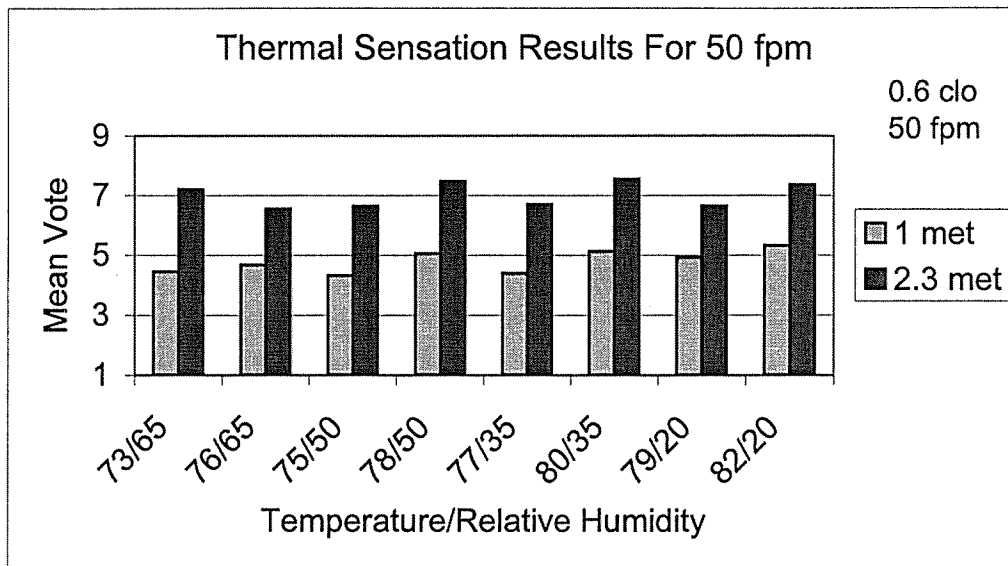


Figure 3.24 Thermal Sensation Results for 50 fpm (1 met and 2.3 met)

Figure 3.25 depicts the effect of velocity on the thermal sensation for the 1-met activity level. Increasing the velocity from 30 fpm to 50 fpm led to a slight decrease in the thermal sensation votes. At 50 fpm, all thermal sensations were in the cooler range, which is from comfort/cool to comfort. There is less than one mean-vote difference in the results between an air velocity of 30 fpm and an air velocity of 50 fpm. Overall, for the 1-met activity level, all the given conditions can be categorized as comfortable.

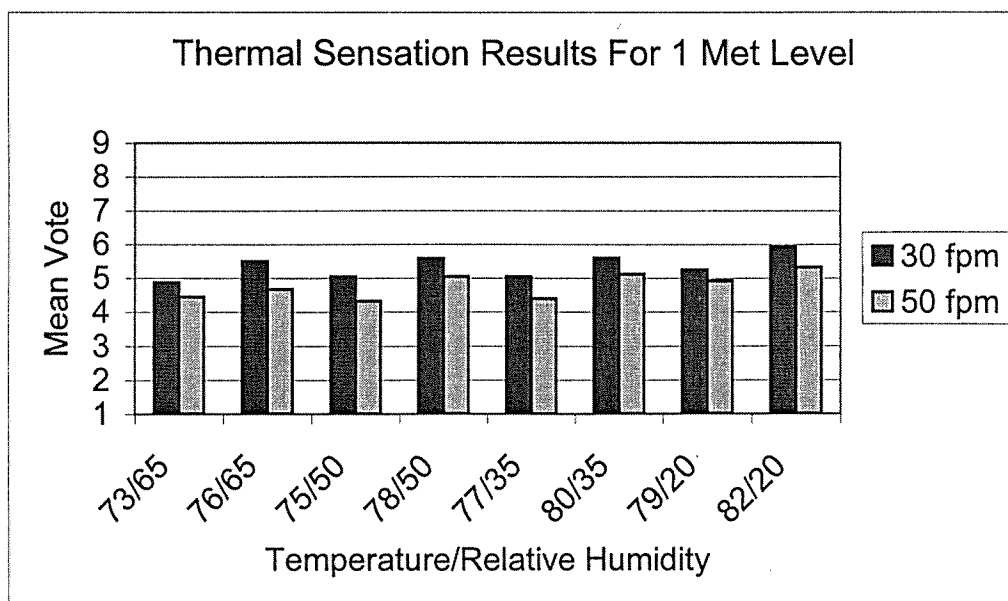


Figure 3.25 Thermal Sensation Results for 1-met Level for Two Different Velocities.

Figure 3.26 presents the influence of velocity on the thermal sensation at the 2.3-met activity level. Figure 3.26 shows that all thermal sensations range from warm/comfort to hot/warm for both lower and higher air velocity. Therefore, increasing the air velocity from 30 fpm to 50 fpm had no effect on the thermal sensation for the higher activity level. This is no surprise. The air velocity experienced by the subjects during the walking activity would be on the order of 100 fpm in still air. From the subjects' point of view, the difference between the 50 fpm and 30 fpm room air velocities superimposed vectorially on a walking velocity of 100 fpm is likely undetectable.

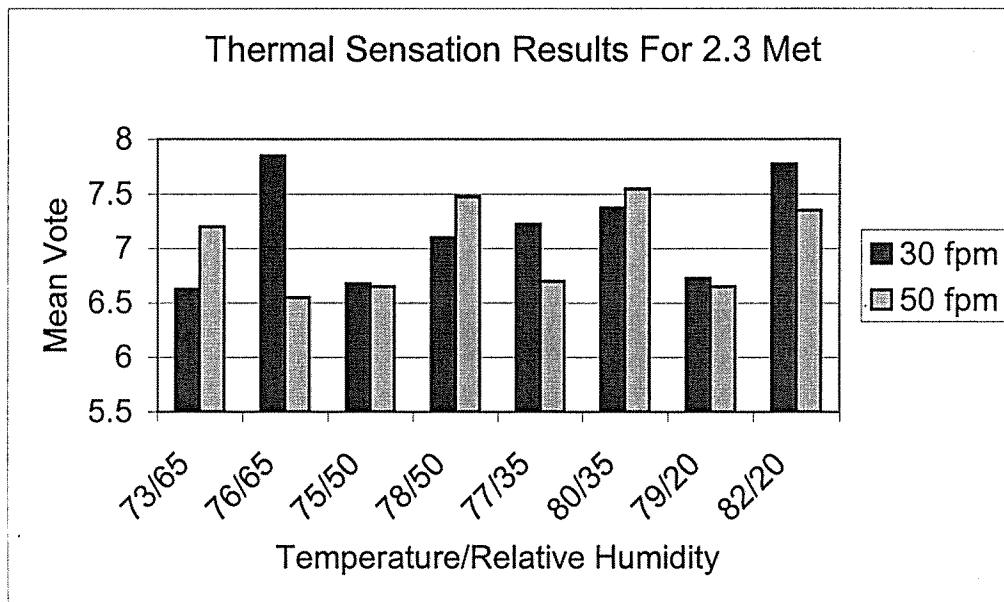


Figure 3.26 Thermal Sensation Results for 2.3-met Level for Two Different Velocities.

Figures 3.27 to 3.30 illustrate the influence of gender on thermal comfort. Figure 3.27 depicts the thermal sensation of males and females for 1-met activity with 30 fpm and a clo of 0.6, for which males and females experienced the same range of thermal comfort. As shown in Figure 3.28, males and females also experienced the same thermal sensation for the 2.3-met level at 30 fpm (all subjects felt warm for all temperature/relative humidity combinations). Figure 3.29 presents the thermal sensations by gender for an air velocity of 50 fpm at 1-met activity level. Thermal sensations for males stayed in the same range as for the 30 fpm velocity. However, thermal sensations for females decreased from “comfort” to “slightly cool.”

The thermal sensation comparison between the genders for 50 fpm and the higher activity level of 2.3-met is shown in Figure 3.30. At the 2.3-met level, an examination of Figures 3.28 and 3.30 indicates the thermal sensations of males and females remained at the same level as for the velocity of 30 fpm.

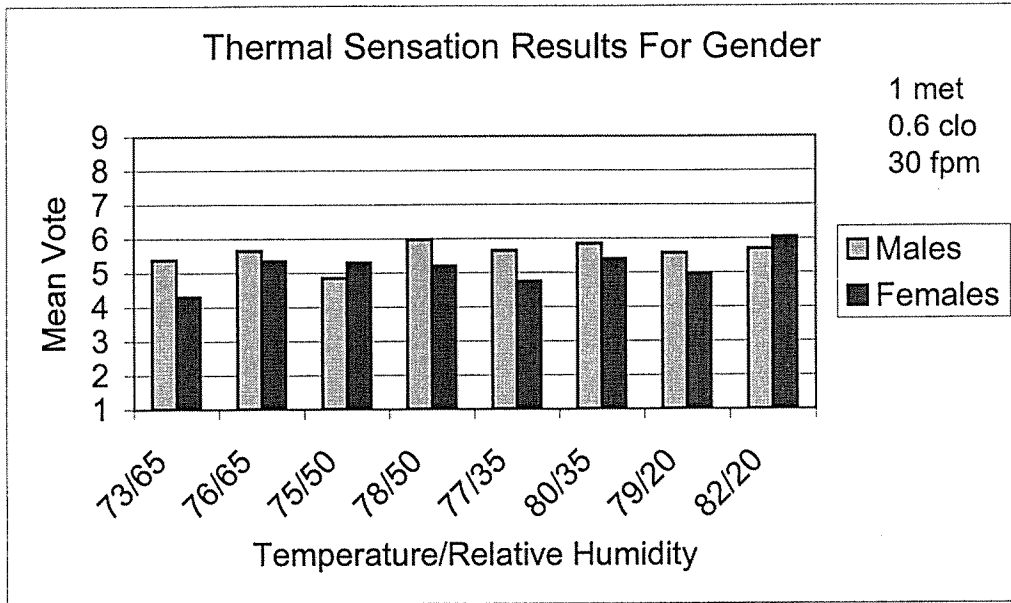


Figure 3.27 Thermal Sensation Results for Gender (1 met, 0.6 clo, 30 fpm)

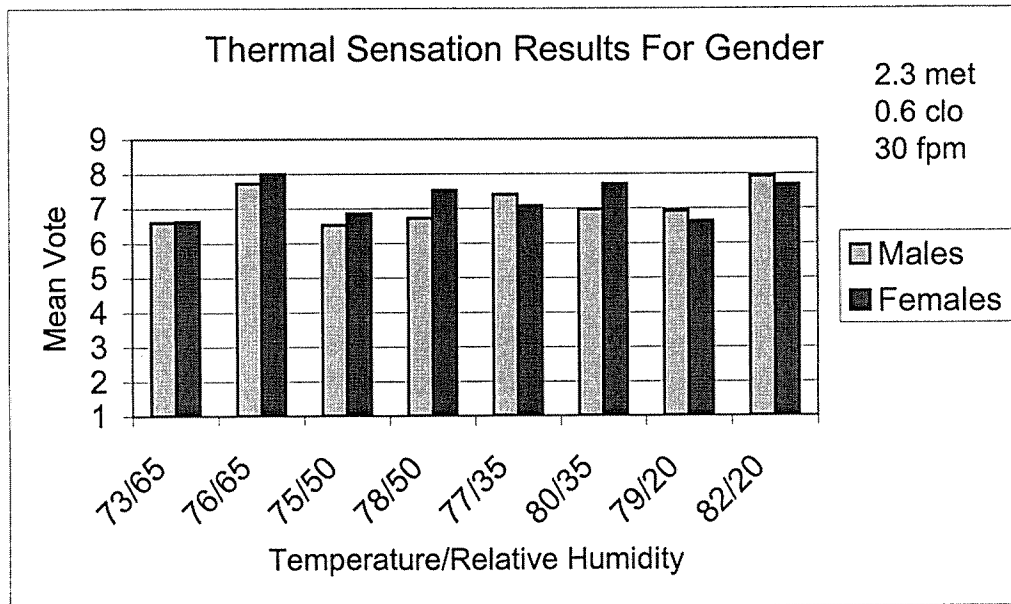


Figure 3.28 Thermal Sensation Results for Gender (2.3 met, 0.6 clo, 30 fpm)

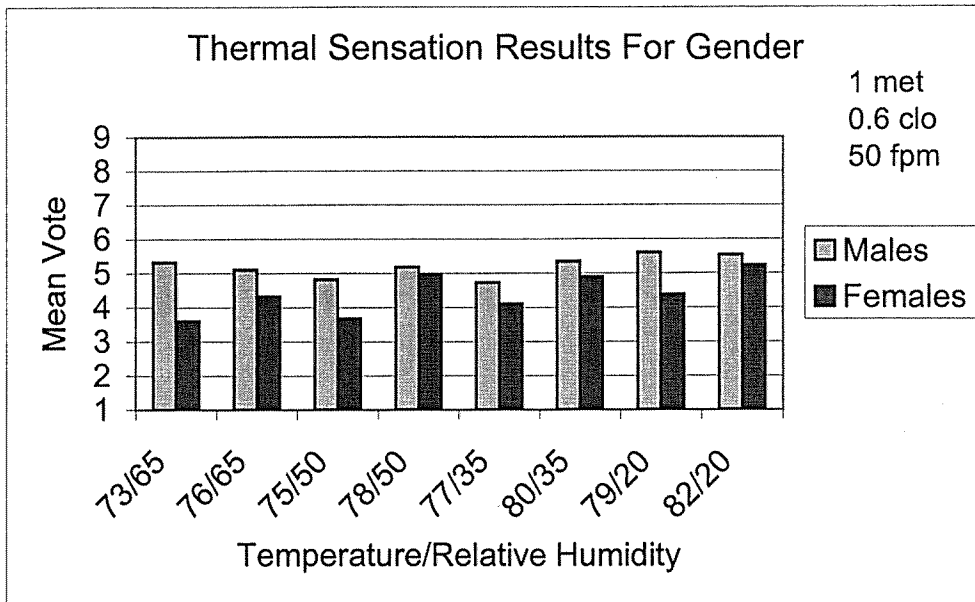


Figure 3.29 Thermal Sensation Results for Gender (1 met, 0.6 clo, 50 fpm)

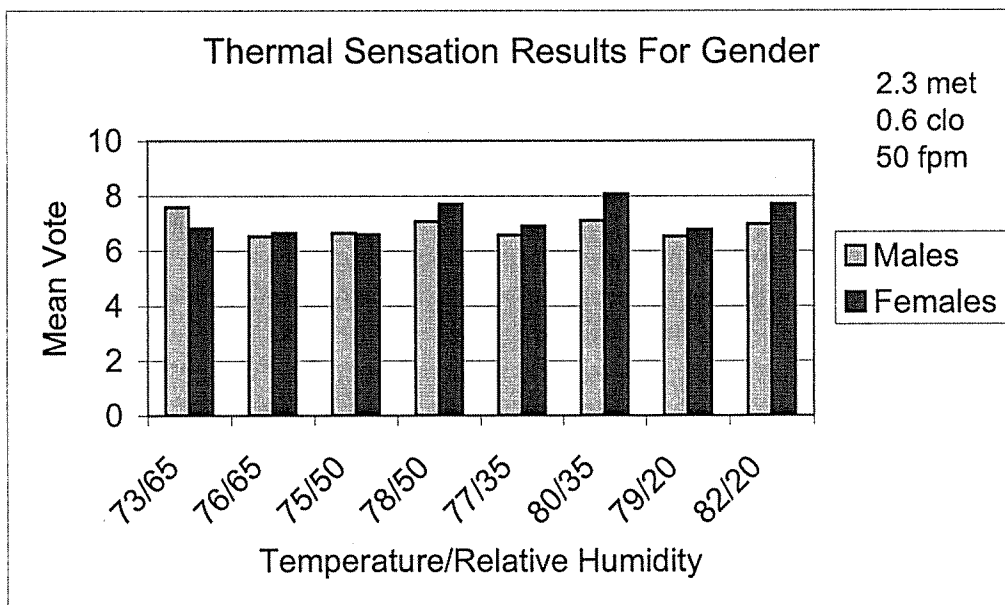


Figure 3.30 Thermal Sensation Results for Gender (2.3 met, 0.6 clo, 50 fpm)

3.3.6 Uncertainty Analysis of Experimental Study

An uncertainty analysis was performed for this study. Since this experiment was subjective, only random uncertainty was considered. The random uncertainty of the experiment

was determined by using the methods given in Coleman and Steele (1999). The expression for determining the random uncertainty is

$$U_{\text{experiment}} = \frac{2 \cdot \text{Std}}{\sqrt{N}} \quad (3.7)$$

where

Std Standard deviation
 N Number of readings

Tables 3.8 through 3.11 present the uncertainty analysis results for this experimental study. As shown in Table 3.8 and Table 3.9, with air velocities of 30 fpm and 0.6 clo insulation, the uncertainties for 1-met are higher than for 2.3-met except for condition 78/50. The same trend appears in Tables 3.10 and 3.11 when the air velocity was increased from 30 fpm to 50 fpm.

The absolute uncertainties associated with the results increased for most of the conditions as the air velocity was changed from 30 fpm to 50 fpm for the 1-met activity. For the 2.3-met level, the uncertainty of the experimental results decreased for most of the conditions when air velocity was increased from 30 fpm to 50 fpm.

Table 3.8 Uncertainty Analysis Results For Present Study (1 met, 30 fpm)

Temperature/Relative Humidity	Absolute Uncertainty Associated Mean Vote
73/65	0.709
76/65	0.813
75/50	0.610
78/50	0.813
77/35	0.769
80/35	0.767
79/20	0.672
82/20	0.778

Table 3.9 Uncertainty Analysis Results For Present Study (2.3 met, 30 fpm)

Temperature/Relative Humidity	Absolute Uncertainty Associated Mean Vote
73/65	0.582
76/65	0.583
75/50	0.573
78/50	1.149
77/35	0.619
80/35	0.680
79/20	0.654
82/20	0.424

Table 3.10 Uncertainty Analysis Results For Present Study (1 met, 50 fpm)

Temperature/Relative Humidity	Absolute Uncertainty Associated Mean Vote
73/65	1.025
76/65	1.008
75/50	0.850
78/50	0.636
77/35	0.742
80/35	0.648
79/20	0.648
82/20	0.869

Table 3.11 Uncertainty Analysis Results For Present Study (2.3 met, 50 fpm)

Temperature/Relative Humidity	Absolute Uncertainty Associated Mean Vote
73/65	0.442
76/65	0.601
75/50	0.760
78/50	0.424
77/35	0.583
80/35	0.600
79/20	0.678
82/20	0.725

3.4 COMPARISON OF PRESENT STUDY WITH THE FANGER (1982) MODEL AND ASHRAE STANDARD-55-1995

3.4.1 Comparison of the Results with the Fanger (1982) Model

The experimental results are compared with the Fanger PMV for all thirty-two cases. All the PMV generated were converted to the Standard Thermal Sensation Scale based on Table 3.1. The Standard Thermal Sensation Scale uses a seven-point thermal sensation scale; however, the present study used a nine-point scale, Table 3.7. The following equation is used to convert the 9-point scale of Table 3.7 to the ASHRAE Standard Thermal Sensation Scale of Table 3.1:

$$ASHRAE, Scale = 4 - \left(\frac{Present\ Scale - 5}{4} \right) \times 3 \quad (3.9)$$

Table 3.12 lists the conversion between both scales.

Table 3.12 Thermal Environment Ratings

Subjective Rating	Present study scale	Equivalent ASHRAE Scale	ASHRAE Scale	Subjective Rating
Cold	1	7		
Cold/Cool	2	6.25	7	Cold
Cool	3	5.5	6	Cool
Cool/Comfort	4	4.75	5	Slightly cool
Comfort	5	4	4	Neutral
Comfort/ Warm	6	3.25	3	Slightly warm
Warm	7	2.5	2	Warm
Hot/Warm	8	1.75	1	Hot
Hot	9	1		

Figures 3.31 through 3.34 present the comparison of the experimental data with the Fanger model predictions. Figure 3.31 shows the thermal sensation results and the Fanger model predictions for 1-met activity level, 30 fpm air velocity, and 0.6 clo insulation. Figure 3.31 demonstrates reasonable agreement between the Fanger model and the experimental data for the temperature/relative humidity combinations corresponding to mid to small relative humidity. The comparison for the 2.3 met level with 30 fpm velocity is depicted in Figure 3.32. At this met level, the agreement between the Fanger model predictions and the experimental data is generally not as good as for the 1-met case except for the temperature/relative humidity combinations corresponding to mid to high relative humidity. For the 82/20 condition at 2.3 met, the thermal sensation predicted by the Fanger model is off the Standard Thermal Sensation Scale and is not shown on Figure 3.32.

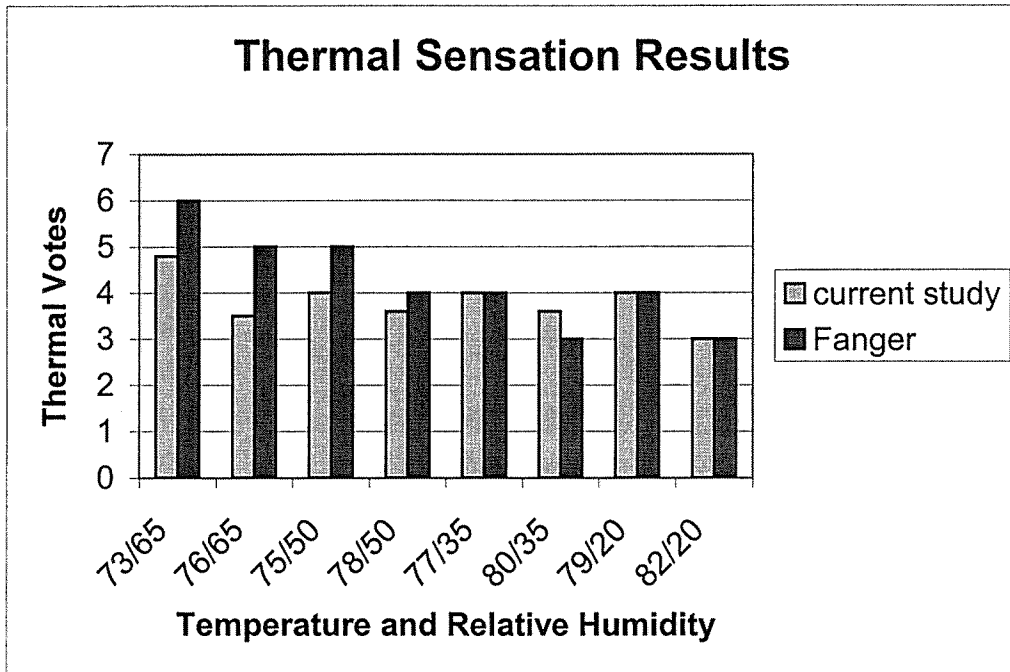


Figure 3.31 Thermal Sensation Prediction Using the Fanger Model for 1 met, 30 fpm, and 0.6 clo.

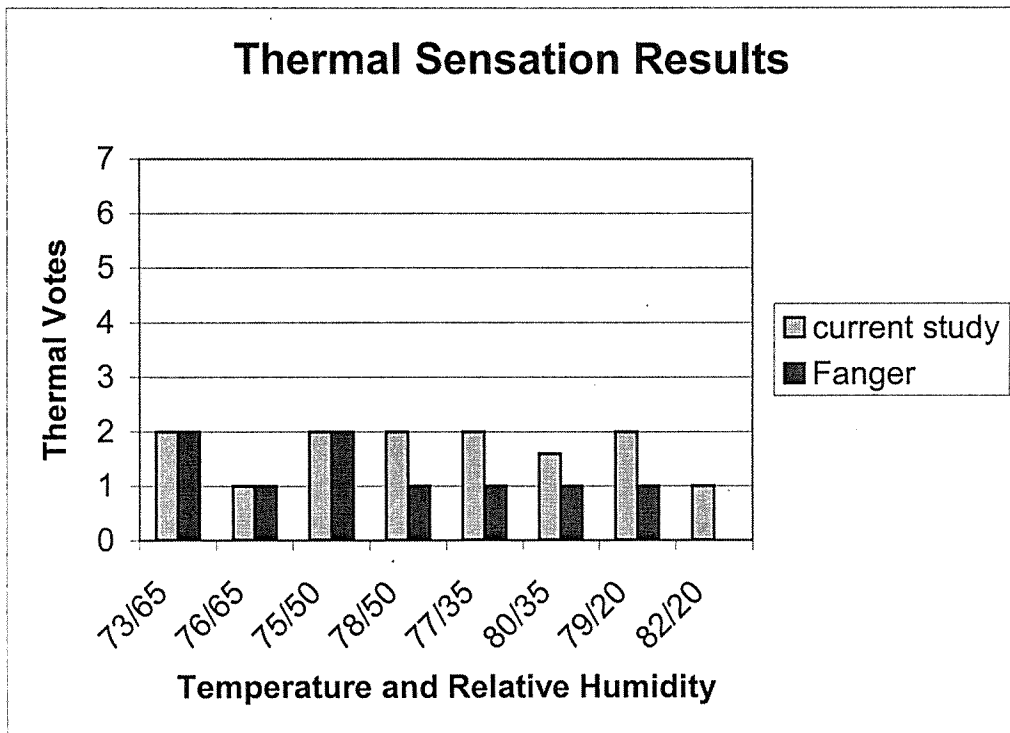


Figure 3.32 Thermal sensation prediction using the Fanger model for 2.3 met, 30 ipm, and 0.6 clo.

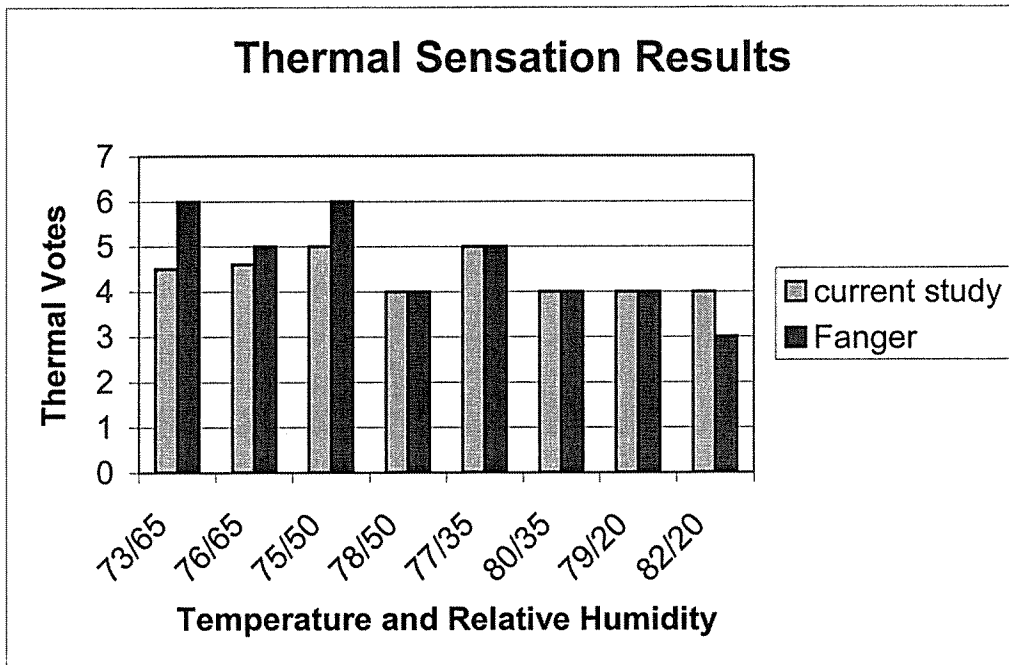


Figure 3.33 Thermal Sensation Prediction Using the Fanger Model for 1 met, 50 fpm, and 0.6 clo.

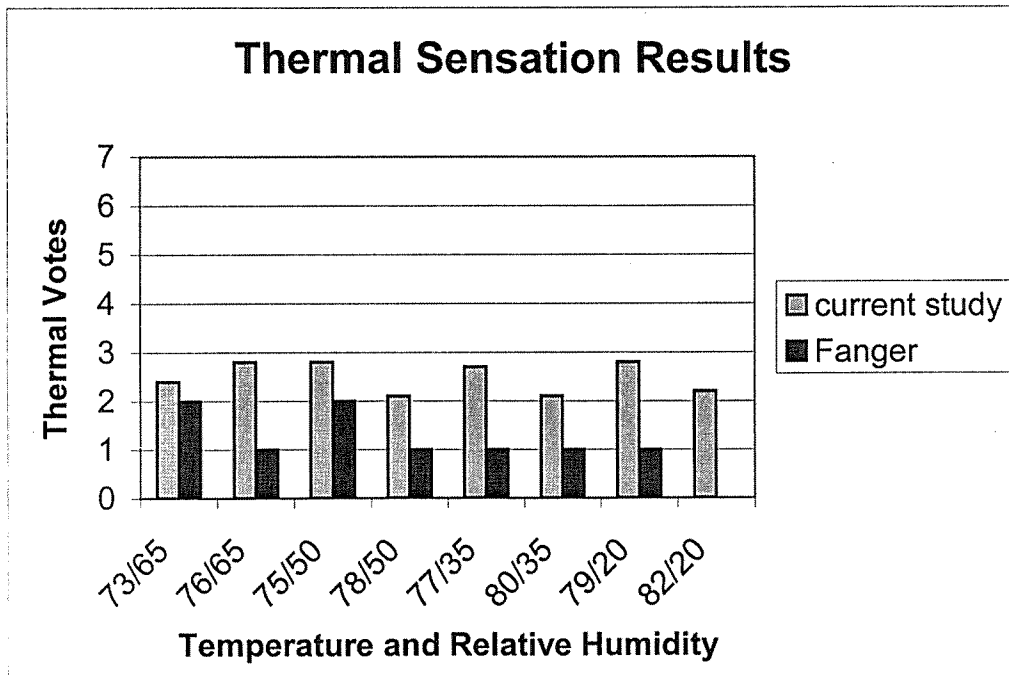


Figure 3.34 Thermal Sensation Prediction Using the Fanger Model for 2.3 met, 50 fpm, and 0.6 clo.

Figures 3.33 and 3.34 present the comparison for an air velocity of 50 fpm with 1-met and 2.3-met activity levels, respectively. Figure 3.33 shows that the thermal sensations between the Fanger model and the present study are in a very good agreement, except for the discrepancy in conditions 73/65 and 75/50. The agreement is better in the low to moderate relative humidity range. For a velocity of 50 fpm at 2.3 met, Figure 3.34, the Fanger model generally does not agree with the results of the experimental study.

In order to better access the degree of agreement between the experimental data and the Fanger model, a detailed uncertainty analysis of the Fanger model is necessary, as discussed in Sections 3.4.2 and 3.4.3.

3.4.2 Uncertainty Analysis of Fanger (1982) Model

The uncertainty of the Fanger model will be determined by using the Coleman and Steele (1999) procedure for uncertainty analysis. The first step in Coleman and Steele's methodology is to determine the uncertainty estimates for the variables. A detailed uncertainty analysis involves predicting both systematic and random errors associated with each measured variable. Systematic error is that portion of the total error that generally remains constant and is due to the physical limits of the sampling physics. Random error is that portion of the total error, which is associated with small changes in operating conditions. The effect of systematic error is to offset the reading from the true value by the amount of the error. The effect of random error is the scatter of the readings around the mean value (Coleman and Steele, 1999). The true value is the actual value of the measured variable which is unattainable since there will always be some error in the sampling instruments

Using the approach of Coleman and Steele, an uncertainty analysis was performed. MathCad was used to calculate the numerical values for the uncertainties. The detailed uncertainty analysis is presented in Appendix 3-A. Table 3.13 through Table 3.16 present the overall absolute uncertainties associated with the calculated PMVs from the Fanger 1982 Model. The overall uncertainty of a calculated PMV is the interval around the best value of PMV within which the true value of PMV is expected to lie.

As presented in Tables 3.13 and 3.14, the uncertainties for 1 met are higher than for 2.3 met, with air velocity of 30 fpm and 0.6 clo insulation. The same trend appears for Tables 3.15 (1 met) and 3.16 (2.3 met), for an air velocity of 50 fpm. The uncertainties of the PMVs calculated from the Fanger model increase with increasing air velocity for both met levels.

In order to determine the major sources of uncertainty, the variables which have the larger uncertainty percentage contribution (UPC) are identified. Table 3.17 and Figure 3.35 show the UPC of each variable to the overall uncertainty for the input condition of 1 met, 30 fpm, 0.6 clo, 73 °F, and 65% relative humidity.

As depicted in Figure 3.35, activity level has the highest overall UPC. Clothing insulation and air velocity are the second and third highest, respectively. The UPC's associated with the rest of the variables are very small compared to that of the activity level and, therefore, can be neglected. Met levels for this study were estimated rather than measured. Accurate measurement of met levels for this study could not have been attained without significant

additional testing. Moreover, the overall uncertainties in the Fanger model resulting from uncertainties in the input data, even with estimated met levels, are within ± 1 PMV, which is considered “close enough” when predicting something as subjective as human *perception* of comfort.

Table 3.13 Uncertainty Analysis Results (1 met, 30 fpm, and 0.6 clo)

Temperature/Relative Humidity	Uncertainty of Fanger Model (\pm)
73/65	0.873
76/65	0.777
75/50	0.809
78/50	0.714
77/35	0.747
80/35	0.659
79/20	0.688
82/20	0.61

Table 3.14 Uncertainty Analysis Results (2.3 met, 30 fpm)

Temperature/Relative Humidity	Uncertainty of Fanger model (\pm)
73/65	0.507
76/65	0.514
75/50	0.504
78/50	0.512
77/35	0.5
80/35	0.508
79/20	0.497
82/20	0.504

Table 3.15 Uncertainty Analysis Results (1 met, 50 fpm)

Temperature/Relative Humidity	Uncertainty of Fanger model (\pm)
73/65	1.019
76/65	0.909
75/50	0.944
78/50	0.834
77/35	0.873
80/35	0.771
79/20	0.804
82/20	0.712

Table 3.16 Uncertainty Analysis Results (2.3 met, 50 fpm)

Temperature/Relative Humidity	Uncertainty of Fanger model (+)
73/65	0.582
76/65	0.59
75/50	0.578
78/50	0.588
77/35	0.574
80/35	0.583
79/20	0.57
82/20	0.578

Table 3.17 Results of UPC for Overall Uncertainty

Variables	UPC
t_a	0.19
t_r	0.13
V	1.84
I_{cl}	30.3
M	67.2
p_a	0.11

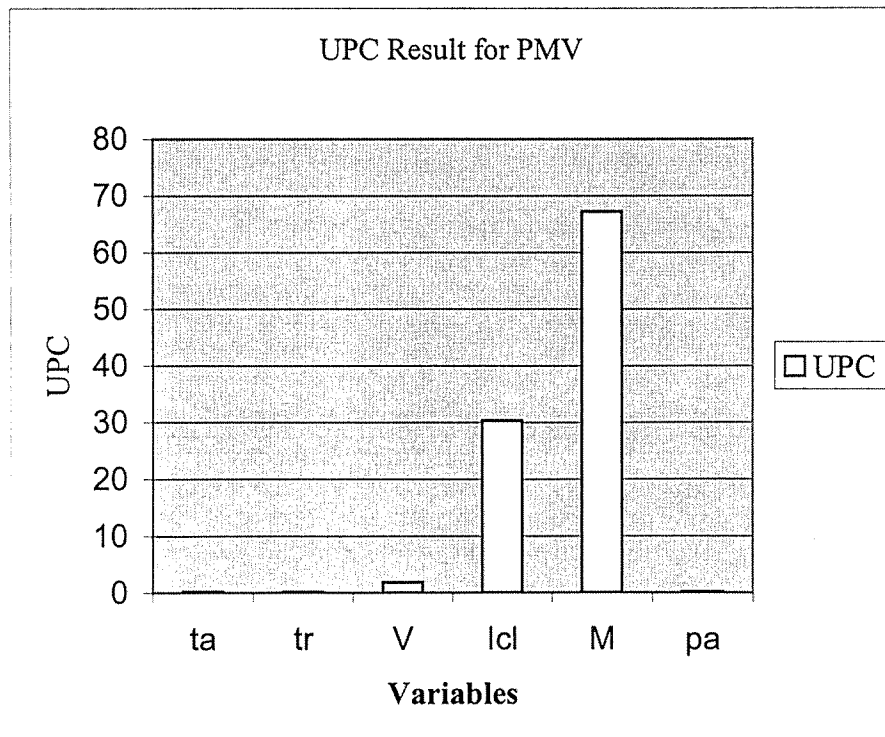


Figure 3.35 Results of UPC for the Overall Uncertainty

3.4.3 Comparison of the Experimental Uncertainty with the Fanger (1982) Model Uncertainty

In order to access the differences in the results of the present study and the Fanger model, a comparative test has to be considered. A comparative test is the comparison of two test results, either from the same facility or from different facilities. In this case, the two tests are this experimental study and the Fanger model results. The difference, δ , between a thermal vote of the present study, converted into seven-point scale using Equation (3.9), and the corresponding thermal sensation predicted from the Fanger model is computed. The uncertainty associated with the difference is

$$U_{\Delta} = \sqrt{U_{\text{experiment}}^2 + U_{\text{PMV}}^2} \quad (3.10)$$

If the thermal sensation difference, δ , is smaller than the uncertainty of the difference, U_{Δ} , then there is no indication that the results of the present study and the Fanger model represent different physical phenomena (Coleman and Steele, 1999), and the results are considered to be in agreement. Tables 3.18 through 3.21 represent the results of the comparative test.

Table 3.18 Uncertainty Results For Comparative Test (1 met, 30 fpm)

Temperature/Relative Humidity	Thermal Sensation Difference (δ)	Uncertainty of Difference (U_{Δ})
73/65	1.2	1.12
76/65	1.4	1.12
75/50	1	1.01
78/50	0.4	1.08
77/35	0	1.07
80/35	0.4	1.01
79/20	0	0.96
82/20	0	0.99

Table 3.19 Uncertainty Results For Comparative Test (2.3 met, 30 fpm)

Temperature/Relative Humidity	Thermal Sensation Difference (δ)	Uncertainty of Difference (U_{Δ})
73/65	0	0.77
76/65	0	0.78
75/50	0	0.76
78/50	1	1.26
77/35	1	0.80
80/35	0.6	0.85
79/20	1	0.82
82/20	0.8	0.66

Table 3.20 Uncertainty Results For Comparative Test (1 met, 50 fpm)

Temperature/Relative Humidity	Thermal Sensation Difference (δ)	Uncertainty of Difference (U_{Δ})
73/65	1.5	1.45
76/65	0.3	1.36
75/50	1	1.27
78/50	0	1.05
77/35	0	1.15
80/35	0	1.01
79/20	0	1.03
82/20	1	1.12

Table 3.21 Uncertainty Results For Comparative Test (2.3 met, 50 fpm)

Temperature/Relative Humidity	Thermal Sensation Difference (δ)	Uncertainty of Difference (U_{Δ})
73/65	0.4	0.73
76/65	1.8	0.84
75/50	0.8	0.95
78/50	1.1	0.73
77/35	1.7	0.82
80/35	1.1	0.84
79/20	1.8	0.89
82/20	2.2	0.93

As shown in Tables 3.18 and 3.20 for the 1-met activity level, the thermal sensation differences are smaller than the uncertainties of the differences except for conditions 73/65 and 76/65 at 30 fpm and 73/65 at 50 fpm. The agreement between the present study and the thermal comfort model are, therefore, considered acceptable.

For the 2.3-met activity level and 30 fpm, the thermal sensation differences are less than the uncertainties of the differences except for conditions 77/35, 79/20, and 82/20 as seen in Table 3.19. This comparison is the same as the earlier comparison of model and test results in Figure 3.32, which seems to indicate agreement at mid to high relative humidities. However, the sample size for each thermal condition (8 people) is not large enough to conclude general agreement at mid to high relative humidity based on agreement at only three conditions. At 2.3 met and 50 fpm, most of the δ values in Table 3.21 are greater than the U_{Δ} values, indicating poor agreement between the model and the data.

In the discussion of the basis for Fanger's model, Section 3.2.6.2, a key assumption of the model was mentioned. The model assumes that all sweat generated is evaporated, thus eliminating clothing moisture permeability concerns. Fanger explains that the assumption is valid for normal indoor clothing with low to moderate activity levels. The agreement between the model and the experimental data at the 1 met activity level affirms the validity of this assumption. The poor agreement between the model and the experimental data at the elevated activity level (2.3 met) may indicate that 2.3 met is above the limits of this assumption. In order

to better determine the activity-level limits of the model, more experimental data are needed at various elevated met levels with observations of skin and clothing wetness.

3.4.4 Comparison with ASHRAE Standard 55

The eight thermal conditions were selected within the ASHRAE Thermal Comfort Zone except for the condition of 80°F and 20% relative humidity which falls outside the zone, as shown in Figure 3.22. Standard 55 was developed for sedentary people (1.2 met) with clothing insulation of 0.6 clo and an air velocity between 30 and 50 fpm. The ASHRAE data were generated using the ASHRAE Thermal Comfort Program version 1.0 (Fountain and Huizenga, 1995) where the software is based on ASHRAE Standard 55-1995 for 1-met activity level. For non-sedentary activity (higher met level), the program is based on the Standard 55 recommendation of lowering the operative temperature based on activity level and clothing insulation up to 3 met.

Figure 3.36 presents the thermal sensation test results as compared with ASHRAE Standard 55 for 1-met activity, 30 fpm velocity, and 0.6 clo. As expected, the figure shows good agreement since the test conditions were chosen within the Comfort Zone. The only exception is the 73/65 condition, which appear slightly cool according to the ASHRAE Comfort Program. For the 82/20 thermal condition chosen outside the ASHRAE Comfort Zone, people should feel slightly warm according to Standard 55. Good agreement with ASHRAE Standard 55 was also achieved for 1 met activity, 50 fpm velocity, and 0.6 clo insulation. The comparison is shown in Figure 3.37. The only exceptions are the 73/65 and the 75/50 thermal conditions where the subjects reported comfortable conditions. Based on the ASHRAE Comfort Program, people should feel slightly cool even though this condition is within ASHRAE Standard 55 Comfort Zone.

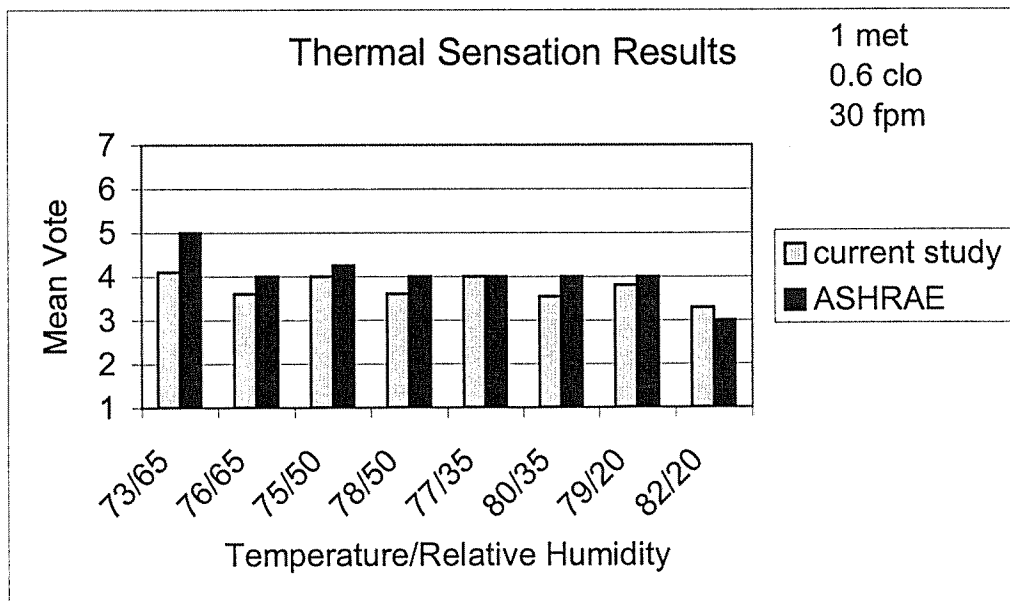


Figure 3.36 Current Study Comparison with ASHRAE Standard 55-1995 for 1 met Activity, 30 fpm Velocity, and 0.6 clo.

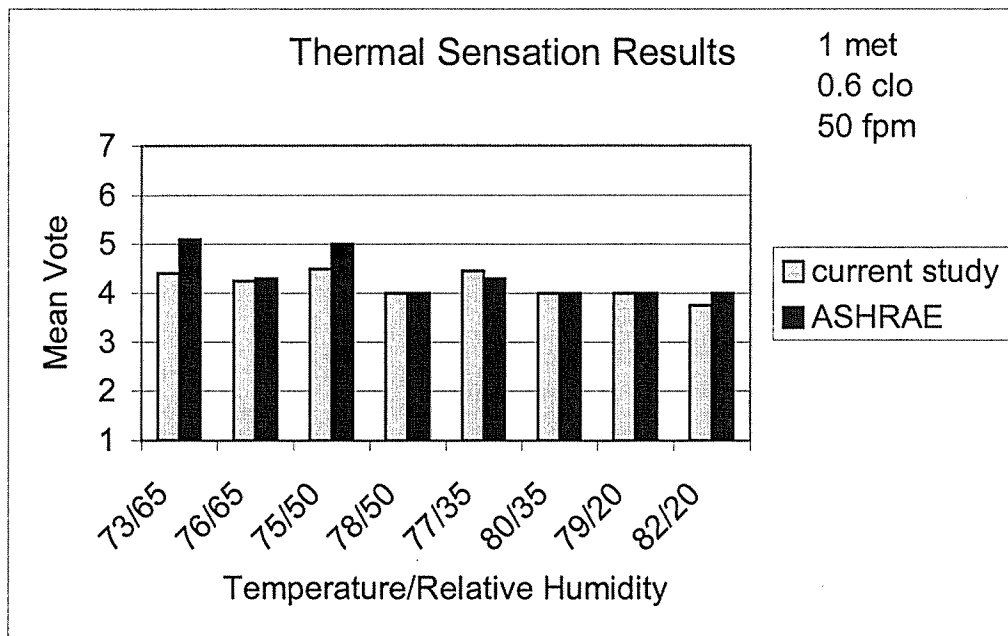


Figure 3.37 Current Study Comparison with ASHRAE Standard 55-1995 for 1 met Activity, 50 fpm Velocity, and 0.6 clo.

3.5 PERCEIVED AIR QUALITY

3.5.1 Introduction

In addition to rating thermal comfort, the 256 subjects also rated the perceived quality of the 32 thermal environmental conditions according to the subjective air quality scale developed by Laviana and Rholes (1987). The descriptors of the air quality scale are as follows:

Positive Descriptors:

Content with
 Agreeable
 Satisfied with
 Good
 Acceptable
 Pleasant
 Comfortable

Negative Descriptors:

Unpleasant
 Undesirable
 Dissatisfied with
 Disagreeable
 Unsatisfactory

These twelve descriptors are combined into a single factor representing the air quality scale which is scaled to fall between -100 (worst) and +100 (best), with "0" representing "neutral." Two scales were developed for describing air quality: the favorable air quality scale (AQ+) and the unfavorable air quality scale (AQ-) expressed in Equations (3.11) and (3.12), respectively.

$$AQ = \left[\left[\sum_{i=0}^6 (\text{Rating}_i \cdot \text{Loading}_i) - 5.752 \right] \cdot 2.90 \right] \quad (3.11)$$

$$AQ = \left[\left[\left[\sum_{i=0}^4 (\text{Rating}_i \cdot \text{Loading}_i) - 4.129 \right] \cdot 4.04 \right] \right] \quad (3.12)$$

The rating and loading are presented below (Laviana and Rohles, 1987):

Rating

- 7 = very accurate
- 6 = accurate
- 5 = slightly accurate
- 4 = Neutral, neither accurate nor inaccurate
- 3 = slightly inaccurate
- 2 = inaccurate
- 1 = very inaccurate

Loading

<u>Descriptors</u>	<u>Loading</u>	<u>Descriptors</u>	<u>Loading</u>
Content with	0.803	Unpleasant	0.823
Agreeable	0.808	Undesirable	0.838
Satisfied with	0.815	Dissatisfied with	0.815
Good	0.848	Disagreeable	0.820
Acceptable	0.813	Unsatisfactory	0.833
Pleasant	0.825		
Comfortable	0.840		

The test subjects rate each air quality descriptor using the 1 through 7 rating scale. The loading factors were developed by Laviana and Rholes in order to weight the descriptors.

3.5.2 Results - Positive (Favorable) Air Quality Scale

Figure 3.38 shows the average positive (favorable) air quality scale for 1 met and 2.3 met with standard clothing insulation (0.6 clo) and 30 fpm air velocity for the eight temperature/humidity conditions. The reported air quality scale is the average vote of all four ballots taken at 0.5, 1.0, 1.5, and 2.0 hours. Figure 3.38 demonstrates that air quality satisfaction ranges from 65% to 80% for all conditions at 1-met activity level. However, the air quality scales become relatively low for the 2.3- met activity level (20% to 55%).

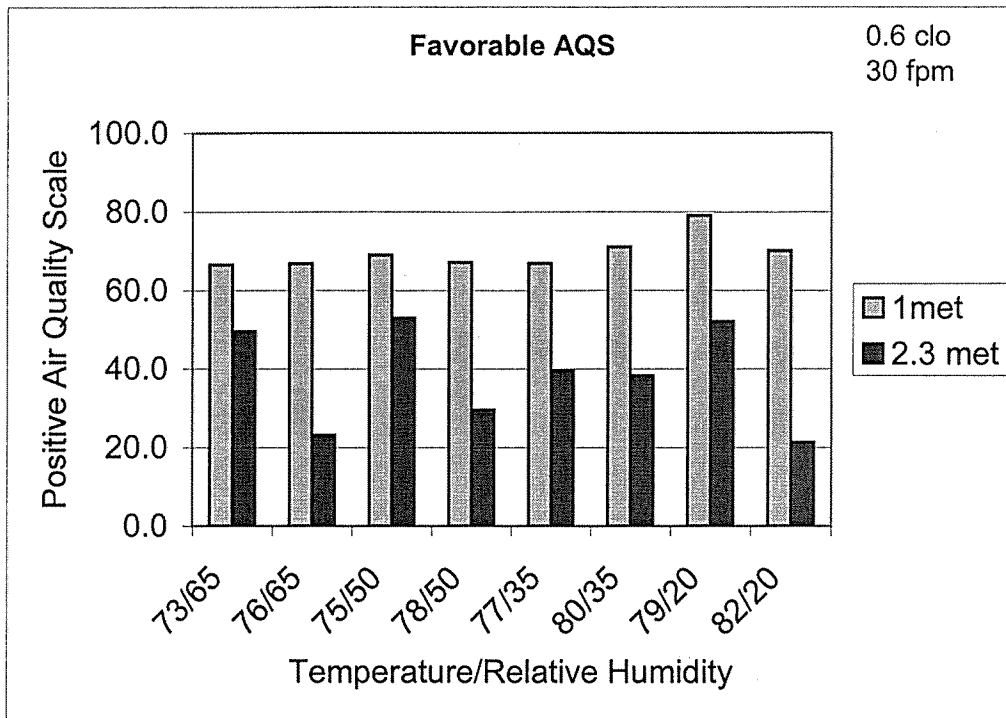


Figure 3.38 Positive Air Quality Scale for 30 fpm and 0.6 clo.

Figure 3.39 depicts the air quality scale for 1-met and 2.3-met activity levels when the air velocity is increased to 50 fpm. The trends are similar to that of Figure 3.38 for 30 fpm. At 1 met, reported air quality scales range from 60% to 75% satisfaction but degrade to between 30% and 60% satisfaction when the activity level is increased to 2.3 met.

Figures 3.40 and 3.41 show the effects of velocity on the positive air quality scale for the 1-met and 3-met activity levels, respectively. For either activity level, increasing the air velocity from 30 fpm to 50 fpm had no consistent effect on positive air quality perceptions.

3.5.3 Results - Negative (Unfavorable) Air Quality Scale

Figures 3.42 through 3.45 present the results of the negative (unfavorable) air quality perceptions. In the case of the negative air quality scale, a higher percentage is less favorable (more unfavorable), while a lower percentage is more favorable (less unfavorable). For all eight thermal conditions and both air velocities examined, the air quality is perceived as being significantly more unfavorable (less favorable) at the higher (2.3 met) activity level. Increasing air velocity from 30 fpm to 50 fpm had no consistent effect on negative air quality perceptions, as was the case with positive air quality perceptions.

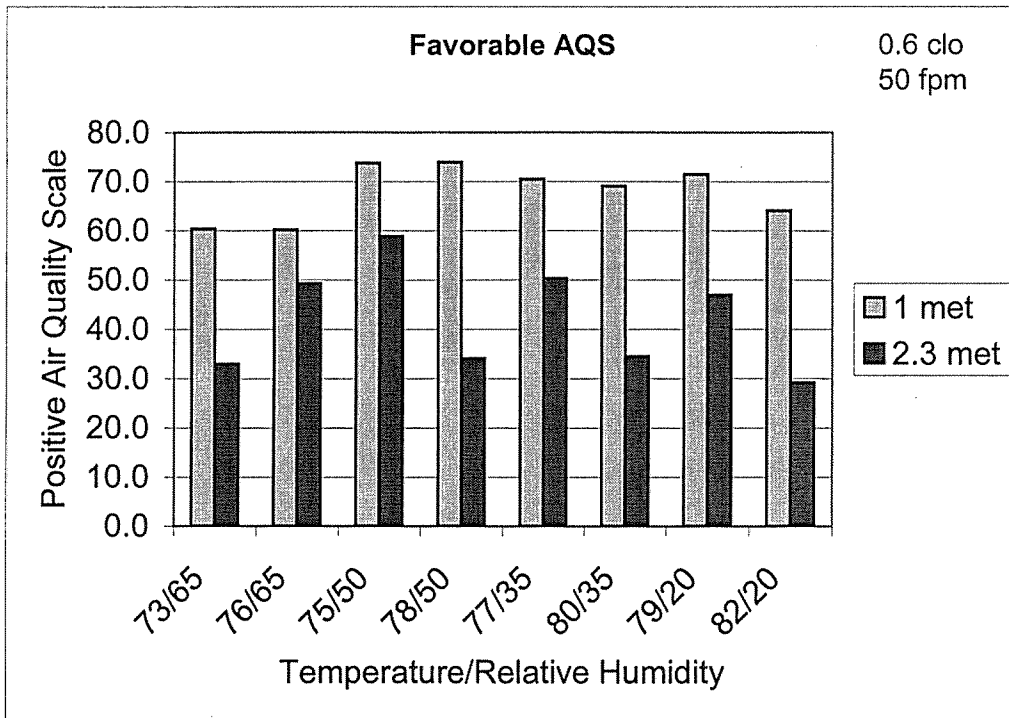


Figure 3.39 Positive Air Quality Scale for 50 fpm and 0.6 clo.

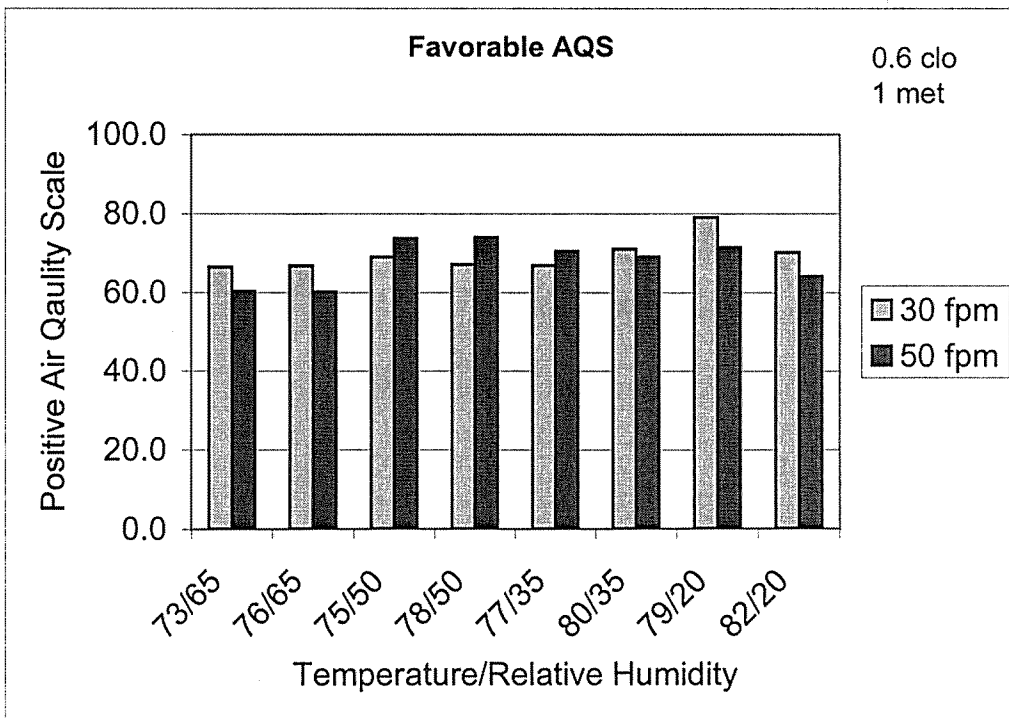


Figure 3.40 Positive Air Quality Scale for the 1-met Level.

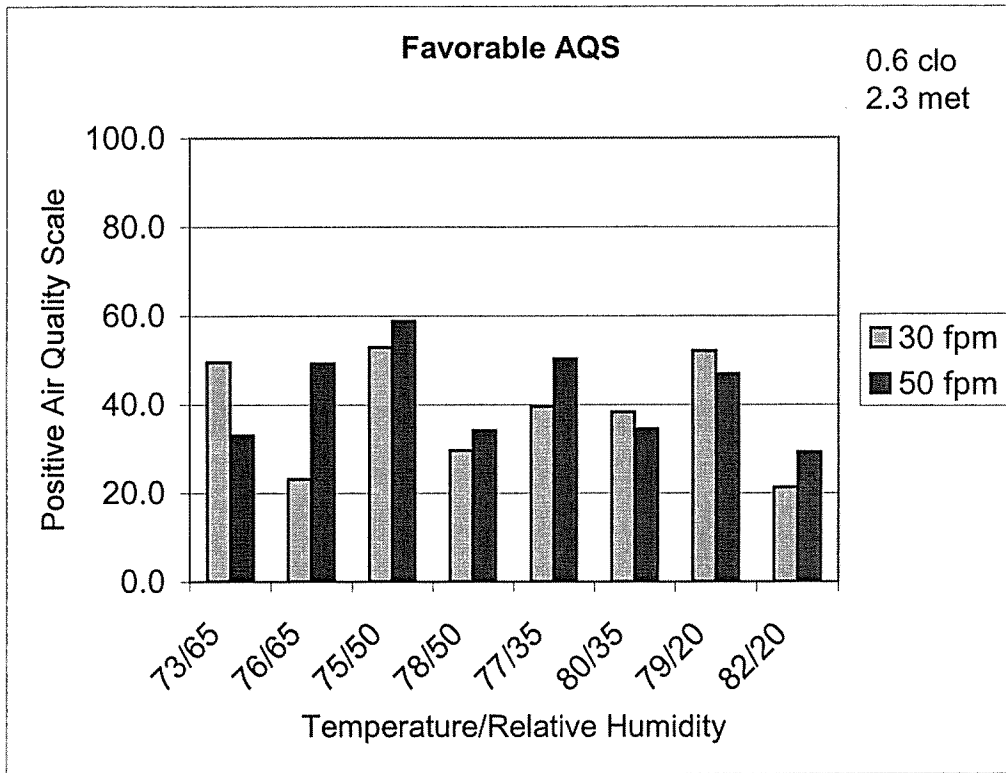


Figure 3.41 Positive Air Quality Scale for the 2.3-met Level.

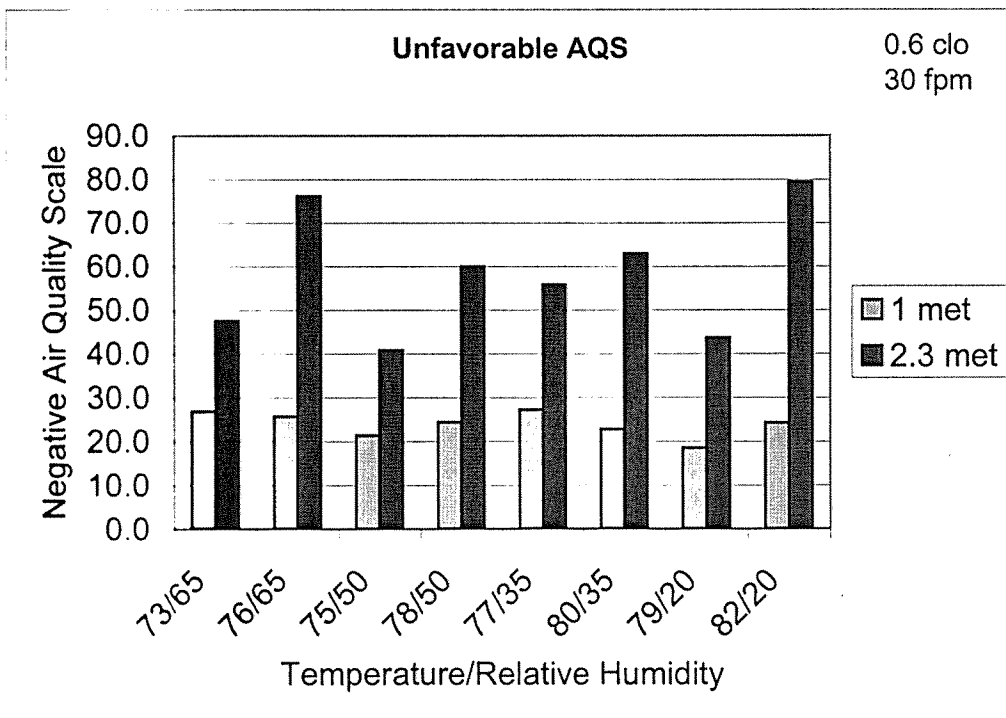


Figure 3.42 Negative Air Quality Scale for 30 fpm.

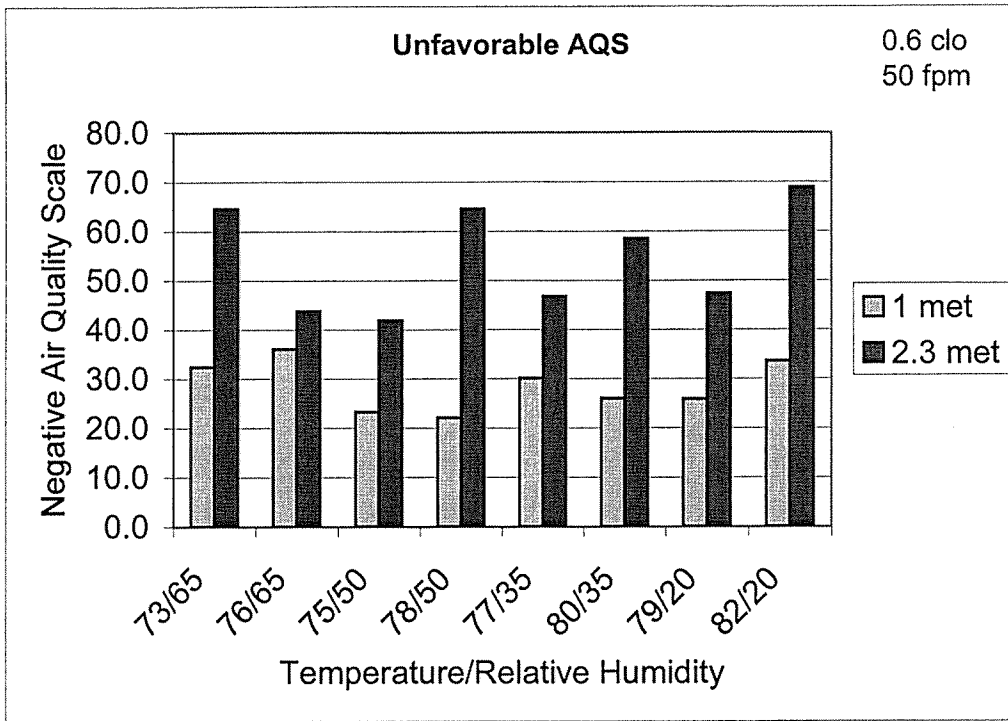


Figure 3.43 Negative Air Quality Scale for 50 fpm.

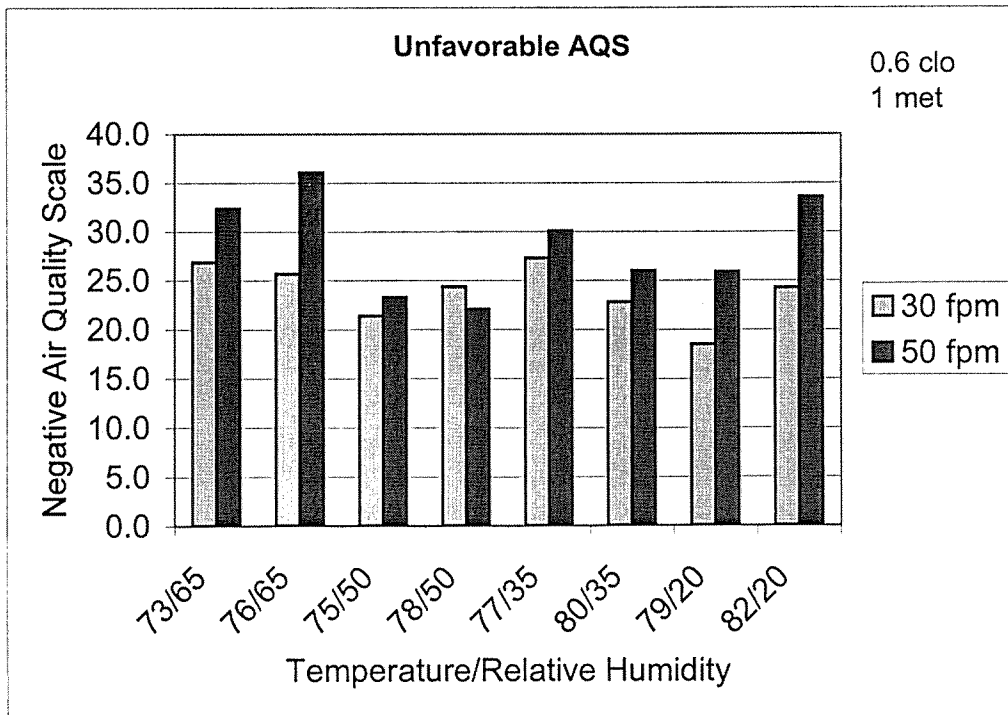


Figure 3.44 Negative Air Quality Scale for the 1-met Level.

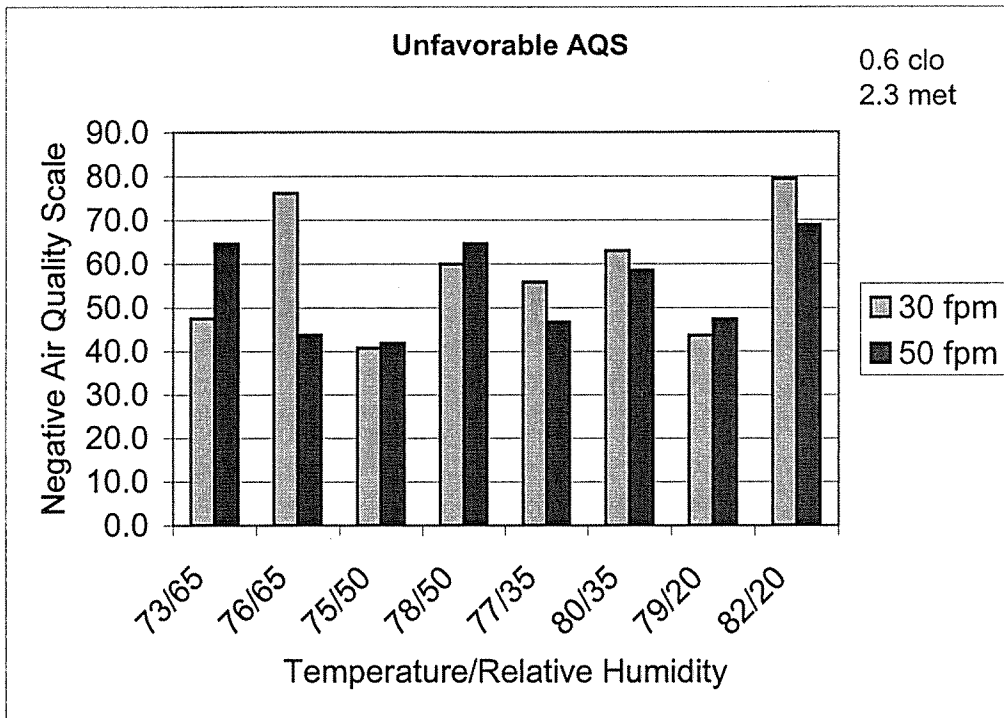


Figure 3.45 Negative Air Quality Scale for the 2.3-met Level.

3.6 SUMMARY AND CONCLUSIONS

Human thermal comfort is influenced by four environmental parameters (dry bulb temperature, mean radiant temperature, relative humidity, and air velocity) and two personal parameters (activity level and clothing insulation). Each parameter is strongly related to the other parameters in affecting thermal comfort. This is evident from the literature survey in that the majority of studies in the survey examined the combined effects of two or more parameters on thermal comfort. The interrelation is also quite evident within the ASHRAE Comfort Chart with the appearance of terms such as *operative temperature*, which combines dry bulb temperature and mean radiant temperature into a single index, and *effective temperature*, which combines dry bulb temperature and relative humidity into a single index. The introduction of the effective temperature concept as early as 1923 (Houghten and Yaglou, 1923) is evidence that the fact has long been recognized that increases in dry bulb temperature can be offset by decreases in relative humidity. However, the nearly vertical slope of the effective temperature lines on the Comfort Chart indicates that humans are much more sensitive to dry bulb temperature than relative humidity (i.e., large changes in relative humidity are required to offset small changes in temperature). As further evidence of interrelation between each of the parameters, ASHRAE Standard 55 gives guidelines for increasing air speed to offset increases in dry bulb temperature and for decreasing operative temperature to compensate for elevated activity levels.

Human perception of thermal comfort is related to human physiological responses to the thermal environment. Fanger's (1967) steady-state energy balance model uses empirical models of physiological responses to the thermal environment (mean skin temperature and sweat secretion rate) to predict human perception of thermal comfort. Much of the ASHRAE Standard

55 is based on studies using this model, which has been validated over a wide range of relative humidities and dry bulb temperatures for sedentary subjects in standard clothing. In the present study, an experimental study was conducted to obtain data suitable for further validation of the ASHRAE Standard 55 Comfort Zone, the ASHRAE Thermal Comfort Program, and the Fanger model upon which much of the Comfort Zone and Thermal Comfort Program are based. In keeping with the overall objective of promoting widespread use of desiccant-based air conditioning equipment, the scope of this experimental study was limited to higher met levels and varying air velocity. Air velocities, however, were limited to 30 fpm and 50 fpm, the maximum velocities recommended for winter and summer applications, respectively, by ASHRAE Standard 55. Higher air velocities and heavier clothing insulations are generally not of interest for typical summer air conditioning applications.

As expected, the experimental data for the baseline condition (1 met activity level) were in agreement with the Fanger model within the limits of the experimental and model uncertainties. Likewise, the baseline 1-met experimental data were in agreement with the ASHRAE Standard 55 Comfort Zone. All temperature/humidity conditions within the Comfort Zone resulted in mean thermal votes within ± 0.5 of a vote corresponding to "neutral" or "comfort." (The borders of Comfort Zone do not necessarily correspond to a predicted mean vote (PMV) of "neutral," but rather a PMV within ± 0.5 of neutral.) All temperature/humidity conditions of the study were chosen within the Comfort Zone with the exception of the 82°F/20% condition. The 82/20 condition (just outside the Comfort Zone) was included to determine if the comfort zone could be stretched to include higher dry bulb temperatures at very low relative humidities attainable with desiccant-based air conditioning equipment. The 82/20 condition was perceived as slightly warmer, yet not uncomfortable. Although the experimental data were in general agreement with the Comfort Chart, the experimental data indicate a stronger dependence on humidity than predicted by the Comfort Chart (i.e., the effective temperature lines corresponding to the data are more horizontal than the effective temperature lines on the Comfort Chart). Evaluation of the data according to the perceived air quality approach (Laviana and Rohles, 1987) showed that occupants involved in the 1-met activity expressed 60% to 80% satisfaction with the quality of the thermal environment on a positive air quality scale and 20% to 35% dissatisfaction on a negative air quality scale. These scales are based on the average occupant's degree of satisfaction or dissatisfaction with the thermal environment and are not to be confused with the basis of the ASHRAE Comfort Zone, which is 80% of the occupants being 100% satisfied while the remaining 20% will be 100% dissatisfied. The two totally different approaches, however, yield results that are at least qualitatively in agreement.

At the elevated activity level (2.3 met), the agreement between the experimental data and the Fanger model is poor. The poor agreement at the elevated activity level (2.3 met) may indicate that 2.3 met is above the limits of the Fanger model assumption that all sweat generated is evaporated (thus eliminating clothing moisture permeability concerns). In order to better determine the activity-level limits of the model, more experimental data are needed at various elevated met levels with special attention given to observation of skin and clothing wetness as well as clothing moisture permeability.

Increasing the air velocity from 30 fpm to 50 fpm had no effect on thermal comfort for men or women at the elevated activity level (2.3 met) nor for men at sedentary conditions (1 met). However, sedentary women felt slightly cooler, yet not uncomfortable, when the air

velocity was increased from 30 fpm to 50 fpm. Higher air velocities (up to 300 fpm) may be tolerated (even preferred) for activity levels above 2.0 met (ASHRAE Standard 55). However, this study was focused on temperature and humidity effects with air velocities limited to 50 fpm.

The ASHRAE Comfort Chart is valid for sedentary and light activity only (≤ 1.2 met). However, ASHRAE Standard 55 contains relations for adjusting operative temperature to maintain comfort for higher activity levels (1.2 to 3 met) and clothing insulations. Although these relations do not explicitly account for humidity, it is implicitly accounted for by shifting the effective temperature lines of the Comfort Zone according to the calculated operative temperature shift. According to these relations, the effective temperature limits for an activity level of 2.3 met should be decreased by about 10°F . None of the eight temperature/humidity conditions examined in the study were within this adjusted comfort zone. Therefore, the 2.3-met experimental data agree, at least qualitatively, with the adjusted Comfort Zone in that subjects reported uncomfortably warm sensations for all eight temperature/humidity conditions outside the 2.3-met-level adjusted Comfort Zone. Similarly, the perceived air quality evaluations for the 2.3 met activity level demonstrate qualitative agreement with the adjusted Comfort Zone and the thermal comfort evaluations. Subjects involved in the 2.3 met activity expressed low levels of satisfaction and high levels of dissatisfaction with the quality of the thermal environment.

Meaningful quantitative assessments of met-level adjusted comfort zones could be made by gathering extensive data for elevated met levels at temperature/humidity conditions near the effective temperature boundary lines of the adjusted comfort zones. According to the Gagge et al. (1971b) analytical relations for effective temperature, the slope of the effective temperature lines at elevated met levels should be more horizontal (i.e., more sensitive to humidity) than those of the standard 1.2 met-level Comfort Zone. Therefore, the usefulness of gathering such data would be to validate this greater sensitivity of comfort to humidity at elevated met levels. Should the data confirm the analytical predictions, the results could be used to promote desiccant-based air conditioning equipment for buildings in which nonsedentary activity levels predominate.

3.7 REFERENCES

ASHRAE, 1995, Thermal Environmental Conditions for Human Occupancy, ANSI/ASHRAE Standard 55-1995, American Society of Heating, Refrigerating, and Air-Conditioning Engineers, Inc., Atlanta, GA.

ASHRAE, 2001, *Handbook – 2001 Fundamentals*, American Society of Heating, Refrigerating, and Air-Conditioning Engineers, Inc., Atlanta, GA, pp. 8.1-8.29.

Berglund, L.G., 1979, "Thermal Acceptability," *ASHRAE Transactions*, Vol. 85, Part 2, pp. 825-834.

Berglund, L.G., and Cain, W.S., 1989, "Perceived Air Quality and the Thermal Environment," *The Human Equation: Health and Comfort*, Proceedings of the ASHRAE/SOEH Conference IAQ '89, Atlanta, GA, pp. 93-99.

Burton, D.R., Robeson, K.A., and Nevins, R.G., 1975, "The Effect of Temperature on Preferred Air Velocity for Sedentary Subjects Dressed in Shorts," *ASHRAE Transactions*, Vol. 81, Part 2, pp. 157-168.

Chappuis, P., Pittet, P., and Jequier, E., 1976, "Heat Storage Regulation In Exercise During Thermal Transients," *Journal of Applied Physiology*, Vol. 40, pp. 384-392.

Coleman, H. W. and Steele, W. G., 1999, *Experimentation and Uncertainty Analysis for Engineers*, John Wiley & Sons, Inc., New York.

Fanger, P.O., 1967 "Calculation of Thermal Comfort: Introduction of a Basic Equation," *ASHRAE Transactions*, Vol. 77, Part II, pp. 200-215.

Fanger, P.O., 1972, "Conditions for Thermal Comfort – A Review," Proceedings of the CIB (W45) Symposium Thermal Comfort and Moderate Heat Stress, September 13-15, Garston, Watford, pp. 3-15.

Fanger, P.O., 1970, *Analysis and Applications in Environmental Engineering*, McGraw-Hill Book Company, New York, NY.

Fanger, P.O., 1982, *Thermal Comfort*, Krieger Publishing Company, Malabar, Florida.

Fanger, P.O., and Langkilde, G., 1975, "Interindividual Differences in Ambient Temperatures Preferred by Seated Persons," *ASHRAE Transactions*, Vol. 81, Part 2, pp. 140-147.

Fanger, P.O., Ostergaard, J., Olesen, S., and Lund Madsen, Th., 1974, "The Effect on Man's Comfort of a Uniform Air Flow from Different Directions," *ASHRAE Transactions*, Vol. 80, Part 2, pp. 142-157.

Fountain, M., and Huizenga, C., 1995, "Thermal Comfort Program, Version 1.0," American Society of Heating, Refrigerating, and Air-Conditioning Engineers, Atlanta, GA.

Gagge, A.P., Burton, A.C., and Bazett, H.D., 1971a, "A Practical System of Units for the Description of Heat Exchange of Man with His Environment," *Science*, Vol. 94, pp. 428-430.

Gagge, A.P., Stolwijk, J.A.J., and Nishi, Y., 1971b, "An Effective Temperature Scale Based on a Simple Model of Human Physiological Regulatory Response," *ASHRAE Transactions*, Vol. 77, Part 1, pp. 247-262.

Givoni, B., and Goldman, R.F., 1972, "Predicting Rectal Temperature Response to Work, Environment and Clothing," *Journal of Applied Physiology*, Vol. 32, pp. 812-822.

Haslam, R.A., and Parsons, K.C., 1988, "An Evaluation of Computer-Based Models that Predict Human Responses to the Thermal Environmental," *ASHRAE Transactions*, Vol. 94, Part 1, pp. 1342-1360.

- Henane, R., Bittel, J., Viret, R., and Morino, S., 1979, "Thermal Strain Resulting from Protective Clothing of an Armored Vehicle Crew in Warm Conditions," *Aviation Space and Environmental Medicine*, Vol. 50, pp. 599-603.
- Houghten, F.C., and Yaglou, C.P., 1923, "Determination of the Comfort Zone," *ASHVE Transactions*, Vol. 29, pp. 361.
- Houghten, F.C., and Yaglou, C.P., 1923, "Determining Lines of Equal Comfort, and Determination of the Comfort Zone," *ASHVE Transactions*, Vol. 29, pp. 163 and 361.
- ISO, 1987, "Hot Environments: Analytical Determination and Interpretation of Thermal Stress Using Calculation of Required Sweat Rate," ISO/DIS 7933, Geneva.
- Kobayashi, K., Horvath, S.M., Diaz, F.J., Bransford, D.R., and Drinkwater, B.L., 1980, "Thermoregulation During Rest and Exercise in Different Positions in a Hot Humid Environment," *Journal of Applied Physiology*, Vol. 48, pp. 999-1007.
- Koch, W., Jennings, B.H., and Humphreys, C.M., 1960, "Environmental Study II, Sensation Responses to Temperature and Humidity Under Still Air Conditions in the Comfort Range," *ASHRAE Transactions*, Vol. 66, pp. 264-287.
- Laviana, J. E., Rohles, F. H., 1987, "Thermal Comfort: A New Approach For Subjective Evaluation" *ASHRAE Transactions*, Vol. 93, Part 1, pp. 1069-1079.
- McIntyre, D.A., 1975, "Determination of Individual Preferred Temperatures," *ASHRAE Transactions*, Vol. 81, Part 2, pp. 131-139.
- McIntyre, D.A., 1978, "Preferred Air Speeds for Comfort in Warm Conditions," *ASHRAE Transactions*, Vol. 84, Part 2, pp. 264-277.
- Nevins, R.G., Gonzalez, R.R., Nishi, Yasunobu, and Gagge, A.P., 1974, "Effect of Changes in Ambient Temperature and Level of Humidity on Comfort and Thermal Sensations," *ASHRAE Transactions*, Vol. 80, Part 1, pp. 169-182.
- Nevins, R.G., Rohles, F.H., Springer, W.E., and Feyerherm, A.M., 1966, "Temperature-Humidity Chart for Thermal Comfort of Seated Persons," *ASHRAE Transactions*, Vol. 72, pp. 283-291.
- Nielsen, P.V., 1975, "Prediction of Air Flow and Comfort in Air Conditioned Spaces," *ASHRAE Transactions*, Vol. 81, Part 2, pp. 247-259.
- Nishi, Y., and Gagge, A.P., 1977, "Effective Temperature Scale Useful for Hypo- and Hyperbaric Environments," *Aviation Space and Environmental Medicine*, Vol. 48, pp. 97-107.
- Olsen, S., and Fanger, P.O., 1971, "Can Man be Adapted to Prefer a Lower Ambient Temperature?" 5th International Congress for Heating, Ventilating and Air Conditioning, Copenhagen, Vol. 1, pp. 27-40.

Rohles, Jr., F.H., and Johnson, M.S., 1972, "Thermal Comfort in the Elderly," *ASHRAE Transactions*, Vol. 78, Part 1, pp. 131-137.

Rohles, F.H., and Nevins, R.G., 1971, "The Nature of Thermal Comfort for Sedentary Man," *ASHRAE Transactions*, Vol. 77, Part 1, pp. 239-246.

Rohles, F.H., Hayter, R.B., and Milliken, G., 1975, "Effective Temperature (ET*) as a Predictor of Thermal Comfort," *ASHRAE Transactions*, Vol. 81, Part 2, pp. 148-156.

Rohles, F.H., Jr., Woods, J.E., and Nevins, R.G., 1974, "The Effects of Air Movement and Temperature on the Thermal Sensations of Sedentary Man," *ASHRAE Transactions*, Vol. 80, Part 1, pp. 101-119.

Smith, C.E., 1991, "A Transient, Three-Dimensional Model of the Human Thermal System (Thermoregulation)," Ph.D. dissertation, Kansas State University, Manhattan, KS.

Sprague, C.H., and McNall, P.E., 1970, "The Effects of Fluctuating Temperature and Relative Humidity on the Thermal Sensation (Thermal Comfort) of Sedentary Subjects," *ASHRAE Transactions*, Vol. 76, Part 1, pp. 146-156.

Sterling, E.M., Arundel, A., and Sterling, T.D., 1985, "Criteria for Human Exposure to Humidity in Occupied Buildings," *ASHRAE Transactions*, Vol. 91, Part 1B, pp. 611-642.

Stolwijk, J.A.J., and Hardy, J.D., 1977, "Control of Body Temperature," *Handbook of Physiology*, Maryland Press, pp. 45-68.

Tanabe, S., and Kimura, S., 1989, "Importance of Air Movement for Thermal Comfort Under Hot and Humid Conditions," Far East Conference on Air conditioning in Hot Climate, October 25-28, Kuala Lumpur, Malaysia.

Takemori, T., Nakajima, T., and Shoji, Y., 1995, "A Fundamental Model of the Human Thermal System for Prediction of Thermal Comfort," *Heat Transfer: Japanese Research*, Vol. 24, Number 2, pp. 147-165.

Wanner, H.U., 1972, "Comfort and Air Quality in Air-Conditioned Rooms." Proceedings of the CIB (W45) Symposium Thermal Comfort and Moderate Heat Stress, September 13-15, Garston, Watford, pp. 65-78.

Wright, D.N., Bailey, G.D., and Hutch, M.J., 1968, "Survival of Airborne Mycoplasma as Affected by Relative Humidity," *J. Bacteriol.*, Vol. 95, pp. 251-252.

Yaglou, C.P., and Drinker, P., 1929, "The Summer Comfort Zone: Climate and Clothing," *ASHVE Transactions*, Vol. 35, pp. 269.

Young, A.J., Muza, S.R., Sawka, M.N., Gonzalez, R.R., and Pandolf, K.B., 1986, "Human Thermoregulatory Responses to Cold Air are Altered by Repeated Cold Water Immersion," *Journal of Applied Physiology*, Vol. 60, pp. 1542-1548.

APPENDIX 3-A

DETAILED UNCERTAINTY ANALYSIS FOR PMV CALCULATIONS

(1): Define the nominal values for the environmental parameters and the personal parameters:

$t_a := 22.8$	Ambient air temperature measured in °C
$t_r := 22.8$	Mean radiant temperature measured in °C
$V := 0.15$	Air velocity measured in m/s
$I_{cl} := 0.6$	Clothing insulation measured in clo unit
$M := 60$	Metabolic rate measured in W/m ²
$RH := 65$	Relative humidity measured in percent

(2): Express the data reduction equation (DRE) in term of the parameters above

However, the DRE is not in term of relative humidity, but the DRE is in terms of vapor pressure so that the relative humidity needs to be converted to vapor pressure.

The vapor pressure (p_a) can be found by using the saturation temperature in the psychrometric chart given the relative humidity and the dry bulb temperature. The uncertainty of readability is neglected so that only the uncertainty for p_a is the uncertainty in how the relative humidity was measured.

For 65% relative humidity and dry bulb temperature of 22.8°C, from the ASHRAE Psychrometric Chart, the saturation temperature is approximately 18.5°C.

Using that temperature, from the Saturated Water and Steam Properties table, vapor pressure (p_a) can be calculated by interpolation (temperature in °C and pressure in bar).

Thus, after the interpolation and conversion from bar to kPa, the vapor pressure is
 $p_a := 2.141$

The following equations are used to solve the DRE. These equations include the units conversion factors so that the result for the data reduction equation (DRE) is dimensionless.

The mechanical work (W) of the equations can be assumed equal zero because: (1) it is small compared to metabolic rate; (2) estimates for metabolic rate can often be inaccurate; and (3) this assumption results in a more conservative estimate.

$$h_c(V) := 12.1 \cdot \sqrt{V} \quad f_{cl}(I_{cl}) := 1.05 + 0.1 \cdot I_{cl} \quad W := 0$$

$$R_{cl}(I_{cl}) := 0.155 \cdot I_{cl}$$

$$t_{cl}(M, t_a, p_a, I_{cl}) := 35.7 - 0.0275 \cdot (M - W) \dots \\ + (-R_{cl}(I_{cl})) \cdot \left[\begin{array}{l} (M - W) \dots \\ + 0 - 3.05 [5.73 - 0.007(M - W) - p_a] \dots \\ + 0 - 0.42 [(M - W) - 58.15] - 0.0173 \cdot M \cdot (5.87 - p_a) \dots \\ + 0 - 0.0014 \cdot M \cdot (34 - t_a) \end{array} \right]$$

$$t_{cl}(M, t_a, p_a, I_{cl}) = 29.889$$

The expression below is the steady-state energy balance of the Fanger (1982) model in the form of the thermal load on the body.

$$L(M, t_a, p_a, I_{cl}, V, t_r) := (M - W) - \left[\begin{array}{l} 3.96 \cdot 10^{-8} \cdot f_{cl}(I_{cl}) \cdot [(t_{cl}(M, t_a, p_a, I_{cl}) + 273)^4 - (t_r + 273)^4] \dots \\ + f_{cl}(I_{cl}) \cdot h_c(V) \cdot (t_{cl}(M, t_a, p_a, I_{cl}) - t_a) \dots \\ + 3.05 [5.73 - 0.007 \cdot (M - W) - p_a] \dots \\ + 0.42 \cdot [(M - W) - 58.15] \dots \\ + [0.0173 \cdot M \cdot (5.87 - p_a)] \dots \\ + 0.0014 \cdot M \cdot (34 - t_a) \end{array} \right]$$

$$L(M, t_a, p_a, I_{cl}, V, t_r) = -25.563$$

This is the data reduction equation for PMV

$$PMV(M, t_a, p_a, I_{cl}, V, t_r) := [0.303 \cdot e^{(-0.036M)} + 0.028] \cdot L(M, t_a, p_a, I_{cl}, V, t_r) \quad \text{DRE}$$

The nominal value of PMV

$$PMV(M, t_a, p_a, I_{cl}, V, t_r) = -1.609$$

(3): Perform design phase uncertainty analysis

(A). Take the partial derivative of PMV with respect to each of the six parameters

$$\theta_M := \frac{d}{dM} PMV(M, t_a, p_a, I_{cl}, V, t_r) \quad \text{Partial derivative of PMV with respect to metabolic rate}$$

$$\theta_{t_a} := \frac{d}{dt_a} PMV(M, t_a, p_a, I_{cl}, V, t_r) \quad \text{Partial derivative of PMV with respect to ambient air temperature}$$

$\theta_{I_{cl}} := \frac{d}{dI_{cl}} PMV(M, t_a, p_a, I_{cl}, V, t_r)$	Partial derivative of PMV with respect to clothing insulation
$\theta_V := \frac{d}{dV} PMV(M, t_a, p_a, I_{cl}, V, t_r)$	Partial derivative of PMV with respect to air velocity
$\theta_{t_r} := \frac{d}{dt_r} PMV(M, t_a, p_a, I_{cl}, V, t_r)$	Partial derivative of PMV with respect to mean radiant temperature
$PMV := PMV(M, t_a, p_a, I_{cl}, V, t_r)$	

(B). Systematic uncertainty associated with each of the parameters (these are reasonable assumptions)

$B_{t_a} := 0.1$	Systematic uncertainty associated with ambient air temperatures
$B_{t_r} := 0.1$	Systematic uncertainty associated with mean radiant temperature
$B_V := 0.015$	Systematic uncertainty associated with air velocity
$B_{I_{cl}} := 0.12$	Systematic uncertainty associated with clothing insulation
$B_M := 6$	Systematic uncertainty associated with activity level
$B_{RH} := 0.056$	Systematic uncertainty associated with relative humidity is $\pm 2\%$ but it is converted to vapor pressure in kPa.

(C). Random uncertainty associated with each of the parameters (these are reasonable assumptions)

$P_{t_a} := 0.05$	Random uncertainty associated with ambient air temperature
$P_{t_r} := 0.05$	Random uncertainty associated with mean radiant temperature
$P_V := 0.003$	Random uncertainty associated with air velocity
$P_{I_{cl}} := 0$	Random uncertainty associated with clothing insulation (Assume KSU standard clothing, constant)
$P_M := 2$	Random uncertainty associated with activity level
$P_{RH} := 0.014$	Random uncertainty associated with relative humidity is $\pm 0.5\%$ but it is converted to vapor pressure in kPa.

No units were given to the systematic and random uncertainty above because the DRE already includes all the conversion factors. The list of units for all systematic and random uncertainty associated with the input parameters is:

Uncertainty associated with ambient air temperature measured in °C

Uncertainty associated with mean radiant temperature measured in °C

Uncertainty associated with velocity measured in m/s

Uncertainty associated with clothing insulation measured in clo unit

Uncertainty associated with activity level measured in (W/m²) unit

Uncertainty associated with relative humidity measured in ±% with the value changed to kPa because vapor pressure in kPa is used in the DRE for PMV calculations.

(D). The systematic uncertainty for PMV is

$$B_{PMV} := \left[\theta_{ta}^2 \cdot B_{ta}^2 + \theta_{tr}^2 \cdot B_{tr}^2 + \theta_M^2 \cdot B_M^2 + \theta_{Icl}^2 \cdot B_{Icl}^2 + \theta_V^2 \cdot B_V^2 + \theta_{pa}^2 \cdot B_{RH}^2 \right]^{0.5}$$

$$B_{PMV} = 0.84$$

(E). The random uncertainty for PMV is

$$P_{PMV} := \left(\theta_{ta}^2 \cdot P_{ta}^2 + \theta_{tr}^2 \cdot P_{tr}^2 + \theta_M^2 \cdot P_M^2 + \theta_{Icl}^2 \cdot P_{Icl}^2 + \theta_V^2 \cdot P_V^2 + \theta_{pa}^2 \cdot P_{RH}^2 \right)^{0.5}$$

$$P_{PMV} = 0.229$$

(F). The overall absolute uncertainty can be expressed as

$$U_{PMV} := \sqrt{B_{PMV}^2 + P_{PMV}^2} \quad U_{PMV} = 0.873$$

(4): Uncertainty Percentage Contributions (UPC) have been used for this experiment. The UPC for a given variable gives the percentage contribution of the uncertainty in that variable to the squared uncertainty in the result. The systematic UPC, random UPC, and overall UPC can be calculated as:

(A). The systematic uncertainty percentage contribution (UPC) of each variable to the squared result of systematic uncertainty can be expressed as

$$UPC_{Bta} := \frac{(\theta_{ta})^2 \cdot (B_{ta})^2}{(B_{PMV})^2} \quad UPC_{Bta} = 0.16\%$$

$$UPC_{Btr} := \frac{(\theta_{tr})^2 \cdot (B_{tr})^2}{(B_{PMV})^2} \quad UPC_{Btr} = 0.12 \%$$

$$UPC_{BV} := \frac{(\theta_v)^2 \cdot (B_v)^2}{(B_{PMV})^2} \quad UPC_{BV} = 1.90 \%$$

$$UPC_{BIcl} := \frac{(\theta_{Icl})^2 \cdot (B_{Icl})^2}{(B_{PMV})^2} \quad UPC_{BIcl} = 32.6 \%$$

$$UPC_{BM} := \frac{(\theta_M)^2 \cdot (B_M)^2}{(B_{PMV})^2} \quad UPC_{BM} = 65.1 \%$$

$$UPC_{Bpa} := \frac{(\theta_{pa})^2 \cdot (B_{RH})^2}{(B_{PMV})^2} \quad UPC_{Bpa} = 0.11 \%$$

(B). The random uncertainty percentage contribution (UPC) of each variable to the squared result of random uncertainty becomes

$$UPC_{Pta} := \frac{(\theta_{ta})^2 \cdot (P_{ta})^2}{(P_{PMV})^2} \quad UPC_{Pta} = 0.54 \%$$

$$UPC_{Ptr} := \frac{(\theta_{tr})^2 \cdot (P_{tr})^2}{(P_{PMV})^2} \quad UPC_{Ptr} = 0.39 \%$$

$$UPC_{PV} := \frac{(\theta_v)^2 \cdot (P_v)^2}{(P_{PMV})^2} \quad UPC_{PV} = 1.03 \%$$

$$UPC_{PIcl} := \frac{(\theta_{Icl})^2 \cdot (P_{Icl})^2}{(P_{PMV})^2} \quad UPC_{PIcl} = 0 \%$$

$$UPC_{PM} := \frac{(\theta_M)^2 \cdot (P_M)^2}{(P_{PMV})^2} \quad UPC_{PM} = 97.9 \%$$

$$UPC_{Ppa} := \frac{(\theta_{pa})^2 \cdot (P_{RH})^2}{(P_{PMV})^2} \quad UPC_{Ppa} = 0.093\%$$

(C). The overall uncertainty associated with each of the variables

$$U_{ta} := \sqrt{B_{ta}^2 + P_{ta}^2} \quad U_{ta} = 0.112$$

$$U_{tr} := \sqrt{B_{tr}^2 + P_{tr}^2} \quad U_{tr} = 0.112$$

$$U_V := \sqrt{B_V^2 + P_V^2} \quad U_V = 0.015$$

$$U_{Icl} := \sqrt{B_{Icl}^2 + P_{Icl}^2} \quad U_{Icl} = 0.12$$

$$U_M := \sqrt{B_M^2 + P_M^2} \quad U_M = 6.325$$

$$U_{RH} := \sqrt{B_{RH}^2 + P_{RH}^2} \quad U_{RH} = 0.058$$

(D). The overall uncertainty percentage contribution (UPC) of each variable to the squared result of overall uncertainty is

$$UPC_{ta} := \frac{(\theta_{ta})^2 \cdot (U_{ta})^2}{(U_{PMV})^2} \quad UPC_{ta} = 0.19\%$$

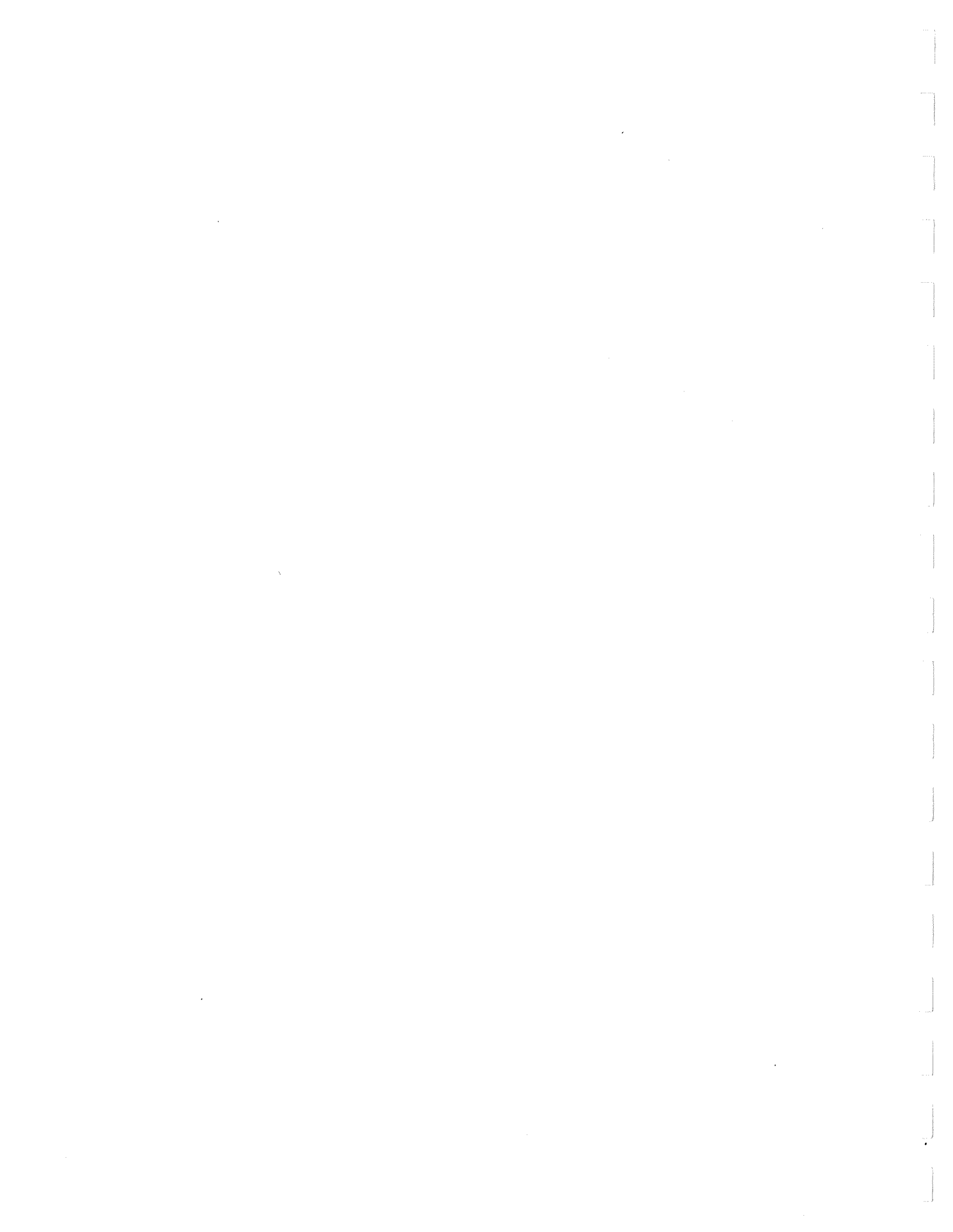
$$UPC_{tr} := \frac{(\theta_{tr})^2 \cdot (U_{tr})^2}{(U_{PMV})^2} \quad UPC_{tr} = 0.13\%$$

$$UPC_V := \frac{(\theta_V)^2 \cdot (U_V)^2}{(U_{PMV})^2} \quad UPC_V = 1.84\%$$

$$UPC_{Icl} := \frac{(\theta_{Icl})^2 \cdot (U_{Icl})^2}{(U_{PMV})^2} \quad UPC_{Icl} = 30.3\%$$

$$UPC_M := \frac{(\theta_M)^2 \cdot (U_M)^2}{(U_{PMV})^2} \quad UPC_M = 67.2\%$$

$$UPC_{pa} := \frac{(\theta_{pa})^2 \cdot (U_{RH})^2}{(U_{PMV})^2} \quad UPC_{pa} = 0.11\%$$



CHAPTER 4

FIELD ENERGY SAVINGS VALIDATION

4.1. INTRODUCTION

The main objective of this task was to validate simulation models designed for performance evaluation of desiccant dehumidification systems. Experimental and field data constitute the benchmarks used in the validation process. The main components of this task were

1. Devise and implement an experimental approach to obtain data from Mississippi State University (MSU) test units.
2. Obtain field data from Oak Ridge National Laboratory (ORNL) and Gas Technology Institute (GTI).
3. Compare the experimental and field data with the results predicted by the model.
4. Describe the findings and suggest means for improving the model.

DesiCalc™ (1998) is the simulation model considered for validation. Although designed primarily as a screening tool, DesiCalc™ implements an elaborate algorithm for simulating performance of desiccant systems for various applications. This is also the same software used in the first task of this project, "National Energy/Cost Savings." The program is designed to simulate the performance of conventional heating, ventilating, and air conditioning (HVAC) systems as well as hybrid systems incorporating desiccant dehumidification for various building applications. DOE-2.1E is the driving engine of the program that facilitates simulation of building/equipment performance. DesiCalc™ utilizes a set of empirical correlations for predicting the performance of desiccant systems. Evaluating the accuracy of this model in predicting desiccant systems performance is the primary interest of this study.

Included in the output of DesiCalc™ are the monthly and yearly estimates of latent load, sensible load, and energy usage (gas and electricity) for a given application considering a conventional HVAC system and a desiccant-based system. To facilitate comparisons between the model results and the experimental and field data, Gard Analytics modified the output algorithm of the program to produce hourly weather data and hourly desiccant system performance parameters.

The key parameters used for comparisons are 1) grain depression (grains of moisture removed per unit mass of process dry air), 2) desiccant system efficiency for dehumidification (regeneration thermal energy input per unit mass of moisture removed), and 3) the process exit temperature. In this report, the terms "grain depression" and "moisture removal capacity" are used interchangeably. The combination of the first two parameters, as will be discussed later, provides a measure for evaluating the validity of the simulation model in predicting the energy usage. The importance of predicting accurate process exit temperature has to do with its direct impact on estimating the post cooling requirement (sensible load) which impacts the total energy consumption.

The mode of operation selected for the system model is characterized as the “ventilation mode,” implying dehumidification of 100% outside air (no recirculated air). For regeneration, 100% outside air is also utilized. As a result, the conditions of the process inlet and regeneration inlet are the same, as are the assumptions for the University of Illinois Chicago (UIC) correlations and for the experimental data used in the comparisons.

The challenges encountered included the difficulties in obtaining applicable field data and in establishing congruity between the system model and the experimental and field data. Of the field data considered, the data furnished by CDH Energy were selected since they provided hourly performance values averaged over the duration of the desiccant system operation. Field data from the Sustainable Energy Group were also considered but not used because the hourly data were representative of the averages that included measurements during the system “off-periods.” A meaningful comparison between the hourly model results and field data is feasible only when the system performance variables are averaged over the operating periods.

Inconsistency between the modeled system and the systems of the field and experimental data also posed a challenge. Since the model does not accept direct specification of the desiccant system characteristics, for meaningful comparisons, normalized variables were utilized.

This section will start with an examination of the dynamics of the selected desiccant dehumidification systems (including the one modeled by DesiCalc™). With this description, the diversities among the commercially available systems will be addressed by considering variations in the design features. Then, the performance parameters pertinent to the validation of the model will be defined. Next, the model will be described and its limitations will be addressed. The criteria and procedures adopted in the validation of DesiCalc™ will be examined. After presentation and discussion of the results, conclusions will be drawn and recommendations for improvement of the model will be made.

4.2. DYNAMICS OF DESICCANT SYSTEMS

Of all types of desiccant systems available in the market, gas-fired, rotary systems utilizing solid desiccant materials are the most widely utilized. Figures 4.1 and 4.2 illustrate two different types of rotary desiccant systems tested at MSU, a Fresh Air Solutions (FAS) unit (model DC026) and a Munters unit (model A10G), respectively. The Oak Ridge National Laboratory (ORNL) has also tested a FAS test unit which is virtually identical to the MSU FAS unit. The Munters unit for the CDH Energy field data, as depicted in Figure 4.3, differs from the MSU Munters unit and will be discussed later. As seen in these figures, two counter-flow air streams, a process air stream and a regeneration air stream, are involved in the operation. The process air represents the air

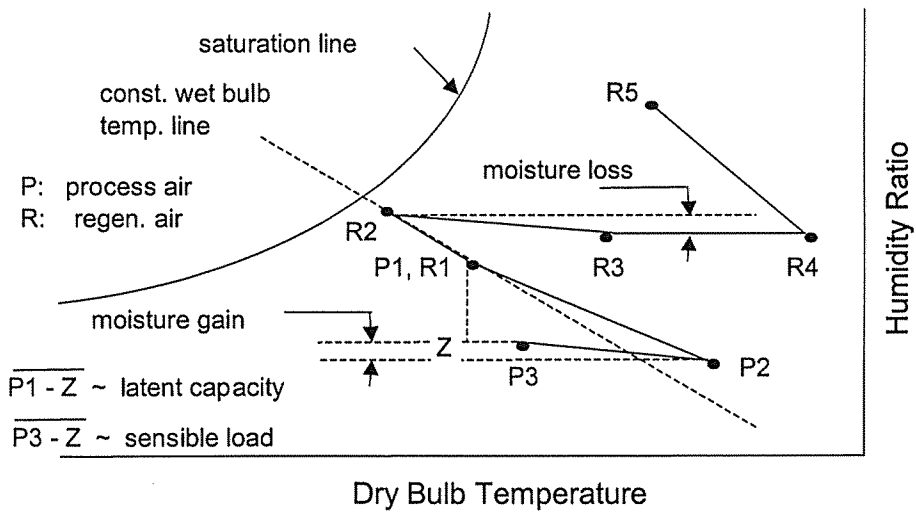
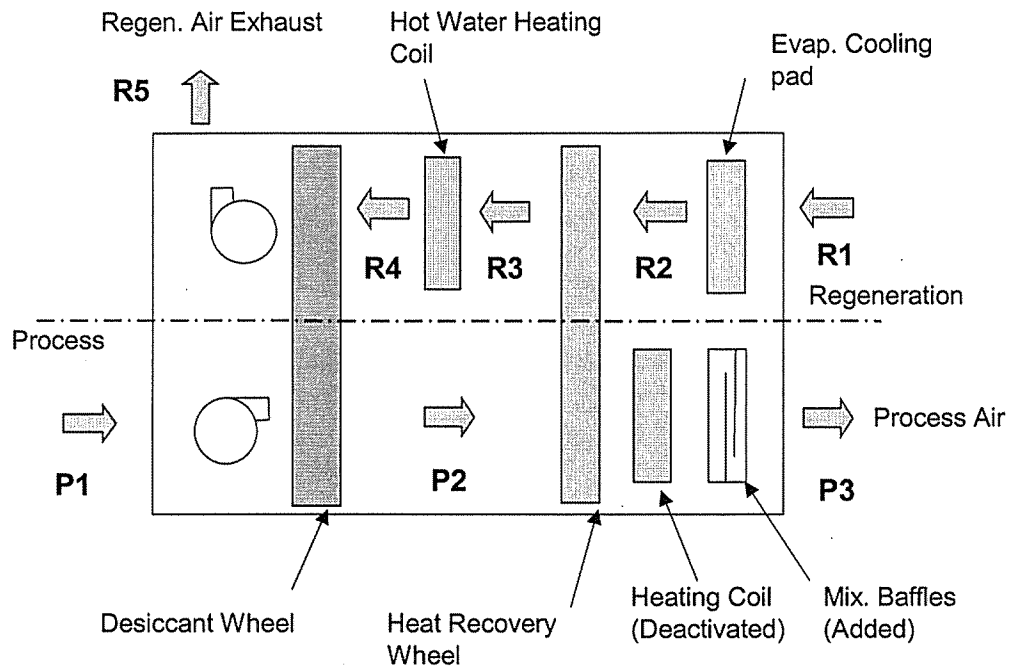


Figure 4.1. Desiccant Dehumidification System (MSU FAS Unit) and Related Psychrometric Processes.

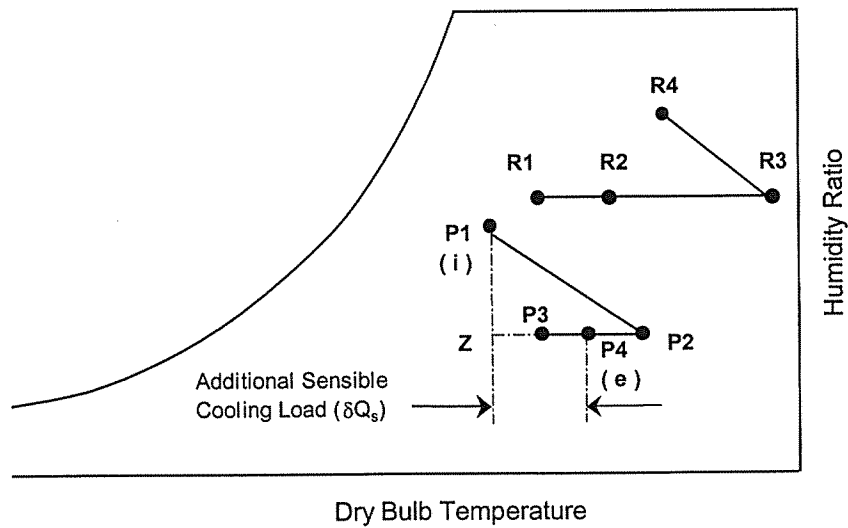
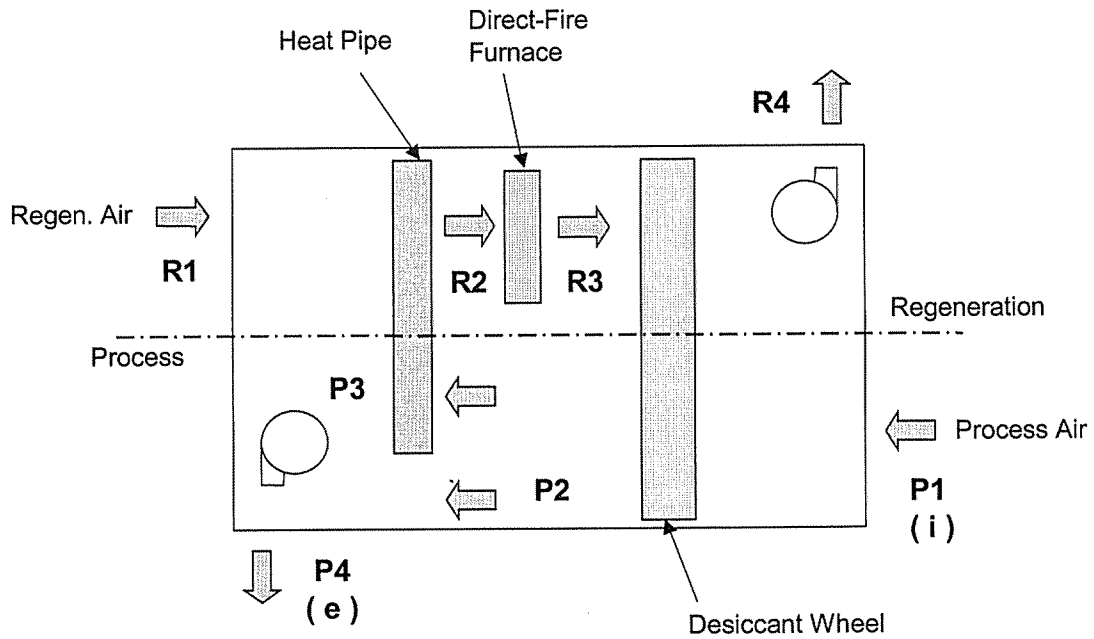


Figure 4.2. Desiccant Dehumidification System (MSU Munters Unit) and Related Psychrometric Processes.

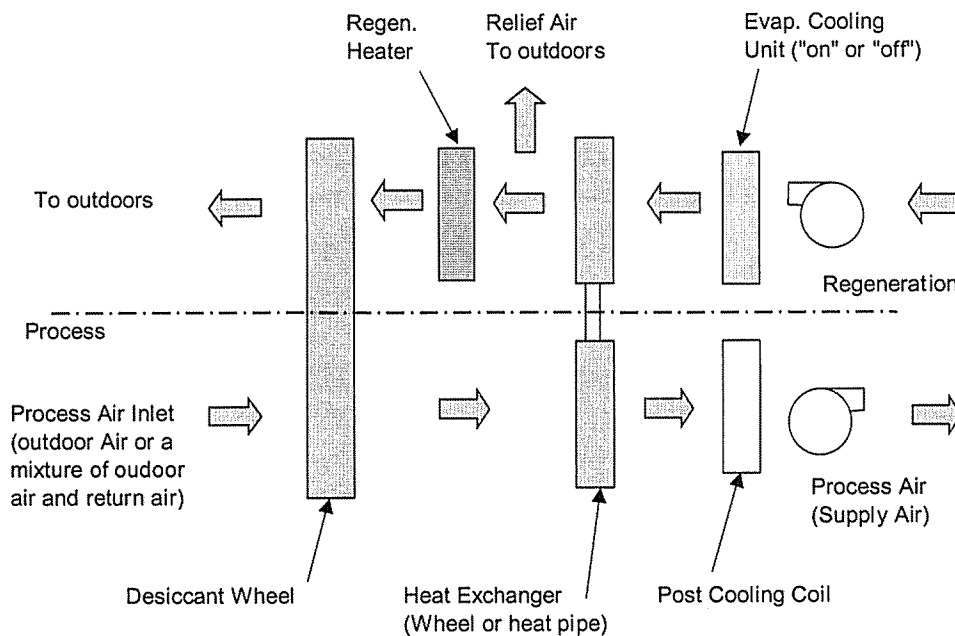


Figure 4.3. CDH Energy Munters Unit and Representative Desiccant Dehumidification System of Desicalc™.

stream to be dehumidified and thermally conditioned before being supplied to an indoor space. The incoming process air can be outside air (OA), return air (RA), or a mixture of the two. The regeneration air is exhausted from the system. Relief air from the indoor space or outside air can be the source of the regeneration air stream.

Moisture is removed from the process air stream by a rotating porous desiccant wheel. The desiccant material is a solid sorbent which collects the water vapor at the surface without involving any chemical reaction or mixing. Therefore, this dehumidification process is classified as “adsorption.” The dehumidification takes place due to the difference in the vapor pressure in the air stream and that at the surface of the desiccant material. The psychrometric charts accompanying Figures 4.1 and 4.2 illustrate the process paths involved with desiccant dehumidification.

The moisture adsorbed by the desiccant material is released into the heated regeneration air stream as the desiccant wheel rotates. The driving force behind the moisture release is the increase in vapor pressure at the wheel surface due to the heat transfer from the regeneration air. To heat the regeneration air upstream of the desiccant wheel, either a hot water heating coil (Figure 4.1) or a direct-fired furnace (Figure 4.2) is used. The heating system is controlled via a thermostat sensing the regeneration air temperature. For the case with the MSU FAS unit, the regeneration air temperature

upstream of the desiccant wheel is maintained at about 190°F. In the MSU Munters unit, the regeneration air temperature downstream of the desiccant wheel is controlled at a set point of about 123°F.

On the process side, as air flows through the desiccant wheel, the air temperature increases (as shown in the psychrometric charts of Figures 4.1 and 4.2). This temperature increase is the result of the dehumidification effect (the release of latent heat) and the heat transfer from the regeneration air stream via the rotating desiccant wheel. The portion of the process air stream coming in contact with the desiccant wheel immediately as it rotates into the process section experiences a high temperature rise and is ineffectively dehumidified due to a relatively high vapor pressure at the wheel surface. For this reason, in some desiccant systems, a section is designated to purge this excessively heated and ineffectively dehumidified portion of the process air stream. Neither the systems used to obtain the field/experimental data nor the systems modeled by DesiCalc™ were equipped with a purge area.

To partially offset the increase in temperature of the process air exiting the desiccant wheel, a heat exchanger is utilized which transfers heat from the hot process air stream to the relatively cool incoming regeneration air. This heat exchanger can be a sensible heat recovery wheel (FAS, Figure 4.1) or a non-moving device such as a heat pipe (Munters, Figure 4.2). Without the heat exchanger, the dehumidified air leaving the desiccant wheel will impose a significant sensible cooling load on the overall HVAC system. To further cool the process air, an evaporative cooler can be installed at the entrance of the regeneration side as seen in Figure 4.1. The evaporative cooling of the regeneration air takes place under a nearly constant-wet bulb temperature process. Although heat recovery wheels are generally considered to be among the most effective (or efficient) heat exchangers used in desiccant systems, heat recovery wheels can adversely affect the net moisture removal capacity of the system since they transfer moisture from the regeneration air stream to the process air stream due to the rotation. This effect is clearly demonstrated in the psychrometric diagram of Figure 4.1. More detailed information on the effects of this moisture transfer can be found in the study by Jalalzadeh-Azar, Sand, and Vineyard (2000a).

Another important role of the heat exchanger is preheating of the regeneration air prior to entering the heating unit. This preheating effect leads to an improvement in the energy efficiency of the system. Description of various types of desiccant systems can be found in the literature, Munters (1990) and Pesaran (1994).

Table 1 provides the design features of the desiccant systems used in this research program: the MSU FAS and Munters units, the ORNL FAS system, and the CDH Munters unit field data. As stated earlier, the FAS systems of MSU and ORNL are similar in design and operating characteristics. The Munters units of MSU and CDH Energy differ from each other in a number of ways as delineated in Table 1. On the process side of the MSU unit (Figure 4.2), a part of the process air stream bypasses the heat pipe. Although this system offers optimum dehumidification efficiency, the full potential for heat recovery is not realized. For the CDH Energy unit (Figure 4.3), the regeneration air flow rate is the same as that of the process until it leaves the heat pipe

where a portion of the air stream is exhausted without going through the heater. With this scheme of operation, a higher dehumidification efficiency than that of the FAS unit can be achieved, while at the same time, the maximum attainable efficiency is also realized by the heat pipe as it is exposed to two balanced air flows. The desiccant systems of DesiCalc™ are modeled by the schematic shown in Figure 4.3 (the CDH Energy Munters configuration). This conclusion is reached by examining the systems for different building applications covered by DesiCalc™ (see Appendix 4.A).

Table 1. Characteristics of Desiccant Systems.

Description	MSU FAS	ORNL FAS	MSU Munters	CDH Munters
Type of desiccant material	Titanium Silicate	Titanium Silicate	Silica gel	Silica gel
Desiccant wheel diameter, inches	48	48	30	42
Desiccant wheel depth, inches	6	6	16	8
Desiccant wheel reg./process split	180°/180°	180°/180°	90°/270°	90°/270°
Process flow rate, scfm	2500	2600	2500	2400
Regen flow rate, scfm	2500	2600	900	800 thru heater 2400 thru HX
Regeneration heating system	Hot water coil	Hot water coil	Direct-fire furnace	Direct-fire furnace
Regeneration, temp., °F (approx.)	190	190	~ 250 (approx.)	~ 256
Regen. control strategy	Regen. temp.	Regen. temp.	Regen. exit temp.	N/A
Heat exch. type / Efficiency	Rotary/ ~ 82%	Rotary/ variable	Heat pipe/ 50-60%	Heat pipe/ ~70%

Uncertainties associated with the experimental and field data stem from a number of sources. The most obvious source is the measuring devices, whose readings carry minimum uncertainties equal to those of the calibration instruments. A potential source of uncertainty is the spatial variation of temperature and humidity ratio of the process and regeneration air streams. In a previous study [Jalalzadeh-Azar, Steele, and Hodge (2000b)] conducted on the MSU FAS unit, the significance of such spatial variations for the exiting process air was demonstrated. This source of uncertainty was remedied by installing mixing baffles downstream of the heat exchanger on the process side (Figure 4.1). Field data considered for system evaluation are not immune to these elemental sources of uncertainties.

4.3. PERFORMANCE PARAMETERS

The process exit temperature, T_{pe} , is one of the important parameters since its accurate determination is necessary for accurate evaluation of the energy input required for post cooling. The post cooling load is determined as

$$\dot{Q}_{sensible} = \dot{m}_{pe} c_p (T_{pe} - T_{SA}) \quad (4.1)$$

where \dot{m}_{pe} is the mass flow rate of the exiting process air, c_p is the specific heat of the air, and T_{SA} is the required temperature of the supply air leaving the post cooling unit.

The rate of thermal energy required for regeneration, \dot{Q}_{reg} , is also of great importance due to its dominance in the total energy input of a desiccant system. This parameter represents the net heat transfer rate to the regeneration air stream required to maintain an adequate air temperature upstream of the desiccant wheel. For a gas-fired desiccant system, the energy input, \dot{Q}_{gas} , accompanying the gas flow can be found as

$$\dot{Q}_{gas} = \dot{m}_{gas} HV_{gas} = \dot{Q}_{reg} / \eta_{reg} \quad (4.2)$$

where \dot{m}_{gas} is the mass flow rate of natural gas, HV_{gas} is the heating value of the gas, and η_{reg} is the efficiency of the regeneration heating system.

Due to the incongruities between the system of the simulation model and those installed in the field and laboratories (in terms of size and features), model validation via experimental and field data requires a normalized form of energy input. The normalized parameter introduced here, which also reflects the dehumidification efficiency of the desiccant system, is as follows:

$$\eta_{dehumid} = \dot{Q}_{gas} / \dot{m}_w \quad (4.3)$$

The moisture removal capacity, \dot{m}_w , is defined as

$$\dot{m}_w = \dot{m}_{a,pi} (w_{pi} - w_{pe}) = \dot{m}_{a,pi} \Delta w = \left(\frac{\dot{m}_{pi}}{1 + w_{pi}} \right) \Delta w \quad (4.4)$$

where Δw represents the grain depression (grains of water per lbm of dry air), w_{pi} and w_{pe} are, respectively, the humidity ratios at the process inlet and exit, \dot{m}_{pi} is the total mass flow rate of the process air entering the desiccant system, and $\dot{m}_{a,pi}$ is the flow rate of the dry air portion of the entering process air.

The effectiveness (or efficiency) of the heat exchanger used in desiccant systems represents the effectiveness in transferring heat from the process to the regeneration side which, in turn, affects the temperature of the exiting process air. As stated earlier, accurate evaluation of the process air temperature is critical in accurately estimating the post-cooling requirement. In addition, the effectiveness of the heat recovery component

dictates the extent to which the regeneration air is preheated. This impacts the amount of the regeneration heat input required from an active heating system. The heat exchanger effectiveness, ϵ_{HX} , is defined as

$$\epsilon_{HX} = \frac{T_{P2} - T_{P3}}{T_{P2} - T_{R2}} \quad (4.5)$$

The temperature variables shown in this equation represent the air temperature at the principal points shown in Figure 4.1. Rotary heat recovery wheels offer the highest efficiency among the types of sensible heat exchangers used in desiccant systems. Depending on the rotational speed, rotary heat exchangers typically have an effectiveness ranging from 55% to 85%.

Typical uncertainties of the variables and performance parameters for the MSU test units are provided in Table 2.

**Table 2. Typical Uncertainties of MSU Experimental Results.
(Jalalzadeh-Azar, Steele, and Hodge, 1996)**

Variables/ Parameters	Symbol	Typical Uncertainty
Dry-bulb temperature, process inlet	T_{pi}	$\pm 1^\circ\text{F}$
Dry-bulb temperature, process exit	T_{pe}	$\pm 1.2^\circ\text{F}$
Humidity ratio at process exit	w_{pi}	$\pm 5\%$
Humidity ratio at process inlet	w_{pe}	$\pm 8\%$
Grain depression	Δw	$\pm 9\%$
Moisture removal capacity	\dot{m}_w	$\pm 10\%$
Air flow rate	\dot{m}_{pi}	$\pm 3\%$
Gas flow rate	\dot{m}_{gas}	$\pm 3\%$
Heat exchanger effectiveness	ϵ_{HX}	$\pm 6\%$
Dehumidification efficiency	$\eta_{dehumid}$	$\pm 11\%$

4.4. DESICALC™

General description:

DesiCalc™ is a simulation software package developed as a screening tool for evaluation of desiccant systems (GRI, 1998). The software is designed to perform hour-by-hour simulation for evaluating a variety of desiccant systems and conventional HVAC equipment for a number of building applications. The program is interfaced with the DOE-2.1E computer program and has built-in default inputs, eliminating the need for specifying complex design parameters. The energy rate schedules, selection of weather data location, building type and operating schedule, and limited input for building and HVAC system configurations are the data entry required to run DesiCalc™. Other parameters such as the seasonal efficiency for cooling systems and the effectiveness of the heat recovery components for desiccant systems can be specified, although default values are provided by the model. Included in the output of the program are the monthly and yearly heating and cooling loads of the equipment, the energy consumption, and the energy cost. Appendix 4.A presents a sample output for a baseline (conventional) system and an alternative system (a hybrid system incorporating desiccant dehumidification).

A set of empirical correlations constitutes the core of DesiCalc™ for evaluation of desiccant systems. The figures of Appendix 4.A depict the configurations of the desiccant systems modeled by the simulation program. The variations among these configurations stem from the source of process and regeneration air (outside air, return air, or a mixture of the two), availability of a preconditioning unit for the process air, and use of an economizer for outside air intake. A close examination of the alternatives given in Appendix 4.A reveals that, regardless of the application, the operation of the desiccant system is the same. Consequently, the same method for evaluation of the system performance is applicable.

Correlations:

In predicting the performance of a desiccant system, DesiCalc™ relies on a set of correlations developed by the University of Illinois at Chicago (UIC). These empirical correlations were developed using an experimental apparatus that incorporated a silica gel desiccant wheel with a 90°/270° split for regeneration/process. The performance parameters for which the correlations were developed are the temperature and humidity ratio of the exiting process air and the net thermal energy required for regeneration (specified in terms of Btu per lbm of moisture removed). The correlations provided by UIC are in a graphical form showing the dependency of these parameters on the inlet temperature and humidity ratio. As seen in Appendix 4.B, the correlations are reported for face velocities of 400, 600, and 800 fpm on the process side. For a given process air flow rate, the lower the face velocity, the larger the wheel diameter required. (Based on the discussions with Gard Analytics, the program apparently sets the face velocity according to the design ambient conditions and the maximum allowable indoor humidity level in an attempt to meet the design dehumidification load.) In developing the correlations, the regeneration air flow rate was modulated in order to optimize the system

performance according to the operating conditions. The same inlet conditions were used for the process and regeneration in generating these correlations.

Before proceeding with the validation process, the conformity of the model to the UIC correlations was established. To do so, the model was run for a hypothetical application involving a department store in Charleston, SC. The model results for the performance parameters corresponding to within $\pm 1^\circ\text{F}$ of the process inlet temperatures of the correlations, 70°F , 80°F , and 90°F , were selected for comparison. For congruity with the approach of the UIC correlations, no heat recovery was used in the desiccant system of the model. As shown in Figures 4.4 through 4.12, excellent, or at least good, agreement between these model results and the correlations was found. In this research task, the UIC correlations for the humidity ratio of the exit process air were rearranged in the form of the grain depression (moisture removal) versus the inlet humidity ratio. This was done to directly reflect the variation of the dehumidification capacity with respect to the inlet conditions. Furthermore, for congruity between the model and the UIC data, DesiCalc™ was run for the case in which the regeneration inlet conditions are the same as those of the process inlet.

Figures 4.4, 4.5, and 4.6, respectively, show the comparisons for the process exit temperature, the grain depression, and the regeneration heat input as functions of inlet humidity ratio for the inlet temperature of 70°F . Figures 4.4 and 4.5 are indicative of excellent agreement between the UIC relationships (for 400 fpm face velocity) and the model for the exit temperature and the grain depression. The fluctuations of the model results, in part, are a consequence of choosing model inlet temperatures within $70 \pm 1^\circ\text{F}$ rather than an exact inlet temperature of 70°F . Comparisons for the 80°F and 90°F inlet temperatures are shown in Figures 4.7 to 4.9 and Figures 4.10 to 4.12, respectively. Again, as expected, the agreement between the UIC relationships (for 400 fpm face velocity) and the model for exit temperature and grain depression are excellent. The model predictions of regeneration heat input for the 70°F and 80°F inlet temperatures are in the general neighborhood of the UIC data but do not exhibit the same trends, falling short of the excellent agreement expected between the model results and the correlations upon which the model is based. For the 90°F inlet temperature, however, the agreement is excellent. The UIC correlations were developed on the basis of modulating the regeneration airflow to achieve optimum regeneration heat input performance (process exit temperature and grain depression are relatively insensitive to regeneration air flow rate). Although typical, well-designed desiccant systems are designed with optimum regeneration air flow rates corresponding to a particular operating condition, most do not incorporate modulating controls to optimize regeneration air flow over the entire range of operating conditions. Likewise, DesiCalc™ evidently chooses an optimum regeneration air flow rate to match the maximum dehumidification load in much the same way that it sets the process air face velocity. In this case, DesiCalc™ (in simulating a real system) evidently sized the desiccant equipment based on a face velocity of 400 fpm and an optimum regeneration airflow rate corresponding to 90°F .

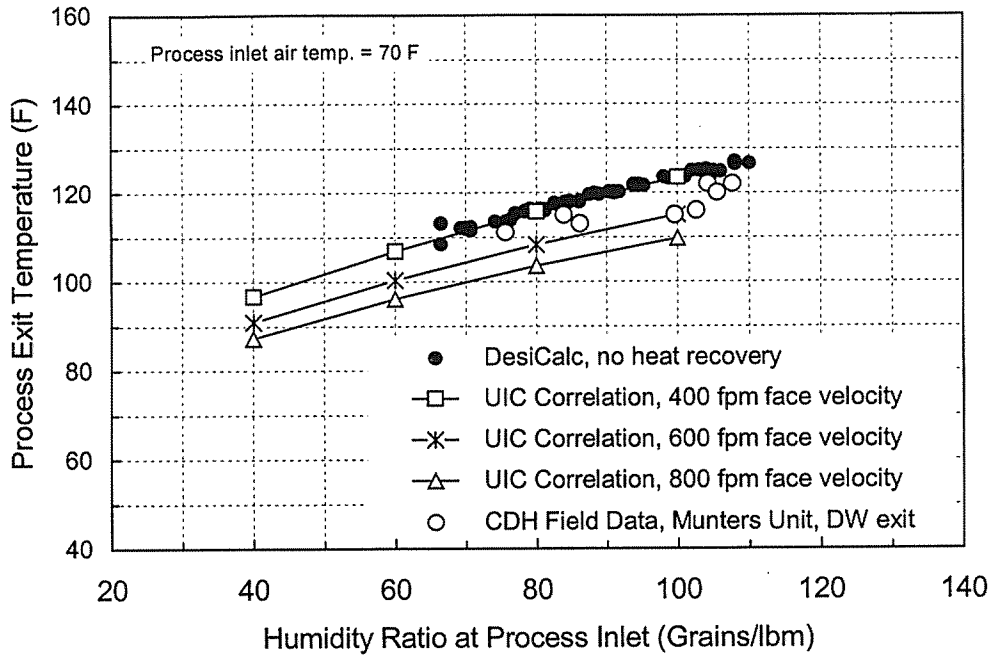


Figure 4.4. Results of Desicalc™ Versus UIC Correlations for Process Exit Temperature (70°F Inlet Temperature).

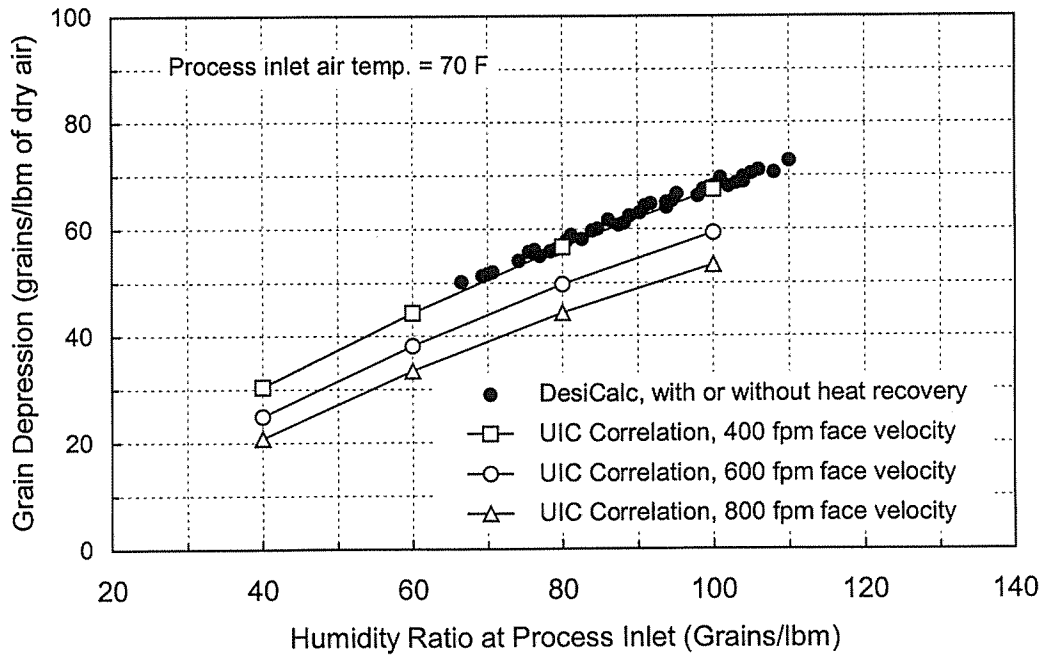


Figure 4.5. Results of Desicalc™ Versus UIC Correlations for Grain Depression (70°F Inlet Temperature).

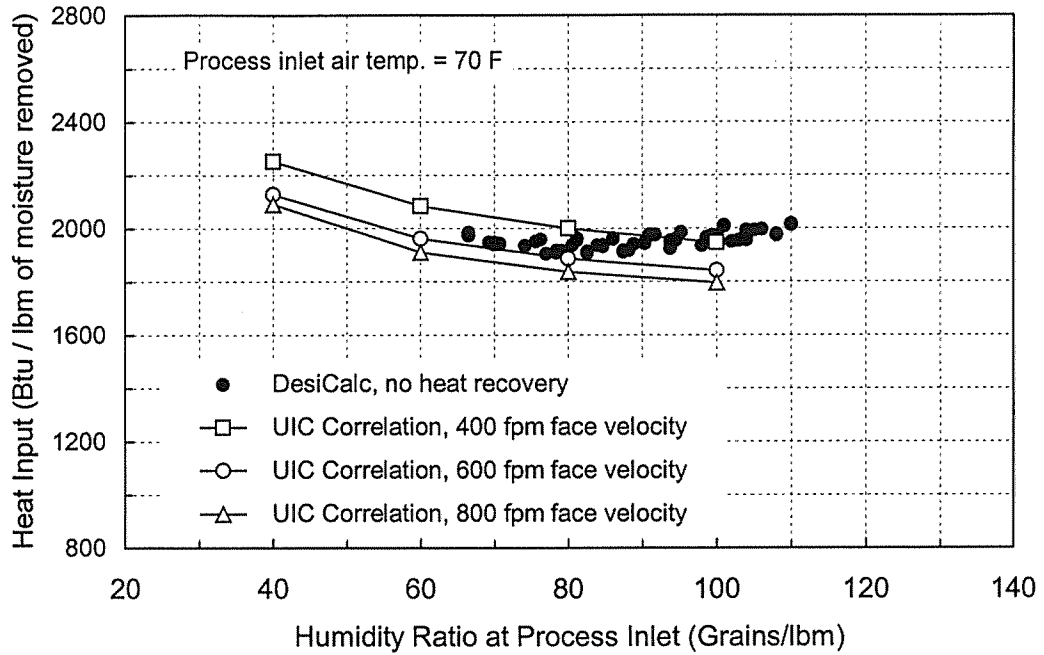


Figure 4.6. Results of DesiCalc™ Versus UIC Correlations for Regeneration Heat Input (70°F Inlet Temperature).

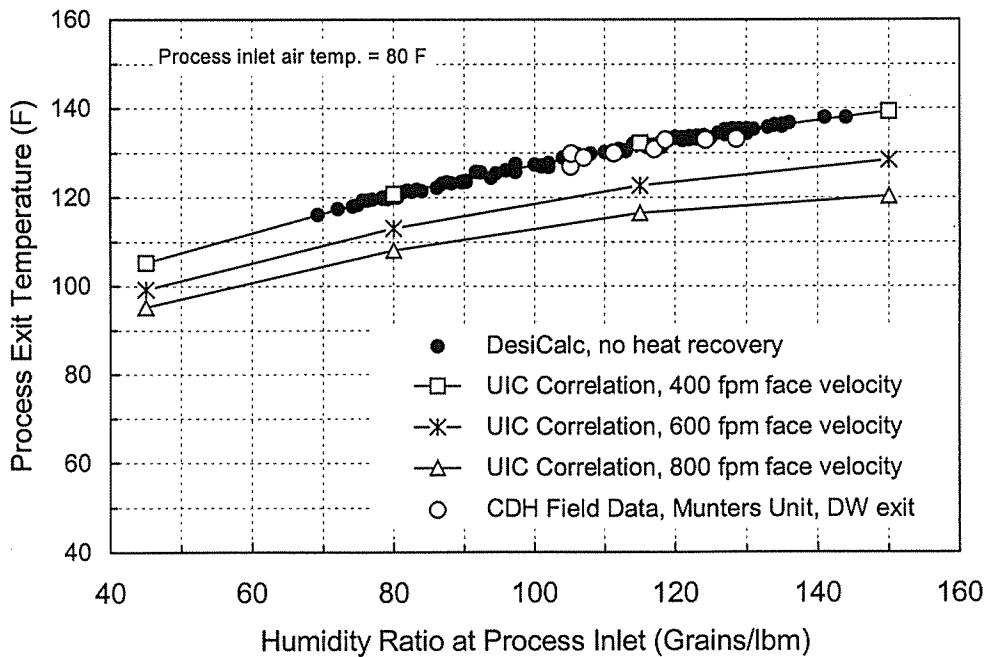


Figure 4.7. Results of DesiCalc™ Versus UIC Correlations for Process Exit Temperature (80°F Inlet Temperature).

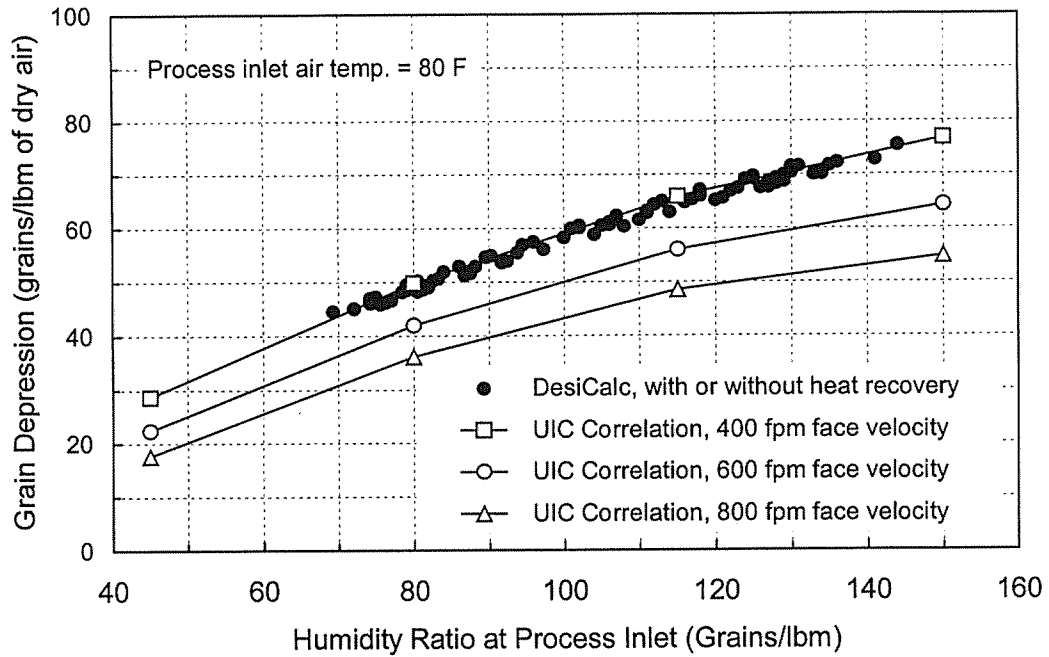


Figure 4.8. Results Of DesiCalc™ Versus UIC Correlations For Grain Depression (80°F Inlet Temperature).

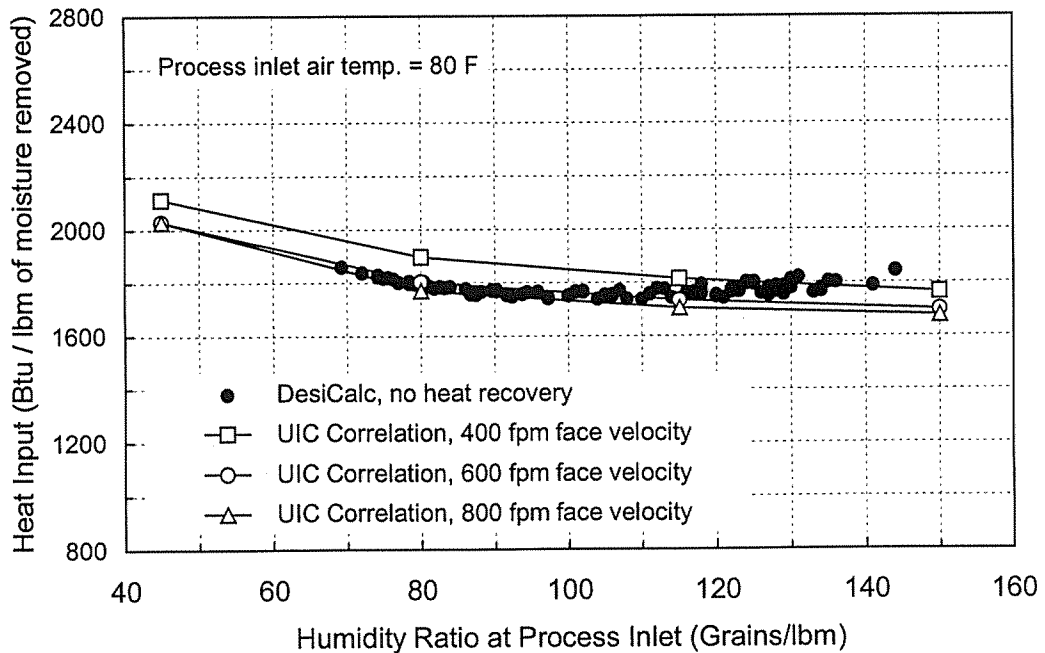


Figure 4.9. Results Of DesiCalc™ Versus UIC Correlations For Regeneration Heat Input (80°F Inlet Temperature).

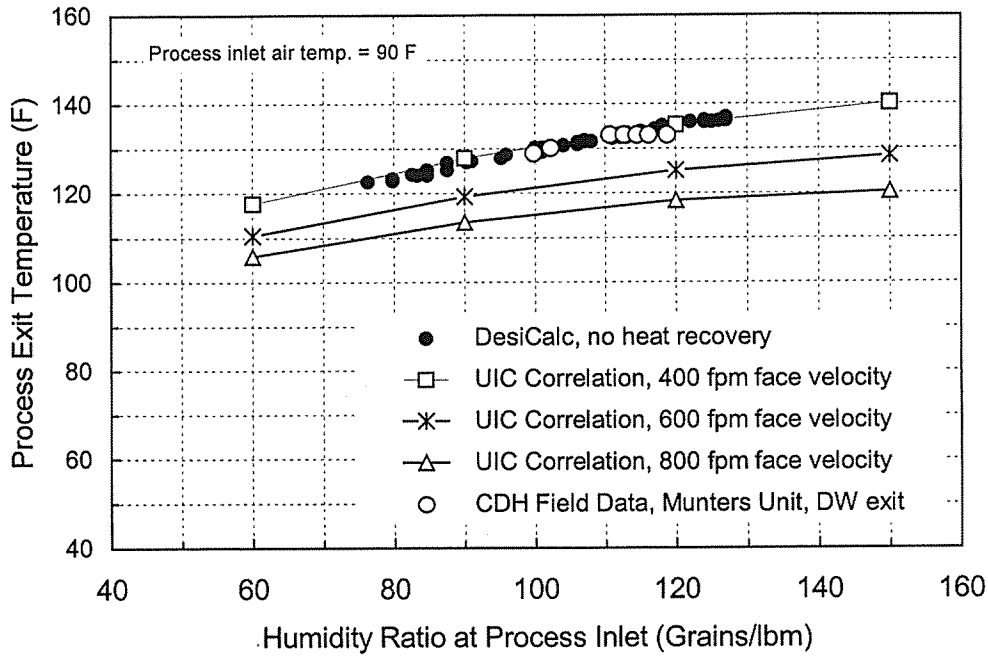


Figure 4.10. Results Of DesiCalc™ Versus UIC Correlations For Process Exit Temperature (90°F Inlet Temperature).

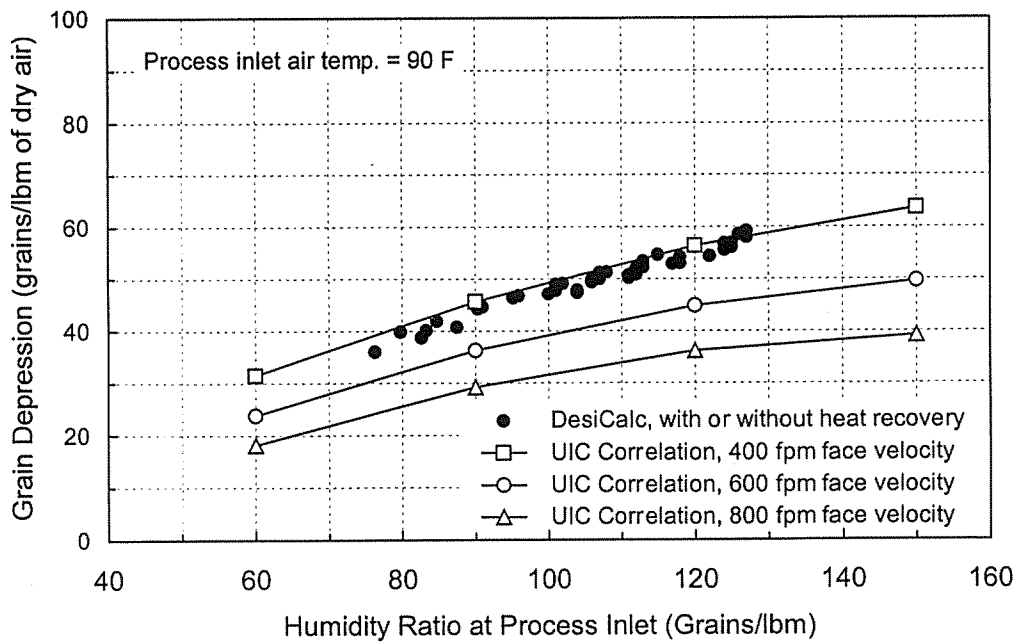


Figure 4.11. Results Of DesiCalc™ Versus UIC Correlations For Grain Depression (90°F Inlet Temperature).

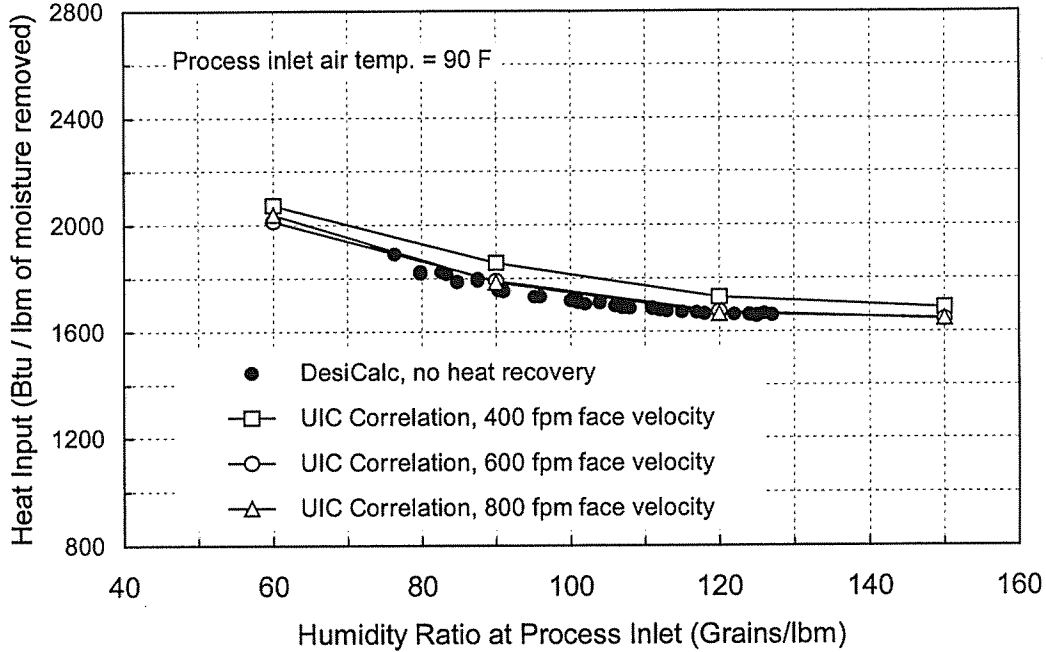


Figure 4.12. Results Of DesiCalc™ Versus UIC Correlations For Regeneration Heat Input (90°F Inlet Temperature).

The results in Figures 4.4 through 4.12 are for a case with no heat recovery in the desiccant system, implying that the process air exit temperature is the same as the air temperature leaving the desiccant wheel. The field data obtained from CDH Energy also include temperature measurements of the process air exiting the desiccant wheel, which are shown in Figures 4.4, 4.7, and 4.10. Except for the case of Figure 4.4, which is for an inlet temperature of 70°F, excellent agreement is found between the model results and the field data.

Limitations of Model:

Although DesiCalc™ is viewed as a screening tool and its accuracy is sufficient for preliminary studies, addressing its limitations can be constructive in two ways: 1) evaluation and interpretation of the predicted results in light of the uncertainties induced by the limitations and 2) future enhancements to the model. The main limitations identified during the course of the project are as follows:

The correlations incorporated in DesiCalc™ are empirical relationships that are obtained for a particular desiccant wheel under a specific set of design/operating parameters. The commercially-available desiccant systems utilize different desiccant materials and differ from one another in design features and operating parameters. Desiccant wheel speed, regeneration temperature set point, face velocity of air at the desiccant wheel, and regeneration-to-process air flow ratio

are among the parameters that influence the performance of desiccant systems. Details on the impact of variation of important parameters on desiccant system performance can be found in the studies by Jalalzadeh-Azar, Steele, and Hodge (2000b) and Vineyard, Sand, and Durfee (2000).

The model does not take into account the moisture transfer from the regeneration air to the process air stream caused by rotary heat recovery wheels. This is not a limitation when non-rotating heat exchangers such as heat pipe and plate-fin heat exchangers are utilized. As a result, the moisture removal capacity for a rotary heat recovery wheel is overestimated by the model compared to that of a real system. This ultimately leads to underestimation of the total energy input for regeneration since any over-estimate of the moisture removal capacity can translate into a shorter duration for system operation. Further discussions are made regarding this issue when the results are presented in this report. The penetration of the desiccant wheel and heat exchanger through the panel separating the process and regeneration streams can potentially be a source of air leakage from one stream to the other. Although quantification of this undesired mass transfer is not included in the model, this effect is not significant in well designed systems with effective seals at the penetration areas.

Desiccant systems, like any other air conditioning systems, are subjected to on-off cycling which translates into a lower energy efficiency than what is achieved in steady-state operations. A study by Jalalzadeh-Azar (2000c) has shown that, for a direct-fired desiccant system, the average system performance can be adversely affected by a preceding lengthy shut-off period. This effect is expected to be even stronger when a hot water heating system as opposed to a direct-fired furnace is used for regeneration. In the model, however, the predicted results are based on steady-state operation of the system.

The efficiency of the regeneration heating system is potentially another source of discrepancy between the model predictions and the actual system performance. In the model, this efficiency is assumed to be 92%, which is a reasonable value for direct-fired systems but not for the systems utilizing gas-fired boilers whose efficiencies are typically around 80%. The efficiency of hot water regeneration systems can be expected to be even less when they are subjected to on-off cycling of the regeneration heater during the dehumidification process. The regeneration heating efficiency of an actual system is not only influenced by the type of the system but also by the quality of the fuel as well. Although the heating value of natural gas is assumed to be 1000 Btu per cubic feet under standard atmospheric conditions, the actual value may be subjected to day-to-day variation.

4.5. VALIDATION CRITERIA

For a screening tool, prediction of the annual energy consumption with a reasonable accuracy is perhaps the most important feature. The thermal energy required for regeneration of the desiccant material comprises over 90% of the total energy consumption in a typical rotary desiccant system. The remainder is the electrical energy required to operate the fans and other accessories. Therefore, accurate prediction of the energy input for regeneration is critical. In this project, only the regeneration thermal energy input is considered. In addition to estimating the energy consumption, predicting the system dehumidification (latent) capacity is also important in evaluating the adequacy of the selected system in conjunction with the time-dependent building latent load.

For comparisons between model predictions and experimental and/or field data, the model results are not readily usable since the system of the model cannot be directly characterized and sized to match those for the experimental and field data. The energy consumption and system dehumidification capacity were normalized to facilitate comparisons. In this study, the normalized energy consumption is defined as the ratio of the rate of energy supplied by the natural gas input to the mass flow rate of moisture removed by the system, which in effect, is the energy efficiency index defined in Equation (4.3). For the dehumidification capacity, the grain depression (Δw in Equation 4.4) specified in terms of grains of moisture per unit mass of process air entering the desiccant system is utilized. Comparisons between the predicted values for grain depression and energy efficiency index and the actual performance data (experimental or field) can be interpreted as follows:

Scenario 1: If the model predictions of a system performance in terms of dehumidification energy efficiency index (Equation 4.3) and grain depression are in agreement with the selected experimental or field data (which are presumed reasonably accurate), then 1) the model would accurately predict the monthly and annual energy consumption of the selected system type since the latent load of the building defined in the model is independent of the dehumidification system and 2) the model would accurately predict the number of hours that the system does not meet the latent load (or the indoor humidity setpoint).

Scenario 2: If the model accurately predicts the grain depression but underestimates (or overestimates) the dehumidification efficiency index, the estimated annual energy consumption is also underestimated (or overestimated).

Scenario 3: If the model overestimates the grain depression of the system but accurately predicts the efficiency index, the predicted annual energy consumption may be subject to an error provided that an indoor humidity setpoint is to be met. When the grain depression is overestimated, the running time of the system of the model would be shorter, and the total number of hours that the indoor humidity level exceeds the setpoint would be underestimated. As a result, to meet the latent load of the building using an actual system, a larger desiccant wheel size may be required, with a potential adverse impact on the system efficiency and energy consumption.

Scenario 4: If the model underestimates the grain depression of the system but accurately predicts the efficiency index, the monthly and annual energy consumption would be either correct or overestimated (the opposite of Scenario 3). In this case, the number of hours that the system does not meet the humidity setpoint would be overestimated.

Scenario 5: If the model predicts accurate results for grain depression but incorrect values for the energy efficiency, the energy consumption can also be expected to be inaccurate.

Comparisons between the predicted values for grain depression and energy efficiency index and the actual performance data are effective in validating the model's ability to predict energy usage associated with dehumidification only. To verify the conformity of the model to real-world systems in predicting total energy usage (natural gas and electricity), the post-cooling requirement must be taken into account. One of the necessary conditions for such conformity is accurate prediction of the process exit temperature, as it directly affects the post-cooling load (Equation 4.1). Therefore, the accuracy of the predicted exit temperatures is also an important criterion in the model validation process.

4.6. RESULTS AND DISCUSSIONS

Comparisons of hourly performance data

Figures 4.13 through 4.15 present the comparisons between the CDH Energy field data (from a Munters unit) and the results of DesiCalc™ for the process inlet temperature of 70°F. Figure 4.13 indicates that the process exit temperature of the field data is underestimated by the model throughout the range of inlet humidity ratios examined. Consequently, the model underestimates the post-cooling requirements. For example, at the inlet humidity ratio of 85 grains/lbm (corresponding to a relative humidity of about 75% for the given inlet temperature), the exit temperature from the field data is about 85°F, roughly 10°F higher than the model predicted temperature. Then, if the supply air to the indoor space has to be 60°F, the sensible load of the post cooling unit predicted by the model would be 40% lower than that based on the field data. This ultimately leads to underestimation of the electrical energy input for post cooling, assuming the field data are the benchmark.

Figures 4.14 and 4.15 show the comparisons for moisture removal capacity and normalized regeneration heat input, respectively. These figures indicate that the model overestimates the grain depression for the entire range of the inlet humidity ratio and underestimates the normalized energy input especially at low inlet humidity levels. Therefore, based on the discussion in Section 4.5, the energy consumption due to the regeneration heat input is underestimated. As an example, at the inlet humidity ratio of 85 grains/lbm.a, the model prediction and the field data are, respectively, 60 and 47 grains/lbm.a for the grain depression (Figure 4.14) and 1700 and 2050 Btu/lbm of moisture for the normalized energy input (Figure 4.15). Then, for this example, the total regeneration input is underestimated by about 17%.

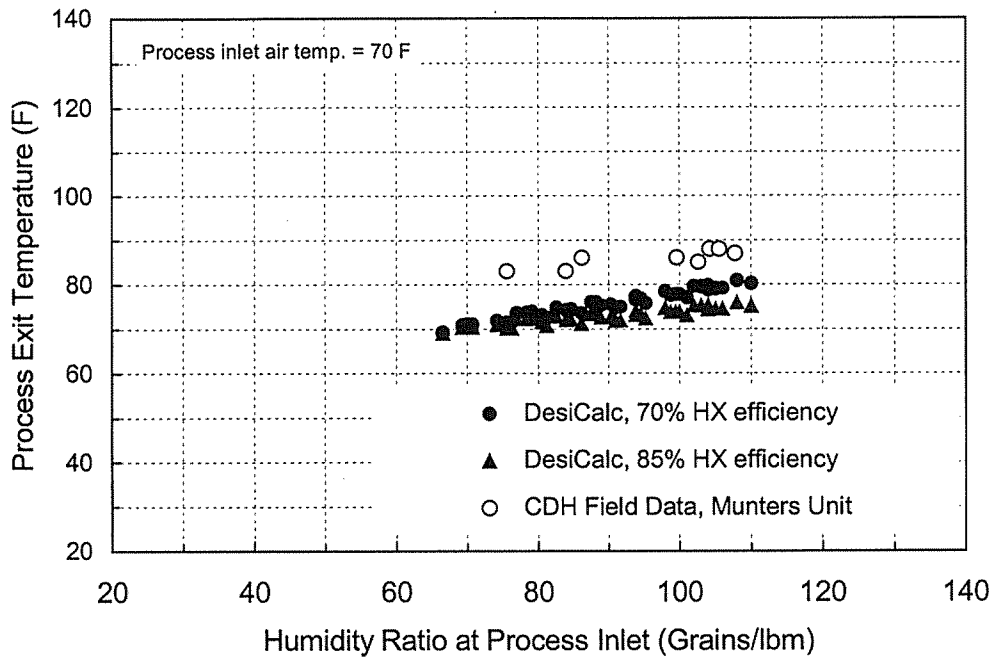


Figure 4.13. Process Exit Temperature Comparisons for Process Inlet Temperature of 70°F - (Munters Unit).

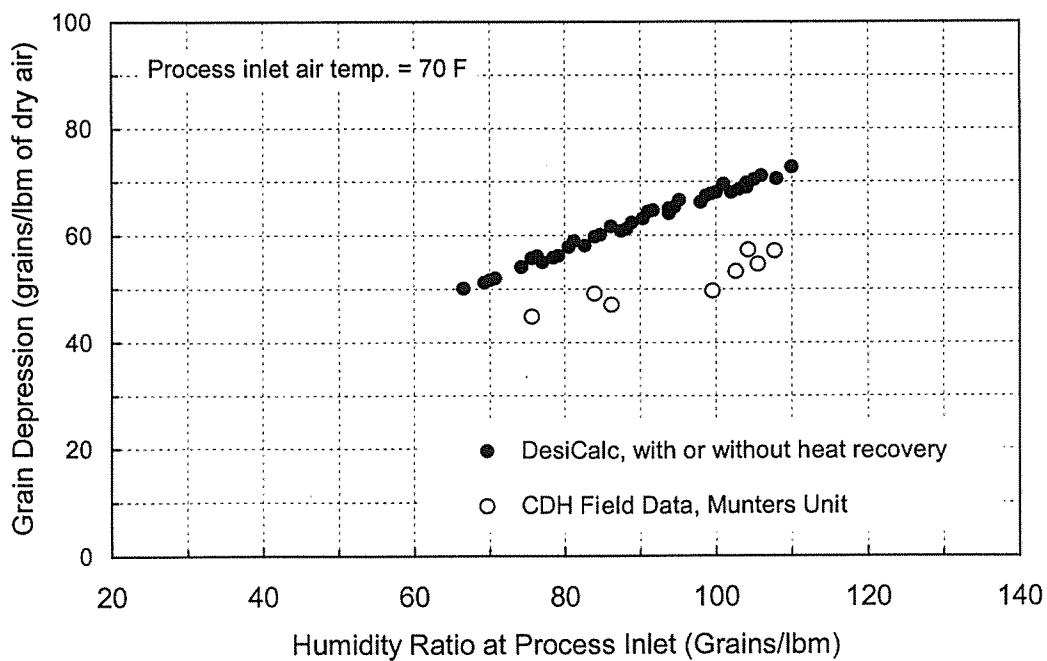


Figure 4.14. Grain Depression Comparisons for Process Inlet Temperature of 70°F - (Munters Unit).

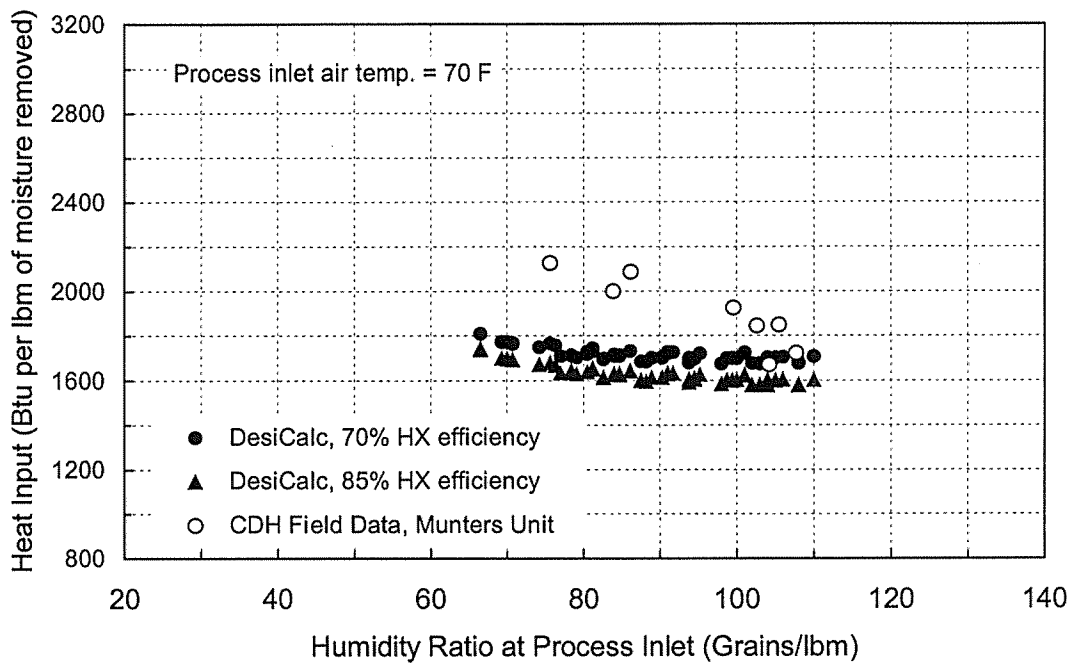


Figure 4.15. Regeneration Heat Input Comparisons For Process Inlet Temperature of 70°F - (Munters Unit).

The comparisons for the inlet temperature of 80°F are presented in Figures 4.16 to 4.21. The first three of these figures present the experimental and field data obtained from the Munters units, and the last three the data obtained from the FAS units. In Figures 4.17 and 4.18, two sets of model results corresponding to two values of heat recovery efficiencies, 57% and 70%, are shown. The efficiency of 70% represents the efficiency of the CDH Energy Munters unit. The lower efficiency, 57%, is the case with the MSU Munters unit. These differences in efficiency are used to establish the dependence of system performance on heat recovery efficiency. For the case of grain depression comparisons provided in Figures 4.17 and 4.20, the model results are independent of the heat recovery efficiency. This poses a potential discrepancy when rotary heat exchangers are used. The source of this discrepancy is the migration of the moisture from the regeneration air stream to the process air stream via the rotary heat exchanger [Jalalzadeh-Azar, Sand, and Vineyard (2000a)].

Figure 4.16 compares the process exit temperature data from the MSU Munters unit with those from the CDH Energy Munters unit. While the exit temperatures reported by CDH Energy are in good agreement with the results of DesiCalc™, the MSU data shows significantly higher exit temperatures, which ultimately leads to significantly higher sensible post-cooling requirements. The difference between the performance characteristics arises from configuration differences between the CDH Energy Munters unit and the MSU Munters unit, as brought out earlier in the discussion of Table 1. For the MSU unit, about two-thirds of the process air bypasses the sensible heat exchanger,

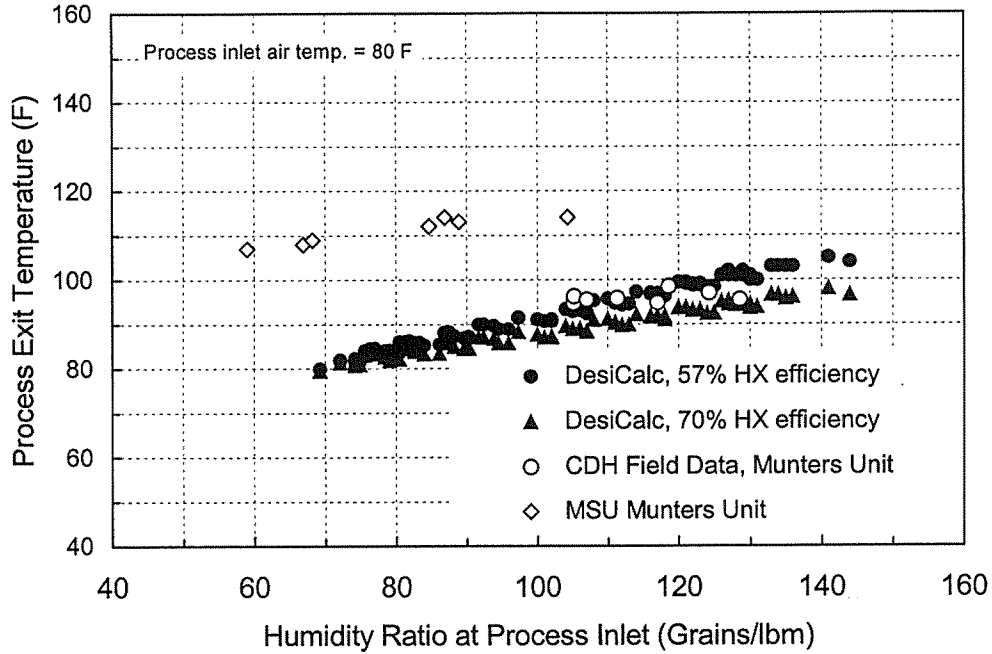


Figure 4.16. Process Exit Temperature Comparisons for Process Inlet Temperature of 80°F - (Munters Units).

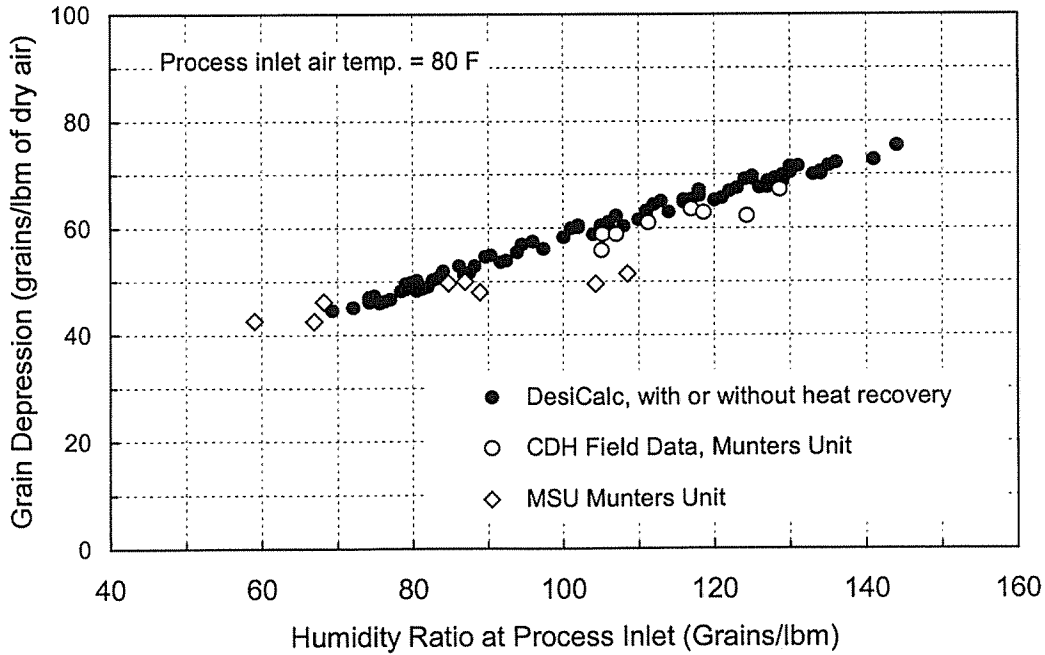


Figure 4.17. Grain Depression Comparisons for Process Inlet Temperature of 80°F - (Munters Units).

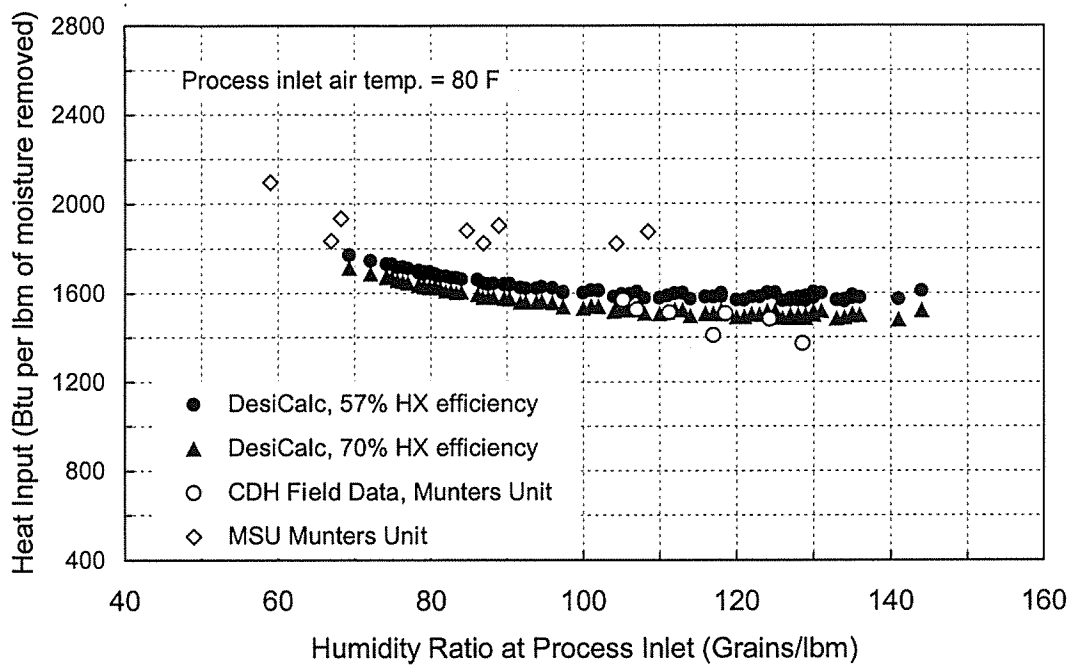


Figure 4.18. Regeneration Heat Input Comparisons for Process Inlet Temperature of 80°F - (Munters Units).

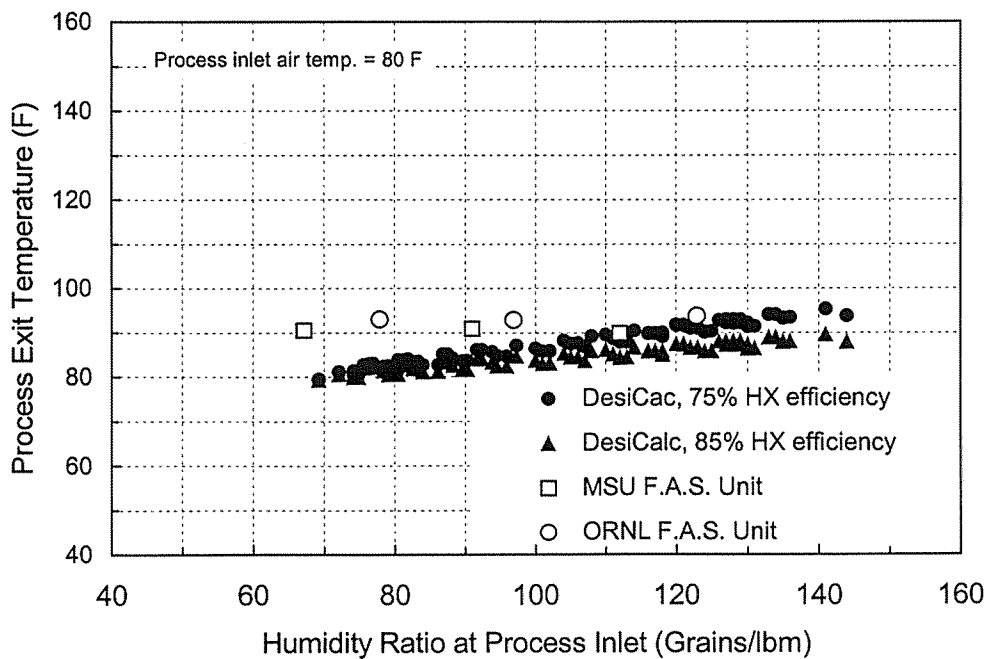


Figure 4.19. Process Exit Temperature Comparisons for Process Inlet Temperature of 80°F - (FAS Units)

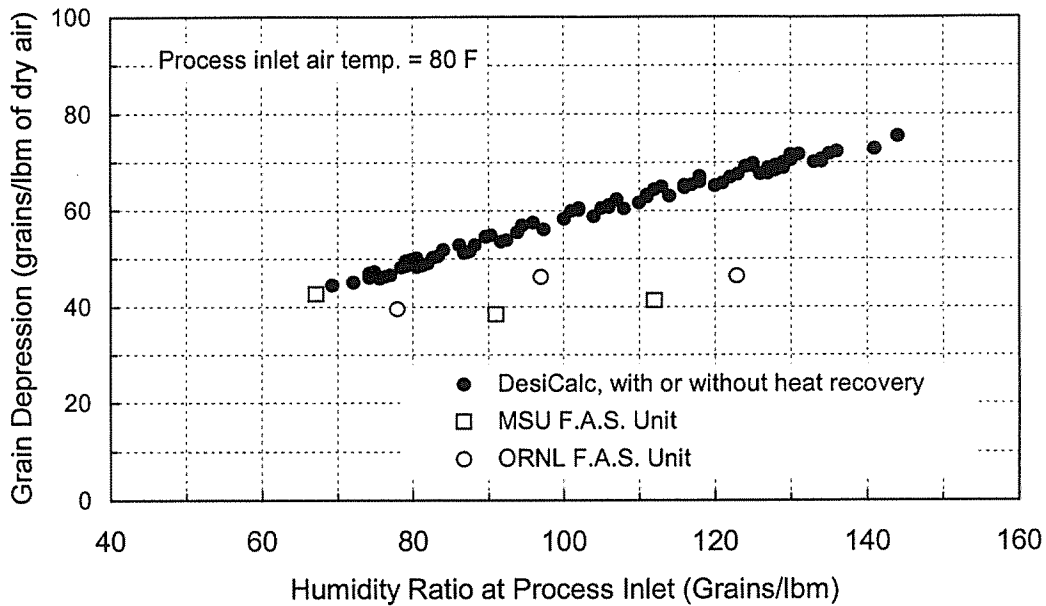


Figure 4.20. Grain Depression Comparisons for Process Inlet Temperature of 80°F - (FAS Units).

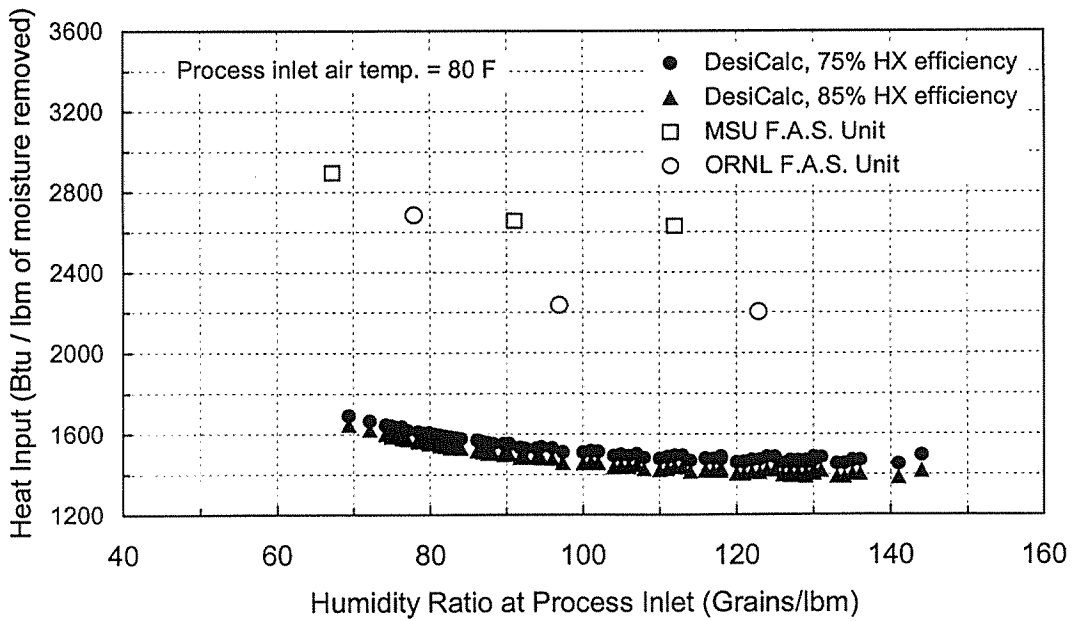


Figure 4.21. Regeneration Heat Input Comparisons for Process Inlet Temperature of 80°F - (FAS Units).

resulting in significantly less sensible cooling of the process air. Good agreement between the DesiCalc™ predictions and the CDH Energy data is expected since the CDH Energy Munters unit is configured identically to the desiccant system modeled in DesiCalc™ (Figure 4.3). Conversely, DesiCalc™ does not accurately predict the MSU Munters exit temperature performance simply because it does not include an option to model the MSU Munters configuration.

As for the moisture removal capacity, the available CDH Energy data for a relatively narrow range of inlet humidity ratio (105 to 130 grains/lbm.a) are in good agreement with the model results as shown in Figure 4.17. The grain depression of the MSU Munters unit is in good agreement with that of the model at relatively low inlet humidity levels but is noticeably lower at higher inlet humidity levels. In conjunction with these observations for grain depression, Figure 4.18 indicates that the model underestimates the regeneration energy input with respect to the MSU data but rather closely follows the CDH Energy data. The largest deviation between the MSU data and DesiCalc™ in terms of the energy usage occurs at the inlet humidity ratio of about 105 grains/lbm.a where the model overestimates the grain depression by about 20% and underestimates the normalized energy input by about 12%. Due to the overestimation of the system dehumidification capacity, the actual energy consumption can be even higher if the indoor humidity set point is not to be compromised.

Figures 4.19 to 4.21 provide comparisons between the model results and experimental data obtained from the two FAS units at MSU and ORNL. In both units, the regeneration and process flow rates are balanced, the regeneration temperature is maintained at about 190°F, and a rotary heat exchanger is used. For the data shown, the rotational speed of the heat recovery wheels for both systems is 10 rpm, which yields an efficiency within 80% to 85%. The model results are shown for 75% and 85% efficiency to illustrate the sensitivity of the results to the heat exchanger efficiency.

Figure 4.19 shows good agreement between the process exit temperatures obtained from the MSU and ORNL FAS units. The agreement between the model predicted temperatures and the experimental values is not quite satisfactory at very low inlet humidity ratios, but improves as the humidity level increases. Furthermore, unlike the model-predicted exit temperatures, which increase with inlet humidity ratio, the corresponding experimental values appear to be nearly constant. Based on the model results, increasing the heat recovery efficiency from 75% to 85% has only a slight impact on the exit temperatures, which diminishes as the inlet humidity ratio decreases.

Referring to the moisture removal performance results in Figure 4.20, the MSU data are in line with the ORNL data, given the uncertainties involved (about 9% for the MSU data for grain depression). This is no surprise since the two experimental systems are FAS units, which utilize the same type of desiccant wheel and have virtually identical operating characteristics. The model tends to overestimate the grain depression with respect to the experimental results. The discrepancy between the model predictions and the experimental data increases with increasing inlet humidity ratio. This is largely due to the differences between the characteristics of the desiccant materials used in the model (silica gel) and the FAS units (titanium silicate).

Figure 4.21 compares the normalized energy input predicted by the model with the experimental data obtained from the MSU and ORNL FAS units. The seemingly inconsistent performance data observed for the two experimental units is a reflection of the following attributes: First, the ORNL data are estimated based on the assumption that the regeneration hot water heating system operates at an efficiency of 80%, a typical value for gas-fired boilers. Such an assumption is required since only the net thermal energy transfer to the regeneration air stream is experimentally determined by ORNL. This is done by taking measurements of hot water temperature at the inlet and exit of the heating coil and applying an energy balance. Second, the energy consumption of the MSU unit is obtained by taking the product of the experimentally determined natural gas flow rate and an assumed heating value of 1000 Btu per cubic foot of gas. In view of these considerations, significant uncertainties can be attributed to the experimental data. Considering a 10% uncertainty for both sets of experimental data, the agreement between the two can be considered at least satisfactory. The uncertainty for the normalized energy input of the MSU unit is about 10% without including the effect of possible day-to-day variation in the heating value of natural gas.

Significant discrepancy between the model results and the experimental data is evident in Figure 4.21. The regeneration heat input predicted by the model is based on an efficiency of 92%, an implicit assumption in the model (presumably for a direct-fired system). If the model had utilized a gas-fired water heating system for regeneration with an overall efficiency of 80% or less, the discrepancy in the results would have been reduced accordingly. In addition, the desiccant system of the model is inherently more efficient in the dehumidification process than the FAS units considered here. The system of the model (or the UIC correlations) requires a regeneration flow rate of about one-third that of the process flow, unlike the FAS units, in which the regeneration and process air flow rates are equal. The studies by Jalalzadeh-Azar, Steele, and Hodge (2000b) and Van den Bulck, Mitchell, and Klein (1986) elaborate on this issue. Allowing the regeneration flow rate to be less than that of the process flow can yield substantial improvement in the dehumidification efficiency as long as the regeneration temperature is fixed. Considering these design/operational differences, the underestimate of the energy input by the model with respect to the experimental values is not surprising.

The performance results for the process inlet temperature of 90°F are shown in Figures 4.22 to 4.24. Figure 4.22 shows that the model-predicted process exit temperatures are in excellent agreement with the CDH Energy field data (from a Munters unit) but are significantly lower (by about 10 to 15°F) than those reported for the MSU Munters unit. As discussed before, this is because the CDH Energy unit utilizes a balanced-flow heat pipe, whereas the MSU Munters unit does not.

For the grain depression, both MSU experimental data and the CDH Energy field data are in good agreement with the model results as shown in Figure 4.23. Referring to Figure 4.24, excellent agreement is also found between the experimental data from the MSU Munters unit and the CDH Energy field data for the normalized energy input. The agreement of these data with the model results is generally good, considering the uncertainties, but excellent for inlet humidity ratios up to 100 grains/lbm.a.

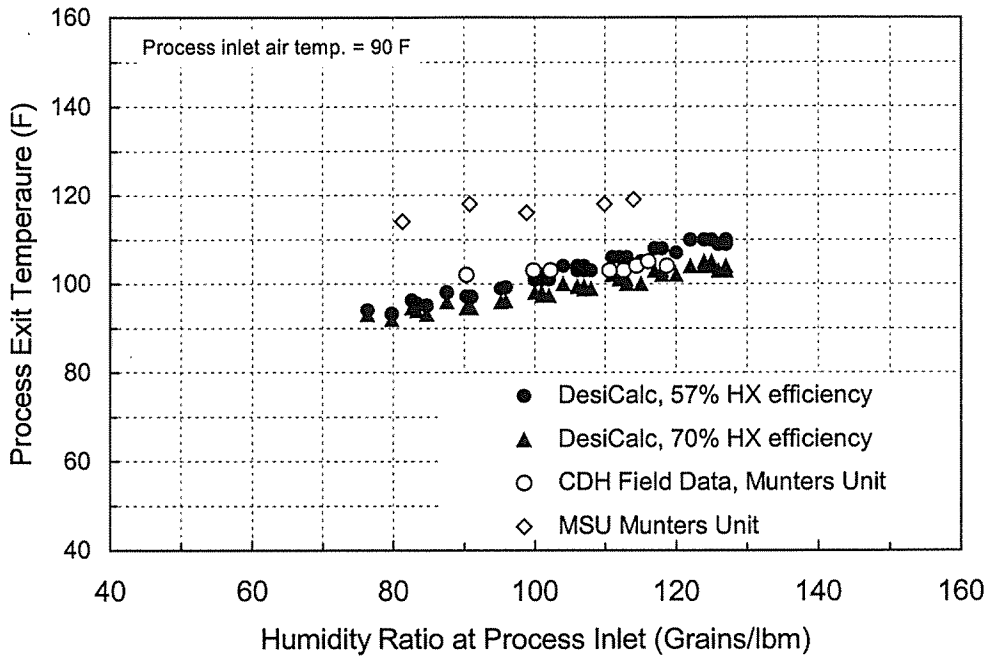


Figure 4.22. Process Exit Temperature Comparisons for Process Inlet Temperature of 90°F - (Munters Units).

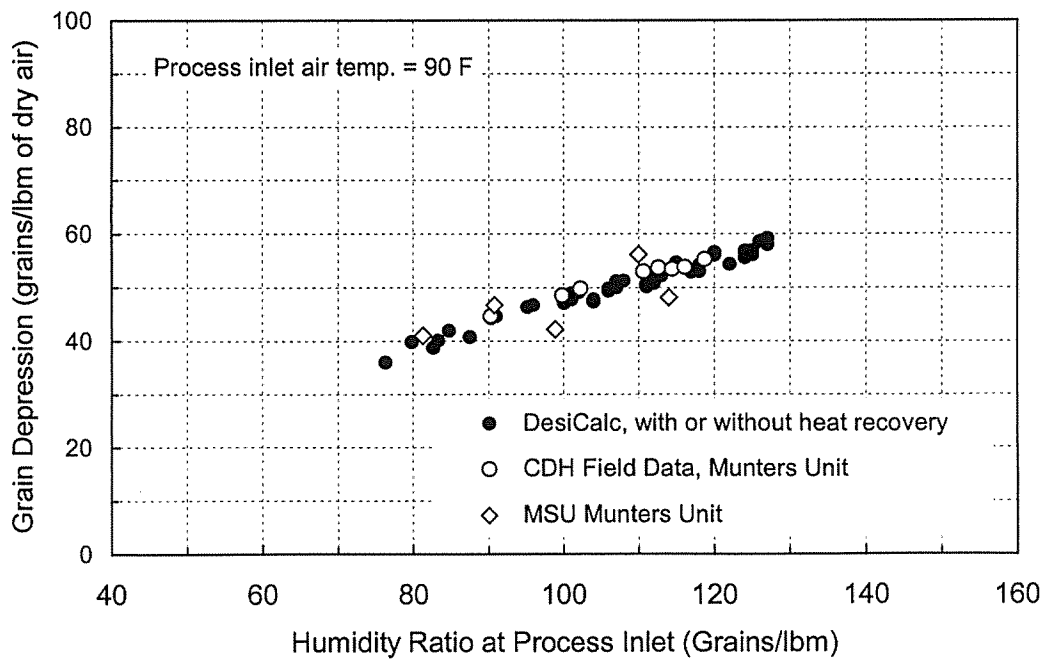


Figure 4.23. Grain Depression Comparisons for Process Inlet Temperature of 90°F - (Munters Units).

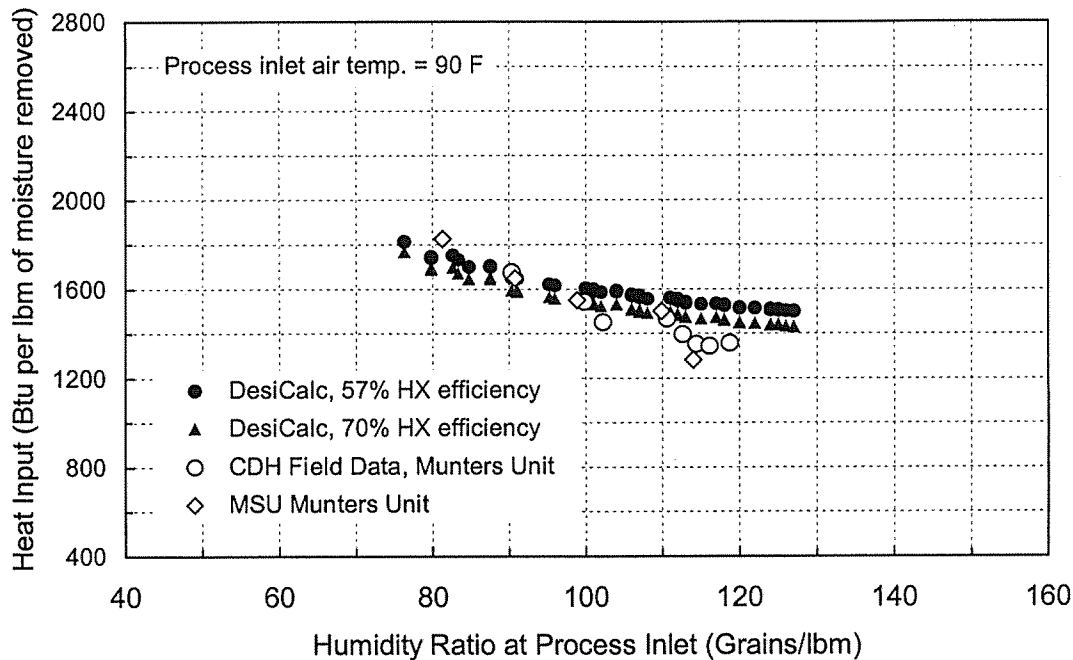


Figure 4.24. Heat Input Comparisons for Process Inlet Temperature of 90°F - (Munters Units).

In obtaining the preceding results, no evaporative cooling was used to enhance the sensible cooling of the process air via the heat exchanger. Further comparisons are made to examine the validity of DesiCalc™ when evaporative cooling takes place on the regeneration side. In doing so, experimental data from the FAS units of MSU and ORNL are compared with the corresponding model predictions. No data from the Munters units of MSU and CDH Energy are included. The MSU Munters system is not equipped with an evaporative cooler, and the CDH Energy data were obtained without evaporative cooling.

Figures 4.25 to 4.27 present the results for an inlet process air temperature of 80°F with evaporative cooling activated. Figure 4.25 exhibits good agreement between the process exit temperatures obtained from the MSU and ORNL units. The model predicts lower exit temperatures, but the discrepancy diminishes as the humidity level increases. For the grain depression and normalized energy input shown in Figures 4.26 and 4.27, respectively, the two sets of experimental data (MSU and ORNL) are in excellent agreement with each other but are noticeably different from the model predictions. With respect to these experimental data, the model underestimates the normalized regeneration energy input. The discrepancy between the model predictions and the real-system results for the regeneration energy input is even greater than what is seen in Figure 4.27 because the grain depression is overestimated by the model.

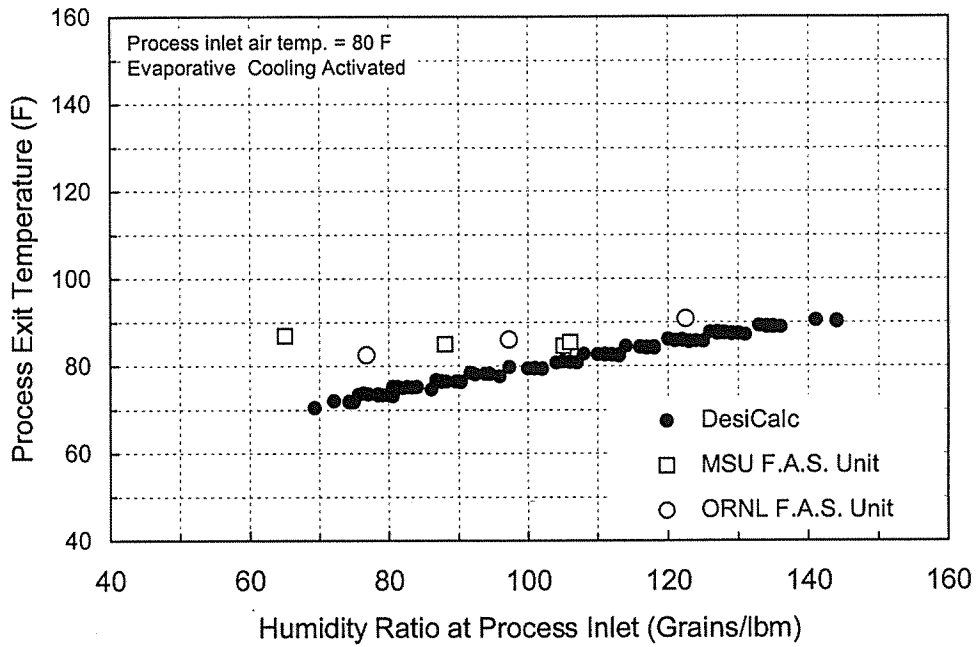


Figure 4.25. Process Exit Temperature Comparisons for Process Inlet Temperature of 80°F - (FAS Units, Evaporative Cooling Activated).

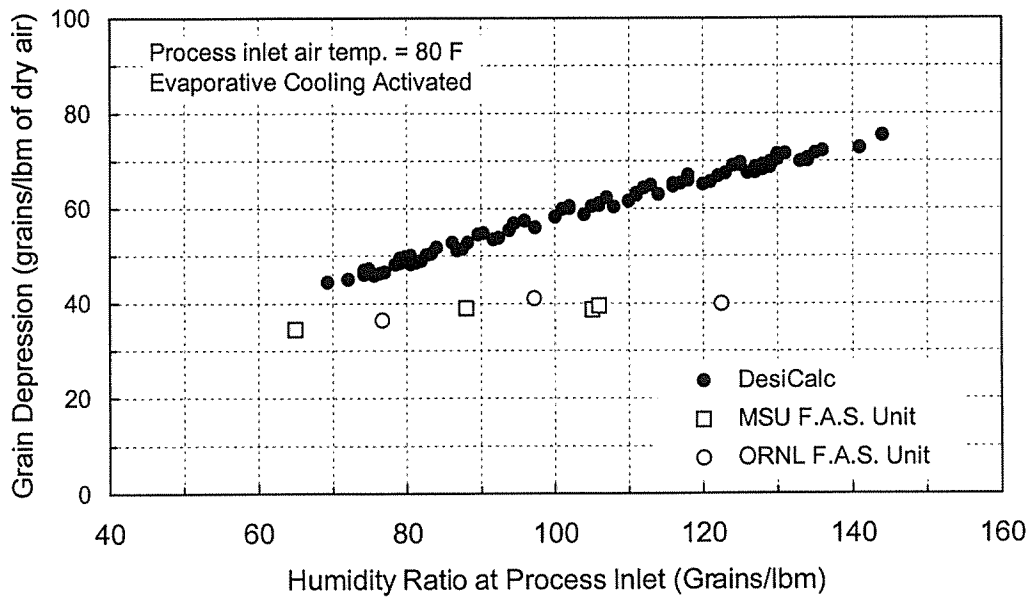


Figure 4.26. Grain Depression Comparisons for Process Inlet Temperature of 80°F - (FAS Units, Evaporative Cooling Activated).

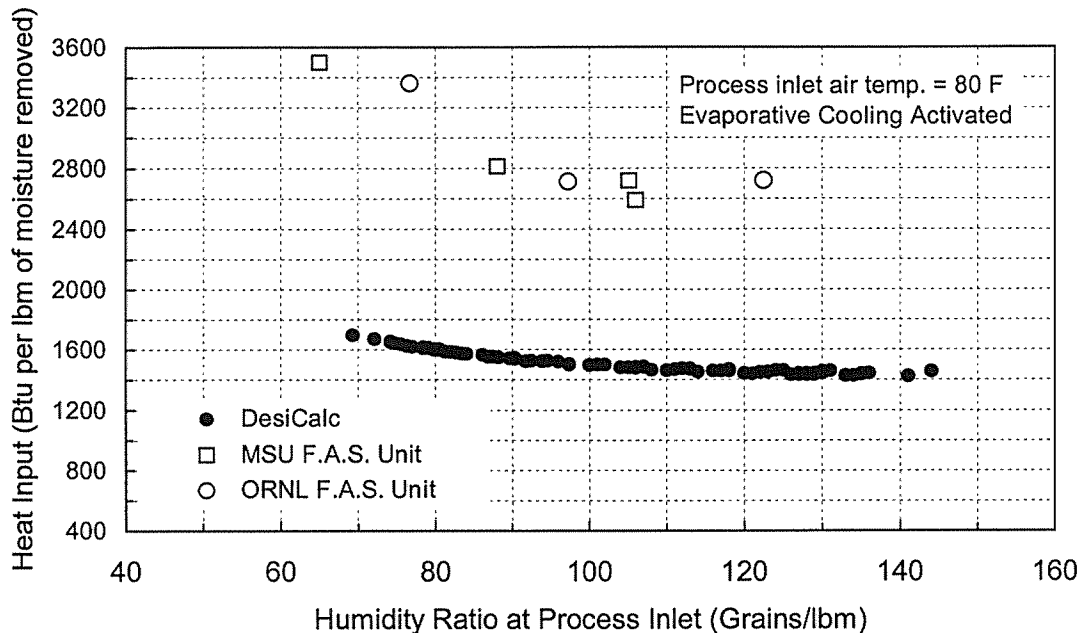


Figure 4.27. Regeneration Heat Input Comparisons For Process Inlet Temperature of 80°F - (FAS Units, Evaporative Cooling Activated).

Similar results are shown for the inlet temperature of 95°F in Figures 4.28 to 4.30. Figure 4.28 reflects good agreement between the model-predicted exit temperatures and those of the MSU and ORNL experimental data. As shown in Figure 4.29, good agreement is also observed between the two sets of experimental data for grain depression. The model-predicted values of grain depression are closer to the experimental data in this case than in the case for the inlet temperature of 80°F (Figure 4.26). For the normalized regeneration energy input, Figure 4.30 indicates that the model results are significantly less than the experimental data. The discrepancies observed between the model predictions and the experimental data from the FAS units (Figures 4.27 and 4.30) can be addressed in the same fashion as was discussed for the case of Figure 4.21.

Rotary heat recovery wheels in desiccant systems generally cause migration of moisture from the regeneration air stream to the process air stream, which adversely affects the net moisture removal capacity of the systems. The migration effect intensifies as the rotational speed of the wheel increases or when evaporative cooling is activated. However, the model does not distinguish a rotary heat exchanger from a non-rotary one with regard to moisture transfer (for example, model grain depression predictions in Figure 4.20, without evaporative cooling, and Figure 4.26, with evaporative cooling, are identical). Consequently, the energy requirement for regeneration tends to be underestimated by the model when a rotary heat exchanger is in use. Figure 4.31 highlights the impact of the rotary heat exchanger and evaporative cooling on the

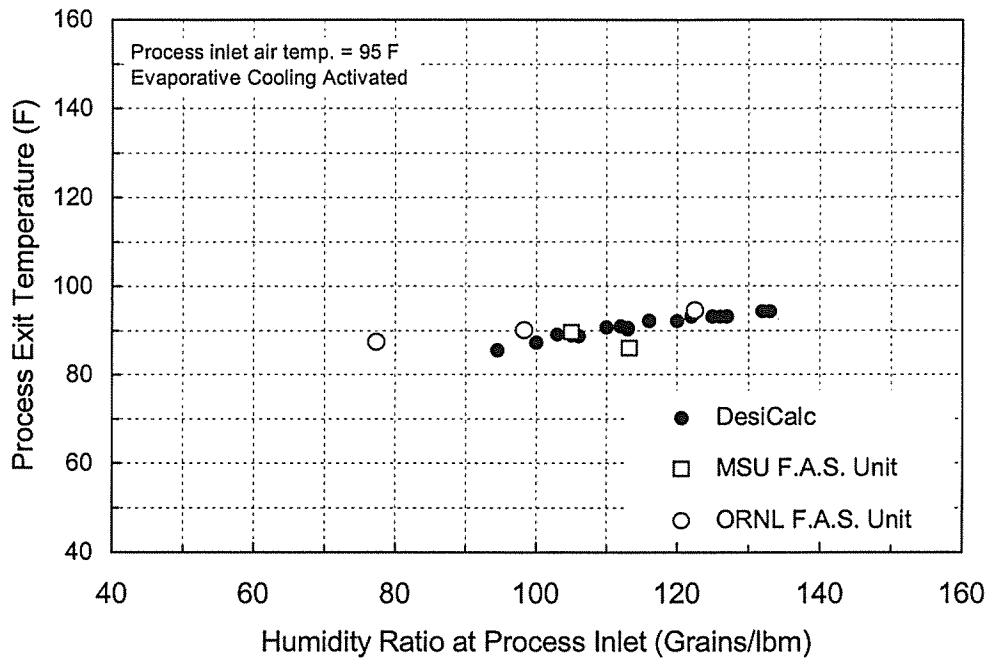


Figure 4.28. Process Exit Temperature Comparisons for Process Inlet Temperature of 95°F - (FAS Units, Evaporative Cooling Activated).

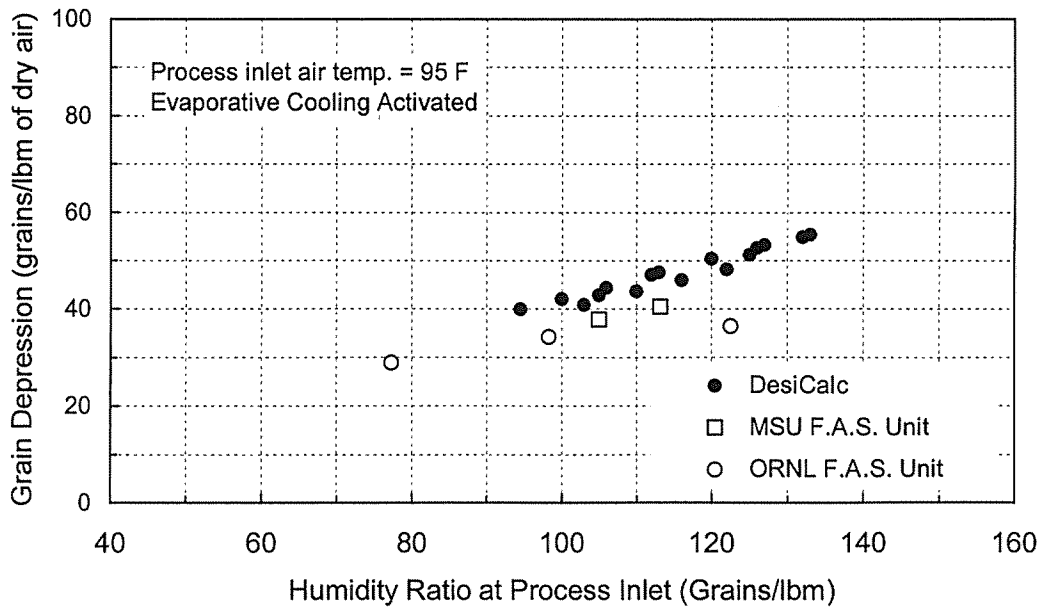


Figure 4.29. Grain Depression Comparisons for Process Inlet Temperature of 95°F - (FAS Units, Evaporative Cooling Activated).

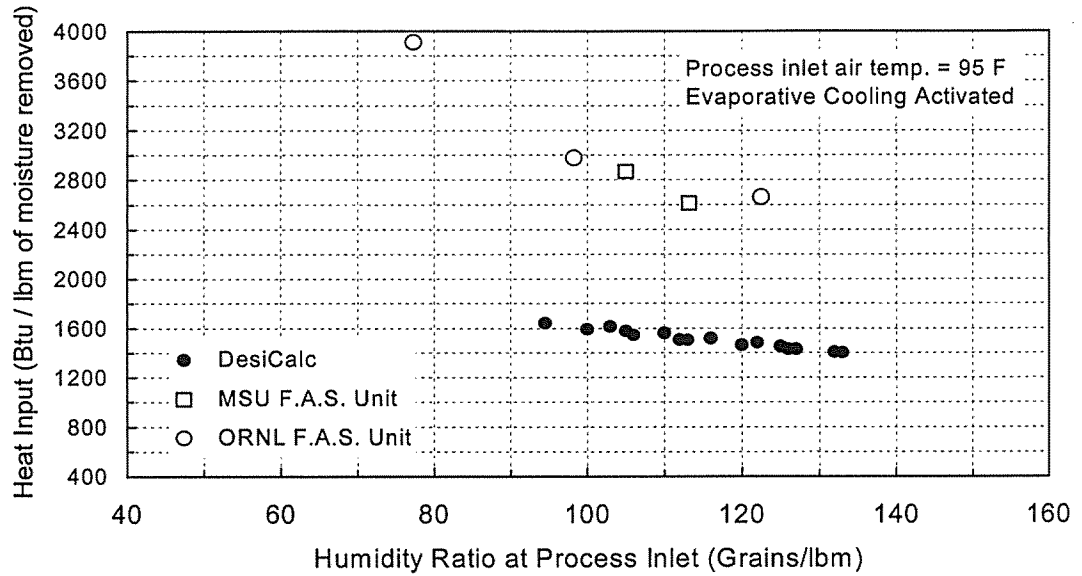


Figure 4.30. Regeneration Heat Input Comparisons for Process Inlet Temperature of 95°F - (FAS Units, Evaporative Cooling Activated).

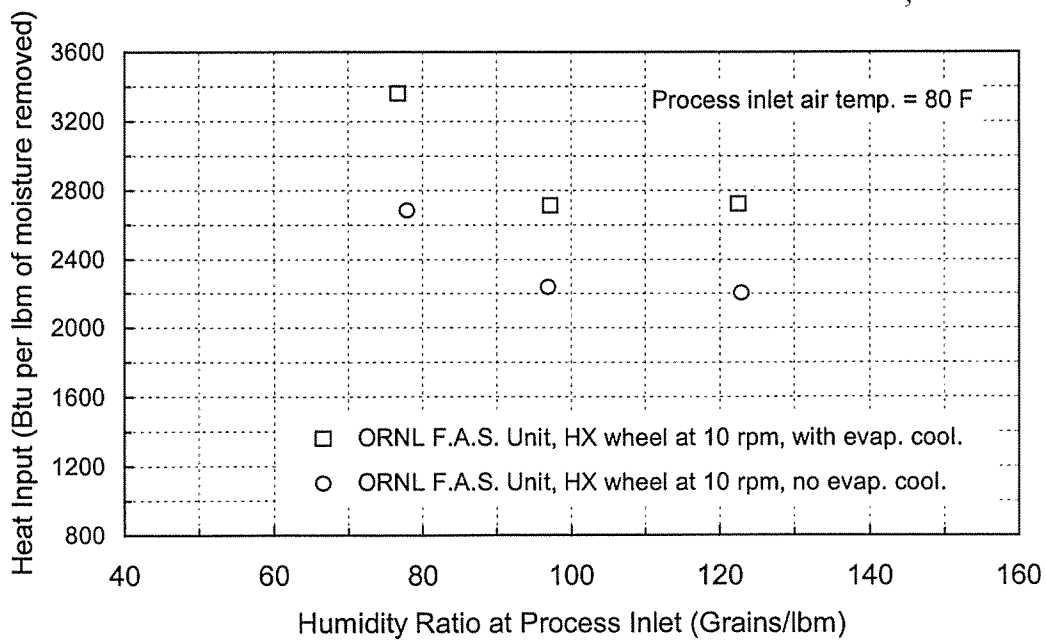


Figure 4.31. Effect of Rotary Heat Recovery Wheel on Grain Depression.

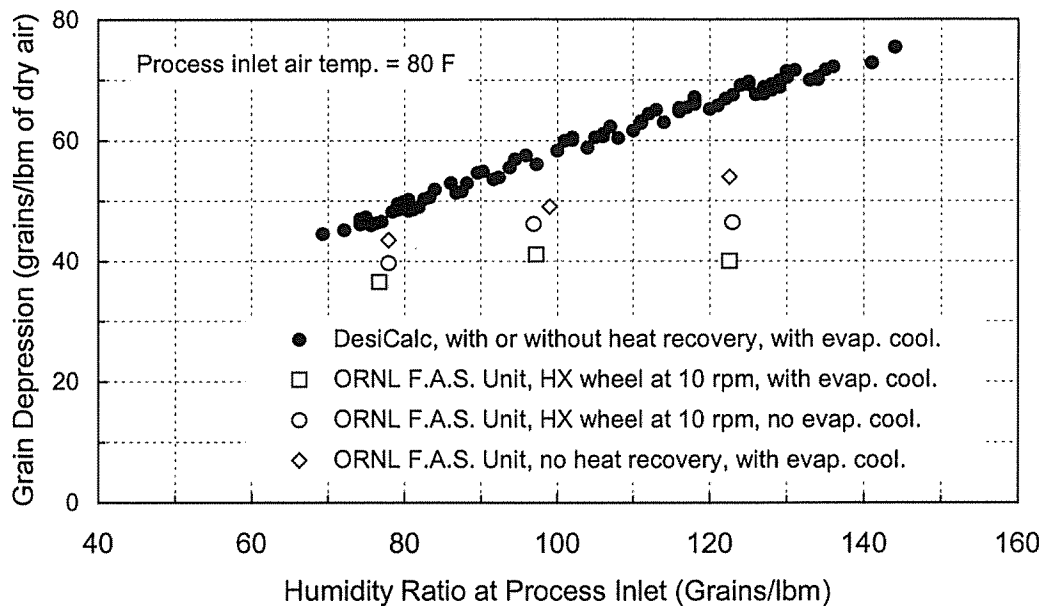


Figure 4.32. Effect of Rotary Heat Recovery Wheel on Regeneration Heat Input.

moisture removal capacity of the ORNL FAS unit. Figure 4.32 demonstrates the adverse impact of activating the evaporative cooler in the ORNL FAS unit on the normalized heat input for regeneration. [See the study by Jalalzadeh-Azar, Sand, and Vineyard (2000a) for an in-depth analysis of the impact of rotary heat recovery wheels on system performance.]

Implications

The comparisons of hourly performance data have confirmed the usefulness of DesiCalc™ in predicting the performance trends of commercially available desiccant systems. However, an assessment of the model would not be complete without addressing the impact of any discrepancies (stemming from generalization of the model results to other types of desiccant systems) on the total energy consumption.

As indicated earlier, when the DesiCalc™ predictions are applied to the FAS units considered in this study, the model significantly underestimates the regeneration heat input of the regeneration system. Referring to Figures 4.21 and 4.30, the predicted regeneration heat input has to be increased by about 50% (on the average) if the results are to be applied to the FAS units. This correction can be directly applied to the monthly gas input predictions for the space cooling indicated in the output of the alternative system. For example, the model predicts 537 MMBtu for the gas usage associated with the space cooling of a retail store in Charleston, SC for the month of July (based on the

default values). The corrected gas consumption for this month would be about 800 MMBtu (1.5 times the predicted value).

Evaluation of the effect of deviations in the predicted process exit temperature on the electrical energy consumption for post cooling requires considering hourly performance data. This is because the time duration of the desiccant system operation has to be taken into account for evaluating the impact of any perturbation in the process exit temperature on the monthly or yearly electrical energy usage. Figure 4.33 depicts the effect of process exit temperature perturbations on the electrical energy input associated with post cooling of the dehumidified ventilation air for a retail store in Charleston, SC in the month of July. These results are based on an average COP of about 2.6 for cooling (equivalent to an efficiency of 8.9 Btu/W used as the default value for the cooling system in DesiCalc™). From Figure 4.33, the predicted electrical energy input for post cooling is about 22,000 kWh. This value increases to about 26,000, 35,000, and 42,000 kWh when the process exit temperature is perturbed by 4, 12, and 20°F, respectively. The temperature discrepancy can exceed 20°F as seen in Figure 4.16. A total electrical energy consumption of 73,400 kWh is predicted by the model for the space cooling via the alternative system in the month of July. Considering an underestimation of the process exit temperature by 20°F, the resulting discrepancy in the energy usage becomes about 20,000 kWh, which translates into about 27% of the electrical energy usage for the month of July. This assessment is based on the default value of 0.3 cfm per square foot of the floor area for outside air intake and on the fact that the modeled HVAC system incorporates desiccant technology for dehumidification of outside air only. Should the amount of ventilation air increase, the impact of this discrepancy on the monthly energy consumption would be even greater.

Another examination performed in this study for the overall assessment of DesiCalc™ is the sensitivity of the annual energy usage to the extent of application of desiccant dehumidification. The total energy consumptions for gas and electricity for the base and alternative systems would be expected to converge as the outside air intake approaches zero. This is based on the notion that desiccant dehumidification is applied for treating the ventilation air only and that gas heating is specified for both scenarios in the example. Figure 4.34 illustrates the variation of the normalized annual electrical energy and gas consumptions with the amount of outside air intake for a quick-service restaurant application in Atlanta, Ga. The normalized energy parameter in this figure is the ratio of the energy usage of the alternative system to that of the conventional system. These results are indicative of reasonable trends in variation of the energy usage for electricity and gas but may point to the existence of a bias error. When the outside air intake vanishes, the gas consumption of the alternative system lags behind that of the conventional system by at least 5%. The corresponding discrepancy for electricity is about 2 or 3%. At the higher values of outside air intake, the conventional system is ineffective in meeting the indoor relative humidity set point. As seen in Figure 4.35, when the outside air intake increases from the default value of 1.6 to 3 cfm per square foot, the number of hours that the humidity set point (60% r.h.) is not met by the

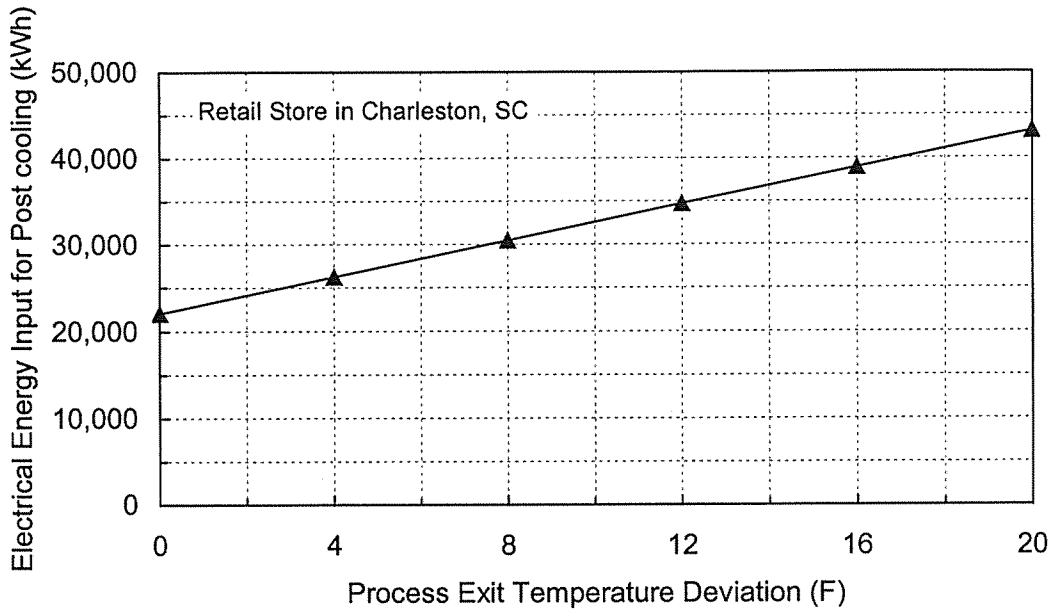


Figure 4.33. Impact of Underestimating Process Air Exit Temperature on Actual Energy Requirements for Post Cooling.

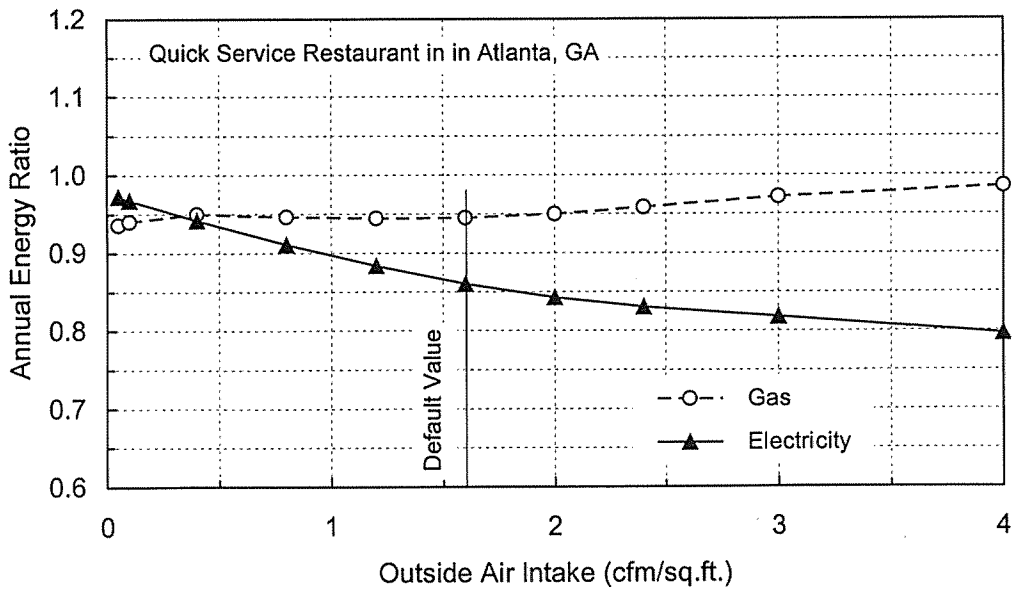


Figure 4.34. Variation of Relative Energy Consumption of Alternative System with Outside Air Intake.

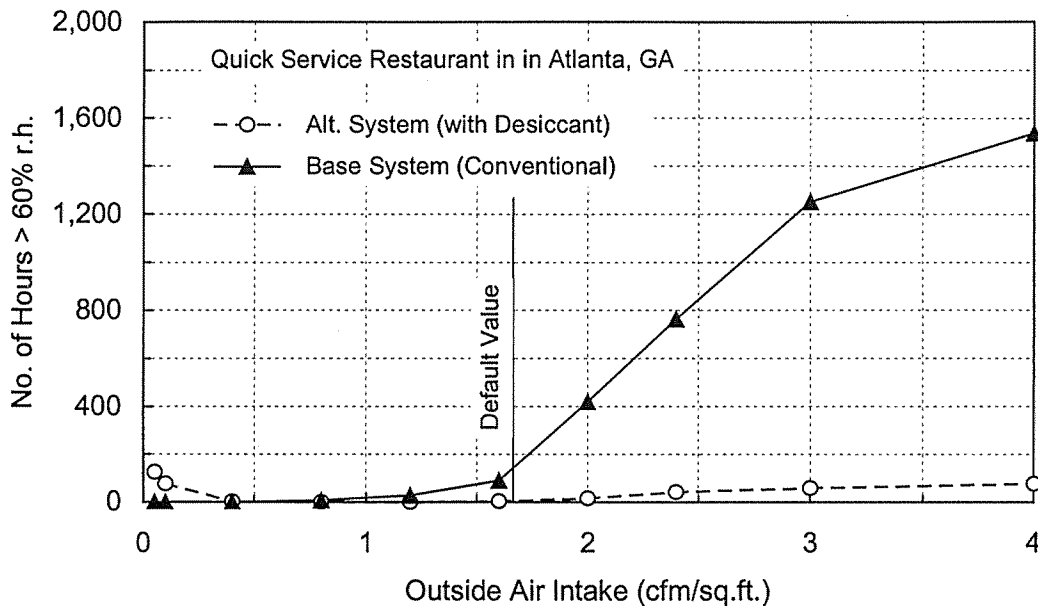


Figure 4.35. Dehumidification Effectiveness with Respect to Outside Air Intake.

conventional system increases from approximately 180 to about 1200 hours, whereas a negligible effect is observed with the case of the alternative system incorporating desiccant dehumidification.

4.7. CONCLUSIONS

The UIC correlations are central to the predictive capability of DesiCalc™ in performance evaluation of desiccant systems. These correlations pertain to the performance of a specific experimental system operated under steady-state conditions. Comparisons between the UIC empirical data and the hourly model results for arbitrary applications have verified the conformity of the model to these correlations. Establishing this conformity is the first crucial step in the model verification process as it reflects an accurate simulation process. Beyond this stage, any significant deviation of the model predictions from the real-world outcome may be construed as a consequence of 1) limitations of the correlations, 2) incompatibilities between the characteristics of the real system and the model system, 3) inaccuracies associated with the real-system data, or 4) a combination of these factors.

The limitations of the model can be largely attributed to its empirical correlations as they do not account for the diversities of the desiccant systems in the market. The model predictions for the energy input were in excellent agreement with the CDH Energy field data obtained from a Munters unit and in satisfactory agreement with the experimental data from the MSU Munters unit. However, the model results did not

accurately represent the performance of the FAS units tested at DOE/ORNL and MSU, largely due to 1) the type of the regeneration heating system used in these experimental units and 2) differences in the system design parameters including desiccant material, desiccant wheel speed, control mode of regeneration heating system, and regeneration-to-process-airflow ratio.

Although experimental and field data have been used as benchmarks for the model validation, the data are subject to uncertainties (as discussed in Section 4.2). In general, unaccounted sources of uncertainties for experimental and field data can create difficulties and challenges to accurate assessment of the predictive models.

Despite all the difficulties and limitations encountered in validating DesiCalc™, two important considerations should be taken into account: 1) the purpose of the model and 2) the availability of relatively simple and practical means for enhancement of the model. The main purpose of DesiCalc™ is to facilitate a preliminary evaluation of HVAC system alternatives considered by end users, engineers, or building managers. To accomplish this purpose, a set of relationships are implemented to predict the performance of desiccant systems in accordance with the established standards of the industry, which is not an unreasonable strategy. However, the model can be modified to accommodate the diversities observed with regard to system configurations. Including the efficiency of the regeneration system as an input parameter as opposed to a built-in default value in a non-interactive fashion would be an enhancement. Another means for improvement would be incorporation of more correlations to cover a greater cross section of the commercially available desiccant systems.

4.10. REFERENCES

GRI, 1998, *DesiCalc™ User's Manual, Version 1.1*, Chicago, IL.

Jalalzadeh-Azar, A. A., Sand, J. R., and Vineyard, E. A., 2000a, "Characterization of Heat Recovery Wheels in Thermally Regenerated Desiccant Systems Utilizing Evaporative Cooling," Proceedings of 34th National Heat Transfer Conference, Paper NHTC2000-12167, August 20-22, 2000, Pittsburgh, PA.

Jalalzadeh-Azar, A. A., Steele, W. G., and Hodge, B. K., 2000b, "Performance Characteristics of a Commercially Available Gas-Fired Desiccant System," *ASHRAE Transactions*, Vol. 106, Part 1, pp. 95- 104.

Jalalzadeh-Azar, A. A., 2000c, "Consideration of Transient Response and Energy Cost in Performance Evaluation of A Desiccant Dehumidification System," *ASHRAE Transactions 2000*, Vol. 106, Part.2, pp.210-216.

Jalalzadeh-Azar, A. A., Hodge, B. K., and Steele, W. G., 1998, "Thermodynamic Assessment of Desiccant Systems with Targeted and Relaxed Humidity Control Schemes," *ASHRAE Transactions*, Volume 104, Part 2, pp. 313-319.

Jalalzadeh-Azar, A. A., Steele, W. G., and Hodge, B. K., 1996, "Design of a Test Facility for Gas-Fired Desiccant Dehumidifiers," Proceedings of the International Joint Power Generation Conference and Exposition, Vol. 2, pp. 149-161, October 14-16, 1996, Houston, TX.

Munters, 1990, *The Dehumidification Handbook*, Munters Cargocaire, Amesbury, MA.

Pesaran, A.A., 1994, "A Review of Desiccant Dehumidification Technology," National Renewable Energy Laboratory, Contract No. DE-AC36-83CH10093, Golden, CO.

Van den Bulck, E., Mitchell, J. W., and Klein, S. A., 1986, "The Use of Dehumidifiers in Desiccant Cooling and Dehumidification Systems," *Journal of Heat Transfer*, Vol. 108, pp. 684-692.

Vineyard, E. A., Sand, J. R., and Durfee, D. J., 2000, "Parametric Analysis of Variables that Affect the Performance of a Desiccant Dehumidification System," *ASHRAE Transactions*, Vol. 106, Part 1, pp. 87-94.

APPENDIX 4.A

DESICALC™ SYSTEM DIAGRAMS AND SAMPLE OUTPUT

Pre-Cool Enthalpy Relief Air Heat Exchanger

The desiccant system utilizes a desiccant wheel to treat the outside air stream. Sensible and latent heat is rejected using an enthalpy heat exchanger, shown here as an enthalpy wheel. Excess latent heat is removed from the outdoor air by the desiccant wheel, producing hot and dry air. In most applications, the enthalpy heat exchange is in the relief air stream (Figure 60). The desiccant wheel performance is representative of state-of-the-art silica wheels. The enthalpy heat exchanger performance (effectiveness) should be based on manufacturer's data with typical effectiveness averaging 70% (default value). If no economizer is selected, the amount of outdoor air is fixed at the minimum *Ventilation* air level input from the *Application* screen. If either a *Temperature* or *Enthalpy* economizer is selected, the economizer controls will vary the outdoor air quantities.

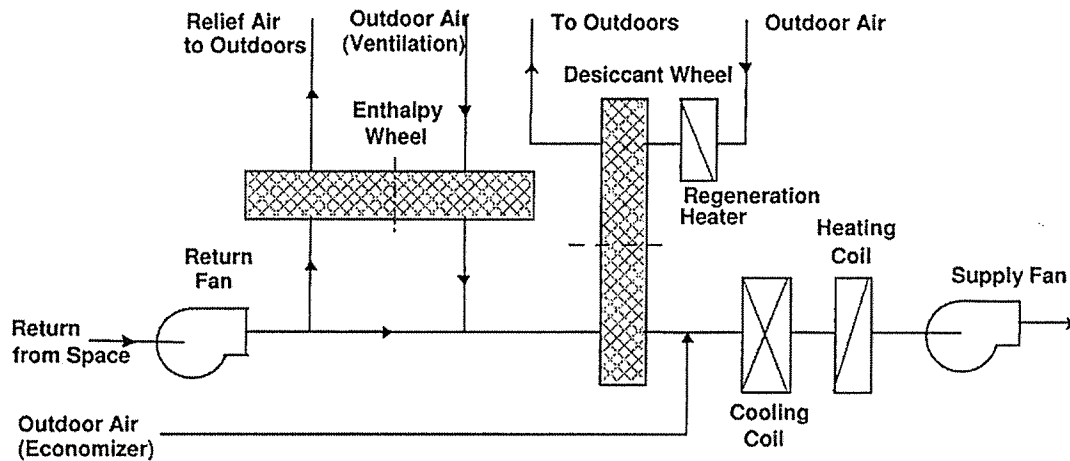


Figure 60 - Pre-Cool Enthalpy Relief Air Heat Exchanger

Post-Cool Sensible Relief Air Heat Exchanger

The desiccant system utilizes a desiccant wheel to treat the outside air stream. The desiccant wheel removes latent heat from the outdoor air, producing hot and dry air. The excess sensible heat is rejected using a sensible heat exchanger, shown here as a run-around heat recovery loop. In most applications, the sensible heat exchange is with the relief air (Figure 61). The desiccant wheel performance is representative of state-of-the-art silica wheels. The sensible heat exchanger performance (effectiveness) should be based on manufacturer's data with typical effectiveness averaging 70% (default value). If no economizer is selected, the amount of outdoor air is fixed at the minimum *Ventilation* air level input from the *Application* screen. If either a *Temperature* or *Enthalpy* economizer is selected, the economizer controls will vary the outdoor quantities.

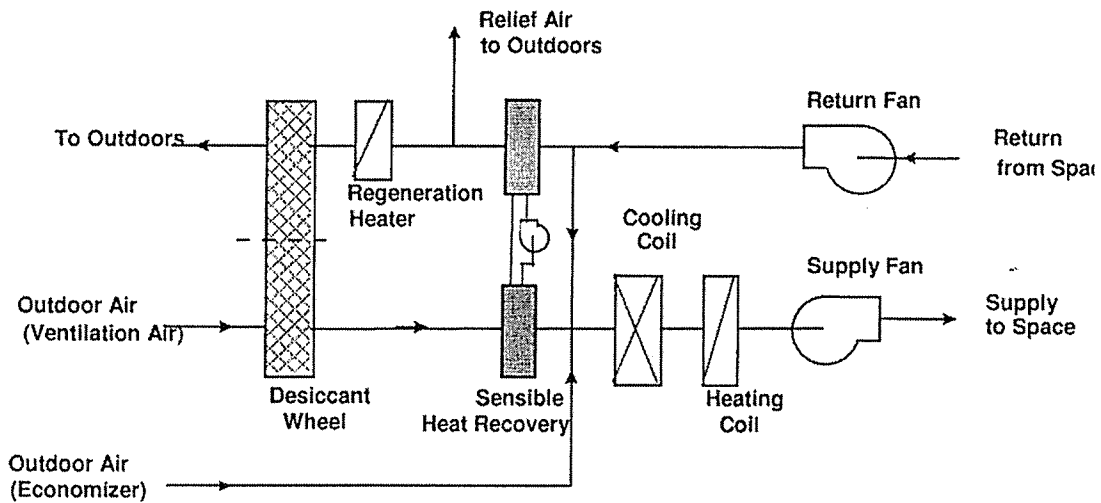


Figure 61 - Post-Cool Sensible Relief Air Heat Exchanger

Post-Cool Sensible Outdoor Air Heat Exchanger

This desiccant dehumidifier with outdoor air sensible heat exchanger (Figure 62) differs slightly from the system described above. In this system, the sensible heat exchanger rejects heat to outdoor air rather than relief air.

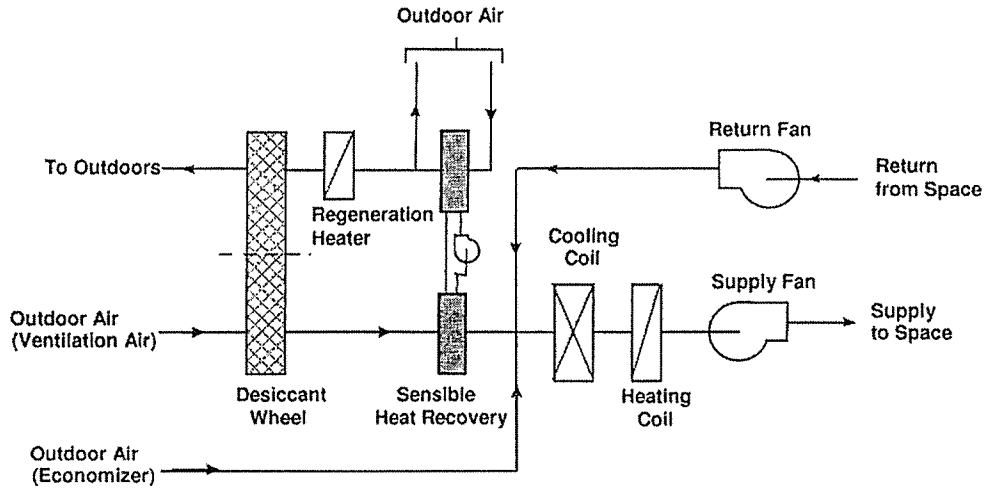


Figure 62 – Post-Cool Sensible Outdoor Air Heat Exchanger

Hospital Desiccant Dehumidification Systems

For the Hospital, the desiccant dehumidifier relief air sensible heat exchanger is the same as described above except that DesiCalc assumes that outdoor air is pre-cooled with a chilled water coil upstream of the desiccant wheel as required to meet the desired setpoint (Figure 63).

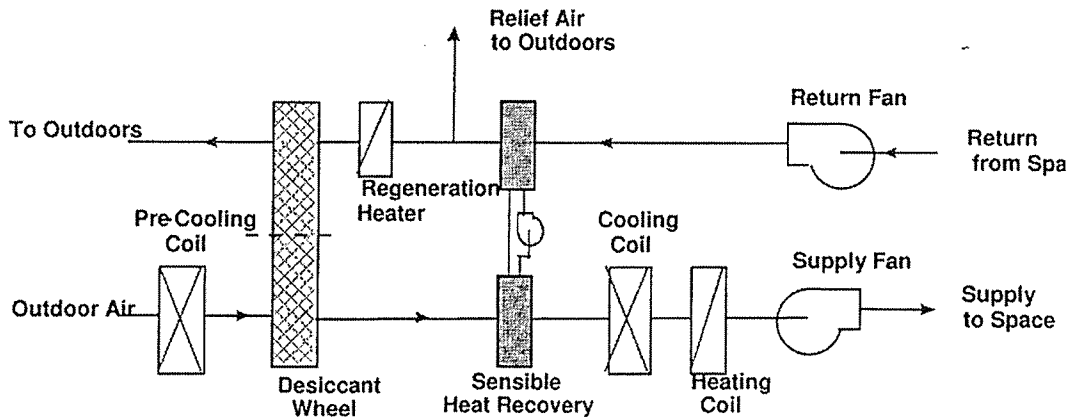


Figure 63 – Hospital Post-Cool Sensible Relief Air Heat Exchanger

Ice Arena Desiccant Dehumidification Systems

For the Ice Arena, the desiccant dehumidifier relief air sensible heat exchanger is the same as described above except that DesiCalc assumes that outdoor air is mixed with air returned from the conditioned space upstream of the desiccant wheel (Figure 64).

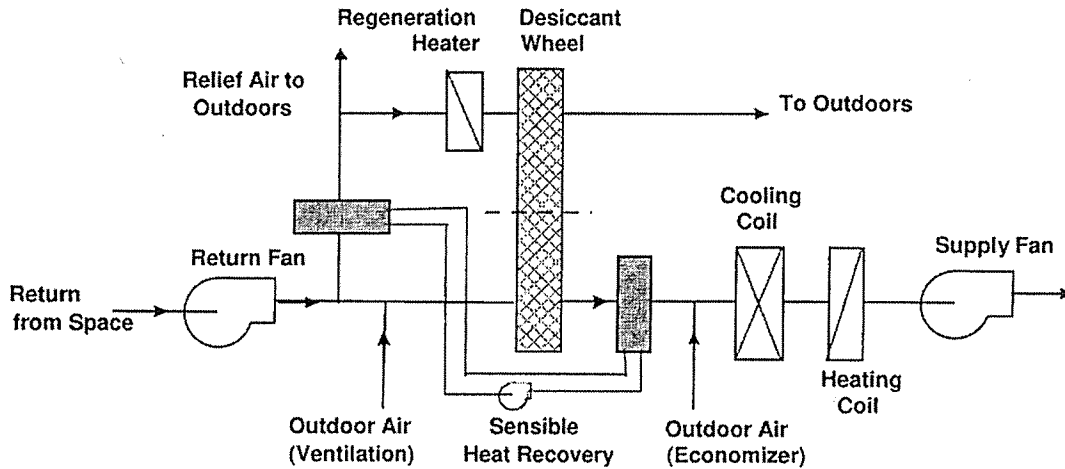


Figure 64 - Ice Arena Post-Cool Sensible Relief Air Heat Exchanger

For the Ice Arena only, the desiccant dehumidifier outdoor air sensible heat exchanger is the same as described above except that DesiCalc assumes that outdoor air is mixed with air returned from the conditioned space upstream of the desiccant wheel (Figure 65).

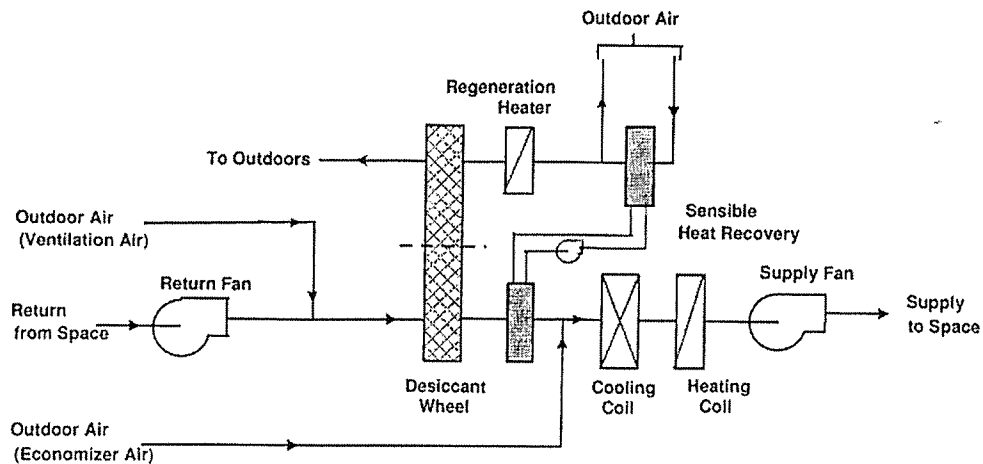


Figure 65 - Ice Arena Post-Cool Sensible Outdoor Air Heat Exchanger

Evaporative Cooler

The evaporative cooler option provides additional sensible cooling capacity to the heat recovery system through the adiabatic cooling principal. That is, using the sensible heat of the outdoor air (Figure 66) or relief air (Figure 67) to evaporate water accomplishes the cooling. Evaporative coolers can range from inexpensive wetted-pad units to more elaborate systems utilizing sprays and eliminators. No moisture is added to the supply air stream. Since the evaporative cooler is used in conjunction with a sensible heat exchanger, this option is disabled if the desiccant dehumidifier *Heat Recovery* is set to [None].

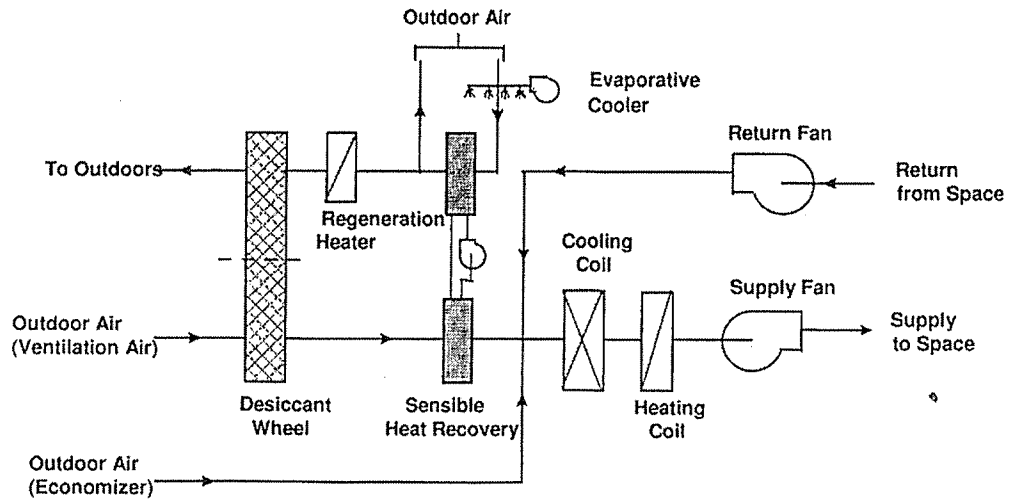


Figure 66 – Sensible Outside Air Heat Exchanger with Evaporative Cooler

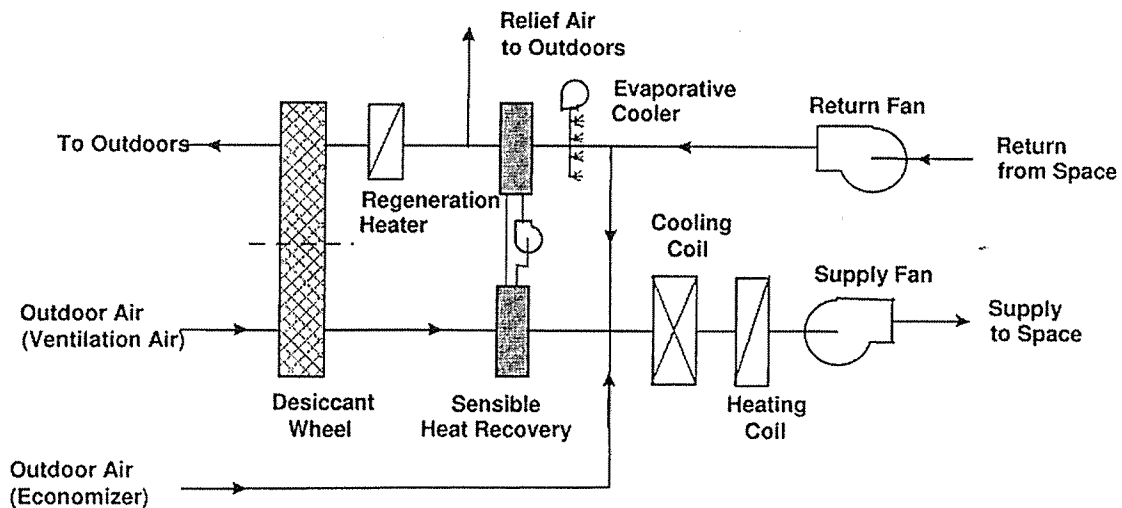


Figure 67 – Sensible Relief Air Heat Exchanger with Evaporative Cooler

JOB DESCRIPTION

Project: January 14, 2001 Location: Charlseton, SC Program User: Jalalzadeh Comments: HX eff: 70% , no evap. cooling

BUILDING

Retail Store; single-story slab on grade construction typical of a larger department store with 10 % wall glazing. Humidity control air treatment applies to 60000 sf floor area. Internal loads and ventilation values apply to humidity controlled areas. Building total floor area is 60000 sf. Application Comfort Controls - Default Controls

Internal Loads and Ventilator

Occupancy:	100.0 sf/person
Lighting:	2.30 Watt/sf
Other Electric:	0.25 Watt/sf
Infiltration:	0.30 air exchanges/hour
Ventilation:	0.30 cfm/sf

LOCATION & DESIGN WEATHER

Charleston SC - Lat./Long. 33N/80W Summer 1% Design Dry Bulb/Mean-Coincident Wet Bulb: 92/77°F (Humidity Ratio 117 gr/lb) Summer 1% Design Dew-Point/Mean-Coincident Dry Bulb: 77/83°F (Humidity Ratio 139 gr/lb). Energy Rates - Default

Equipment Sizing Design Point: 1% DB & 1% DP
 Equipment Oversize: 20 %

Comfort Controls	Baseline	Des. Enhanced
Cooling Temp./Setback	75 / 75 F	75 / 75 F
Heating Temp./Setback	72 / 72 F	72 / 72 F
Maximum Humidity	60 %	60 %
Minimum Humidity	0 %	0 %

EQUIPMENT & ENERGY

<u>Baseline Equipment Alternative</u>	<u>Desiccant Enhanced System Alternative</u>
Constant volume 8.9 EER packaged DX rooftop unit without economizer. System does not use relief air heat recovery. System equipped with electric source heating. Humidifier not used. Default Config.	Constant volume 8.9 EER packaged DX rooftop unit without economizer. System equipped with gas source heating. Outside air treated by a gas-fired desiccant dehumidifier with 70 % eff. heat exch. (downstream sensible exchange with outside air heat recovery). Dehumidifier configured without evap. cooler option. Humidifier not used. Default Config.
Design Cooling Capacity: 219.29 RT Design Heating Capacity: 902,870 Btu/hr Supply Fans Capacity: 77,658 CFM Outside Air: 18,017 CFM	Design Cooling Capacity: 159.77 RT Design Heating Capacity: 915,577 Btu/hr Supply Fans Capacity: 65,218 CFM Outside Air : 18,000 CFM
Annual Electric Energy Use: 3,010,395 kWh Annual Gas Energy Use: 0 MMBtu	Annual Electric Energy Use: 1,734,206 kWh Annual Gas Energy Use: 4,023 MMBtu
Annual Electric Energy Cost: 227,271 \$ Annual Gas Energy Cost: 0 \$ Total Annual Energy Cost 227,271 \$	Annual Electric Energy Cost: 129,336 \$ Annual Gas Energy Cost: 19,699 \$ Total Annual Energy Cost 149,035 \$
Annual Occupied Hours @ RH>60% 1,077	Annual Occupied Hours @ RH>60% 1

DesiCalc
Input/Output Data Short Report
 Version 1.1g

1/14/01 10:39:08AM

Page 2 of 2

DESICCANT DEHUMIDIFIER UNIT PERFORMANCE SPECIFICATION
 (ARI Standard 940P Rating Conditions)

		Process Air Flow Face Velocity: 400 fpm		
		Dehumidifier Capacity: 18,000 CFM		
DB (F)	WB (F)	Humidity (gr/lb)	Water Removed (lb/hr)	Specific Energy Input (Btu/lb_removed water)
95	75	100.0	460	1,559
80	75	124.5	768	1,397

Regeneration air source is outside air preheated by post-cool sensible HX.

DESICCANT WHEEL MATRIX PERFORMANCE SPECIFICATION
 (ARI Standard 940P Rating Conditions)

		Process Air Flow Face Velocity: 400 fpm		
DB (F)	WB (F)	Humidity (gr/lb)	Water Removed (lb/hr)	Specific Energy Input (Btu/lb_removed water)
95	75	100.0	460	1,772
80	75	124.5	768	1,776

Note. The annual energy consumption and costs given in this report reflect facility total energy use including lights, equipment, and HVAC equipment. Details of monthly energy consumption by end use are given in Detailed Report.

Units Used
 RT = 12,000 Btu/hr
 MMBtu = 1,000,000 Btu

Cooling and Heating Coil Loads

January 14, 2001
Charleston, SC
Jalalzadeh
HX eff: 70% , no evap. cooling

Baseline System

Month	Cooling Sensible MMBtu	Cooling Latent MMBtu	Cooling Total MMBtu	Heating/Reheat Total MMBtu
JAN	59	9	68	206
FEB	122	32	154	206
MAR	283	83	367	193
APR	449	111	560	198
MAY	789	315	1,104	342
JUN	887	383	1,270	344
JUL	951	483	1,434	298
AUG	969	534	1,503	304
SEP	907	432	1,339	329
OCT	552	160	711	218
NOV	294	75	369	162
DEC	209	62	271	230
Total	6,471	2,679	9,150	3,030

Alternative System

Month	Cooling Sensible MMBtu	Cooling Latent MMBtu	Cooling Total MMBtu	Heating Total MMBtu
JAN	26	4	30	183
FEB	42	9	51	138
MAR	144	25	169	61
APR	250	43	293	15
MAY	478	85	563	0
JUN	594	95	689	0
JUL	739	112	851	0
AUG	773	110	882	0
SEP	647	102	750	0
OCT	331	58	389	2
NOV	156	25	181	33
DEC	86	18	104	118
Total	4,265	687	4,951	550

DesiCalc
Monthly Loads, Energy Consumption and Costs Report

1/14/01 10:39:21AM

Version 1.1g

Page 2 of 5

Electric Energy Consumption by End Use

Baseline System

Month	Lights kWh	Misc. Equip. kWh	Space Cooling kWh	Pumps & Misc. kWh	Fans Vent. kWh	Space Heating kWh	Heat Reject. kWh	Refrig. kWh	Dom.Hot Water kWh	Total kWh
JAN	82,137	8,928	5,349	1,114	14,849	60,311	0	0	2,910	175,598
FEB	74,188	8,064	12,243	1,918	13,412	60,423	0	0	2,670	172,918
MAR	82,137	8,928	29,280	4,280	14,849	56,492	0	0	2,991	198,957
APR	79,487	8,640	45,763	6,676	14,370	57,954	0	0	2,846	215,736
MAY	82,137	8,928	90,591	10,059	14,849	100,290	0	0	2,837	309,691
JUN	79,487	8,640	106,298	10,481	14,370	100,701	0	0	2,613	322,590
JUL	82,137	8,928	122,598	10,916	14,849	87,238	0	0	2,523	329,189
AUG	82,137	8,928	128,059	10,930	14,849	88,968	0	0	2,467	336,338
SEP	79,487	8,640	112,062	10,496	14,370	96,525	0	0	2,344	323,924
OCT	82,137	8,928	57,820	7,833	14,849	63,911	0	0	2,516	237,994
NOV	79,487	8,640	29,334	4,861	14,370	47,383	0	0	2,548	186,623
DEC	82,137	8,928	21,575	3,083	14,849	67,473	0	0	2,795	200,840
Total	967,095	105,120	760,972	82,647	174,835	887,669	0	0	32,060	3,010,398

Alternative System

Month	Lights kWh	Misc. Equip. kWh	Space Cooling kWh	Pumps & Misc. kWh	Fans Vent. kWh	Space Heating kWh	Heat Reject. kWh	Refrig. kWh	Dom.Hot Water kWh	Total kWh
JAN	82,137	8,928	2,210	766	12,470	0	0	0	0	106,511
FEB	74,188	8,064	3,981	1,256	11,263	0	0	0	0	98,752
MAR	82,137	8,928	14,202	3,439	12,470	0	0	0	0	121,176
APR	79,487	8,640	24,953	5,457	12,068	0	0	0	0	130,605
MAY	82,137	8,928	50,370	8,440	12,470	0	0	0	0	162,345
JUN	79,487	8,640	63,255	8,790	12,068	0	0	0	0	172,240
JUL	82,137	8,928	79,506	9,178	12,470	0	0	0	0	192,219
AUG	82,137	8,928	82,654	9,179	12,470	0	0	0	0	195,368
SEP	79,487	8,640	68,884	8,834	12,068	0	0	0	0	177,913
OCT	82,137	8,928	33,383	6,769	12,470	0	0	0	0	143,687
NOV	79,487	8,640	14,806	4,004	12,068	0	0	0	0	119,005
DEC	82,137	8,928	8,547	2,296	12,470	0	0	0	0	114,378
Total	967,095	105,120	446,751	68,408	146,825	0	0	0	0	1,734,199

Gas Energy Consumption by End Use

Baseline System

Month	Space Heating MMBtu	Space Cooling MMBtu	Dom. Water MMBtu	Hot Misc. Domestic MMBtu	Suppl. Heating MMBtu	Ext. Misc. MMBtu	Total MMBtu
JAN	0	0	0	0	0	0	0
FEB	0	0	0	0	0	0	0
MAR	0	0	0	0	0	0	0
APR	0	0	0	0	0	0	0
MAY	0	0	0	0	0	0	0
JUN	0	0	0	0	0	0	0
JUL	0	0	0	0	0	0	0
AUG	0	0	0	0	0	0	0
SEP	0	0	0	0	0	0	0
OCT	0	0	0	0	0	0	0
NOV	0	0	0	0	0	0	0
DEC	0	0	0	0	0	0	0
Total	0	0	0	0	0	0	0

Alternative System

Month	Space Heating MMBtu	Space Cooling MMBtu	Dom. Water MMBtu	Hot Misc. Domestic MMBtu	Suppl. Heating MMBtu	Ext. Misc. MMBtu	Total MMBtu
JAN	245	3	12	0	0	0	260
FEB	184	24	11	0	0	0	219
MAR	82	78	12	0	0	0	173
APR	20	86	12	0	0	0	118
MAY	0	366	12	0	0	0	378
JUN	0	463	11	0	0	0	474
JUL	0	615	10	0	0	0	625
AUG	0	712	10	0	0	0	722
SEP	0	540	10	0	0	0	550
OCT	2	148	10	0	0	0	161
NOV	44	65	11	0	0	0	120
DEC	158	57	12	0	0	0	227
Total	736	3,158	132	0	0	0	4,025

Total Monthly Electric Consumption and Electric Energy Cost

Baseline System

Month	Metered Energy kWh	Metered Demand kW	Energy Charge (\$)	Demand Charge (\$)	Energy Cost Adj (\$)	Taxes (\$)	Surch. (\$)	Fixed Charge (\$)	Min. Charge (\$)	Total Charge (\$)
JAN	175,599	562	12,102	0	0	0	0	13	0	12,115
FEB	172,918	578	11,918	0	0	0	0	13	0	11,931
MAR	198,957	542	13,710	0	0	0	0	13	0	13,723
APR	215,736	528	14,865	0	0	0	0	13	0	14,878
MAY	309,691	562	24,350	811	0	0	0	13	0	25,174
JUN	322,591	555	25,365	794	0	0	0	13	0	26,171
JUL	329,189	546	25,884	770	0	0	0	13	0	26,667
AUG	336,339	543	26,446	762	0	0	0	13	0	27,221
SEP	323,924	547	25,469	771	0	0	0	13	0	26,254
OCT	237,995	528	16,397	0	0	0	0	13	0	16,410
NOV	186,623	553	12,861	0	0	0	0	13	0	12,874
DEC	200,841	522	13,840	0	0	0	0	13	0	13,853
Total	3,010,403	6,565	223,207	3,908	0	0	0	156	0	227,271

Alternative System

Month	Metered Energy kWh	Metered Demand kW	Energy Charge (\$)	Demand Charge (\$)	Energy Cost Adj (\$)	Taxes (\$)	Surch. (\$)	Fixed Charge (\$)	Min. Charge (\$)	Total Charge (\$)
JAN	106,513	198	7,347	0	0	0	0	13	0	7,360
FEB	98,754	219	6,813	0	0	0	0	13	0	6,826
MAR	121,177	251	8,356	0	0	0	0	13	0	8,369
APR	130,607	286	9,005	0	0	0	0	13	0	9,018
MAY	162,347	293	12,758	111	0	0	0	13	0	12,882
JUN	172,240	321	13,536	184	0	0	0	13	0	13,734
JUL	192,220	331	15,108	210	0	0	0	13	0	15,331
AUG	195,369	337	15,356	226	0	0	0	13	0	15,595
SEP	177,914	321	13,983	184	0	0	0	13	0	14,180
OCT	143,688	279	9,906	0	0	0	0	13	0	9,919
NOV	119,006	240	8,207	0	0	0	0	13	0	8,220
DEC	114,379	239	7,889	0	0	0	0	13	0	7,902
Total	1,734,214	3,313	128,264	915	0	0	0	156	0	129,336

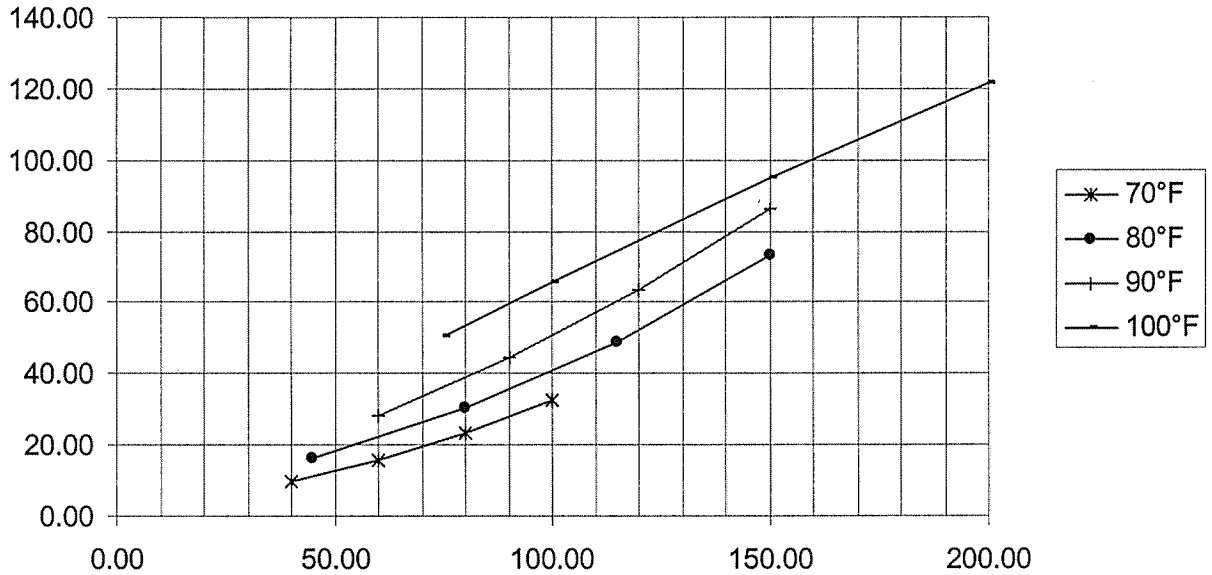
Total Monthly Gas Consumption and Gas Energy Cost
--

Baseline System										
Month	Metered Energy Therms	Metered Demand Therms/Day	Energy Charge (\$)	Demand Charge (\$)	Energy Cost Adj (\$)	Taxes (\$)	Surch. (\$)	Fixed Charge (\$)	Min. Charge (\$)	Total Charge (\$)
JAN	0	0	0	0	0	0	0	9	0	0
FEB	0	0	0	0	0	0	0	9	0	0
MAR	0	0	0	0	0	0	0	9	0	0
APR	0	0	0	0	0	0	0	9	0	0
MAY	0	0	0	0	0	0	0	9	0	0
JUN	0	0	0	0	0	0	0	9	0	0
JUL	0	0	0	0	0	0	0	9	0	0
AUG	0	0	0	0	0	0	0	9	0	0
SEP	0	0	0	0	0	0	0	9	0	0
OCT	0	0	0	0	0	0	0	9	0	0
NOV	0	0	0	0	0	0	0	9	0	0
DEC	0	0	0	0	0	0	0	9	0	0
Total	0	0	0	0	0	0	0	108	0	0

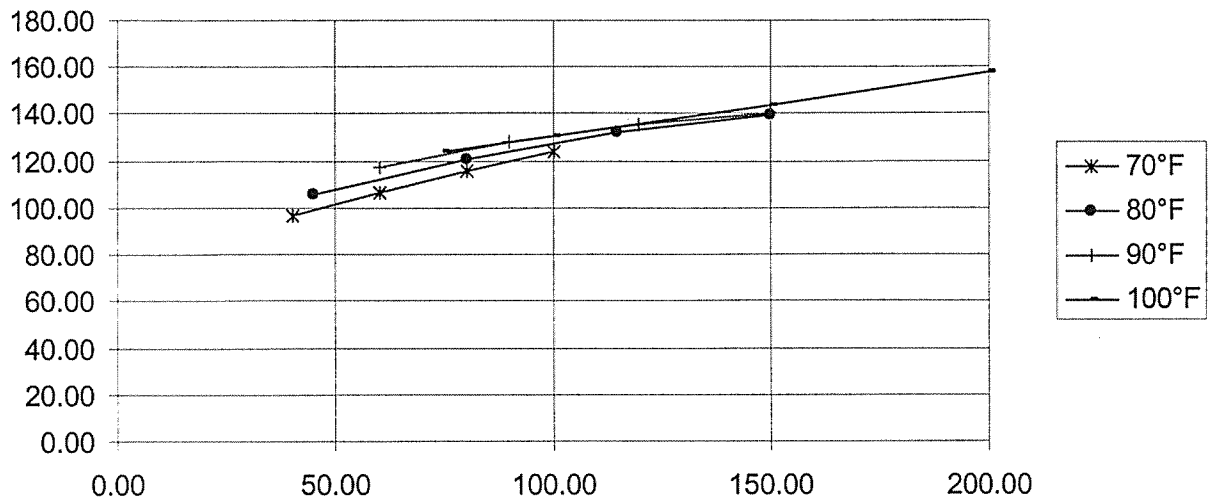
Alternative System										
Month	Metered Energy Therms	Metered Demand Therms/Day	Energy Charge (\$)	Demand Charge (\$)	Energy Cost Adj (\$)	Taxes (\$)	Surch. (\$)	Fixed Charge (\$)	Min. Charge (\$)	Total Charge (\$)
JAN	2,598	335	2,096	0	0	0	0	9	0	2,105
FEB	2,193	208	1,767	0	0	0	0	9	0	1,776
MAR	1,728	162	1,392	0	0	0	0	9	0	1,400
APR	1,174	126	943	0	0	0	0	9	0	951
MAY	3,776	259	1,390	0	0	0	0	9	0	1,399
JUN	4,737	277	1,728	0	0	0	0	9	0	1,736
JUL	6,253	265	2,266	0	0	0	0	9	0	2,275
AUG	7,216	275	2,608	0	0	0	0	9	0	2,617
SEP	5,498	249	1,995	0	0	0	0	9	0	2,003
OCT	1,608	199	620	0	0	0	0	9	0	629
NOV	1,197	120	961	0	0	0	0	9	0	970
DEC	2,270	182	1,830	0	0	0	0	9	0	1,838
Total	40,248	2,656	19,596	0	0	0	0	108	0	19,699

APPENDIX 4.B
UIC CORRELATIONS

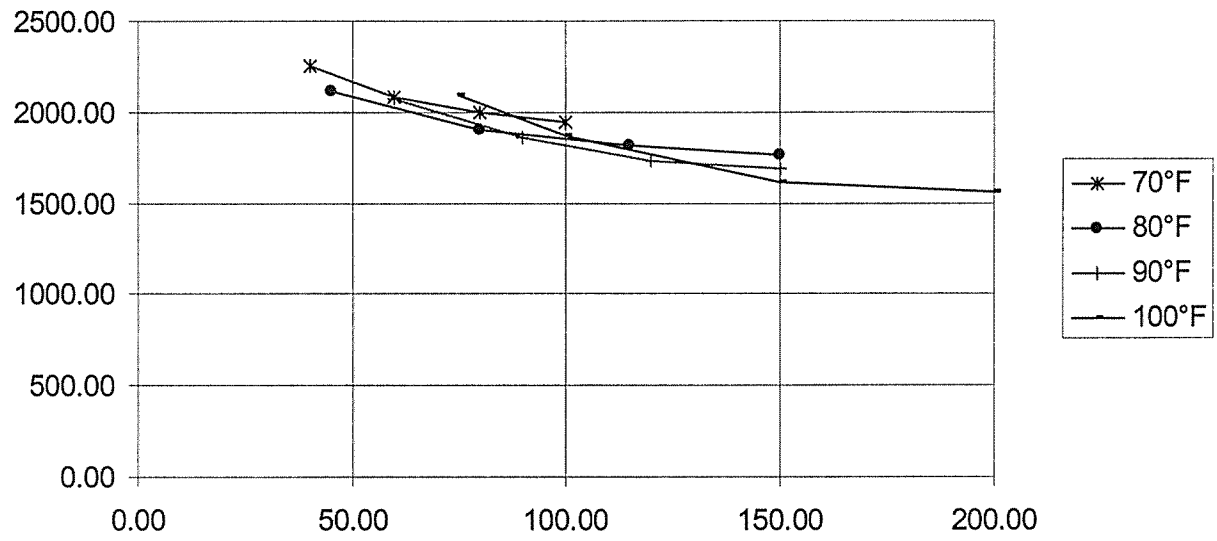
Outlet Grains (y axis) Dependence on Inlet Grains (x axis) and Inlet Temperature - 400 fpm Face Velocity



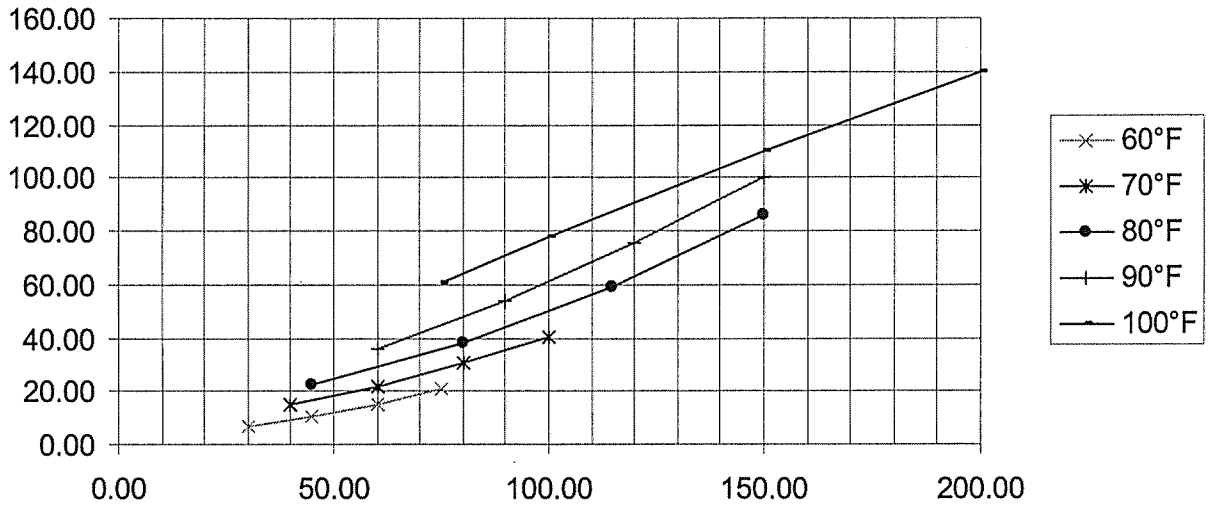
Outlet Temperature (y axis) Dependence on Inlet Grains (x axis) and Inlet Temperature - 400 fpm



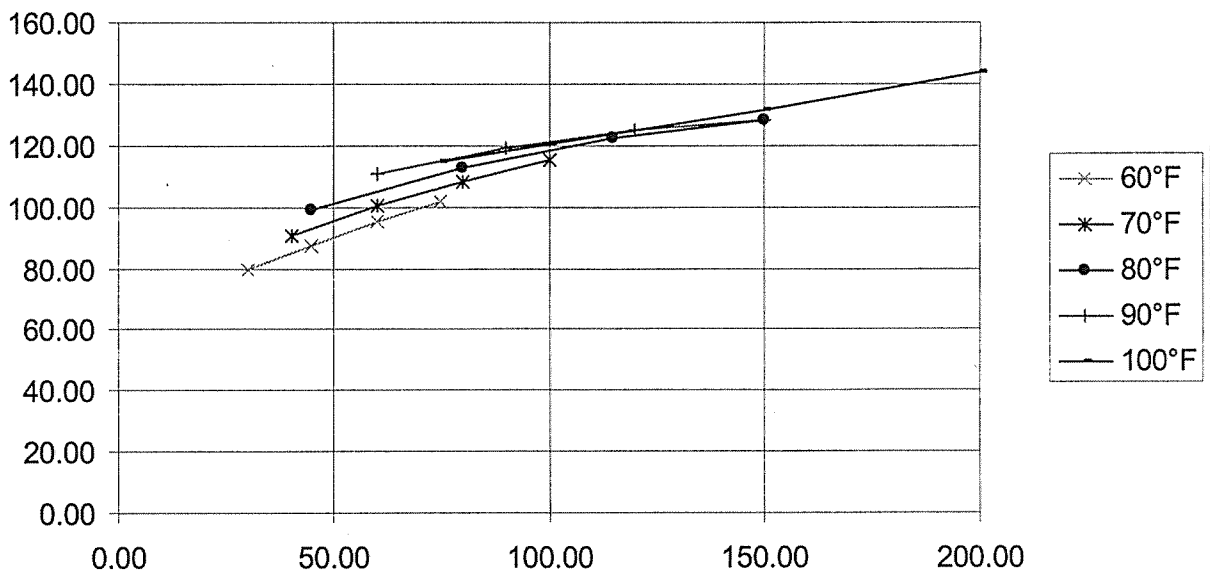
**BTU/lb H₂O Removed (y axis)
Dependence on Inlet Grains (x axis)
and Inlet Temperature - 400 fpm**



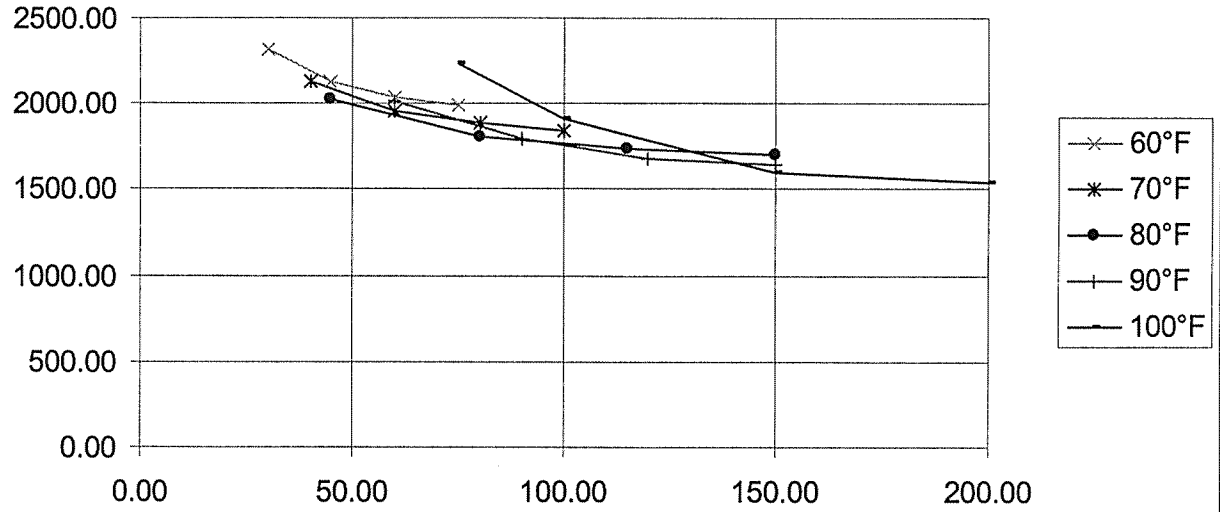
Outlet Grains (y axis) Dependence on Inlet Grains (x axis) and Inlet Temperature - 600 fpm Face Velocity



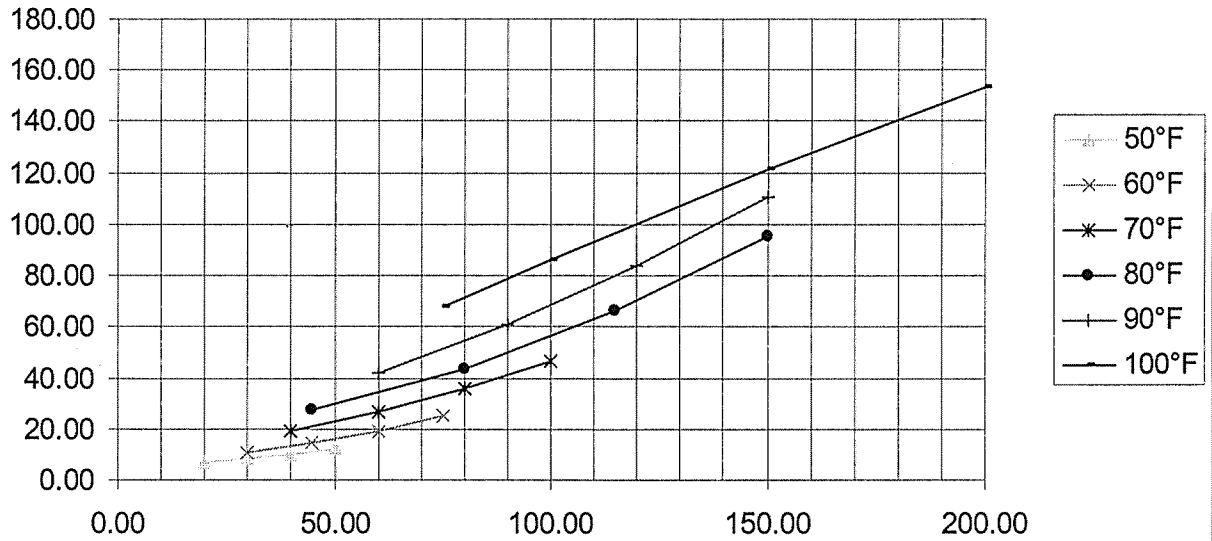
Outlet Temperature (y axis) Dependence on Inlet Grains (x axis) and Inlet Temperature - 600 fpm



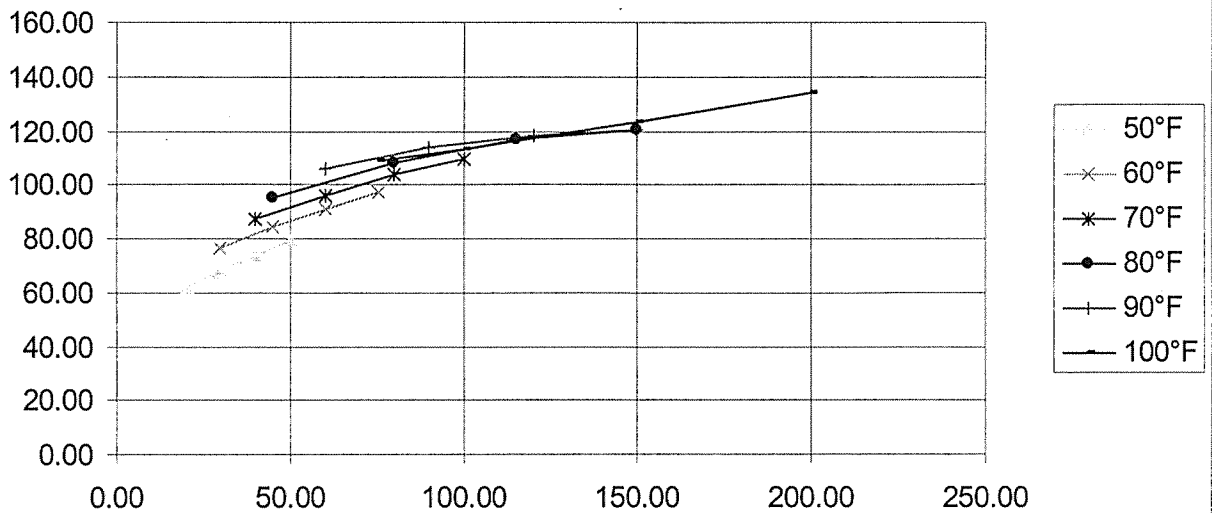
**BTU/lb H₂O Removed (y axis)
Dependence on Inlet Grains (x axis)
and Inlet Temperature - 600 fpm**



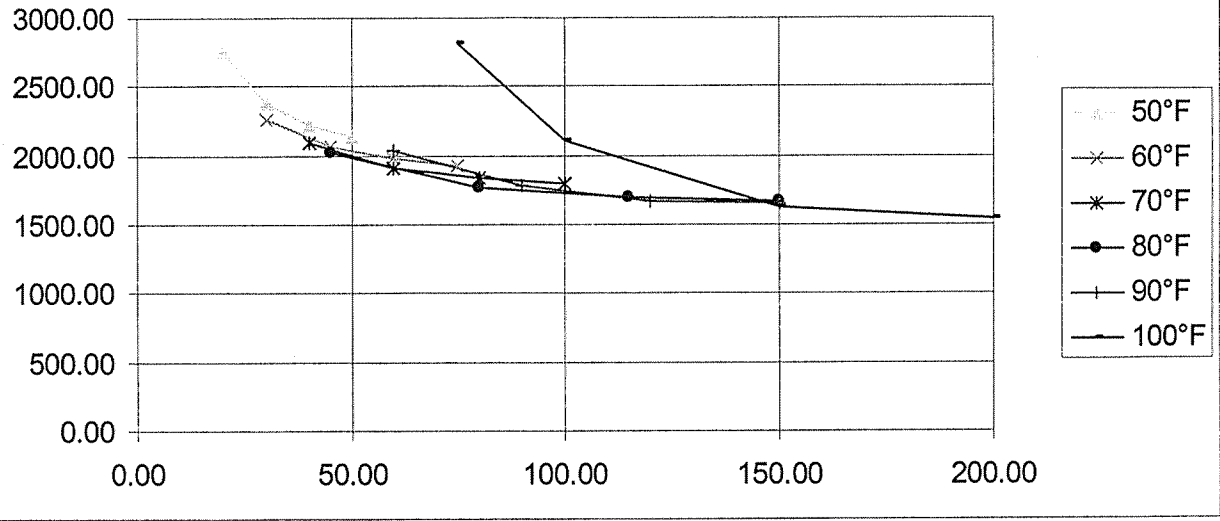
Outlet Grains (y axis) Dependence on Inlet Grains (x axis) and Inlet Temperature - 800 fpm Face Velocity



Outlet Temperature (y axis) Dependence on Inlet Grains (x axis) and Inlet Temperature - 800 fpm



**BTU/lb H₂O Removed (y axis)
Dependence on Inlet Grains (x axis)
and Inlet Temperature - 800 fpm**



Baseline Comparison Metrics:

Present day electric grid delivered energy to the end-use is baselined at an average of 32% for generation and nine percent line losses yielding 29.1%. The future electric grid is assumed to use a Combined Cycle Turbine (CCT) and average annual transmission and distribution losses are projected at nine percent. Using this data, the delivered energy (HHV) is 47.6% of the fuel input energy. (Figure 1)

The efficiency of electricity generation in power-only plants is measured simply by dividing the net electrical output by the amount of fuel consumed (simple efficiency). However, CHP plants produce useable heat as well as electricity. Total CHP efficiency is equal to the sum of the net electrical output and the net useful thermal output of the CHP system divided by the fuel consumed by the CHP system. Both simple and total efficiency are commonly expressed as percentages. CHP plant efficiency is often represented using the total efficiency measure. However, the total efficiency concept does not reflect the quality of electrical output versus heat output (e.g., ability to be transmitted over long distances, to do different types of work, to be converted to work or another form of energy).

An important definition of CHP efficiency is Effective Electrical Efficiency. It expresses CHP efficiency as the ratio of net electrical output to net fuel consumption, where net fuel consumption excludes the portion of fuel that goes to producing useful heating or cooling output. The fuel used to produce useful heating or cooling is calculated assuming specific conversion efficiency (typically 80% boiler efficiency). This measure is useful because of its accuracy in capturing the value of both the electrical and thermal outputs of CHP plants, and its specific measure of the efficiency of generating power through the incremental fuel consumption of the CHP system when compared to the baseline electric grid.

Equivalent Electric Efficiency²

CHP System Equivalent Electric Efficiency	2003	2004	2005	2006
Microturbine / Hot Water CHP	50% ^a			58% ^b
Microturbine / Chilled Water CHP	38% ^c			63% ^d
Reciprocating Engine / Hot Water CHP	^e			^f
Reciprocating Engine / Chilled Water CHP	^g			^h
Combustion Turbine / Steam CHP	56% ⁱ			^j
Combustion Turbine / Chilled Water CHP	43% ^k			63% ^l

² Equivalent Electric Efficiency equals $\text{CHP System (Energy Output}_{\text{ELECTRIC}}) / [\text{Input}_{\text{FUEL}} - (\text{Boiler Fuel Necessary to Generate Thermal Energy Recovered}) \times (\text{Cooling Factor} - \text{if required})]$

Energy Efficiency Metric for Integrated Combined Heat and Power systems:

Project Development Metrics:

The project energy metric for CHP systems is defined as the system's electric energy output plus thermal energy output delivered to a building or industrial process divided by the fuel energy used. This metric is always calculated using Higher Heating Value¹.

This metric is useful in benchmarking project integration progress and should be used in the context of the other metrics. For, example increasing reliability and reducing installation costs leads toward the development of tightly integrated prepackaged components that require considerable size reduction. Size reduction is usually associated with performance penalties. Therefore, improving system integration, reducing installed cost and reducing size, while maintaining performance, is a considerable accomplishment.

$$\frac{\text{Energy Output}_{\text{ELECTRIC}} + \text{Energy Output}_{\text{THERMAL}}}{\text{Energy Input}_{\text{FUEL}}}$$

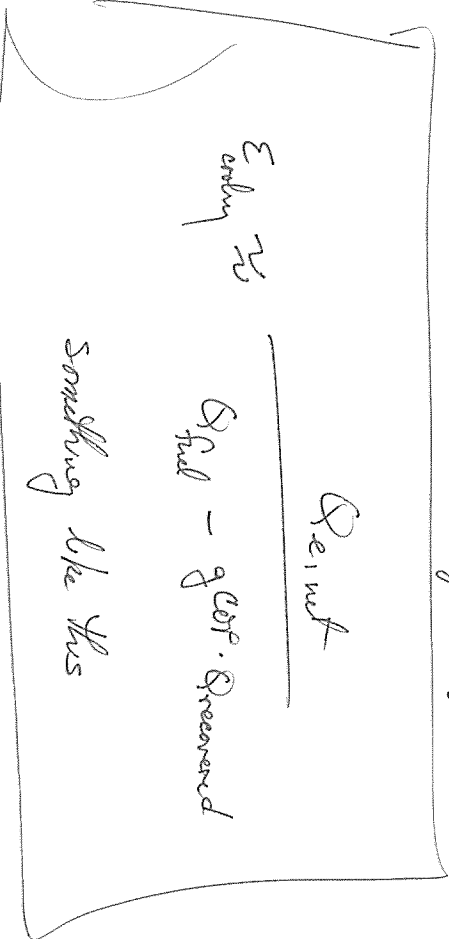
CHP System Performance Metric	2003	2004	2005	2006
Microturbine / Hot Water CHP	65% ^a			70% ^b
Microturbine / Chilled Water CHP	49% ^c			73% ^d
Reciprocating Engine / Hot Water CHP	66% ^e			69% ^f
Reciprocating Engine / Chilled Water CHP	53% ^g			59% ^h
Combustion Turbine / Steam CHP	68% ⁱ			69% ^j
Combustion Turbine / Chilled Water CHP	56% ^k			74% ^l

- ^a Average microturbine characterization assuming 220F leaving exhaust from all HR devices
- ^b Average microturbine characterization assuming 180F leaving exhaust from all HR devices
- ^c Bowman Power microturbine and Broad Air Conditioning USA – HEB project projected performance
- ^d UTC Power IES project projected performance
- ^e Avg. Caterpillar 3516bLE & 3616 and Cummins QSV81G
- ^f Avg. Caterpillar 3516bLE & 3616 and Cummins QSV81G with G Gurber improvement estimates
- ^g Avg. Caterpillar 3516bLE & 3616 and Cummins QSV81G with 0.60 single effect hot water absorber
- ^h Avg. Caterpillar 3516bLE & 3616 and Cummins QSV81G improved with 0.70 single effect hot water absorber
- ⁱ Solar Turbine catalogue average for Centaur, Taurus, Mars with unfired HRSG
- ^j Solar Turbine catalogue average for Centaur, Taurus, Mars with unfired HRSG with improved electronics
- ^k Solar Turbine catalogue average for Centaur, Taurus, Mars with unfired HRSG and 0.7 CHP single effect chiller
- ^l Solar Taurus and Broad exhaust gas fired double effect chiller

¹ Natural gas is often selected as the fuel for these systems. There are two ways to define the energy content of natural gas in common use -- Higher Heating Value (HHV) and Lower Heating Value (LHV). Higher Heating Values for a fuel include the full energy content as defined by bringing all products of combustion to 77°F (25° C). Natural gas typically is delivered by the local gas company with values of 1,000 - 1,050 Btu per cubic foot on this HHV basis. Lower Heating Values (LHV) neglect the energy in the water vapor formed by the combustion of hydrogen in the fuel. This water vapor typically represents about 10% of the energy content. Therefore the lower heating values for natural gas are typically 900 - 950 Btu per cubic foot.

GAS TURBINE
CHP PERFORMANCE (natural gas)

Engine Manufacturer	Solar Turbines	Solar Turbines	Solar Turbines
Engine Model	Centaur 50	Taurus 60	Mars 100
Basic Performance Characteristics			
Base/Load Electric Capacity (kW)	4,425	5,291	10,275
Fuel Input (MMBtu/hr), HHV	58.3	67.21	122.32
Electric Heat Rate (Btu/kWh), HHV	13,175	12,703	11,905
Electrical Efficiency (%), HHV	25.9%	26.9%	28.7%
Other Fuel Types	distillate	distillate	distillate
Fuel Gas Pressure (psig)	216	241	373
CHP Characteristics			
Steam CHP (150 psig saturated) - UNFIRED	Steam	Steam	Steam
Exhaust Flow (1000 lb/hr)	150.3	172	328.2
Turbine Exhaust Temperature (F)	956	960	916
Exhaust Temperature at Burner (F)	956	960	916
Exhaust Temperature after HRSG (F)	320	320	320
Ductburner Fuel Input (MMBtu/hr), HHV	0.0	0.0	0.0
Heat Recovered from Exhaust (MMBtu/hr)	24.9	28.6	50.9
HRSG Losses	2%	2%	2%
Steam Pressure (psig sat)	150.0	150.0	150.0
Steam Saturation Temperature (F)	366	366	366
Boiler Feedwater Temperature (F)	228	228	228
Heat Recovered as Steam (MMBtu/hr)	24.4	28.0	49.8
Total Steam Generated (1000 lb/hr)	24.4	28.1	49.9
HRSG Steam Blowdown (%)	2%	2%	2%
Net Steam to Process (1000 lbs)	24.3	28.0	49.7
Net Heat to Process (MMBtu/hr)	24.3	28.0	49.7
Total CHP Efficiency (%), Steam	67.6%	68.5%	69.3%
Thermal Output/Fuel Input	0.42	0.42	0.41
Power/Heat Ratio	0.62	0.65	0.71
Fuel Chargeable to Power (Btu/kWh)	6,311	6,092	5,856
Efficient Electrical Efficiency	54%	56%	58%
Chilled Water CHP			
Net Heat to Chiller	24.3	28.0	49.7
Chiller COP	1.1	1.1	1.1
Total Chilled Water Produced (MMBtu/hr)	26.7	30.8	54.7
Total CHP Efficiency (%), Chilled Water	71.8%	72.7%	73.4%
Thermal Output/Fuel Input	0.46	0.46	0.45
Power/Heat Ratio	32.94	39.43	78.43
Fuel Chargeable to Power (Btu/kWh)	5,625	5,431	5,251
Efficient Electrical Efficiency	61%	63%	65%



**GAS TURBINE
CHP PERFORMANCE (natural gas)**

Engine Manufacturer	Solar Turbines	Solar Turbines	Solar Turbines
Engine Model	Centaur 50	Taurus 60	Mars 100
Cost Components (\$/Hr)			
Equipment			
Gen Set Package			
Heat Recovery, 150 psig saturated, unfired			
Interconnect/Electrical			
Other equipment			
Total Equipment (150 psig unfired, no SCR)			
Emission Control - SCR (w/unfired HRSG)			
Emission Control - Oxidation Catalyst			
Total Equipment (150 psig unfired, w/SCR and Oxid Cat)			
Installation			
Contractors			
Project Management/Engineering			
Shipping and Misc.			
Permits			
Total Installation			
Total Equipment and Installation (no SCR/Oxid)			
Full Service Maintenance Contract (SRMh)			

**GAS TURBINE
CHP PERFORMANCE (natural gas)**

Engine Manufacturer	Solar Turbines	Solar Turbines	Solar Turbines
Engine Model	Centaur 50	Taurus 60	Mars 100
Engine Emission Controls Only (Unifired HRSG)			
Emission Control Technology	DLN	DLN	DLN
NOx (ppmv @ 15% O2)	15	15	25
CO (ppmv @ 15% O2)	25	25	50
UHC (THC) (ppmv @ 15% O2)	25	25	25
CO2 (lb/MMWh)	1,541	1,486	1,392
Carbon (lb/MMWh)	420	405	380

**GAS TURBINE
CHP PERFORMANCE (natural gas)**

Engine Manufacturer	Solar Turbines	Solar Turbines	Solar Turbines
Engine Model	Centaur 50	Taurus 60	Mars 100
Engine Emission Controls + After Treatment (Unfired HRSO)			
Emission Control Technology	DLN/SCR/CO	DLN/SCR/CO	DLN/SCR/CO
NOx (ppmv @ 15% O2)	2.5	2.5	2.5
CO (ppmv @ 15% O2)	2.5	2.5	5.0
UHC (THQ) (ppmv @ 15% O2)	2.5	2.5	2.5
CO2 (lb/MMWh)	1,541	1,486	1,392
Carbon (lb/MMWh)	420	405	380

Boiler Eff

90%
90%
90%
99%

**MICROTURBINE
CHP PERFORMANCE (natural gas)**

Engine Manufacturer	Capstone	Capstone	Bowman	Ingersoll Rand
Engine Model	C60	C30	1G80	70LM
Basic Performance Characteristics				
Engine Cycle	Recup	Recup	Recup	Recup
<i>Without Gas Boost Compressor (GBC)</i>				
Baseload Electric Capacity (kW)	60	30	80	70
Fuel Input (MMBtu/hr), HHV	0.804	0.433	1.08	0.92
Electric Heat Rate (Btu/kWh), HHV	13,400	14,433	13,480	13,080
Electrical Efficiency (%), HHV	25.5%	23.6%	25.3%	26.1%
Fuel Gas Pressure (psig)	75-80	52-55	80-85	70
<i>With Gas Boost Compressor (GBC)</i>				
Baseload Electric Capacity (kW)	57	28	76.0	67
Fuel Input (MMBtu/hr), HHV	0.804	0.422	1.078	0.91
Electric Heat Rate (Btu/kWh), HHV	14,230	15,071	14,190	13,550
Electrical Efficiency (%), HHV	24.0%	22.6%	24.1%	25.2%
Fuel Gas Pressure (psig)	0.5	0.2-1.5	0.2-6	0.2

MICROTURBINE
CHP PERFORMANCE (natural gas)

Engine Manufacturer	Capstone	Capstone	Bowman	Ingersoll Rand
Engine Model	C60	C30	TG80	70LM
CHP Characteristics				
Hot Water CHP				
Exhaust Flow (lb/hr)	3,852	2,448	6,000	5,760
Turbine Exhaust Temperature (F)	580	530	500	450
Estimated Exhaust Temp after WHRU (F)	220	220	220	220
Heat Recovered from Exhaust (MMBtu/hr)	0.340	0.186	0.412	0.325
Heat Recovered as Hot Water (MMBtu/hr) - no heat loss	0.340	0.186	0.412	0.325
Total CHP Efficiency (%) (without GBC)	67.7%	66.6%	63.5%	61.5%
Thermal Output/Fuel Input	0.42	0.43	0.38	0.35
Power/Heat Ratio	0.60	0.55	0.66	0.74
Fuel Chargeable to Power (Btu/kWh)	6,322	6,686	7,049	7,284
Effective Electrical Efficiency	54%	51%	48%	47%

CHP Characteristics				
Chilled Water CHP				
Exhaust Flow (lb/hr)	3,852	2,448	6,000	5,760
Turbine Exhaust Temperature (F)	580	530	500	450
Estimated Exhaust Temp after WHRU (F)	220	220	220	220
Heat Recovered from Exhaust (MMBtu/hr)	0.340	0.186	0.412	0.325
Heat Recovered as Hot Water (MMBtu/hr) - no heat loss	0.340	0.186	0.412	0.325
COP	1.200	1.200	1.200	1.200
Chilled Water Produced (MMBtu/hr)	0.408	0.223	0.494	0.389
Total CHP Efficiency (%) (without GBC)	76.2%	75.2%	71.1%	68.6%
Chiller Output/Fuel Input	0.51	0.52	0.46	0.43
Power/Cool Ratio	0.50	0.46	0.55	0.61
Fuel Chargeable to Power (Btu/kWh)	4,906	5,137	5,763	6,125
Effective Electrical Efficiency	70%	66%	59%	56%

MICROTURBINE
CHP PERFORMANCE (natural gas)

Engine Manufacturer	Capstone C60	Capstone C30	Bowman TG80	Ingersoll Rand 70LM
Engine Model				
Cost Component				
Equipment				
Gen Set Package				
Gas Compressor				
Heat Recovery				
Interconnect/Electrical				
Total Equipment				
Installation				
Contractors				
Project Management/Engineering				
Shipping and Misc.				
Permits				
Total Installation				
Total Equipment and Installation				
S/KW for Equipment				
S/KW for Equipment and Installation				
Full Service Maintenance Contract (\$/KW)				

MICROTURBINE
CHP PERFORMANCE (natural gas)

Engine Manufacturer	Capstone C60	Capstone C30	Bowman TG80	Ingersoll Rand 70LM
Engine Model	Capstone C60	Capstone C30	Bowman TG80	Ingersoll Rand 70LM
Engine Emission Controls Only (Unfired WHRU)				
Emission Control Technology	DLN	DLN		DLN
NO _x (ppmv @ 15% O ₂)	9	9	25	9
CO (ppmv @ 15% O ₂)	40	40	50	9
UHC (THC) (ppmv @ 15% O ₂)	9	9	9	9
VOC (NMHC) (ppmv @ 15% O ₂)	0.9	0.9	0.9	0.9
CO ₂ (lb/MWe)	1,608	1,732	1,618	1,570
Carbon (lb/MWh)	439	472	441	428

RECIPROCATING ENGINE

CHP PERFORMANCE PROFILE (natural gas)

Engine Manufacturer	Teegen	Cummins	Caterpillar	Caterpillar	Caterpillar
Engine Model	GM-75	QSV8G	G3516B LE	G3520C LE	G3616
Engine Make	GM 454, 8 cyl	Cummins, 16 cyl	Cat, 16 cyl	Cat, 20 cyl	Cat, 16 cyl
Turbo/ Natural Aspirated (NA)	NA	Turbo	Turbo	Turbo	Turbo
Basic Performance Characteristics					
Engine Combustion (Rich or Lean)	Rich	Lean	Lean	Lean	Lean
Base/Load Electric Capacity (KW)	75	1100	1400	2055	3480
Fuel Input (MMBtu/hr) HHV	0.92	10.58	14.26	20.33	31.67
Electric Heat Rate (Btu/kWh) HHV	12,240	9,614	10,188	9,893	9,101
Electrical Efficiency (%), HHV	27.9%	35.5%	33.5%	34.5%	37.5%
Fuel/Gas Pressure (psig)	0.14-0.5	3.5 to 43	1.5-5	1.5-5.0	4.3
Engine RPM	1800	1200	1800	1800	900
Power Factor			0.8	0.8	0.8
Induction (I), Synchronous (S)	I	S	S	S	S
CHP Characteristics					
Hot Water Recovery (190F - 210F)	hot water	hot water	hot water	hot water	hot water
Hot Water Outlet Temperature (F)	230	203	200	194	210
Hot Water Flow Rate (gpm)	22				
Jacket Outlet Water Temperature (F)		203	198	194	210
Lube Oil Outlet Water Temperature (F)		217	198	194	210
Heat Recovered from Exhaust (MMBtu/hr)	0.245	2.290	3.570	4.740	5.105
Heat Recovered from Jacket Water (MMBtu/hr)	0.245	0.910	0.521	4.229	2.340
Heat Recovered from HT Aftercooler (MMBtu/hr)		0.500	0.535	inc in JW	1.403
Heat Recovered from HT Aftercooler (MMBtu/hr)		0.400	0.540	inc in JW	1.161
Total Heat Recovered (MMBtu/hr)	0.490	3.922	4.851	8.381	9.557
Total CHP Efficiency (%)	81%	73%	68%	76%	68%
Thermal Output/Fuel Input Ratio	0.53	0.37	0.34	0.41	0.30
Power/Heat Ratio	0.52	0.96	0.84	0.99	1.24
Fuel Chargeable to Power (Btu/kWh)	4.073	5.157	5.857	4.795	5.668
Effective Electrical Efficiency	84%	66%	58%	71%	60%
Chilled Water Recovery	n/a	steam	steam	steam	steam
Heat recovered (MMBtu/hr)	0.49	3.92	4.85	8.38	9.56
Chiller COP	0.7	0.7	0.7	0.7	0.7
Chilled Water-Produced (MMBtu/hr)	0.34	2.75	3.40	5.87	6.69
Total CHP Efficiency (%)	69%	61%	57%	63%	59%
Thermal Output/Fuel Input Ratio	0.37	0.26	0.24	0.29	0.21
Power/Heat Ratio	0.75	1.37	1.41	1.20	1.78
Fuel Chargeable to Power (Btu/kWh)	8.238	7.430	8.066	7.395	7.419
Effective Electrical Efficiency	41%	46%	42%	46%	46%

RECIPROCATING ENGINE

CHP PERFORMANCE PROFILE (natural gas)

Engine Manufacturer	Teegen	Cummins	Caterpillar	Caterpillar	Caterpillar
Engine Model	CM-75	QSV81G	G35168 LE	G3520C LE	G3616
Engine Make	GM 454, 8 cyl	Cummins, 16 cyl	Cat, 16 cyl	Cat, 20 cyl	Cat, 16 cyl
Turbo/natural aspirated (NA)	NA	Turbo	Turbo	Turbo	Turbo
Cost Estimates					
Electric Capacity (kW)					
Equipment					
Gen. Set Package ¹					
Three-Way Catalyst (rich burn only)					
Heat Recovery					
Interconnect/Electrical ²					
Total Equipment					
Installation					
Contractors					
Project Management/Engineering					
Shipping/Misc					
Permitting					
Total Installation					
Equipment Costs, \$/kW					
Equipment and Installation Costs, \$/kW					
SCR Costs for Lean Burn Engines, (\$/kW) ³					
Full Service Maintenance Contract, (\$/kW)					

Date: Wed, 23 Jul 2003 12:45:25 -0400
From: Richard Sweetser <rsweetser@cox.net>
Subject: metrics
To: Phil Fairchild <fairchildpd@ornl.gov>

Sincerely yours,

Richard S. Sweetser

President

EXERGY Partners Corp.

12020 Meadowville Court

Herndon, VA 20170

Phone: 703.707.0293

Fax: 703.707.0138

E-mail rsweetser@exergypartners.com



Recip Engine Performance MetricsR1.xls



Microturbines Performance MetricsR1.xls

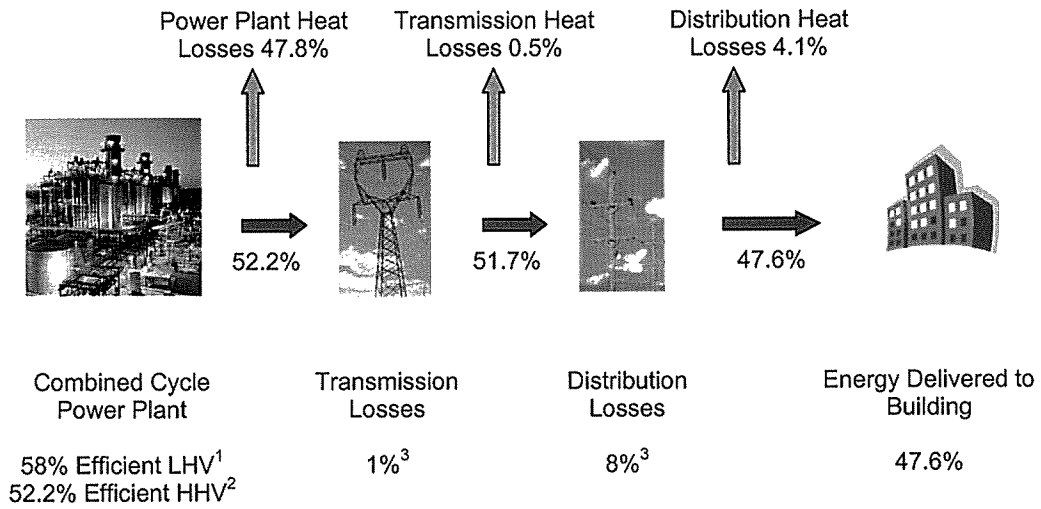


Gas Turbine Performance Metrics.xls



Untitled9

Figure 1: Best Available Grid Technology Combined Cycle Combustion Turbine



¹ 58% (LHV) GE G class Turbine <http://asme.pinetec.com/ijpgc2000/data/html/15084.html>

² Higher Heating Value efficiency is 10% less than Lower Heating Value – see footnote on page 1

³ T&D Losses are estimated at 9% of gross generation--EIA/Annual Energy Review 2001, page 219

Date: Wed, 23 Jul 2003 11:41:51 -0400
From: Richard Sweetser <rsweetser@cox.net>
Subject: next add
To: Bruce Hedman <bhedman@eea-inc.com>
Cc: Phil Fairchild <fairchildpd@ornl.gov>

Sincerely yours,

Richard S. Sweetser

President

EXERGY Partners Corp.

12020 Meadowville Court

Herndon, VA 20170

Phone: 703.707.0293

Fax: 703.707.0138

E-mail rsweetser@exergypartners.com



Untitled8